DISCLAIMER NOTICE

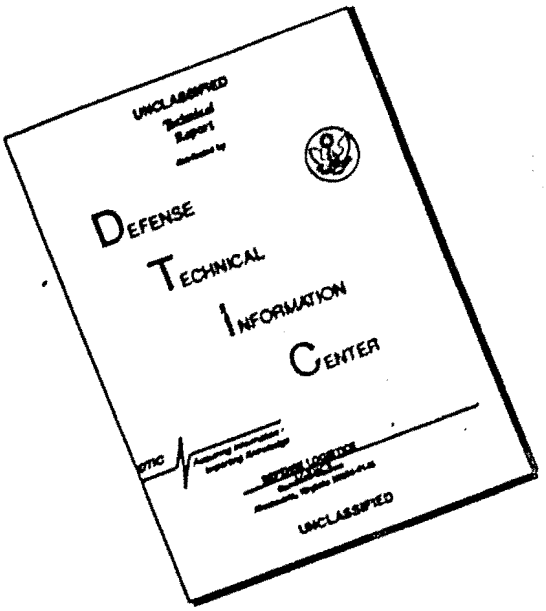

THIS DOCUMENT IS BEST QUALITY AVAILABLE. THE COPY FURNISHED TO DTIC CONTAINED A SIGNIFICANT NUMBER OF PAGES WHICH DO NOT REPRODUCE LEGIBLY.

PRINCETON UNIVERSITY

DEPARTMENT OF AERONAUTICAL ENGINEERING

DEPARTMENT OF THE AIR FORCE
AIR FORCE OFFICE OF SCIENTIFIC RESEARCH
PROPULSION RESEARCH DIVISION

Grant AF-AFOSR-92-63

SOLID PROPELLANT IGNITION STUDIES: IGNITION OF THE REACTION FIELD ADJACENT TO THE SURFACE OF A SOLID PROPELLANT

Final Technical Report

1 October 1962 to 30 September 1963

Aeronautical Engineering Report No. 674

Prepared by: Clarke E. Hermance
Clarke E. Hermance
Research Associate

Reuel Shinnar CEH
Reuel Shinnar
Visiting Research Engineer

Joseph Wenograd
Joseph Wenograd
Research Staff Member

Approved by: Martin Summerfield
Martin Summerfield
Principal Investigator

1 December 1963

Guggenheim Laboratories for the Aerospace Propulsion Sciences
Department of Aerospace and Mechanical Sciences
PRINCETON UNIVERSITY
Princeton, New Jersey

The contents of this report have been submitted by Clarke E. Hermance in partial fulfillment of the requirements for the degree of Doctor of Philosophy from Princeton University, 1963, under the title of "Ignition of the Reaction Field Adjacent to the Surface of a Solid Propellant."

ACKNOWLEDGEMENTS

This dissertation was completed with the assistance of a large number of kind persons to whom I am very grateful.

It was my great privilege and pleasure to carry out this research under the direction of Professor Martin Summerfield who suggested the research program. His continued support and encouragement were vital for the completion of this work, and are deeply appreciated.

Many fruitful and stimulating hours of discussion concerning the theoretical developments in this program were spent with Professor Reuel Shinnar, Visiting Professor in the Department of Aeronautical Engineering. The completion of this program is in a large measure due to his steadfast interest, for which I am wholeheartedly grateful.

Dr. Joseph Wenograd's technical help and personal interest is acknowledged gratefully. Special thanks are due the Department of Mechanical Engineering, and particularly to Professors R. M. Drake and J. B. Fenn of that Department, for continued support and encouragement.

Mr. L. L. Hoffman deserves great credit for his unselfish help in the digital computation part of this work, and I wish to thank him very much. Messrs. G. Barnock and N. Carney were most helpful in the experimental part of this program and their efforts are gratefully acknowledged. The final manuscript was typed by Miss Yolanda Pastor; her skill and unswerving effort are truly appreciated. Many other members of the technical staff of the Guggenheim Laboratories for the Aerospace Propulsion Sciences contributed their time and effort. I would like to thank all of them at this time.

Finally, I would like to take this opportunity to thank my wife, for her love and encouragement were essential for the completion of this work.

Financial support was provided by the U. S. Air Force Office of Scientific Research on Grant AF-AFOSR 92-63. This work made use of computer facilities supported in part by National Science Foundation Grant NSF-GP579.

ABSTRACT

Early experimental and theoretical investigations of solid propellant ignition seemed to indicate that ignition was caused by exothermic solid phase reactions stimulated at the exposed surface of a propellant by applied heat. Later experiments, in which nitrate ester and composite propellants were exposed to various gases at controlled high temperatures and pressures, showed that the ignition delay was influenced not only by the nature of the propellant, but by the quantity of oxidizer present in the external gas and the gas pressure. Log-log plots of experimental ignition delay versus the gaseous oxidizer concentration exhibited a range of slopes from zero to minus two or more. These experiments indicated that the igniter gas plays a specific role in the ignition process, and that propellant ignition could be due either to a reaction of propellant fuel molecules with the gaseous oxidant in a gas phase reaction, or to a heterogeneous surface reaction between oxygen and the solid phase fuel.

The object of this research was to further elucidate the ignition mechanism of solid propellants, to identify the component processes, and to lay the basis for a theory of ignition.

Experiments were performed in which composite propellant samples and polymeric fuel samples were exposed to high and low speed flows of oxygen containing gases at high temperature and pressure in a shock tunnel. Ignition of either propellant or fuel could not be obtained in high speed flows (ca. 5000 ft/sec) even in pure oxygen; in addition, no charring or decomposition of the fuel was observed. At low flow speeds, on the other hand, ignition of the composite propellant and the polymeric fuel did occur, and the ignition delay was found to depend on the gas phase oxygen concentration. The non-ignition at high flow speeds indicated that dilution or sweeping away of the gaseous reaction zone inhibited the ignition. An ignition limit for the fuel samples near 50% oxygen mole fractions was observed, suggesting that boundary layer flame establishment required a longer fuel sample.

These results indicate that a pure solid phase ignition mechanism is incorrect, and strongly suggest that the site of ignition is in a gaseous reaction boundary layer adjacent to the surface of the propellant and not on the fuel surface itself.

A previous approximate theory of solid propellant ignition by gas phase reaction, developed by McAlevy and Summerfield, did not predict the correct dependence of ignition delay on oxygen concentration; therefore, the theoretical situation was in doubt. A special point of interest for the

theoretical development is that proportionality of the ignition delay to the gaseous oxidizer concentration raised to a power substantially greater than minus one has been observed in solid propellant ignition. Therefore, the theory of thermal, gas phase ignition was extended to check whether a gas phase ignition mechanism could admit a dependence on oxidizer concentration raised to a power greater than minus one.

A mathematical model was formulated for the thermal, gas phase ignition of a reaction field adjacent to a condensed phase fuel suddenly exposed to a hot, stagnant, oxidizing gas. The characteristic ignition properties of this model were treated first by similarity theory and then by numerical methods. Two cases were treated: in the first case the concentration of fuel vapors at the condensed phase surface was taken constant; in the second case a constant mass flux of fuel vapors from the surface was assumed. The surface temperature of the condensed phase was assumed constant (a restrictive assumption to be removed in later work), and the chemical reaction was represented by a second order reaction with an Arrhenius function temperature dependence.

It is significant that the system of three, coupled, nonlinear, partial differential equations of this mathematical model could be integrated by digital techniques. The integrations were both stable and convergent, showing that the solution of similar problems of nonlinear nature should be possible.

An important conclusion was that when $(RT/E)_{gas} > 1/5$, a classical induction period does not exist; the reaction temperature rises continuously and the definition of the state of ignition becomes arbitrary. Consequently, two experiments could show differing effects of oxidizer concentration on the ignition delay unless identical ignition detection methods were used. Furthermore, at least to a limited degree, a theory of ignition can be made to fit experimental results by deliberate choice of an ignition criterion.

It was shown that for any ignition criterion, the sensitivity of the ignition delay to changes in the concentration of gaseous oxidizer can vary strongly. A log-log plot of these quantities can exhibit a slope between zero and minus infinity. Therefore, the gas phase ignition delay of a heterogeneous system can depend on the gaseous oxidizer concentration raised to a power greater than one over some range of oxidizer concentration.

The presence of diffusional processes was found to result in a falsification of the activation energy of the chemical reaction. The apparent activation energy found from a plot of log (t_{ign}) versus $(1/T_{gas})$ was lower than the actual activation energy. Activation energies reported on the basis of such experimental data are thus invalid.

The analysis indicated that gas pressure increases could have an adverse effect on the ignition delay under certain restrictions on the physical parameters of the system. This is contrary to the prediction of a heterogeneous surface ignition theory, but unfortunately there is no experimental data to support it.

This work is significant in that it points out the type of decisive experiments needed to test the validity of either the gas phase or surface reaction ignition mechanism. Conclusive interpretation of the results of these experiments, however, require that the gas phase theory be extended by relaxing the restriction of constant temperature at the surface of the condensed phase. In addition, theoretical extension to include the case of a flowing igniter gas should be carried out.

TABLE OF CONTENTS

TABLE OF CONTENTS-contd.

TABLE OF CONTENTS-contd.

TABLE OF CONTENTS-contd.

LIST OF FIGURES
FOR PART I

LIST OF FIGURES
FOR PART I-contd.

LIST OF FIGURES
FOR PART II

LIST OF FIGURES
FOR PART II-contd.

LIST OF FIGURES
FOR PART II-contd.

TABLE OF SYMBOLS

A	dimensionless constant characteristic of oxidizer consumption; $(n y_F^\circ / y_{ox}^\infty)$ in case I, $\left(\frac{n \dot{m}_F^\circ}{\sqrt{\rho^3 (y_{ox}^\infty)^3 \rho D}}\right)$ for Case II
B	dimensionless constant characteristic of heat generation; $\left(\frac{\rho R}{\varphi E} y_F^\circ\right)$ case I, $\left(\frac{\rho R}{\varphi E} \cdot \frac{\dot{m}_F^\circ}{\sqrt{\rho^3 y_{ox}^\infty \rho D}}\right)$ for Case II
c	specific heat of solid
c_p	specific heat of gas
C_F	fuel concentration in gas phase
C_F°	fuel concentration at surface of condensed phase
C_{ox}	oxidizer concentration in gas phase
C_{ox}^∞	initial value of C_{ox}
D	mass diffusion coefficient
E	activation energy or voltage
$f(C_F)$	any specified function of C_F or its spatial gradient
h	convective heat transfer coefficient
H_1	characteristic time of homogeneous induction period
H_2	characteristic time of heat exchange in a homogeneous system
L	characteristic length
Le	Lewis number, D/α
$L^*(\theta)$	functional representation of ignition criterion
$\dot{m}_F^\circ$	mass flux of fuel from surface of condensed phase
n	stoichiometric ratio or surface reaction order
$\dot{q}$	heat transfer rate or heat flux
q_R	heat of reaction
q	heat of reaction per mole of oxidizer
P	pressure

TABLE OF SYMBOLS-contd.

R	universal gas constant
S	surface area
T	temperature
V	volume
t	time
t_{ign}	ignition delay time
y	mole fraction of reactant in gas phase
y_F°	mole fraction of fuel at surface of condensed phase
y_{ox}^∞	initial mole fraction of oxidizer in gas phase
α	thermal diffusivity, dimensionless number, temperature coefficient of resistivity
α'	value of empirical ratio, from B. L. Hicks (19)
β	dimensionless number
γ	dimensionless number, ratio of gas specific heats
δ	dimensionless number
η_F	dimensionless fuel concentration
η_{ox}	dimensionless oxidizer concentration
θ	dimensionless temperature, $\theta = RT/E$ or $\theta = (T - T_{wall})/T_o$
λ	thermal conductivity
μ	viscosity
ξ	dimensionless distance
ρ	density
σ	dimensionless number
τ	dimensionless time
τ^*	dimensionless ignition delay
φ	dimensionless function,

TABLE OF SYMBOLS-contd.

Subscripts

I or II	reference to case I or case II
o	initial state
F	fuel, solid or gas
G	gas
P	propellant
s	solid or surface
ign	ignition

CHAPTER I-1

DISCUSSION OF PREVIOUS IGNITION STUDIES

A. INTRODUCTION

The ignition of energetic chemical reactants is a critical part of any system in which combustion is a necessary part of its operation. In such a system, the reactants to be ignited may be present as either a homogeneous mixture of identical phases, or a heterogeneous mixture of unlike phases. From the standpoint of technological application, it is clearly desirable to understand the properties of ignition in both types of reactant mixtures.

In the past, the ignition of combustible mixtures has been quite intensively studied by a large number of investigators. Two general classes of combustible mixtures were studied and in each case a variety of experimental methods were used. These two classes were those in which both reactants were gaseous, and those in which one of the reactants was a liquid, hydrocarbon fuel. A brief review of typical experiments and results for each of these cases is given in a later section of this chapter.

Now in each class of mixture, the common manifestation of ignition was a rapid acceleration of the chemical reaction rate which caused a sudden temperature increase in the system. Two alternative explanations for this accelerating chemical reaction rate exist. The first alternative is the control of the reaction rate through a predominance of chain branching over chain breaking chemical reactions and subsequent acceleration of heat release. The other alternative is that the reaction rate is governed purely by the relative thermal processes of heat generation and heat loss, regardless of the detailed form of the chemical reaction. The former alternative may be termed "chain branching" explosion or ignition; in the latter alternative ignition is considered as being purely thermal in nature, and arising out of a favorable thermal unbalance in the system.

Having certain experimental results, then, one is faced with the problem discerning which of these alternatives is best supported by the data. In the case of "chain branching" ignition, the data persuades one to conclude that the previous history of the reaction rate is important in the total ignition process. Consequently, the experimental data is used in the development of a detailed description of the chemical reactions including the formation and propagation of free radicals and

activated complexes. It is only recently, however, that adequate treatment of such formulations has been made possible through the advent of high speed computing devices. On the other hand, the experimental data may indicate that the ignition was purely thermal in nature.

It should be noted that the latter interpretation of experimental data is based on the previous theoretical developments of the properties of thermal ignitions. An essential feature of thermal ignition theory is the assumption of a chemical reaction rate represented by an instantaneous function of reactant concentration and temperature. Consequently, the chemical reaction rate is assumed to be independent of its previous history. Clearly, our present understanding of ignition processes has been profoundly influenced by early theoretical and experimental studies.

Actually, the ignition of most homogeneous--and heterogeneous--mixtures probably involves a combination of chain branching and breaking processes, and thermal effects. Even so, the assumption of simple, one-step chemical reaction often constitutes an adequate description of the chemical processes during ignition. Consequently, the theoretical description of the properties inherent in thermal ignition of combustible mixtures is a fundamental area of present, and past, investigations.

B. REVIEW OF EARLY THERMAL IGNITION THEORY

The basic concept of thermal ignition was developed by van't Hoff (I.1), who defined this type of ignition as the impossibility of thermal equilibrium being established between a reacting system and its surroundings. Le Chatelier (I.2) qualitatively formulated this condition as a contact between the curve of heat generation and the straight line of heat loss.

Quantitative formulation of thermal ignition was first done for a homogeneous mixture confined in a reaction vessel in order to determine the characteristic behavior of such a system. Thus, it is informative to determine critical explosion conditions in terms of vessel size, pressure, and initial temperature. In this case, one wishes to know what steady, or stationary, states can be tolerated by the mixture. Secondly, one may wish to determine the induction period of the explosion and its dependence on the mixture's initial conditions. The theoretical description of this case requires formulation and solution of the transient, or nonstationary, behavior of the confined mixture.

The following two sections provide a brief review of the early theoretical developments describing these two

cases. These developments provide the basic understanding of thermal ignition which is essential for the developments in thermal ignition theory which follow in the next chapter.

1. Stationary Theory of Thermal Ignition

The theoretical development for determination of the limiting or critical stationary state for a confined homogeneous mixture has been done by Semenov (I.3) and others. Recently, limitations and extension of the early developments of this case were discussed in references (I.4) and (I.5).

In the stationary theory of thermal explosion, one assumes that the heat generated by chemical reaction is continuously distributed throughout the reactant mixture. Heat loss is assumed to take place by conduction to the vessel walls which are maintained at a constant temperature. Because all possible states of the reactant mixture up to the conditions of explosion are assumed to be stationary, the time derivative of the temperature is equal to zero. It is further assumed that the temperature rise at the critical conditions for explosion is small compared to the initial temperature of the mixture. This assumption allows approximation of the exponential term in the chemical reaction rate term, simplifying the final differential equation. The most important consequence of this approximation is that all the physical parameters of the system can be grouped into one constant, δ , appearing only in the differential equation.

$$\delta = \frac{Q E r^2 Z}{\lambda R T_0^2} e^{-E/RT_0}$$

The constant, δ , characterizes the solution of the differential equation in that for some critical value of δ a stationary state cannot exist and explosion will occur. This method is quite accurate in its prediction of the critical conditions for explosion as a function of vessel wall temperature, pressure, and vessel size, see reference (I.6). The effect of free convection in the mixture have been ignored, but under normal experimental situations this effect can be neglected justifiably.

2. Nonstationary Theory of Thermal Ignition

In the nonstationary theory developed by Todes (I.7), Rice (I.8) and Frank-Kamenetskii (I.6), one deals with the reaction vessel as a whole, assuming that the temperature is uniform over all points in the vessel. Under conditions in which explosion is imminent, heat conduction

within the mixture is ignored, an assumption which is equivalent to replacing all temperature dependent quantities by their value at some mean temperature. It is tacitly assumed, then, that the reactant mixture remains well mixed, and always homogeneous.

Errors introduced by these assumptions, however, are relatively minor compared to the assumptions that density is independent of temperature and that the chemical reaction can be approximated by an Arrhenius rate term. Pragmatically, however, the two assumptions just mentioned are justifiable in the sense that their use in theoretical developments of steady state gaseous flames has produced reasonably correct results.

Under all the above assumptions, one then considers the time rate of change of temperature inside a vessel containing a homogeneous reactant mixture. The competing processes in this case are chemical heat generation, reactant consumption, and heat transfer to the walls of the vessel. It has been normally assumed the chemical reaction does not deplete the concentration of either/any reactant during the induction period because the total temperature rise during the induction period is taken to be small compared to the initial temperature. Consequently, the Semenov approximation of the temperature dependent exponential term of the Arrhenius function has been made. Heat loss to the vessel walls is assumed to take place through Newtonian cooling.

After suitable nondimensionalization of the temperature, the nonstationary behavior of the reaction vessel is characterized by the two dimensionless groups contained in the following differential equation. One should note that the reaction vessel is assumed to have a surface area and volume of S and V respectively, and that the heat transfer coefficient between the mixture and the vessel walls is defined as h . Other symbols are standard, and their definitions may be found in the Table of Symbols.

$$\frac{d\theta}{dt} = \frac{e^{\theta}}{H_1} - \frac{\theta}{H_2} \qquad [1]$$

where $H_1 = \left(\frac{E Q \rho Y_1^{\circ} Y_2^{\circ} Z e^{-E/RT_0}}{c_p R T_0^2}\right)^{-1}$, $H_2 = \left(\frac{hS}{c_p \rho V}\right)^{-1}$; $\theta = 0$ at $t = 0$.

The group, H_1 , may be termed the characteristic time of the chemical induction period; H_2 is the characteristic time of heat exchange in the system.

The form of the solution of [1] above, is

$$\theta = f\left(\frac{t}{H}, \frac{H_1}{H_2}\right) \qquad [2]$$

where (H) may be chosen to be either (H_1) or (H_2). It is clear from this formulation that the ratio (H_1/H_2) completely determines the form of the solution [2].

Often the vessel is considered adiabatic, or the time of heat exchange is long compared to the induction period. In either case, the right hand term of equation [1] can be neglected, and the solution of the resulting equation is

$$e^{\theta} = \left(1 - \frac{t}{H_1}\right)^{-1} \qquad [3]$$

Well into the ignition range, equation [3] will be valid; however, near the ignition limit, H_1 and H_2 are equally important.

It should be noted that at some critical constant value of the ratio (H_1/H_2) there will be a sharp change in the form of equation [2]. When (H_1/H_2) is much greater than its critical value, the real induction delay which is necessary for θ to reach some value θ^* depends upon the pressure or initial concentration of either reactant in the manner shown below.

$$t_{INDUCTION} \sim \varphi^{-1} \qquad [4]$$

where φ = pressure, Y_1° or Y_2° . The dependence of on temperature and activation energy is

$$t_{INDUCTION} \sim \frac{E e^{-E/RT_0}}{RT_0^2} \qquad [5]$$

Note that the criterion selected to define explosion or ignition does not affect the induction delay's dependence on the physical parameters of the system as shown in equations [4] and [5] above.

One should note that the above results are commonly accepted as defining thermal ignition or explosion. Experimental results which follow the predictions of equations [4] and [5] are often used as proof that the reaction mechanism was thermal. If the results of experiments did not follow these patterns, it was often concluded that the ignition or explosion initiation was not governed by thermal processes.

However, when the ratio of characteristic times, (H_1/H_2) is not greatly larger than the critical value, equations [4] and [5] are no longer true. In addition, it is entirely possible that one of the reactants is consumed as the ignition or explosion progresses. Consequently, one must re-examine the formulation of the nonstationary thermal theory, as is done in Chapter I-2.

Recently, the thermal theory of ignition for quiescent, gaseous homogeneous systems has been extended to ignition in flowing systems by Khitrin and Goldnberg (I.9) They examined the critical characteristics of flammability including concentration limits and their dependence on pressure and initial temperature, limit burning velocities, and flame front stabilization criteria. Khitrin (I.10) discussed the consequences of the thermal theory of homogeneous mixture ignition in a fast, laminar or turbulent flow past heated wall or planar body. The ignition by heated, bluff bodies could not be treated except in the case of an ellipse which approached a planar body. Ignition delays, as functionally related to temperature, pressure, and oxidizer concentration were not discussed because stationary state theory was used.

Toong, reference (I.11), has presented a theory for the steady state ignition and combustion of a homogeneous mixture flowing over a heated flat plate. A second order, thermally controlled chemical reaction was assumed. The necessary wall to free stream temperature ratio for establishment of a flame was calculated for variations in pressure, plate length, free stream velocity, and free stream temperature. Reasonable agreement between theory and experiment was obtained; however, the results of this theory are difficult to compare with those of a transient analysis of homogenous mixture ignition.

In 1955, reference (I.12), Marble and Adamson presented a theoretical treatment of the steady, constant pressure combustion of a flowing, homogeneous mixture. They

considered two parallel flows, one of high temperature combustion products and the other of a premixed combustible, and the development of ignition as the separate flows mixed; a perturbation analysis of the pertinent equations was made. The dependence of ignition of the stream was noticed in this treatment, but the effect was not considered important; consequently no investigation of this point was undertaken.

Dooley, in (I.13), treated the case of initially unmixed, different temperature reactants in parallel flow; after mixing by diffusion, ignition and steady combustion ensued. The analytical treatment of this case of heterogeneous combustion was treated by a perturbation analysis similar to that of (I.12). Again, the problem of ignition definition was noted, but remained univestigated.

A nonstationary treatment of thermal ignition was treated recently by Thomas (I.4) including the consumption of one reactant by an n^{th} order reaction during the induction period. By employing the quadratic approximation to the exponential reaction rate term, analytic solutions were obtained for several interesting cases. The use of this approximation, however, limits the applicability of his treatment to cases in which the temperature rise at explosion is less than 100° C. Primary emphasis was placed on the behavior of the system just above its critical condition, and the effect of reactant consumption on this condition and on the induction period.

In reference (I.5), the ignition of ammonium perchlorate and cuprous oxide by simple self-heating was treated by nonstationary thermal theory. Through the use of an effective heat transfer coefficient characterizing the system's heat loss, reasonable agreement between theory and experiment was obtained. The work of Thomas, above, was used to justify the assumption of uniform temperature in the reacting system, during the ignition delay necessary to reach a chosen temperature.

A theoretical treatment of spark ignition has been presented by Jost (I.14) where the spark was represented by a point source of energy in a homogeneous, combustible mixture. Under the assumptions of a threshold source energy value, quasi-steady state after some specified time t_o up to which no reaction occurred, a time independent equation was solved. Heat generation and dissipation were included. The theory predicts the correct order of minimum spark ignition energies in terms of measurable quantities like the mixtures thermal conductivity and burning velocity for some assumed thickness of the combustion wave.

C. PAST EXPERIMENTS ON THE IGNITION OF COMBUSTIBLE MIXTURES

At this point, let us turn to a discussion of past ignition experiments in which homogeneous gaseous mixtures, and mixtures of liquid fuels and oxidizing gases, were ignited. Although a primary aim in these investigations has been the attainment of a homogeneous mixture of the various chemical reactants, it should be noted that this was not always achieved. The gaseous mixtures were usually premixed, or the mixing could be considered fast enough that the mixture was homogeneous at the time of ignition. However, the ignition of liquid fuels and oxidizing gases must be considered as occurring in a heterogeneous mixture. This distinction has not often been made in the open literature, however. Consequently, in the discussion of past ignition experiments which follows, ignition in homogeneous and heterogeneous mixtures will be discussed separately. The reason for this separation is that significant differences exist in the ignition of these two types of mixtures; as will be described in Chapter I-2.

Before preceding with a discussion of the past experiments, some further comments must be made. In the past, there has been a preoccupation with the determination of an ignition temperature and/or the ignition energy of various combustible systems. Measurements of the ignition delay were often ignored or not reported. It has been recognized, however, that neither the ignition energy or temperature is an absolute property of any specific system. Providing sufficient cognizance is taken of the experimental conditions under which either of these quantities was determined, however, such knowledge can be valuable. For example, such measurements do indicate the relative ignitabilities of various fuels under the same environmental conditions. When available, data on the variation of ignition delay with environmental changes preferable if quantitative understanding of the ignition process is to be obtained and used in practical situations.

Three reviews, references (I.15), (I.16), and (I.17), in the general field of ignition of gaseous and liquid fuels, are easily available and provide large bibliographies for those who are interested. The most recent of these are (I.16) and (I.17), published in 1955 and 1956, respectively. The review of ignition, which follows, is not intended as a complete survey of the field, but a brief summary of experimental methods and results up to the present time. It provides a background for the discussion of heterogeneous system ignition in the following chapters of this work.

1. Ignition of Gaseous Mixtures (Homogeneous Ignition)

True attainment of a homogeneous mixture for ignition studies is difficult, and generally can be achieved

only in fully mixed gaseous systems. Thus, the gaseous mixture should be fully mixed before injection into the test apparatus.

The experimental method used for igniting such homogeneous gas mixtures varied considerably with the investigator. Methods which have been used include electrical sparks, hot wires, heated bodies in contact with the mixture, propagation of shock waves into the mixture, and injection of a fuel gas into a hot, isothermal flow of a carrier gas containing oxygen. Ignition delays, when reported, were given for various pressures, reactant concentration, and temperature of the system.

In the last type of experiments, the carrier gas was preheated and passed through a duct into which the fuel gas was injected. The degree and effect of any unmixedness were, in general, not considered exhaustively.

The results of the spark ignition experiments were reported in terms of ignition energy versus equivalence ratio, flow velocity, pressure, and the fuel tested, but ignition delays were not reported. References (I.18), (I.19), and (I.20) are representative of spark ignition experiments. The lack of ignition delay data makes these experiments useless as sources of information on the effect of environmental conditions on the ignition delay.

In other experiments, such as those reported in references (I.11), (I.21), (I.22), and (I.23), premixed combustible mixtures were ignited by heated bodies in contact with the mixture. The results are reported in terms of the body temperatures necessary for ignition and the minimum ignition energy, for various conditions of flow velocity, equivalence ratio, and fuel type. Again, no ignition delay data was given.

In the shock tube experiments (I.24), (I.25), (I.26), and (I.27), ignition was observed behind either the incident or reflected shock wave. This shock wave established the initial high temperature conditions in the mixture before ignition. Generally, the pressure and temperature were varied, and the effect on ignition delay reported. The most interesting of these experiments of this type were those reported in reference (I.27) in which methane-oxygen-nitrogen mixtures ignited behind the reflected shock wave. It was observed that the ignition of methane rich mixtures appeared to be of a thermal nature, and could be obtained only at high temperatures. Lean mixtures could be ignited at lower temperatures and the data was found to be correlated by a modification of the branched chain mechanism presented in reference (I.28). It is

interesting to note that the ignition delay of the methane rich mixture was reported as being inversely proportional to the product of methane and oxygen concentration, each raised to a power of one. This behavior is predicted by a thermal theory of homogeneous mixture ignition, assuming no reactant consumption and a second order reaction.

The experimental results obtained from injecting a fuel gas into a carrier gas containing oxygen, varied considerably among the different experiments. For example, reference (I.29) reports that in propane-oxygen-nitrogen mixtures, the ignition delay was inversely proportional to the first power of propane concentration times the oxygen concentration raised to the power 1/4. At constant mixture ratio and temperature, the ignition delay was proportional to the logarithm of the ratio of system pressure to some reference pressure. In contrast, reference (I.30) reports that the ignition delay of "calor" gas was inversely proportional to the first power of the oxygen concentration and was unaffected by the fuel concentration. However, reference (I.31) reported that the ignition delay of propane oxygen mixtures decreased with temperature and was proportional to the oxygen concentration raised to the -0.74 power.

The effect of pressure on the ignition delay of gaseous mixtures was reported in references (I.31) and (I.32). It was generally found that increased pressure resulted in decreased ignition delays, but some reversal of this trend was reported in (I.33) at subatmospheric pressures for hydrogen, ethane, and carbon monoxide. Unfortunately, all these experiments were done at pressures of less than two atmospheres, and no high pressure data was found.

The effects of composition, pressure, and temperature on the ignition of gaseous mixtures has been very well summarized in the review paper by Brokaw (I.17). It is mentioned in (I.17) that ignition delay data on gaseous mixtures is "generally distressing in (it's) discord." One must only agree with the above quotation. Indeed, from this brief survey, it is evident that little more than a qualitative understanding of the factors affecting the ignition of homogeneous and quasi-homogeneous gaseous mixtures can be obtained at present. Similar experiments with identical or similar mixtures have given conflicting results, and correlation of results from different experimental methods is extremely difficult. Furthermore, it is evident that the present development of the thermal theory of ignition is able to predict and correlate experimental results only under some conditions. However, it will be shown in the next chapter that further development of the thermal theory of ignition may be able to explain some of the varied results just reviewed.

2. Ignition of Heterogeneous Mixtures of Gases and Liquid Fuels

An interaction of chemical and diffusional processes may certainly be very important in experiments on the ignition of heterogeneous mixtures, and in practical systems in which liquid fuel drops or sprays are ignited. Therefore, differences in experimental methods may produce markedly different ignition behavior if interaction of the processes of evaporation, and reactant diffusion and consumption, depend strongly upon pressure and temperature of the system.

A number of experimenters, using a variety of experimental techniques and environments, have investigated the ignition of heterogeneous mixtures of gases and liquid fuels. The experimental methods which have been used include suspension of liquid fuel droplets in heated chambers, injection of liquid fuels into heated bombs, CFR engines, and the injection of fuel sprays into a hot, oxygen containing carrier gas. In general, the ignition delay was reported as a function of oxygen and fuel concentration, pressure, and temperature in the experimental environment. As might be expected, a variety of correlations between the ignition delay and the aforementioned environmental parameters were obtained.

In reference (I.34), hydrocarbon fuel droplets were suspended on a fiber and surrounded by a high temperature chamber filled with an oxidizing gas. The total ignition delay was reported to consist of two parts; the first delay involved the period of time necessary to establish steady evaporation, and the second delay was the period between the start of the steady evaporation and actual ignition. The first delay was independent of oxygen concentration and the second delay was strongly dependent on the oxygen concentration. Consequently, the total delay had a variable dependence upon the oxygen concentration. This experiment provides excellent documentation of the necessity of establishing a significant fuel concentration in the gas phase before ignition can occur. Therefore, diffusional processes are important during the ignition of heterogeneous systems.

The CFR engine experiments, references (I.35), indicated that oxygen-liquid fuel reaction was bimolecular for mixtures which were stoichiometric or leaner.

The ignition of kerosene droplets injected into a constant temperature and pressure flow of oxygen containing carrier gas, was reported in reference (I.36). Experimentally, it was observed that the ignition delay depended upon the inverse square of the oxygen mole fraction for mole fractions less than that of air. Reference (I.37) reports that the ignition delay of liquid fuels in a heated bomb was controlled by the partial pressure of oxygen present in the bomb.

It should be noted that the effect of pressure variation on the ignition was not reported in any of the above experiments. The experiments do indicate that oxygen concentration has a nonconstant effect upon the ignition delay. The relation between this variable effect on the ignition delay cannot be determined clearly; however, (I.34) indicates that two different fuels exhibited similar ignition characteristics under the same environmental conditions.

On the other hand, other experiments have given the variation of ignition delay with pressure level under otherwise constant environmental conditions. In reference (I.38), it was reported that the ratio of ignition temperatures to system pressure was constant and that the ignition delay was inversely proportional to pressure raised to the 0.6 power. These results were for hydrocarbon oils ignited in a heated bomb. A similar experiment with diesel fuels, reference (I.39), gave the result that the product of ignition delay and pressure raised to the 1.19 power, was proportional to an Arrhenius function of temperature.

D. DISCUSSION

All of the above reports on the ignition of heterogeneous systems seem to indicate that the ignition delay may be more strongly dependent upon environmental properties of the system than is the ignition delay of homogeneous systems. Thus, clear support is given to the previous suggestion that there are significant differences between the ignition of heterogeneous and homogeneous systems. In fact, the experimental results point to a nonconstant dependence of the ignition delay on environmental conditions as an essential feature of heterogeneous system ignition.

Of course, realizing that processes involved in the ignition of either homogeneous or heterogeneous systems may be quite complicated, the question arises whether any further development of the thermal theory of ignition is worthwhile. Regarding this question, let us note the remarks concerning the theory of flame propagation made by Hirschfelder in reference (I.40). These remarks are quite apropos to this question of extending the development of the thermal theory of ignition; after some modification they are given below.

"It must be concluded that if one is interested in the ignition properties of a particular combination of reactants, an experimental study is the wisest course of action. However, theory is useful if one is interested in

1. The general features which are common to the ignition of some general classes of combustion systems.

2. The differential effects that may be expected when small changes are made in the pressure, the ignition system, the ambient temperature, etc.

3. The effects of scaling the system.

4. Or effects of changing the initial or ambient oxidizer concentration.

On the basis of the above remarks, it seems quite clear that additional theoretical development of the thermal theory of ignition would be a useful aid in understanding ignition in both homogeneous and heterogeneous mixtures.

In the following chapter, the thermal theory of ignition in homogeneous mixtures will be extended and discussed with respect to the results of homogeneous mixture experiments. Following this development for homogeneous mixtures, the ignition process undergone in heterogeneous systems will be discussed. Afterward, two related but different cases of ignition in a heterogeneous system will be treated quantitatively, in which the effects of reactant supply, diffusion, and consumption on the ignition delay are determined.

At present, the study of the ignition of solid propellants and polymeric fuels in the presence of a hot, oxidizing gas is of great interest, and a review of a number of studies of this solid propellant ignition appears in Part II. Certainly either one of these instances constitutes a heterogeneous system; therefore, the ignition of heterogeneous systems is technologically important at the present time.

CHAPTER I-2

THERMAL THEORY OF IGNITION FOR HOMOGENEOUS AND HETEROGENEOUS SYSTEMS

In past developments of thermal ignition theory, it has been quite well shown that the critical, physical conditions for explosion of a quiescent, homogeneous mixture of reactants are adequately predicted by the stationary theory of thermal explosion developed by Semenov. One may refer, for example, to the remarks made by Frank-Kamenetskii (I.6) concerning such explosions. Therefore, no further development of this theory appears necessary.

On the other hand, the nonstationary theory of thermal explosion (ignition) has had only moderate success in predicting the dependence of the induction delay on the physical parameters of the system. This theory, as formulated by Frank-Kamenetskii (I.6), seems to have had its best application when the total induction period is quite large. When the induction period is on the order of a few milliseconds, as was the case in many of the experiments reported in the previous chapter, the nonstationary theory of (I.6) appeared to have had much less success. Therefore, it is interesting to investigate the extension of the above theory, and to discuss the consequences of this extension.

A brief review of the assumptions made in the formulation of the nonstationary theory of (I.6) is helpful at this point. Basically, these assumptions were that

(1) the chemical reaction was adequately represented by an instantaneous function of concentration and temperature

(2) the reactant concentration remained constant and uniform up to the occurrence of explosion

(3) the mixture temperature remained uniform at all times up to explosion

(4) the heat loss from the system was characterized by an overall heat transfer coefficient times the temperature difference between the mixture and the wall of the vessel.

Now, within the framework of thermal ignition, there can be no quarrel with the first assumption. However, the assumption (2) of constant reactant concentration is particularly shaky when the conditions of lean reactant mixtures and short

ignition delays prevail. The assumption of uniformity of temperature and reactant concentration amount to the assumption that the reactant mixture is well stirred. If the mixture is stirred, either mechanically or by some other mechanism, the uniformity and heat loss assumptions are justifiable. On the other hand, if no stirring occurs, then energy and reactant diffusion processes must be considered in a nonstationary theory of thermal ignition.

Thus, two basic modifications of the simple nonstationary theory of (I.6) clearly exist. The first of these is the inclusion of reactant consumption in the case of a stirred, or uniform, mixture. Secondly, the assumption of uniformity should be dropped, and the effects of energy and reactant diffusion investigated in addition to allowing reactant consumption. Let us separately discuss these modifications by similarity analysis and investigate their implications with respect to the results of experiments on the ignition of homogeneous mixtures. Note that these modifications are particularly, and logically, applicable to instances in which the ignition delay of the homogeneous mixture is short.

A. EFFECT OF REACTANT CONSUMPTION

In many homogeneous ignition experiments, two reactants are present, and one might consider the effect which consumption of both reactants could have on the ignition delay. However, the normal experimental condition is one in which one reactant is in great excess compared to the other. Therefore, the concentration of the excess reactant undergoes little change compared to the changes of the lean reactant during the development of ignition. In homogeneous gas mixtures, induction delays are often quite short. Therefore, it would be interesting to extend Thomas' treatment and investigate the effect of reactant consumption on the rate of temperature rise in a homogeneous system once explosion has started. Qualitatively, the result can be analyzed as follows.

Using the above assumptions, the energy and reactant concentration equations can be written in the form shown below. The symbols Y_i and Y_i° are the current and initial values of the reactant mole fractions, respectively; other symbols are the same as those of the preceding chapter.

$$\frac{dT}{dt} = \frac{9\rho^2 Y_2^\circ}{c_p} Y_1 e^{-E/RT} - \frac{T-T_0}{H_2} \qquad [6]$$

$$\frac{dY_1}{dt} = -\rho^2 Y_2^\circ Y_1 e^{-E/RT} \qquad [7]$$

with the boundary conditions of $T = T_o$, $Y_1 = Y_1^\circ$ at $t = 0$ where $H_2 = (hS/c_p \rho V)$. The parameter "H_2" can be regarded as the characteristic time of heat transfer in the system.

If equation [7] is multiplied by q/c_p and added to equation [6], the resulting differential equation can be integrated formally to obtain

$$Y_1 = Y_1^\circ - \frac{(T-T_o)}{q/c_p} - \frac{1}{H_2 (q/c_p)} \int_o^t (T-T_o)\,dt \qquad [8]$$

such that Y_1 is expressed as an integral function of temperature. Substitution of [8] into [6], taking account of the boundary conditions, results in the single, integro-differential equation of the form shown below.

$$\frac{dT}{dt} = \rho z Y_2^\circ \left(\frac{q}{c_p} Y_1^\circ - (T-T_o) - \frac{1}{H_2} \int_o^t (T-T_o)\,dt \right) e^{-E/RT} - \frac{(T-T_o)}{H_2} \qquad [9]$$

In the interesting case of short induction periods or small total ignition delays, the mixture can be considered as quasi-adiabatic. Therefore, H_2 is very large and heat losses from the mixture can be neglected; in this event, equation [9] simplifies, with $\theta = RT/E$ to

$$\frac{d\theta}{d\tau} = \left[\left(\frac{qRY_1^\circ}{c_p E} + \theta_o \right) - \theta \right] e^{-1/\theta} \qquad [10]$$

with the boundary condition that $\theta = \theta_o$ at $t = 0$ and where

$$\tau = (\rho z Y_2^\circ)\, t \,. \qquad [11]$$

The solution of equation [10] is of the form

$$\theta = \theta\left(\tau ;\ \theta_o,\ \frac{qRY_1^\circ}{c_p E} \right) \qquad [12]$$

whose behavior is characterized by the two dimensionless groups θ_o and $(q R Y_{i}^{\circ}/c_p E)$. These groups represent the initial and maximum adiabatic combustion temperatures of the system, respectively.

It is quite clear that for each value of θ_o, there exists some critical value of the sum $[\theta_o + (q R Y_{i}^{\circ}/c_p E)]$ for which the mixture temperature will just rise slightly and then fall back to its initial value. The set of such critical $[\theta_o ; \theta_o + (q R Y_{i}^{\circ}/c_p E)]$ values constitute the boundary of the envelope where ignition is possible. Within this envelope, the sum $[\theta_o + (q R Y_{i}^{\circ}/c_p E)]$ is greater than the critical value for some value of θ_o ; ignition will occur and the temperature will exhibit a sharp rate of rise to some large value.

If the sum $[\theta_o + (q R Y_{i}^{\circ}/c_p E)]$ is sufficiently large to allow ignition, the problem arises of specifying exactly when ignition is considered to have occurred. This specification may determine the form of the functional relationship between the real ignition delay and the physical parameter whose effect on ignition is being investigated, as shown in the following qualitative argument.

Assume some ignition criterion, $L^*(\theta)$, of the form shown below, where the superscript (*) is used to denote the value of a variable at ignition. When $L^*(\theta)$ is satisfied

$$L^*(\theta) = f(\tau^*; \theta_o, q R Y_{i}^{\circ}/c_p E) \qquad [13]$$

Formally, some inverse function of the form

$$\tau^* = g(\theta_o, q R Y_{i}^{\circ}/c_p E ; L^*(\theta)) \qquad [14]$$

may be obtained from equation [13]. The form of this function clearly depends on the specification of $L^*(\theta)$; therefore, the effect of variations in either θ_o or Y_{i}° on the behavior of the real ignition delay is dependent on the specification of an ignition criterion because of equation [14].

The above development and discussion has definitely shown that both reactant consumption and ignition criterion will affect the form of the data obtained from experiments on homogeneous ignition, when the total induction delay is short.

It would be desirable if the ignition criterion in an experiment were specified with reference to some thermodynamic state; unfortunately, this is not always possible. Therefore, difficulties arise in comparing results between different experiments, and in relating these results to theory. It should be pointed out that exact specification of the ignition event has not always been appreciated up to this time.

In addition, no a priori reason exists for saying that τ^*, and therefore t_{ign}, is not continuously dependent on the mole fraction of the lean reactant, Y_1°. Over a range of values for θ_o and (qRY_1°/c_pE), the dependence of t_{ign} on Y_1° may have slopes which are greater or less than the negative unit slope normally assumed as being indicative of thermal ignition. Therefore, an experimental curve of t_{ign} versus Y_1° that does not have a negative unit slope, is not sufficient reason to conclude that the ignition of a particular homogeneous mixture is not controlled by purely thermal processes.

Another interesting observation can be made from the previous development of thermal ignition theory. This has to do with the usefulness of plotting the logarithm of the induction delay versus inverse temperature for purposes of ferreting out a global activation energy value. Evidently such a plot may have no value per se. In the first place, the activation energy certainly affects both constants in the differential equation for adiabatic ignition when reactant consumption is included. Besides, the ignition criterion probably will vary among investigators. Indeed, even if such a plot is linear, it need not necessarily have any direct relation to the actual activation energy. As far as is known, Thomas (I.4) was the first to make this diagnosis concerning the intrinsic value of this plot, but considered it to be of minor importance in the explosion of homogeneous gas mixtures.

These facts have not previously been appreciated in the past growth of thermal ignition theory of homogeneous mixtures, nor have they been included in the interpretation of experimental data. That they may affect such interpretation is clear, but only numerical solution of equations [9] and [10] can determine the extent of their importance.

B. EFFECT OF QUIESCENT OR UNSTIRRED MIXTURES

The case in which the whole homogeneous mixture is raised to a high temperature and remains completely mixed during the ignition has just been considered. Although interesting information was obtained, this case was of a rather specialized nature. Let us, therefore, consider the characteristic properties of fast thermal ignition in

homogeneous gas mixtures which remain quiescent, or unstirred, during the ignition's initiation and growth.

The assumption of a quiescent mixture, however, forces at least the inclusion of a heat diffusion process in describing the ignition process mathematically. Again, it may be necessary to include reactant diffusion and consumption processes depending upon the limiting case one wishes to investigate.

If reactant diffusion and consumption processes are included in the mathematical formulation, however, two important consequences result. First, the set of equations change from ordinary to partial differential equations, while still containing at least one dimensionless group that cannot be removed by any process of nondimensionalization of the equations. Secondly, this set differs from that describing a similar case of ignition in a heterogeneous system only by the boundary conditions on the reactants. A discussion of the effects which variations in the physical parameters of the system have on the form of the relationship between the real ignition delay and any one of these parameters, is identical to that for ignition in a heterogeneous system. This discussion is postponed, therefore, until ignition in heterogeneous systems is considered.

However, if only energy diffusion is considered in the fast ignition of a quiescent, homogeneous mixture it is interesting to make a comparison between local and wi.espread ignition in the confining vessel. Consider an initially cold, homogeneous mixture contained in a reaction vessel or system in which some surface in contact with the mixture is suddenly raised to a high temperature.

If the reaction vessel is large and one decides that some local detection or occurrence of ignition is characteristic of the whole ignition event, then the local ignition can be considered as if it occurred in a semi-infinite mixture. Under such conditions, it is easily shown that the differential equation can be made completely nondimensional through the definitions of time, distance, and temperature given below

$$\tau = t\left(\frac{\alpha \rho C_p E}{g C_1^{\circ} C_2^{\circ} Z R}\right)^{-1} \qquad [15]$$

$$\xi = x\left(\frac{\alpha \rho C_p E}{g C_1^{\circ} C_2^{\circ} Z R}\right)^{-1/2} \qquad [16]$$

$$\theta = RT/E \qquad [17]$$

Evidently, the dependence of the real ignition delay upon pressure and reactant concentration is completely specified by equation [15]. Of course, it is not clear that the activation energy can be determined, because the value of τ_{ign} depends upon the initial condition, $\theta_o = RT_o/E$ and the selected ignition criterion as discussed in the preceding section.

If the reaction vessel is very small, or if it is required that reaction must occur over a large portion of the volume of the vessel, the semi-infinite assumption cannot be made. The removal of all physical parameters from both the differential equation and boundary conditions is no longer possible in this case, and a single dimensionless group will remain. This group is of the form

$$\delta = \left(\frac{\rho C_1^{\circ} C_2^{\circ} Z R L^2}{\alpha \rho C_p E} \right)$$

where (L) is the characteristic dimension of the system. Again, the effect of variations in any of the parameters contained in (δ) on the real ignition delay is dependent upon both the ignition criterion and the magnitude of the dimensionless parameter of the system.

C. SUMMARY

In the last chapter, a number of the results of ignition experiments in homogeneous and heterogeneous mixtures of reactants were reviewed. It may be recalled that one of the striking features of these experiments was the wide variations reported for the dependence of the real ignition delay on various physical parameters of the system, such as pressure and initial reactant concentration. In many cases where the experimental results did not appear to agree with the available developments of thermal ignition theory, it was concluded that the ignition was not controlled by purely thermal process. Of course, this was a perfectly valid conclusion at the time.

Now, however, it has been shown that the properties and implications of thermal ignition in homogeneous mixtures have been widely misinterpreted because of the many simplifying assumptions made in the theoretical developments up to this point. If some of these assumptions are not made, it was shown in the previous sections that thermal ignition theory is not limited to prediction of certain fixed dependences of

ignition delay on the physical parameters of homogeneous systems. A continuous range of these dependences is clearly possible.

In addition, there has been a common lack of distinction between ignition in homogeneous and heterogeneous systems. The properties of heterogeneous mixtures are discussed in the following sections.

D. INTRODUCTION TO THE THERMAL THEORY OF IGNITION IN HETEROGENEOUS SYSTEMS

Now, having discussed the thermal ignition of homogeneous mixtures of gases, let us turn to the consideration of ignition in systems which are completely unmixed initially. Such a system is heterogeneous, innately, and will be referred to as a heterogeneous system. It is understood that the reactants may be of either similar or dissimilar phases at any point in time during the ignition process. For those interested in combustion processes, several examples of heterogeneous systems come readily to mind. These are the cases of chemical reaction at the gas-solid interface, a gas phase reaction between reactant supplied by the solid and reactants initially present in the atmosphere external to the solid, or a gas phase reaction in which both reactants were initially gaseous but unmixed. In each case, of course, the chemical reaction is taken to be exothermic.

It should be apparent that the interaction of reactant diffusion and consumption must govern thermal ignition in heterogeneous systems. Therefore, it behooves the mathematical analyst to be very careful in his choice of simplifying assumptions. For example, any approximation of the exponential part of the reaction rate function may be inappropriate because two, widely different initial temperatures are often a fundamental part of the system. In many practical instances of heterogeneous ignition, the ignition is often quite fast and of the order of milliseconds or tens of milliseconds. Consequently, any a priori assumption concerning the relative importance of reactant diffusion and consumption may easily change the basic character of the mathematical model used to describe a particular system.

Throughout the following discussion, only heterogeneous systems in which the fuel component of the reaction is supplied by a solid body, and the oxidizing component is present only in the gas external to the solid will be considered. Choice of this type of system was dictated by current concern with the technologically important problem of the ignition of solid propellants and polymeric fuels by hot, oxidizing gases in contact with these substances.

In order to treat the above cases in a mathematically feasible fashion and at the same time retaining all essential elements unique to heterogeneous systems, a stagnant environmental atmosphere was selected. Further general mathematical formulation of such cases depends upon what assumptions are made concerning the site of the chemical reaction.

An interesting case of heterogeneous ignition is that in which ignition takes place at the gas-solid interface. A similarity analysis of this case is given in Appendix A-8 where some comments are made on the consequences of this model in terms of the effect of the system's oxidizer concentration and pressure on the ignition delay. No further treatment of this case was undertaken for two reasons. In the first place, the numerical solution of a model similar to that given in Appendix A-8 has been reported in reference (I.41). It was felt that extension of this solution to the case in which the gas was not stagnant, would result in no additional, fundamental information concerning the case's basic properties.

On the other hand, the instance of heterogeneous ignition in the gas phase adjacent to the solid supplying the fuel vapors is interesting from a practical and fundamental viewpoint. This case has not been treated in a manner which includes the diffusion and subsequent reaction of both reactants during the ignition delay period. Consequently, the characteristic features of such a gas phase ignition have not been adequately described up to the present time.

In reference (I.42), McAlevy has presented a treatment of gas phase ignition near a cold wall from which the fuel was supplied by a pyrolysis process. The assumption was made, however, that chemical reaction effects could be ignored up to the point at which chemical heat generation first became equal to the local heat loss. The point in time and space at which this occurred somewhere in the gas phase, was assumed to be the ignition point. A critical discussion of his treatment is presented in Appendix A-7. It is sufficient to note here that this treatment neglected precisely those effects--namely, combined diffusion and consumption of both reactants--which have been indicated as governing ignition in a heterogeneous system.

Clearly, the distinction between ignition in homogeneous and heterogeneous systems was appreciated in the theory presented in (I.42). However, this theory cannot be considered as describing typical heterogeneous ignition near a cold wall except possibly under very special conditions.

Let us turn, therefore, to a rather more detailed examination of heterogeneous ignition occurring in the gas phase adjacent to a cold solid. The solid is assumed to be the source of supply of one of the reactant (fuel) vapors. Therefore, the general, basic properties of the thermal ignition of a diffusion flame near a cold wall will be examined in some detail.

CHAPTER I-3

SIMPLIFIED MODEL FOR THE THERMAL IGNITION OF A DIFFUSION FLAME NEAR A COOL SURFACE

A. SPECIFICATION OF THE PHYSICAL PROBLEM

Although a variety of heterogeneous systems exist, and the study of the ignition characteristics of each could be informative, a quite specific problem of heterogeneous ignition has been selected for investigation. The thermal, gas phase ignition of fuel vapors produced by sudden contact of a vaporizable, condensed phase with a hot, stagnant gas containing an oxidizer was chosen. No specification is made about the nature of the condensed phase, and this condensed phase may be taken as being either a solid or a liquid fuel. For purposes of convenience, however, the surface of this condensed phase will often be referred to as a "solid wall" or merely a "wall"; in either case, though, it should be clear that reference is being made to the vaporizable surface.

The surface of the condensed phase was taken as a fixed plane, and the origin of a one-dimensional, semi-infinite coordinate system. Certain assumptions were made in order to formulate a mathematical model describing the selected system, while still maintaining the essential features of a heterogeneous system. These assumptions are listed below:

(1) the chemical reaction rate is an instantaneous function of temperature and reactant concentration, of second order overall, and can be adequately represented by

$$\text{Reaction Rate} = C_F C_{Ox} Z e^{-E/RT}$$

(2) the chemical reaction is of the form $[F] + n\,[Ox] \rightarrow m[P]$ where $n \geq m$.

(3) the density is constant over the gas phase field at all times, and independent of temperature

(4) the molecular weights of all gaseous species are constant and equal

(5) the mass diffusivities of all gaseous species are constant, and equal to the thermal diffusivity of the gas phase mixture--i.e.-- $Le = D/\alpha = 1$

(6) the effect of mass addition to the system can be ignored; therefore, mass and energy convection can also be neglected.

(7) the surface temperature of the condensed phase is independently specifiable and constant for all time.

Concerning the justification of these assumptions, it may be noted that the first five frequently have been used in theoretical developments of steady state flame theory, and, in general, their use allowed the prediction and understanding of many basic properties of flame propagation. In fact, these assumptions are so standard in the field of combustion that there use in the following development is justified in a purely pragmatic sense, because useful results have been obtained from other theoretical developments in which they were used. One may see, for example, references (I.6), (I.41), (I.42), (I.46), (I.47), and (I.48). A discussion of the neglect of convective transport in this model is presented in Appendix A-10. It is shown that this neglect results in an error of approximately 10% or less, which is in accord with the discussion presented in reference (I.50), pages 594-598.

Regarding the assumption of a constant pressure independent temperature at the surface of the condensed phase, it is realized that any coupling between the surface temperature and gas phase processes is removed. The basic properties of a thermal, gas phase ignition of a diffusion flame near a cool surface can be found even with this assumption, and the mathematical solution of the problem is made considerably easier.

With the above assumptions, the following set of partial differential equations are written to describe the thermal, gas phase ignition of a diffusion flame near a cool surface.

Mass Diffusion:
$$\frac{\partial C_F}{\partial t} = D\frac{\partial^2 C_F}{\partial x^2} - C_F C_{ox} Z e^{-E/RT} \qquad [23]$$

$$\frac{\partial C_{ox}}{\partial t} = D\frac{\partial^2 C_{ox}}{\partial x^2} - n C_F C_{ox} Z e^{-E/RT} \qquad [24]$$

Energy Diffusion:
$$\frac{\partial T}{\partial t} = \alpha\frac{\partial^2 T}{\partial x^2} + \frac{Q}{\rho C_p} C_F C_{ox} Z e^{-E/RT} \qquad [25]$$

On the basis of the above assumptions, the following initial and boundary conditions are written:

$$t \leq 0 \qquad\qquad t > 0$$

$$\left.\begin{aligned} T &= T_\infty \\ C_{ox} &= C_{ox}^\infty \\ C_F &= 0 \end{aligned}\right\} x > 0 \qquad \left.\begin{aligned} T &= T_s \\ -D\frac{\partial C_{ox}}{\partial x} &= 0 \\ f(C_F) &= \text{CONSTANT} \end{aligned}\right\} x = 0 \qquad [26]$$

$$\left.\begin{aligned} T &\rightarrow T_\infty \\ C_{ox} &\rightarrow C_{ox}^\infty \\ C_F &\rightarrow 0 \end{aligned}\right\} x \rightarrow \infty$$

Two simple specifications were selected for the boundary condition on the supply of fuel from the surface of the condensed phase, which was written above simply as $f(C_F)$ = constant. These two conditions were:

I) the concentration of fuel was some constant, specified value, independent of time, or

$$f(C_F) = C_F^\circ = \text{constant} \qquad [27]$$

II) the mass flux of fuel was some constant, specified value, independent of time or pressure, or

$$f(C_F) = -D\frac{\partial C_F}{\partial x} = \dot{m}_F^\circ = \text{constant} \qquad [28]$$

Case I, above, quite clearly corresponds to the condensed phase being considered as a boiling liquid, or possibly a sublimating solid. On the other hand, case II corresponds somewhat closely to the condensed phase being a polymer undergoing irreversible decomposition.

In order to facilitate analysis and numerical solution,

the following set of dimensionless variables were defined:

$$\left.\begin{aligned} \tau &= (\epsilon Y_{ox}^{\infty} Z)\, t \\ \xi &= X \left(\frac{D}{\epsilon Y_{ox}^{\infty} Z}\right)^{-1/2} \end{aligned}\right\} \qquad \left.\begin{aligned} Y_{ox}^{\infty} &= \frac{C_{ox}^{\infty}}{\epsilon} \\ \eta_{ox} &= \frac{C_{ox}}{\epsilon Y_{ox}^{\infty}} \end{aligned}\right\} \qquad \left.\theta = \frac{RT}{E}\right\} \qquad [29]$$

However, different dimensionless variables for the fuel concentration were used to make both the equations and boundary conditions completely dimensionless. Thus, for case I--constant fuel vapor concentration at the wall--define

$$\eta_F = C_F / \epsilon Y_F^{\circ} \qquad [30]$$

where Y_F° is the fuel's mole fraction at the solid surface. For case II--constant fuel mass flux from the solid fuel wall--define

$$\eta_F = \frac{C_F \sqrt{\epsilon Y_{ox}^{\infty} Z D}}{\dot{m}_F^{\circ}} \qquad [31]$$

Use of these definitions reduced the set of differential equations [23], [24], and [25] to

$$\frac{\partial \eta_F}{\partial \tau} = \frac{\partial^2 \eta_F}{\partial \xi^2} - \eta_F \eta_{ox} e^{-1/\theta} \qquad [32]$$

$$\frac{\partial \eta_{ox}}{\partial \tau} = \frac{\partial^2 \eta_F}{\partial \xi^2} - A \eta_F \eta_{ox} e^{-1/\theta} \qquad [33]$$

$$\frac{\partial \theta}{\partial \tau} = \frac{\partial^2 \theta}{\partial \xi^2} + B \eta_F \eta_{ox} e^{-1/\theta} \qquad [34]$$

with the initial and boundary conditions of

$\tau \le 0$:

$$\left.\begin{aligned} \theta &= \theta_0 \\ \eta_{ox} &= 1 \\ \eta_F &= 0 \end{aligned}\right\} \quad \xi > 0$$

$\tau > 0$:

$$\left.\begin{aligned} \theta &= \theta_s \\ \frac{\partial \eta_{ox}}{\partial \xi} &= 0 \\ \text{CASE I:}\ \eta_F &= 1 \\ \text{CASE II:}\ \frac{\partial \eta_F}{\partial \xi} &= 0 \end{aligned}\right\} \quad \xi = 0 \qquad \left.\begin{aligned} \theta &\to \theta_0 \\ \eta_{ox} &\to 1 \\ \eta_F &\to 0 \end{aligned}\right\} \quad \xi \to \infty \qquad [35]$$

Before proceeding any further, let us modify some of the preceding nondimensionalizing procedures to allow consideration of the limiting instance of zero activation energy. This instance is interesting as a part of this investigation of the properties in our mathematical model describing the thermal ignition of a diffusion flame.

In this instance, the dimensionless temperature, had to be redefined as

$$\theta = \frac{T - T_{WALL}}{T_o} \qquad [36]$$

Then, using the same nondimensional parameter definitions as in the finite activation energy instance, the set of dimensionless equations were written as

$$\begin{aligned} \frac{\partial \eta_F}{\partial \tau} &= \frac{\partial^2 \eta_F}{\partial \xi^2} - \eta_F \eta_{ox} \\ \frac{\partial \eta_{ox}}{\partial \tau} &= \frac{\partial^2 \eta_{ox}}{\partial \xi^2} - A \eta_F \eta_{ox} \\ \frac{\partial \theta}{\partial \tau} &= \frac{\partial^2 \theta}{\partial \xi^2} + B \eta_F \eta_{ox} \end{aligned} \qquad [37]$$

with the same initial and boundary conditions as before, namely,

$\tau \leq 0$:

$$\left.\begin{aligned} \theta &= \theta_o \\ \eta_{ox} &= 1 \\ \eta_F &= 0 \end{aligned}\right\} \xi > 0$$

$\tau > 0$:

$$\left.\begin{aligned} \theta &= 0 \\ \frac{\partial \eta_{ox}}{\partial \xi} &= 0 \\ \text{CASE I:}\quad \eta_F &= 1 \\ \text{CASE II:}\quad -\frac{\partial \eta_F}{\partial \xi} &= 1 \end{aligned}\right\} \xi = 0 \qquad \left.\begin{aligned} \theta &\to \theta_o \\ \eta_{ox} &\to 1 \\ \eta_F &\to 0 \end{aligned}\right\} \xi \to \infty \qquad [38]$$

One will note that even in this limiting instance, the set of differential equations and boundary conditions remains nonlinear, and solvable only by numerical techniques. In addition, the same number of dimensionless groups are present as in the instance of finite activation energy. Consequently, the properties of both sets must be similar in a qualitative sense, and they may be discussed together in the similarity analysis which follows.

The constants which remain in these nondimensional equations have been abbreviated simply as (A) and (B) for purposes of convenience. Thus, for cases I and II, (A) and (B) were defined as

Case I:	Case II:
$A = \frac{n Y_F^\circ}{Y_{ox}^\infty}$	$A = \frac{n \dot{m}_F^\circ}{\sqrt{e^3 (Y_{ox}^\infty)^3 Z D}}$
$B = \frac{q R Y_F^\circ}{c_p E}$	$B = \frac{qR}{c_p E} \cdot \frac{\dot{m}_F^\circ}{\sqrt{e^3 Y_{ox}^\infty Z D}}$
$B_{E=0} = \frac{q Y_F^\circ}{c_p T_o}$	$B_{E=0} = \frac{q}{c_p T_o} \cdot \frac{\dot{m}_F^\circ}{\sqrt{e^3 Y_{ox}^\infty Z D}}$

[39]

In summary, one may note that regardless of the value of activation energy, the set of differential equations and boundary conditions for both cases I and II are characterized by the four groups (A), (B), (θ_o), and (θ_s). Of these groups, only (A) and (B) are contained in the differential equations themselves, while (θ_o) and (θ_s) are contained in the boundary conditions of the problem. Once reasonable values for these groups are selected, particular solutions of the following general form can be obtained:

$$\eta_F = \eta_F (\tau, \xi; A, B, \theta_o, \theta_s) \quad [40]$$

$$\eta_{ox} = \eta_{ox} (\tau, \xi; A, B, \theta_o, \theta_s) \quad [41]$$

$$\theta = \theta (\tau, \xi; A, B, \theta_o, \theta_s) \quad [42]$$

Interesting as these solutions are, the variation of the value of any one group or combination of groups, on the dimensionless ignition delay, τ^*, is desired. Once τ^* is known, of course, the real ignition delay, t_{ign}, can be determined.

Let us define, then, an ignition criterion such that

$$L^*(\theta) = F(\tau^*, \xi^*; A, B, \theta_o, \theta_s) \qquad [43]$$

Then from the numerical solution, the form of the inverse function $F^{-1} = f$ which defines the dimensionless ignition delay τ^* can be found. Let us write this inverse function, formally, as

$$\tau^* = f(A, B, \theta_o, \theta_s; \xi^*, L^*(\theta)) \qquad [44]$$

Given an ignition criterion, $L^*(\theta)$, the whole (τ, ξ) field can be examined, and the minimum value of τ^* determined for which $L^*(\theta)$ is satisfied at any ξ^* Specification of ξ^* is unnecessary if only the value of the dimensionless time at the achievement of $L^*(\theta)$ is desired; therefore, equation [44] can be written as

$$\tau^* = G(A, B, \theta_o, \theta_s; L^*(\theta)) \qquad [45]$$

It is important to note that the choice of ignition criterion could have a strong effect on the behavior of equation [45]. For convenience, an $L^*(\theta)$ of $\theta^* = \alpha\theta_o$ was selected, for a range of (α) values between one and two, and used to determine the behavior of the function

$$\tau^* = g(A, B, \theta_o, \theta_s; \alpha) \qquad [46]$$

from the numerical solution of the set of differential equations and boundary conditions for cases I and II.

By writing equation [46], it is by no means implied that the form of the solution will be the same for case I as it is for case II. In fact, one should observe that for common values of θ_o and θ_s in both cases, the function " g " should be different because of the differences in the boundary condition and possible differences in the numerical values of (A) and (B).

B. DISCUSSION OF VARIATIONS IN THE CHARACTERISTIC GROUPS

Before turning to a diagnosis of limiting solutions of our set of differential equations, and the subsequent limiting behavior of the real ignition delay t_{ign}, it is useful to discuss the characteristic groups which were formed.

Therefore, let us review the definitions of these groups and consider which groups must be varied to investigate certain physical effects. For both cases I and II, θ is a dimensionless temperature of the form

$$\theta = RT/E \quad \text{or} \quad \theta = \frac{T - T_{WALL}}{T_0} \qquad [47]$$

depending on whether the activation energy is finite or zero, respectively. The dimensionless group (A) characterizes the relative abundance of fuel and oxidizer, and is of the form

Case I	Case II
$A = \frac{n Y_F^\circ}{Y_{ox}^\infty}$	$A = \frac{n \dot{m}_F^\circ}{\sqrt{\rho^3 (Y_{ox}^\infty)^3 Z D}}$

[48]

which is independent of activation energy. On the other hand, (B) characterizes the maximum heat released in the system, and depends on the activation energy. The definitions of (B) for each case, were

Case I	Case II
$B = \frac{q R Y_F^\circ}{c_p E}$	$B = \frac{qR}{c_p E} \cdot \frac{\dot{m}_F^\circ}{\sqrt{\rho^3 Y_{ox}^\infty Z D}}$
$B_{E=0} = \frac{q Y_F^\circ}{c_p T_0}$	$B_{E=0} = \frac{q}{c_p T_0} \cdot \frac{\dot{m}_F^\circ}{\sqrt{\rho^3 Y_{ox}^\infty Z D}}$

Clearly, it is desirable to determine the effect of activation energy, alone, on the form of equation [46], and three values were selected. These were a high ($\sim$ 24 kcal), a medium ($\sim$ 8 kcal), and a zero activation energy. One may note

that B , θ_o , and θ_s values change by an equal factor with a change in activation energy. On the other hand, only θ_s and θ_o must be changed to investigate various temperature effects, except in the instance of zero activation energy.

Now, in both cases I and II, the (A) and (B) groups contain the physical quantities which represent the intial conditions of pressure and oxidizer concentration in the system. When considering these effects, the following three instances must be included for a complete investigation:

1. Constant pressure, variable (y_{ox}^{∞})
2. Constant (y_{ox}^{∞}) , variable pressure
3. Constant $(\epsilon y_{ox}^{\infty})$, variable pressure

Let us consider what variations of (A) and/or (B) correspond to each of the above instances for both cases I and II in turn. For the non, take (θ_o) and (θ_s) as being constant, as well as assuming some constant ignition criterion.

1. Constant Pressure, Variable (y_{ox}^{∞})

a. Case I: In this instance, observe that only (A) contains the term (y_{ox}^{∞}). Consequently the characteristic shape of the function

$$\tau^* = g(1/A) \qquad [50]$$

is desired over a range of (A) values, for various constant values of B , θ_o , θ_s , and ignition criterion $L^*(\theta)$. The selection of ($1/A$) rather than (A) was made because ($1/A$) is directly proportional to (y_{ox}^{∞}). In addition, one should note that value of ($1/A$) corresponding to $y_{ox}^{\infty} \equiv 1$ for some specified value of (y_F°) , is determined by the value of (n) chosen in the stoichiometric chemical reaction equation

$$[F] + n[O_x] \longrightarrow m\,[\text{PRODUCTS}] \qquad [51]$$

In fact, no matter what effect is investigated, the positioning of the $y_{ox}^{\infty} = 1$ point is determined by (n) for any other set of physical parameters.

b. Case II: For this case, one should recall that both (A) and (B) contain the factor (y_{ox}^{∞}); both will change, therefore, when (y_{ox}^{∞}) is changed, providing all other physical parameters are constant. On the other hand,

the ratio (B^3/A) is independent of (γ_{ox}^{∞}), but contains all the other physical parameters; therefore, the effect of (γ_{ox}^{∞}) variation may be determined from the function

$$\tau^* = g(B/A) \qquad [52]$$

providing (B^3/A) is constant. Similarly to case I, the value of (B/A) which corresponds to ($\gamma_{ox}^{\infty}=1$) depends upon the value of (n) in equation [44].

2. Constant (γ_{ox}^{∞}), Variable Pressure

a. Case I: If (γ_F°) is independent of pressure, then (A) and (B) are also independent of pressure, and pressure changes will not affect the value of any parameters in the numerical solution. On the other hand, if (γ_F°) is dependent upon pressure through some functional relationship, both (A) and (B) will be changed equally by pressure variation. Therefore, the pressure effect can be determined from the form of the function

$$\tau^* = g(1/A) \qquad [53]$$

for various values of (A) and (B).

b. Case II: In this case, the ratio (B/A) is independent of pressure, while the ratio (B^3/A) is inversely proportional to the square of pressure, or

$$(B^3/A) = (B^3/A)_o \left(P_o/P\right)^2 \qquad [54]$$

where the subscript " o " refers to some reference pressure level. Therefore, the function

$$\tau^* = g(B/A) \qquad [55]$$

must be found for several values of the ratio (B^3/A).

3. Constant ($\epsilon\gamma_{ox}^{\infty}$), Variable Pressure

a. Case I: Consider the simple cases of $\gamma_F^{\circ} \sim p^0$ and $\gamma_F^{\circ} \sim p^{-1}$. In the first instance, $A \sim p$ and $B \sim p^0$ while in the second instance, $A \sim p^0$ and $B \sim p^{-1}$. Therefore, the pressure effects may be deduced from the same

function [53], above, providing comparisons are made at appropriate values of (A) as just outlined.

b. Case II: From the definitions of (A) and (B) for case II, and assuming that ($\dot{m}_F^o$) is no function of pressure,

$$A \sim \sqrt{P}$$

$$B \sim \frac{1}{\sqrt{P}} \qquad [56]$$

Consequently, the ratios (B/A) and (B^3/A) both change with pressure such that

$$(B/A) \sim 1/P$$

$$(B^3/A) \sim 1/P^2 \qquad [57]$$

In this case, our investigation has the same need as in case 2b above. However, instead of comparing

$$\tau^* = g\,(B^3/A) \qquad [58]$$

at the same points (B/A), the values of this ratio at which comparison is made, depend on the pressure ratio (P/P_o).

This completes the discussion of the meaningful variations in the characteristic groups of the sets of dimensionless differential equations, and their initial and boundary conditions, for the two cases of the thermal ignition of a diffusion flame. However, it is possible to diagnose the limiting manner in which the ignition delay may be expected to vary with pressure and oxidizer supply from this set of dimensionless equations. Before turning to numerical integration, then, let us proceed with a discussion of these limiting cases.

C. DIAGNOSIS OF LIMITING CASES

1. Variation of the Ignition Delay for Large Initial Values of Oxidizer Concentration

If, for some large initial value of oxidizer concentration; $\eta_{ox} \cong 1$ everywhere, the oxygen diffusion equation can be removed from consideration. In this instance, it is immediately apparent that

Case I: $$\tau_I^* = g\left(\frac{qRY_F^o}{c_p E}, \theta_o, \theta_s\right) \qquad [59]$$

Case II: $$\tau_{II}^{*} = g\left(\frac{qR\dot{m}_F^{\circ}}{c_p E\sqrt{\rho^3 Y_{ox}^{\infty} ZD}}, \theta_o, \theta_s\right) \qquad [60]$$

Let us assume that θ_o and θ_s remain constant. Then, we immediately observe from equation [59] that for case I, (τ_I^*) is independent of the oxidizer concentration, therefore

$$t_{I_{IGN.}} \sim \frac{1}{Y_{ox}^{\infty}} \qquad [61]$$

For case II on the other hand, τ_{II}^* is functionally related to the initial oxidizer mole fraction (Y_{ox}^{∞}) via equation [60]. However, (τ_{II}^*) decreases for increasing values of " β "--at least for small values of $\dot{m}_F^{\circ}$ --or $\tau_{II}^* \sim (Y_{ox}^{\infty})^{\alpha/2}$ for some range of (Y_{ox}^{∞}) values, and consequently,

$$t_{II_{IGN.}} \sim \frac{1}{(Y_{ox}^{\infty})^{k}} \; ; \; k = 1 - \frac{\alpha}{2} \qquad [62]$$

Only numerical solution of the complete set of equations [28] and [29] will enable finding of a range of " A " values, in both cases, for which $\eta_{ox} \cong 1$ everywhere. This range probably is different in cases I and II, and dependent upon the ignition criterion, $L^*(\theta)$. When oxidizer consumption cannot be neglected, the dimensionless ignition delay, τ^*, becomes a function of A, B, θ_o , and θ_s , and it is not possible to predict the relationship between (τ^*) and (Y_{ox}^{∞}) a priori.

2. The Sensitivity of Ignition Delay to Changes in Pressure

Only a qualitative discussion of the effect of pressure changes on the ignition in either case I or II is possible, because (A) and (B) are sensitive to pressure. No dependence is assumed, however, between $\dot{m}_F^{\circ}$, θ_o , or θ_s and pressure, and all pressure effects are contained in the various dimensionless groups which contain a density term. A very important consequence of this is the difference in expected pressure effects when (ρY_{ox}^{∞}) is kept constant instead of (Y_{ox}^{∞}) being constant. This difference should exist in both cases I and II, in which either the fuel concentration or fuel mass flux is constant at the fuel surface, respectively. Of course, the observed pressure effect will be

dependent on the selection of the ignition criterion, but the effect may be discussed if some constant ignition criterion is assumed. Qualitative discussion of the pressure effect can now proceed for the instances in which either (Y_{Ox}^{∞}) or (ϵY_{Ox}^{∞}) is constant in both cases I and II.

a. Constant (Y_{Ox}^{∞}):

Case I: It can be expected that if (Y_F°) is inversely proportional to pressure as would be the case for a boiling liquid; then only the (B) group is dependent upon pressure if oxidizer diffusion and consumption can be neglected. Now, increased pressure will decrease (B) in this case; consequently

$$\tau_I^* \sim P^{\beta} \quad \text{AND} \quad t_{I_{IGN}} \sim P^{-1+\beta} \qquad [63]$$

The magnitude of (β), in the above relations, must be found from numerical solution of case I. When oxidizer diffusion and consumption processes must be included, then the above proportionality will vary because of the direct relationship between (A) and pressure.

On the other hand, if (Y_F°) is independent of pressure, then both (A) and (B) are independent of pressure and it must be expected that

$$\tau_I^* \sim P^{0} \quad \text{AND} \quad t_{I_{IGN}} \sim P^{-1} \qquad [64]$$

Note that if (Y_F°) is independent of pressure, then the above proportionalities are true for the whole range of (A) and (B) values; the pressure dependence of $t_{I_{IGN}}$ is completely contained in the definition of the dimensionless time.

Case II: Examining the limiting case where oxidizer diffusion and consumption can be neglected, it may be noted that (B) is inversely proportional to pressure. As discussed in the derivation of the proportionality given by [62], $\tau_{II}^* \sim B^{-\delta}$ therefore

$$\tau_{II}^* \sim P^{\delta} \quad \text{AND} \quad t_{II_{IGN.}} \sim P^{-1+\delta} \qquad [65]$$

Again, the magnitude of (δ) must be found from the numerical solution of this case.

When oxidizer diffusion and consumption are important, it is not possible to predict, a priori, any ignition delay dependence on pressure.

b. Constant ($e y_{ox}^{\infty}$), Variable Pressure

Case I: In this case, the magnitude of the real time (t) is independent of pressure. On the other hand, τ_I^* may be a function of pressure, as discussed above in the constant (y_{ox}^{∞}) case. If (y_F^o) is inversely proportional to pressure, (A) is a constant with respect to pressure changes, and $\tau_I^* \sim P^{\alpha}$ through the variation of (B) with pressure as discussed above. Therefore, the variation of t_{Iign} with pressure should be of the form

$$t_{I_{IGN}} \sim \tau_I^* \sim P^{\alpha} \qquad [66]$$

The above equation should not by any means be taken to imply that (α) is a constant over all ranges of pressure, and some variation of the value of (α) should exist. In addition, a certain amount of coupling between pressure and the fuel supply should exist because of the increased heat transfer rate to the condensed phase as the pressure is raised. Intuitively, one would expect that in any real case the adverse effect of pressure would be less than that given in the above equation [66].

Case II: In this case, one may recall that (A) is proportional to the square root of pressure and (B) is inversely proportional to the square root of pressure. Once again, if the oxidizer diffusion and consumption equation is neglected, then

$$\tau_{II}^* \sim \bar{B}^{\delta} \sim P^{\delta/2} \qquad [67]$$

as before. Since (t_{IIign}) is independent of pressure for constant values of ($e y_{ox}^{\infty}$), one may observe that

$$t_{II_{IGN.}} \sim P^{\delta/2} \qquad [68]$$

As before, this result is traceable to the initial assumption of boundary conditions for this problem, where we neglected any coupling between pressure, wall temperature, and fuel vapor supply. The numerical solution of case II can be expected, therefore, to result in an ignition delay versus pressure relationship similar to that of equation [68].

D. IGNITION LIMITS IN THE THERMAL IGNITION OF A DIFFUSION FLAME

In case I, where the fuel concentration at the surface of the condensed phase is assumed to be constant, it is easy to show the existence of a "go-no go" ignition limit. Consider that the consumption of oxidizer during the ignition process is negligible, and that ignition is defined to be the attainment of some temperature $(\theta^* > \theta_0)$ somehwere in the gas phase.

Clearly, the existence of an ignition limit is entirely dependent on the amount of fuel which is available in the system. Now, in case I, the (B) parameter is the only group containing a specification of the maximum amount of fuel available for ignition. Therefore, ignition should depend solely on the size of the (B) parameter, as is shown in what follows.

With the assumption that (η_{ox}) is constant, and equal to unity, the (η_F) equation and boundary conditions can be multiplied by B and added to their counterparts which describe the dimensionless temperature, θ . This operation results in the elimination of the nonlinear exponential term in the combined equation; it is allowable, in a mathematical sense, by the similarity of boundary conditions for the two equations. Thus, defining $\varphi = (\theta + B\eta_F)$ the following simple equation and boundary conditions remain:

$$\frac{\partial \varphi}{\partial \tau} = \frac{\partial^2 \varphi}{\partial \xi^2} \qquad [69]$$

$$\left.\begin{aligned} \tau \leq 0: &\quad \varphi = \theta_0 \ ; \ \text{ALL } \xi \\ \tau > 0: &\quad \varphi = \theta_s + B \ ; \ \xi = 0 \\ &\quad \varphi \to \theta_0 \ ; \ \xi \to \infty \end{aligned}\right\} \qquad [70]$$

The solution of the above is

$$\varphi = \theta + B\eta_F = (\theta_s + B - \theta_0)\,\mathrm{erfc}\left(\frac{\xi}{\sqrt{4\tau}}\right) + \theta_0 \qquad [71]$$

where $\mathrm{erfc}\, y = \frac{2}{\sqrt{\pi}} \int_y^\infty e^{-x^2} dx$, the complementary error function.

A plot of φ versus the argument $(\xi/\sqrt{4\tau})$ has the form sketched below.

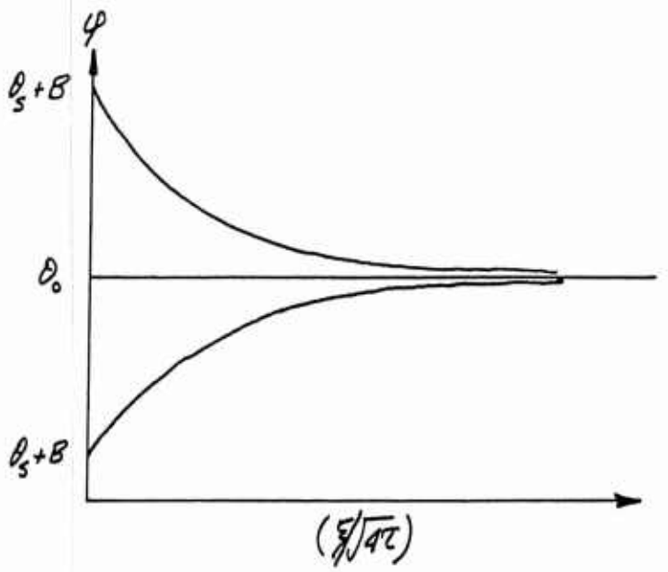

The energy equation can now be written in terms of the known function as

$$\frac{\partial\theta}{\partial\tau} = \frac{\partial^2\theta}{\partial\xi^2} + (\varphi-\theta)\,e^{-1/\theta} \qquad [72]$$

From the form of the function φ, it is evident that the above equation changes its form when $(\theta_s + B - \theta_o)$ is identically zero, and φ is identically equal to θ_o. Therefore, the maximum possible temperature that can be attained is θ_o, when $B \equiv (\theta_o - \theta_s)$, and absolutely no ignition can occur.

Now let us consider what the minimum value of (B) which allows some temperature $\theta^* > \theta_o$ to exist. From equation [71], the maximum attainable temperature in the system, $\overline{\theta}$, must identically equal to $\varphi_{max} - (B\eta_F)_{min}$. But φ_{max} occurs at $\xi = 0$ where $\theta = \theta_s$, and $(B\eta_F)_{min}$ occurs at $\eta_F = 0$; therefore

$$\overline{\theta} = \theta_s + B \qquad [73]$$

A reasonable assumption of a temperature, θ^*, denoting ignition, is that of $\theta^* \leq \bar{\theta}$ Therefore

$$\theta_o \leq \theta^* \leq (\theta_s + B) \qquad [74]$$

or

$$B \geq (\theta^* - \theta_s) \qquad [75]$$

and

$$B_{CRITICAL} \equiv (\theta^* - \theta_s) \qquad [76]$$

Clearly, if $B < B_{critical}$, ignition cannot occur, and (Bcritical) defines the ignition limit for case I, even when $\eta_{ox}^{\infty} \cong 1$ always.

However, similar conditions should exist if the oxidizer consumption is not negligible, but not excessive. If the oxidizer consumption is greatly excessive, of course, ignition may not occur. Numerical solution of the set of equations [32] and [34] agreed with these statements incidentally.

It should be noted that the activation energy disappears from the relation just given, and the critical value of B depends solely upon the heat of reaction, the specific heat, and--most importantly--the mass fraction of fuel present at the surface of the solid. One may hypothesize the existence of a $(B'critical) > (B\,critical)$ if oxidizer consumption is considered. For the case of zero activation energy, it is the initial temperature To which appears in B and θ_o, not activation energy. Otherwise, the analysis just completed is valid, as are the conclusions.

Finally, it must be emphasized that the maximum temperature which can be attained in the system is identically ($\theta_s + B$). Thus, the maximum temperature is dependent on the lowest temperature of the system and <u>not</u> on the system's average temperature as is commonly assumed.

In case II, where the mass flow rate of the fuel from the surface of the condensed phase is assumed to be constant, it is concluded that ignition will always occur because of the semi-infinite extent of the model. In this case it is also assumed that $\eta_{ox} \cong 1$ everywhere. Therefore, a combustible mixture must occur and react somewhere in the system--after some perhaps excessive time--and cause (θ^*) to be reached. The reason for this behavior is the constantly increasing fuel concentration in the system, and the assumption of a finite reaction rate at all temperatures. However, the

present model should be inadequate for this instance because convection should not be neglectible under these conditions.

E. SUMMARY OF RESULTS OF NON-NUMERICAL ANALYSIS

At this point, the general properties of the proposed model for the thermal ignition of a diffusion flame, have been discussed without recourse to numerical solution. This discussion included the qualitative prediction of the effects of pressure and oxidizer mole fraction on the ignition delay, for the cases of constant wall fuel concentration (I) and constant fuel mass flux (II). Analysis showed that a fundamental difference exists between the effects of these quantities on the ignition delay in homogeneous and heterogeneous systems. Specifically considering a one-dimensional, semi-infinite, unsteady system in both cases, this difference is the following:

> In the ignition of the homogeneous system, the effects of pressure and reactant concentration may be unique and independent of the ignition criterion specification. In contrast, the ignition delay of even the most simple heterogeneous system is functionally related to these parameters as well as to the ignition criterion. Therefore, the effect of these parameters on the ignition delay depends upon the specification of the ignition criterion.

The existence of ignition limits in the two cases I and II were considered, and it was shown that an ignition limit exists in case I, but not in case II, providing there is sufficient oxidizer present. Finally, it was found that in the presence of large system heat losses, the adiabatic combustion temperature of a heterogeneous system is based upon the cold fuel temperature alone, and not on the average temperature of the system as commonly assumed. A check on the preceding discussions and predictions requires numerical solution of cases I and II of the proposed model. In the next chapter, the results of the numerical solution, for both non-zero and zero activation energy, are discussed. For those who are interested, the technique used in the numerical integration of the differential equations is discussed in Appendix A-9. Major considerations of convergence and stability of the solutions are also included in this appendix, as is a generalized Fortran program for the numerical solution of each case of interest.

CHAPTER I-4

THERMAL IGNITION OF A DIFFUSION FLAME NEAR A COOL SURFACE; PRESENTATION AND DISCUSSION OF RESULTS OF THE NUMERICAL SOLUTION

The data obtained from the computer program for the solution of the equations describing the thermal ignition of a diffusion flame was in the form of numerical values for each of the dependent variables of the problem, η_F , η_{ox} , and θ . The value of these variables was recorded, at successive time intervals, over the range of values for the space coordinate, ξ , necessary for the solution to have reached the $\xi \to \infty$ boundary condition. From these records, the form of the solution could be learned for each of the cases investigated. An example of a typical solution is given in Figure (I-1) in which a normalized value of the dependent variables for each point in the space field is plotted at a number of successive dimensionless times. The particular solution shown in this figure is for case II, and a comparatively low initial concentration of oxidizer. It is interesting to note the development of the temperature "bulge" or ignition, and the limiting effect of oxygen consumption on the maximum temperature in the system.

From such solutions of cases I and II, the form of the inverse function given below,

$$\tau^* = g\left(A, B, \theta_o, \theta_s ; L^*(\theta)\right) \qquad [77]$$

was obtained for variations in the characteristic dimensionless groups which make up the arguments of the above function. This function was obtained for several values of the ignition criterion $L^*(\theta)$, where $L^*(\theta)$ was specified as $\theta^* = \alpha\theta_o$ for several values of (α), for each set of arguments A, B, θ_o , and θ_s . Once the form of this inverse function over a wide range of values of the dimensionless arguments was known, the characteristic relationships between the real ignition delay and the real physical parameters of oxidizer mole fraction or concentration, pressure, temperature, and activation energy were determined.

A complete discussion of the numerical integration technique is contained in Appendix A-9 , but it is worthwhile to mention the important problems of stability and convergence of the numerical solutions. Extensive effort was devoted ascertaining the necessary conditions for stability and

convergence of these solutions. The analysis of John (I.44) of the conditions necessary for stability and convergence of a quasi-linear, parabolic differential equation of the type formulated in the present work, provided a basis for this effort. Written in terms of the present problem, John's conditions for stable, convergent solutions of each of the present equations, take the form

$$\Delta\tau\left(K\bar{e}^{1/\theta}\right) \leq 1$$

AND

$$\lambda = \frac{\Delta\tau}{(\Delta\xi)^2} < 1/2$$

where (K) is largest of the coefficients of the nonlinear terms--i.e.--either 1.0, (A), or (B).

It should be emphasized that it was not completely certain, a priori, that the simultaneous integration of three, coupled partial differential equations of the type treated in (I.44) would be stable, even if each one were stable under the conditions found by John. Extensive computation showed that stable, convergent solutions for all cases could be obtained, in general, only if the above criteria remained of the form

$$\Delta\tau\left(K\bar{e}^{1/\theta}\right) \leq 10^{-3}$$

and

$$\lambda = \frac{\Delta\tau}{(\Delta\xi)^2} < 1/2$$

throughout the integration of the set of equations. Fortunately, a decrease in ($\Delta\tau$) was a sufficient correction; however, increased computational time was the penalty paid for this reduction in ($\Delta\tau$). In the present calculations, convergence was taken to be agreement in the calculated values η_{0x}, η_F, θ (or $U(I, 2, K)$, $I = 1, 3$) to four decimal places between the results for a certain ($\Delta\tau$) value and ($\Delta\tau$) value four times smaller. Admittedly, this convergence criterion was empirical; however, such an empirical choice is standard practice when completely analytical criteria, or closed form solutions, are unavailable.

A. SIMPLIFYING ASSUMPTIONS AND THEIR VALIDITY

From an analytical point of view, an important question is: "What simplifying assumptions are valid in the

mathematical formulation of the ignition process in simple heterogeneous systems?" A discussion of various possible simplifying assumptions follows, but it must be emphasized that the numerical solutions were absolutely necessary for determining the error--and/or limiting ranges of applicability--of these assumptions. Specifically, it was desirable to determine:

1) the validity of the McAlevy (I.42) extension of the Hicks' ignition criterion, wherein it was assumed that the ignition delay was characterized by an equality between chemical heat generation and heat loss by conduction, or

$$\frac{\partial \theta}{\partial \tau} \geq 0$$

2) under what conditions it is justifiable to assume that fuel consumption is unimportant during the ignition delay.

3) under what conditions it is justifiable to neglect the consumption of the oxidizer and assume a constant value of the oxidizer concentration during the total ignition delay.

Regarding McAlevy's extension of the Hicks' criterion, 1) above, the numerical solutions indicated that ($\partial\theta/\partial\tau$) became positive well before there was any temperature in the system that exceeded the system's initial temperature, in both cases I and II. In general, the elapsed time necessary to cause ($\partial\theta/\partial\tau$) to be positive was ten percent or less of the total ignition delay, based on a temperature. This result is in contrast to Hicks' (I.46) empirical finding which resulted from his numerical solution of the ignition of a solid phase mixture undergoing continuous external heating. It must be concluded that the occurrence of a positive rate of change of temperature with time is an invalid ignition criterion for heterogeneous systems; this is because the ignition occurs in a region normally subjected to a cooling process. In such a system, the chemical reaction must release sufficient heat to overcome a cooling process. On the other hand, the heat released by chemical reaction only supplements the external heating in Hicks' case; therefore, rapid temperature runaways are allowed because the temperature in the region of ignition is normally rising, even if an exothermic chemical reaction is not present.

The simplifying assumption, 2) above, that the consumption of fuel can be ignored up to the time at which $(\partial\theta/\partial\tau) \geq 0$ is made quite often. The numerical solutions indicated that at the time $(\partial\theta/\partial\tau)$ became positive, the local fuel concentration was on the increase.

It is interesting to estimate the minimum amount of fuel consumption which must occur before $(\partial\theta/\partial\tau)$ can become positive. This estimate can be made, a priori, only for case I.

Consider the function defined in equation [71] of the last chapter. Upon differentiation with respect to the dimensionless time τ, one obtains

$$\frac{\partial\varphi}{\partial\tau} = \frac{\partial\theta}{\partial\tau} + B\frac{\partial\eta_F}{\partial\tau} = (\theta_s + B - \theta_o)\frac{\xi e^{-\frac{\xi^2}{4\tau}}}{\sqrt{4\pi\tau^3}} \qquad [78]$$

Now, if there were no fuel consumption in case I, the dimensionless fuel concentration at any time would be given by

$$\eta_F = \operatorname{erfc}\left(\xi/\sqrt{4\tau}\right) \qquad [79]$$

therefore, when there is no fuel consumption by chemical reaction

$$\left(\frac{\partial\eta_F}{\partial\tau}\right)_{\text{NO CONSUMPTION}} = \left(\frac{\partial\eta_F}{\partial\tau}\right)_o = \frac{\xi e^{-\frac{\xi^2}{4\tau}}}{\sqrt{4\pi\tau^3}} \qquad [80]$$

On the other hand, when $(\partial\theta/\partial\tau) = 0$, then

$$\frac{\partial\varphi}{\partial\tau} = B\left(\frac{\partial\eta_F}{\partial\tau}\right) = (\theta_s + B - \theta_o)\frac{\xi e^{-\frac{\xi^2}{4\tau}}}{\sqrt{4\pi\tau^3}} \qquad [81]$$

or the rate of change of dimensionless fuel concentration with respect to the dimensionless time is

$$\left(\frac{\partial \eta_F}{\partial \tau}\right)_{CONSUMPTION} = \left(\frac{\partial \eta_F}{\partial \tau}\right)_c = \frac{(\theta_s+B-\theta_0)}{B} \frac{\xi\, e^{-\xi^2/4\tau}}{\sqrt{4\pi\tau^3}} \qquad [82]$$

The ratio of equations [80] and [82] allows estimation of the amount of fuel consumption which is occurring when ($\partial\theta/\partial\tau$) = 0 . This ratio is, identically,

$$\frac{\left(\frac{\partial \eta_F}{\partial \tau}\right)_c}{\left(\frac{\partial \eta_F}{\partial \tau}\right)_0} = \frac{\theta_s+B-\theta_0}{B} < 1 \qquad [83]$$

The conclusion to be reached is that when the system is far from the ignition limit, or B $>>(\theta_0 - \theta_s)$, then the assumption that no fuel is consumed--up to the point at which ($\partial\theta/\partial\tau$) becomes zero--is quite good, providing the system is one which can be approximately described by the present case I. From equation [82], it is clear that this assumption becomes progressively poorer as B approaches the minimum value of ($\theta_0 - \theta_s$), the absolute ignition limit. Incidentally, the numerical solutions for case I agreed very well with the above analysis. In addition, the numerical solutions showed that for case II, the assumption of negligible fuel consumption, up to the point of a change in sign of the derivative ($\partial\theta/\partial\tau$), is always invalid.

The above analytical development and the numerical results lead to an important conclusion with respect to ignition delay experiments in heterogeneous systems. If, in a particular experiment, the detection of the first appearance

of combustion products is used as the ignition criterion, serious errors can be made with regard to the real ignition delay under various environmental conditions.

The third simplifying assumption will be discussed in detail in a later section.

Now, let us turn to a presentation of the form and behavior of the inverse function for τ^*, equation [77]. During all the discussion which follows, the previous distinctions between the two cases of fuel supply will be kept; for reference, these cases are mentioned again.

Case I: Constant fuel concentration at the cool wall

Case II: Constant mass flux of fuel from the cool wall.

It should be remembered that in each case, the fuel supply is assumed to be independent of the surface temperature of the condensed phase, θ_s .

B. BEHAVIOR OF THE DIMENSIONLESS IGNITION DELAY

1. Changes in (A) and/or (B), and the Ignition Criterion

a. Case I: Plots of the dimensionless ignition delay versus ($1/A$) values are shown in Figures (I-2), (I-3), and (I-4) in the order of decreasing activation energy. The separate curves in each figure correspond to constant values of (α) for the ignition criterion $L^*(\theta)$ of $\theta^* = \alpha\theta_o$; all other parameters were held constant in each figure. These figures clearly demonstrate the importance of ignition criterion specification when one talks about the effect of some physical parameter on the ignition delay. Although the curves are similar in each figure, the magnitude of the ignition delay and its local rate of change at any (A) value and activation energy is determined by the ignition criterion.

As discussed in section A, one will note that for each activation energy, there exists a range of ($1/A$) values for which τ_I^* is virtually independent of ($1/A$). In this range, oxidizer consumption is quite unimportant in the delay of the overall ignition event. Thus, the ignition of some heterogeneous system under certain conditions can be quite similar to some homogeneous systems in that the dependence of the real ignition delay on oxidizer concentration may be the same.

One may recall that the (B) parameter should also affect the value of the dimensionless ignition delay τ_I^*. Figures (I-5), (I-6), and (I-7), ordered in the direction of decreasing activation energy, are plots of τ_I^* versus $(1/A)$ for different (B) values. Note that τ_I^* decreased with increases in (B), as was discussed in the preceding chapter. In addition, the range of $(1/A)$ values over which τ_I^* does not depend strongly on $(1/A)$ evidently increases as (B) increases, regardless of the activation energy.

Furthermore, the numerical calculations showed that unless $B \geq (\theta^* + \theta_s)$, an ignition corresponding to the attainment of a dimensionless temperature, θ^*, could not occur; thus the ignition limits for case I, which were indicated in the preceding chapter, were found. The numerical calculations showed that for (B) less than some (Bcritical), the fuel and oxidizer were just consumed as time increased. However, there was insufficient fuel to allow the generation of sufficient heat to raise any local temperature above the initial temperature of the gas external to the condensed phase.

b. Case II: As was previously discussed, this case requires a different type of plot since the (A) and (B) groups both contain the initial mole fraction of oxidizer in the system. One may recall that determination of the effect of oxidizer concentration requires knowledge of the relationship between τ_{II}^* and (B/A) for various constant values of (B^3/A). Figures (I-8), (I-9), and (I-10) contain curves of the dimensionless ignition delay τ_{II}^* versus (B/A) for a high, medium, and zero activation energy respectively. These figures clearly show the strong dependence of the form of these plots on the ignition criterion $L^*(\theta)$, which is $\theta^* = \alpha\theta_o$, as used in case I.

These numerical calculations for case II indicate the existence of practical ignition limits at each value of (B^3/A), even though fuel is supplied at a constant rate to this semi-infinite system, and the reaction rate is finite at all temperatures in the system. At small values of (B/A), a practical ignition limit occurs because a balance is created between the oxidizer consumption by chemical reaction and its supply by diffusion. Therefore, the temperature rise is limited by the oxidizer diffusion rate. At sufficiently large values of (B/A), it is apparent from the medium and zero activation energy numerical solutions, that the ignition delay becomes strongly influenced by the fuel supply. Figures (I-9) and (I-10) indicate this behavior by the sharp increases in the dimensionless ignition delay at larger values of (B/A).

c. General Discussion

Several important characteristics of thermal gas phase ignition in simple heterogeneous systems are pointed out by the dimensionless ignition delay curves, and deserve particular emphasis. Two of these characteristics are common to both cases I and II, and therefore are probably common to the thermal, gas phase ignition of all heterogeneous systems, since cases I and II represent the two limits of such systems with regard to fuel supply.

First, the variation of the dimensionless ignition delay--and, consequently, the real ignition delay--with respect to any of the dimensionless groups depends upon the selection of ignition criterion. Therefore, one must be careful in the interpretation of the experimental data from different ignition experiments on identical or similar fuels, because the ignition criteria may not be the same. Even in identical systems and experimental conditions, different data on ignition may be obtained if the ignition criteria are different.

Second, the sensitivity of the real ignition delay to initial oxidizer concentration can have very wide limits of behavior in cases I and II, depending upon the value of (1/A) and (B/A), respectively, which corresponds to an initial oxidizer mole fraction of unity. Logarithmic plots of the real ignition delay versus initial oxidizer concentration may exhibit almost any slope from zero to minus two or more.

A characteristic of case II, is that under high initial oxidizer mole fractions, the slope of the above-mentioned plot may be positive in some systems. It is questionable whether such positive slopes could exist in reality, because of the difficulty in matching the boundary conditions specified in case II. However, some experiments have indicated a slope of almost zero on such a plot.

On the other hand, the limiting behavior of case I at high initial oxidizer concentrations is quite different. As has been mentioned, this case degenerates to linear inverse dependence of the real ignition delay on the initial oxidizer concentration, at constant system pressure.

Thus, it is now possible to determine the validity of the simplifying assumption that oxidizer diffusion and consumption can be neglected. Apparently this assumption is valid for case I when the adiabatic combustion temperature based on oxidizer mole fraction, (B/A), is much greater than the ignition criterion temperature $\theta^{*} = \alpha\theta_0$. However, this simplifying assumption is never valid in case II, even at very high adiabatic combustion temperatures based on the oxidizer content in the external gas environment.

2. Equal Changes in B, θ_o , and θ_s

Equal changes in the three parameters B, θ_o , and θ_s correspond to a change in the assumed activation energy of the chemical reaction. As previously mentioned, three different values of activation energy were used in the investigation of cases I and II.

a) Case I: A decrease in activation energy decreased the extent of the region in which τ_I^* depends on the value of (1/A). In addition, the rate of change of τ_I^* with respect to changes in (1/A) also decreased in the strongly varying region of the curves as the activation energy was lowered. Finally, the general level of the τ_I^* versus (1/A) curves is dependent upon the value of the activation energy. These characteristics are graphically shown in Figure (I-11).

Now for case I, two definite limits of behavior are apparent in Figure (I-11). The one limit is the ignition limit at small values of (1/A) where the curves tend toward very large or infinite values of τ_I^* . The other limiting behavior is at large values of (1/A) where τ_I^* becomes essentially independent of the value of (1/A). These two limits are joined, asymptotically, by a transition curve. The extent of this joining region is a function of activation energy, which should become very small as the activation energy approaches very large values.

b) Case II: In case II, qualitatively the same behavior was found in that the extent of the slowly varying region, and the general level, of the τ_I^* versus (B/A) curves decreased with decreased activation energy. It is interesting to note that the range of (B/A) values for which the derivative [$d(\tau_I^*)/d(B/A)$] does not vary rapidly, decreased as the activation energy was lowered, see Figure (I-12). This characteristic behavior is a direct consequence of increased rates of chemical reaction as the activation energy was decreased. At large values of (B/A) it was the fuel which was rapidly consumed; conversely, the oxidizer was consumed rapidly as B/A decreased.

3. Changes in θ_o

It was interesting to determine the effect of changes in the initial gas temperature, θ_o , on the dimensionless ignition delay, with otherwise constant conditions. Figure (I-13) shows this effect, for three different levels of initial gas temperature. In this figure, a constant temperature ignition criterion, $\mathcal{L}^*(\theta)$, was selected, such that $\theta^* = 0.4$.

By comparing Figures (I-11) and (I-13), it is evident that changing the initial gas temperature affects the

shape of the τ_I^* versus (1/A) curves in a manner which is qualitatively similar to changing the activation energy. As is apparent, the general changes in the magnitude of are not as great when just (θ_o) is changed and (B) is kept constant. The functional relationship between τ_I^* and (B) or (θ_o) appears to be quite similar, however.

Because of the computer time involved in these computations as a whole, the effect of gas temperature on ignition was investigated only for case I, at the medium activation energy. The surface temperature of the condensed phase, (θ_s), was not varied for the same reason.

This completes the description of the results of the numerical integration for both cases I and II of the thermal ignition of a diffusion flame in terms of dimensionless parameters. Let us now turn to a discussion of these results describing the manner in which changes in oxidizer mole fraction, pressure, and temperature affect the real ignition delay. The rational choice of absolute values for such quantities as e, Z, D, etc. is, however, very difficult and also causes a loss of generality of calculations based on the assumed values. In the following section, ratios of real quantities will be used whenever possible. Use of this technique reduces the number of physical parameters which had to have exact numerical specification, maintains the generality of the dimensionless results as far as possible, and still demonstrates the real time, characteristic features of the thermal ignition of a diffusion flame.

C. BEHAVIOR OF THE REAL IGNITION DELAY IN THE THERMAL IGNITION OF A DIFFUSION FLAME

1. Variable (y_{ox}^{∞}), Constant Pressure

Variations in the oxidizer mole fraction or concentration are equivalent when the total pressure of the system is kept constant. It is completely adequate, therefore, to discuss the effect of oxidizer mole fraction variations on the real ignition delay of the system. In this discussion, the mole fraction of oxidizer will be the only independent variable which is varied once a specific value of the stoichiometric coefficient, (ν), has been chosen. Several (ν) values are used, however, to demonstrate the variation in the functional relationship that can exist between the real ignition delay and the initial oxidizer mole fraction, (y_{ox}^{∞}). As was discussed in the preceding section, the value of the stoichiometric coefficient (ν) determines the initial value of (1/A) and (B/A) when (y_{ox}^{∞}) equals one, in

cases I and II respectively, and is defined by the assumed chemical reaction equation

$$[F] + n\,[O_x] \longrightarrow m\,[P] \qquad [84]$$

It should be recalled that increased (n) values cause the initial values of (1/A) and (B/A) to become smaller, and closer to the region in which the dimensionless ignition varies strongly with changes in these parameters.

For case I, a plot (t/t_o) versus (Y_{ox}^{∞}) is shown in Figure (I-14), for four different values of the stoichiometry coefficient (n). The reference ignition delay, (t_o), is the real ignition delay when the initial oxidizer mole fraction is unity. This plot was made for medium activation energy case where (E/R) equals 4000° K. The dashed line having a slope of minus one corresponds to the limiting behavior of case I, when there is a linear inverse relationship between ignition delay and oxidizer mole fraction. The strong influence of (n) on the shape of the curves, and the tendency of increased (n) to increase the slope of these curves should be noted.

Similar plots for case II, for the high and medium activation energy used in the present calculations, are shown in Figures (I-15), (I-16), and (I-17). Once again, the influence of (n) should be noted. In the first two figures the activation energy is such that (E/R) equals 12000° K., but the ratio ($\dot{m}_F^{\circ}/\sqrt{\rho_3 Z D}$) in Figure (I-16) is increased by a factor of one hundred over that used in Figure (I-15). Thus, the value of ($9R/c_p E$) remained unchanged in Figures (I-15) and (I-16) while (B^3/A) was 10^{-6} and 10^{-2}, respectively. Figure (I-17) is drawn for an (E/R) value of 4000° K., except for the curve labeled " $n = 6$." In this case, the activation energy and heat of reaction were changed, as noted in the figure, while B, θ_o , and θ_s were kept constant. On the other hand, the value of the value of (B/A) corresponding to $(Y_{ox}^{\infty}) = 1$ was reduced by a factor of $2 \cdot \sqrt{2}$. These changes caused a marked increase in the slope of the (t/t_o) versus (Y_{ox}^{∞}) curve. Mathematically, this behavior is caused by the increased sensitivity of the dimensionless ignition delay to the value of (B/A) as this ratio is reduced. Physical interpretation is difficult because the changes in (E/R) and (9) necessitated changes in the parameter ($\dot{m}_F^{\circ}/\sqrt{\rho_s Z D}$) and the temperatures in the system, in order to keep B, θ_o , and θ_s constant. The primary value in showing the result of this change, is in demonstrating the ease with which strong variations in

ignition characteristics can occur with rather small variations in the physical properties of a heterogeneous system.

The curves of (t/t_o) versus (y_{ox}^{∞}) which have just been discussed, illustrate some important properties of thermal, gas phase ignition of heterogeneous systems at constant pressure.

A constant ignition criterion was used in each one of the above-mentioned figures, as is noted on each figure. It must be emphatically pointed out that any of the figures could be changed radically if a different ignition criterion were used. Therefore, it cannot be mentioned to strongly that in any ignition experiment, the choice of ignition criterion can determine the form of the experimental correlations to a large extent. For example, it was shown in section A of this chapter that for a heterogeneous system, the detection of fuel consumption alone can give completely erroneous information about the ignition event. In fact, there can be a large amount of fuel consumption and still no ignition in the sense of attaining temperature which is greater than the initial temperature of the system, or in the sense of a fast temperature rise.

In particular, one should note the nonconstant nature of the ignition delay's dependence on the initial oxidizer mole fraction, even for a constant ignition criterion. Plots of the logarithm of the ignition delay versus the logarithm of the initial oxidizer mole fraction, for a heterogeneous system, have no special slope which definitely characterizes a thermal, gas phase ignition. In fact, it is evident that such plots can have slopes ranging from minus two or more, to some zero or possibly positive slope, even if the ignition is always of a thermal, gas phase nature. It is perhaps most interesting to note that the slope of these plots can easily exceed the order of the reaction with respect to the gaseous oxidizer reactant concentration. Therefore, such plots of experimental data are alone of little use for the determination of the characteristic chemistry of the ignition reaction of heterogeneous systems, even if it is known that the site of ignition is in the gas phase.

As has been mentioned before, the form of the (t/t_o) versus (y_{ox}^{∞}) or (ρy_{ox}^{∞}) curves at constant pressure is very sensitive the physical properties, of the heterogeneous system, such as activation energy, heat of reaction, and stoichiometric coefficient. This is especially apparent in the " n = 6" and " n = 7" curves of Figure (I-17), and in the effect of (n) in Figures (I-14) through (I-17).

In the next section, the pressure sensitivity of the present model of gas phase ignition in heterogeneous systems, is discussed with respect to two restrictions on the initial oxidizer supply.

2. Variable Pressure

If the assumption is made that the surface temperature of the condensed phase is independent of the pressure level, then it is possible to discuss the effect of pressure changes on the ignition in a semi-quantitative fashion. This discussion requires the assumption of some relationship between pressure and the fuel supply in cases I and II. In addition, a constant ignition criterion must be assumed, and must be independent of the pressure level.

Finally, two restrictions on the oxidizer supply must be considered during the following discussion. These restrictions are that the oxidizer mole fraction is constant during pressure level changes, or that the oxidizer concentration is constant. With these two restrictions, and the assumption of constant surface temperature of the condensed phase at all pressures, the pressure sensitivity of cases I and II will be discussed.

a. Case I: In the completely uncoupled case, the partial pressure of the fuel must be constant; therefore, the fuel mole fraction at the surface of the condensed phase, (y_F°), is linearly related to the inverse of the pressure level. For constant (y_{ox}^∞), there is an adverse pressure effect on the ignition delay, see Figure (I-18), if the initial value of (1/A) is sufficiently large for τ_I^* to be almost independent of (1/A). If the initial value of (1/A) is sufficiently small such that is strongly dependent upon (1/A), this adverse pressure effect may be reduced or become a favorable pressure effect, because (1/A) is directly proportional to pressure in this instance. Favorable pressure effects on the ignition delay at constant (y_{ox}^∞) are also obtained if the coupling between pressure and the fuel supply is of such form that (y_F°) is independent of pressure. This is also shown in Figure (I-18).

On the other, in both the completely uncoupled case where $(y_F^\circ) \sim (1/P)$, or the case where the coupling is such that $(y_F^\circ) \sim (P^\circ)$, the pressure effect on the ignition

delay of case I is always adverse if the oxidizer concentration (ρY_{ox}^{∞}) is constant. This is shown in Figures (I-19), (I-20), and (I-21).

The degree of adversity of these pressure effects could be reduced if the coupling between pressure surface temperature, and (Y_F^o) were taken into account, but this cannot be determined from the present solution.

b. Case II: The case II analogue of the completely uncoupled instance of case I is the situation in which the mass flow rate of fuel coming from the surface of the condensed phase is independent of the pressure level. Now case II can be considered as being similar to the steady pyrolysis of a polymeric fuel. If the pressure is raised, then more heat is transferred to the condensed phase and in reality, the surface temperature, and mass pyrolysis rate would both increase. Assuming the surface temperature to remain constant, an indication of the pressure sensitivity of the ignition delay can be gained by the assumption that the mass flux is proportional to pressure raised to some positive power (γ). There is a slight justification to this procedure because a short numerical investigation of case II showed that the ignition delay was only slightly affected by small changes in the surface temperature.

Figure (I-22) indicates that the effect of pressure increases is always favorable in case II, when the oxidizer mole fraction is kept constant. This is true when the value of (E/R) is large, but the behavior is not clear when (E/R) has a low value. On the other hand, Figure (I-23) indicates an adverse pressure effect on the ignition delay when the partial pressure of oxidizer is maintained at a constant value. It is apparent from both figures that pressure sensitivity of the ignition delay becomes more favorable as (γ)--or the extent of coupling between pressure and mass flux--is increased.

The description of the pressure sensitivity of the ignition delay in cases I and II is now complete. It must be pointed out that the present numerical calculations do not demonstrate the pressure sensitivity of thermal, gas phase ignition in heterogeneous systems because of the assumed boundary conditions. This is because the fuel supply and the surface temperature of the condensed phase were assumed to be uncoupled to the pressure, and independently specifiable; matching these boundary conditions in any real or experimental situation is extremely difficult.

It is interesting to note, though, that a thermal, gas phase ignition might exhibit the adverse pressure sensitivity indicated by the present numerical solutions. Normally, such effects are attributed to the occurrence of chain reactions in the ignition process. Another noteworthy item is that the pressure and oxygen effects interact and cannot be separated from each other completely.

Let us now turn to a discussion of the effect of initial gas temperature on the ignition delay in heterogeneous systems.

3. The Effect of Variations in Initial Gas Temperature

The influence which variation of the initial gas temperature had on the real ignition delay in case I is shown in Figures (I-24) and (I-25), in which the ratio of real ignition delays are plotted versus the reciprocal of the initial gas temperature. These two figures are for the high and medium activation energy, respectively, which have been used in the previous discussions. As might be expected, decreased initial gas temperature resulted in increased ignition delays for all other parameters held constant.

From the point of view of determining global activation energies for ignition of heterogeneous systems, Figures (I-24) and (I-25) indicate an important property of these systems. One may note that the apparent activation energy, found by plotting $(\ln t/t_o)$ versus (1/T) and calculating the activation energy according to the commonly accepted relationship

$$E = -R \frac{d \ln (t_{IGN})}{d(1/T)} \qquad [85]$$

is lower than the actual activation energy used in the assumed reaction rate. Evidently the fuel diffusional processes can result in a falsification of the activation energy of the chemical reaction. A similar diffusional falsification of activation energy has been noted by Rosner (I.49) in connection with a heterogeneous catalytic reaction in a steady flow system. As was discussed in Chapter (I-2), the use of equation [85] for homogeneous mixture ignition experiments can give correct global activation energy values if the induction delay is long. Even in homogeneous systems, however, a priori use of equation [85] will not give correct activation energy values if the induction period is short. It must be emphasized that a falsification of activation energy has been shown to occur in the ignition of even the simplest possible heterogeneous system.

Further comments concerning the applicability of equation [85] for determining the activation energy of ignition in heterogeneous systems must be made. Assume that equation [85] has been used to correlate some experimental data on the ignition

of a particular heterogeneous system. Now, it is commonly assumed that if changes in the quantity of oxidizer in the gas phase produce changes in the slope of the $\ln(t_{ign})$ versus $1/T$ curve, the reaction mechanism or activation energy changed. This interpretation may be incorrect for heterogeneous systems, as is evidenced by the broken line curves in Figure (I-25). It is apparent that diffusional processes can cause a deviation from the straight line relationship predicted by equation [85]. Therefore, some possibly serious error in global activation energy determination and in interpretation of ignition reaction mechanism may result from the application equation [85] to the ignition of heterogeneous systems.

The discussion of the results of the numerical solution of the partial differential equations describing the ignition of a basic, heterogeneous system is now complete. Let us now turn to a summary of the results obtained during the course of the present investigation of thermal ignition processes.

CHAPTER I-5

SUMMARY OF RESULTS

Previous theoretical treatments of thermal ignition in purely homogeneous systems of reactant mixtures have been described, and their limitations were discussed. The theory of thermal ignition in homogeneous systems was then extended to include the situation where one reactant is consumed during the ignition process. Similarity analysis was used to obtain the basic properties of this system; this analysis showed that the implications of thermal ignition in homogeneous systems have been widely misinterpreted. In particular, it was shown that the ignition criterion can have a significant effect on the theoretical and experimental results when the total induction period of the explosion is short. Furthermore, the ignition delay of homogeneous, bicomponent, gaseous systems is not necessarily related in a linear, inverse manner to the concentration of both of the reactants. This result was discussed with respect to some of the experimental results which have been obtained from the ignition of homogeneous mixtures.

It was pointed out that fundamental differences exist between the ignition of homogeneous and heterogeneous systems. A model for the thermal, gas phase ignition of a simple heterogeneous was presented. This model considered the diffusion of fuel vapors from a cool, constant temperature condensed phase into a hot, stagnant gas containing an oxidizer, and the subsequent thermal, gas phase ignition of the resulting mixture. The properties of this model of the thermal ignition of a diffusion flame near a cool surface were investigated by both similarity and numerical analysis.

Several important properties of thermal, gas phase ignition in heterogeneous systems were found, and it was shown that even in this simplest of models, the ignition of heterogeneous systems fundamentally differs from the ignition of homogeneous systems. The important properties of thermal, gas phase ignition of heterogeneous systems can be summarized, briefly, as follows:

1. Even in the most simplified instance of heterogeneous, thermal ignition in the gas phase, the functional relation between the ignition delay and the physical parameters of the system depends upon the definition of the ignition criterion. This dependence has not been recognized heretofore, and constitutes a basic difference between simple cases of heterogeneous and homogeneous ignitions.

2. In two specific heterogeneous systems, differing only in the boundary condition of the fuel supplied from the condensed phase, the ignition delay is not a simple, constant power function of the oxidizer mole fraction (or partial pressure) in the hot, external environment. The theoretical relation between ignition delay and oxidizer mole fraction exhibits a strongly variable slope on a log-log plot. This slope can have a value of zero to minus two or more. The form of this relation strongly depends on the specification of the ignition criterion and the activation energy.

3. In one simple case, ignition limits were theoretically predicted. In addition, it was found that the maximum temperature that can be achieved in the system depends on the lowest temperature in the system, and not on the system's average temperature as commonly assumed.

4. The simplifying assumption that the ignition delay is completely characterized by the change in the time derivative of the gas phase temperature from negative to positive was shown to be invalid. It was interesting to note that over quite wide ranges of parameter values, the numerical results indicate that this gas phase ignition process lacks one essential characteristic of the classical ignition process--a sudden sharp temperature rise. In some ranges the classical sharp temperature rise does indeed appear, but it must be emphasized that the ignition criterion of $(\partial\theta/\partial\tau = \partial T/\partial t)$ equal zero is an incorrect characterization of ignition even in this case. It was found, furthermore, that the characterization of the ignition delay by the start of fuel consumption by chemical reaction will lead to serious errors in determining the ignition properties of a heterogeneous system.

The simplifying assumption that oxidizer consumption by chemical reaction can be neglected was shown to be valid only under a rather limited range of conditions.

5. It was shown that thermal, gas phase ignition in heterogeneous systems may be affected adversely by increases in the system's total pressure.

6. A falsification of the actual activation energy of the chemical reaction was shown to exist, because of the necessary diffusional processes in heterogeneous ignition. The apparent activation energy obtained from a semi-logarithmic plot of ignition delay versus the inverse of the environmental temperature, was shown to be lower than the actual activation energy. In addition, such plots are not necessarily straight lines even though chemical reaction and the activation energy remain unchanged.

In the future, additional investigation of the properties of gas phase ignition in heterogeneous systems should be undertaken. A desirable extension of the present work would be the inclusion of the coupling that must exist between the surface temperature of the condensed phase and the heat transfer rate into the solid.

A second interesting case of the gas phase ignition of a heterogeneous system that could be treated is the substitution of a simple, two step chemical reaction for the second order, thermal reaction assumed in the present work. This would allow an estimation of the importance of chemical relaxation times on ignition processes.

CHAPTER II-1

REVIEW OF RECENT RESEARCH ON THE MECHANISM OF SOLID PROPELLANT IGNITION

A. INTRODUCTION

An understanding of the details of the physical and chemical processes by which a solid propellant rocket motor is brought to a state of steady combustion is obviously of considerable importance to the designer of propellant ignition systems. By such understanding he may, for example, be able to design a system which avoids excessive ignition pressures, minimizes the weight of an igniter for a given rocket, eliminates excessive ignition delays, causes the ignition transient to follow a given program, or accomplishes other desirable objectives.

A fundamental part of the development of steady combustion is the ignition of some portion of the propellant surface. In a practical sense, this ignition requires the supply of a heating impulse to the propellant by some type of igniter. Depending upon the igniter type, the propellant is heated by convection, radiation and conduction from hot particles, liberation of heat of condensation of metallic vapors, reaction of hypergolic materials, or combinations of these and other processes.

Though the igniter may influence later stages of the development of steady combustion, its most basic function is to cause the appearance of a solid propellant flame. A part of the designers task, then, is to control the development of this flame. In order to accomplish this control it is necessary to have knowledge of the mechanism by which this flame first appears. Therefore, this review will be confined to considering the mechanism which controls the first appearance of a solid propellant flame.

Studies of this controlling process have occupied a number of investigators in recent years. A number of experimental techniques varying in form and concept have been used to study the ignition of composite and nitrate ester propellants. Both slow and fast ignitions have been studied, and ignition delays have ranged from 20 seconds down to less than a millisecond.

In the experiments which have been conducted, the propellants have been heated by hot wires, test furnaces of various types, flowing gas streams at elevated temperatures,

shock tubes and shock tunnels, highly reactive oxidizing gases, arc-image furnaces, etc. This review will contain a description of the various theories which have been used to account for the phenomenon of propellant ignition, a discussion of the experimental methods which have been applied to this study, and an evaluation of the reported results.

B. THEORIES OF PROPELLANT IGNITION

1. Discussion of Ignition Criteria

A solid rocket propellant is a solid substance which is capable of burning at a constant rate varying from approximately 0.1 to 5 cm/sec at a fixed pressure. In the steady-state burning of such materials, it is commonly postulated that the components of the solid gasify at the surface and then form a thin, intense gaseous flame in the vicinity of the surface. This extremely simplified picture of the combustion of a solid propellant, of course, ignores complications due to fizz and flame zone structure and it ignores the possible participation of surface and subsurface reactions in the overall combustion process.

The ignition of such a solid propellant is the process whereby the quiescent solid achieves a state of steady combustion. Experimentally, of course, it is difficult or impossible to define precisely when a propellant may be said to be ignited. However, in experimental studies of the ignition process, two criteria to define the onset of ignition are in general use. The first of these criteria is the detection of the first luminous flame or the first light output from the igniting propellant. The second criterion of ignition is based on the initiation of the pressure rise in a combustion chamber. The effectiveness of the light detection experiment depends, of course, on the sensitivity of the detecting system, whereas the pressure record depends on the response time of the chamber as well. It should be pointed out that the two measurements may detect different states of the ignition event.

When the ignition process being studied is a rapid one, the difference between the results obtained from the two ignition criteria may be quite important. However, when the ignition being studied is a slow one, this distinction is probably unimportant. At the same time, if the ignition of a solid propellant is marginal or incomplete, the difference between the times obtained by the two ignition criteria will be quite significant. (See, for example, the remarks under section C-5 below.) The experimental criterion for ignition, then, can be important in interpreting the data in terms of some model for the propellant ignition mechanism.

Three basic models for the physico-chemical processes which control solid propellant ignition have been proposed. These models consider chemical reactions: a) in the solid phase, b) in the gas phase adjacent to the solid surface, and c) at the solid-gas interface. These three models will be discussed in the following sections.

2. Solid Phase Ignition

In steady state burning of a solid propellant a significant part of the reaction always occurs in the gas phase. The assumption that the ignition process is controlled in the solid phase only implies that the ignition is triggered by an exothermic solid phase reaction and that the time needed to establish a gas phase flame is very small as compared to the total ignition time. It is reasonable, under this assumption, to neglect the influence of the gas phase reactions on the ignition process. At present, it is not known whether exothermic solid phase reactions can occur in all practical propellants. It is generally assumed that such reactions contribute to the steady state burning process of nitrate ester propellants. However, in ammonium perchlorate propellants, the situation is much less clear and most investigators claim that endothermic sublimation precedes any exothermic decomposition reaction.

The most complete mathematical treatment of ignitions caused by exothermic solid phase reactions, specifically applied to solid propellants, has been reported by Hicks (18). His treatment is similar to that used by others (1,2,3,4) in studies of the thermal initiation of explosion. Hicks considered the case of a solid decomposition of zero order (with respect to both external pressure and reactant concentration) and a convective heat flux at the surface. It was assumed that the temperature dependence of the reaction rate could be described by an Arrhenius function. The partial differential equation describing the flow of heat for this case is

$$\frac{\partial T}{\partial t} = \alpha_p \frac{\partial^2 T}{\partial x^2} + \frac{q_r Z e^{-E/RT}}{\rho c_p} \qquad [1]$$

The boundary conditions stated by Hicks were:

$$T = T_0 \quad x \longrightarrow \infty \qquad \text{(in the solid)}$$

and

$$-\lambda_p \frac{\partial T}{\partial x} = h(T_g - T_s)\,; \; x = 0 \qquad \text{(at the surface).}$$

Hicks solved this equation numerically, and found from this solution an easily calculated, empirical method of

estimating the propellant ignition delay. In this method, the solid was considered nonreactive until purely conductive heat transfer brought the propellant surface to a certain temperature at which temperature ignition occurred. In other words, the heat evolution due to exothermic decomposition is neglected up to the time at which its effect on the energy transport is comparable to that of heat transfer. A parameter α^L was defined by equation [2] and it was found by comparison with the numerical solution that ignition occurred when a T_{si}^L was reached such that α^L had a value of 0.833.

$$\alpha^L = \frac{q_R Z e^{-E/RT_{si}^L}}{q_R Z e^{E/RT_{si}^L} + \left(\rho c \frac{\partial T}{\partial t}\right)_i^L} \qquad [2]$$

The surface temperature was calculated from equation [1] neglecting the non-linear term $q_R Z e^{E/RT}$. This empirical criterion gave results which were in good agreement with the numerical solutions of equation [1] providing the calculated ignition delay was much less than that of an adiabatic system at the same temperature. For any T_{si}^L, equation [2] may be rewritten, (10), to obtain a relation between the applied heat flux and the ignition delay.

$$\frac{d \ln t_{ign}^{1/2}}{d \ln \dot{q}} = \frac{\frac{E}{R}(T_{si}^L - T_o) - (T_{si}^L)^2}{\frac{E}{R}(T_{si} - T_o) + (T_{si}^L)^2} \qquad [3]$$

Equation [3] implies that a plot of log $t_{ign}^{1/2}$ against log $(\dot{q})$ should be linear with a negative slope having an absolute value less than one.

Several properties of this empirical method must be emphasized. Hicks showed that the influence of various physical parameters on t_{ign} depends on the mathematical choice of ignition criterion. Also, it should be pointed out that the ignition criterion specified by equation [2] does not correspond directly with any ignition event commonly measured. Finally, the method of plotting expressed by equation [3] must be limited to cases in which the time delay between the start of appreciable reaction and fast burning is very small compared to the time, t_{ign}, needed to raise the surface temperature to (T_{si}^L).

A common feature of many high activation energy ignition processes is that the exact definition of the ignition event is of minor importance when the heating rate is low.

Exact definition and measurement of the ignition event does become important when high heating rates or high initial temperatures prevail and ignition times are relatively short.

Hicks' work is a valuable contribution to our understanding of the ignition process, for it provides the first accurate numerical solution of the pertinent, non-linear differential equation. His results have been widely misinterpreted, however.

The relation between ignition time and heat flux given by equations [2] and [3] were derived for an ignition controlled by solid phase reactions, but the experimental demonstration of the linear relation predicted by equation [3] neither proves nor disproves the solid phase mechanism. Indeed, it can be shown that this relation will hold for many high activation energy ignition processes, particularly if they are slow. Thus, the same behavior might be expected for all the previously postulated ignition models. A proper experimental discrimination among the models can be approached only through the variation of parameters other than the heat flux.

3. Gas Phase Ignition

Ambient pressure and oxygen concentration have been found to be important parameters influencing solid propellant ignition in experimental studies to be described below. The existence of such effects has led some investigators to postulate dominant participation of gas phase processes in the ignition mechanism. The discussion of gas phase ignition will include only ignitions in which the major exothermic processes leading to temperature rise occur in the gas phase and are governed by gas phase kinetics.

In the description of this type of model it is postulated that the heating of a solid propellant by an external heat flux causes evaporation or chemical decomposition at the surface. Such gas evolutions have indeed been observed at the temperatures estimated to prevail during ignition processes. The evolved gases then enter into a rapid exothermic reaction in the small region adjacent to the surface. Heat produced by this rapid reaction then increases the temperature of the surface by heat feedback until a steady state of combustion is reached. This type of reaction would be very rapid indeed at the high gas temperatures that exist during the ignition of current solid rocket motors. It is evident that the presence of oxidizing gases and increases in ambient pressure would tend to accelerate these reactions.

An interesting and practical case of the gas phase ignition of a solid propellant would be an ignition

caused by propellant decomposition and subsequent gas phase reaction of oxidizer and fuel product gases. Such an ignition is quite possible conceptually, but has never been treated. A quantitative treatment of such a model would be quite interesting.

Attempts have been made to treat another gas phase ignition model in which the fuel binder of a composite propellant decomposes and the products' vapors ignite through a gas phase oxidation with externally supplied oxygen. This type of ignition could be the controlling process in the ignition of a composite propellant having an easily vaporizable binder exposed to a hot oxidizing gas.

Of course, such an ignition process could take place under the influence of conductive, radiative or convective heat sources in either stagnant or moving gases. In a simple formulation of such a model, the propellant is brought into sudden contact with a hot stagnant gas. Under assumed conditions of conduction heat transfer and constant surface temperature, the following set of diffusion equations may be written for events occurring in the gas phase and at its boundary.

Mass Diffusion:

$$\frac{\partial C_F}{\partial t} = D\frac{\partial^2 C_F}{\partial X^2} - C_F C_{Ox} Z e^{-E/RT} \qquad [4]$$

$$\frac{\partial C_{Ox}}{\partial t} = D\frac{\partial^2 C_{Ox}}{\partial X^2} - n C_F C_{Ox} Z e^{-E/RT} \qquad [5]$$

Energy Diffusion:

$$\frac{\partial T}{\partial t} = \alpha\frac{\partial^2 T}{\partial X^2} + \frac{q}{\rho C_p} C_F C_{Ox} Z e^{-E/RT} \qquad [6]$$

with boundary conditions:

$t \le 0$:

$$\left.\begin{aligned} C_F &= 0 \\ C_{Ox} &= C_{Ox}^{\infty} \\ T &= T_o \end{aligned}\right\} \text{ALL } X$$

$t > 0$:

$$\left.\begin{aligned} f(C_F) &= \text{CONSTANT} \\ -D\frac{\partial C_{Ox}}{\partial X} &= 0 \\ T &= T_s \end{aligned}\right\} X = 0$$

$$\left.\begin{aligned} C_F &\to 0 \\ C_{Ox} &\to C_{Ox}^{\infty} \\ T &\to T_o \end{aligned}\right\} X \to \infty$$

The following assumptions are, of course, inherent in this model:

1) all transport properties are constant,
2) convective mass transport can be neglected everywhere,
3) the gas density is independent of temperature,
4) the overall chemical reaction is of second order and of a thermal kinetic nature.

McAlevy, Summerfield, and Cowan (12) have treated this case of a cold fuel coming into contact with a stagnant, hot oxidizing gas. They assumed that the surface mass flux of fuel was constant and that oxidizer diffusion and consumption was unimportant. However, because of simplifying assumptions made in the analysis, the applicability of their result is rather limited. A more complete discussion of the inadequacy of the formulation is given in Appendix A-7.

A more general treatment of equations [4], [5], and [6] has been carried out, and the results are discussed in Part I of this report. A numerical solution of the complete set of equations [4,5,6] with two different boundary conditions on the fuel supply was a part of this treatment.

Previous investigators have inferred the mechanism of the ignition process from the magnitude of the dependence of ignition delay on oxygen concentration. Among the findings of the more general treatment of Part I, was the observation that this magnitude depends on the exact specification of the ignition event. Another finding was that the slope of a plot of the logarithm of ignition delay versus the logarithm of oxygen concentration is not necessarily constant and can vary over wide ranges. These effects occur as a consequence of the influence of oxygen diffusion and consumption. They are important because they indicate that the slopes of the ignition delay-oxygen concentration curves cannot in themselves prove or disprove the validity of any ignition model. Although the available theoretical treatments of gas phase ignition are limited to cases of externally supplied oxygen, the concept of the gas phase ignition may realistically be applied to situations in which the oxidizer is supplied by the decomposition process of the solid.

4. Ignition Due to Heterogeneous Reactions at the Gas-Solid Interface

It has been suggested that the effect of gaseous oxygen on ignition delay could be due to an exothermic oxygen

attack on the solid material at the gas-solid interface. This heat generated at the surface would lead to a subsequent increase in the heat flux to the solid and thus, to ignition. Similar reactions could occur in composite propellants, even in neutral gas environments, where oxidizing gases from the decomposing ammonium perchlorate could react with the organic binder at the interfaces between the binder and oxidizer particles. Some support for this assumption can be found in the fact that ammonium perchlorate starts to decompose at much lower temperatures than most of the polymeric binders in use, (20).

A mathematical model for such a surface reaction can be formulated under the assumption of a one-dimensional, semi-infinite domain of stagnant, oxidizing gas, bounded at one side by a semi-infinite solid with which the gaseous oxidizer reacts at the surface. With this picture in mind, the following transient diffusion equations may be written.

Energy Diffusion:

Gas: $$\frac{\partial T_G}{\partial t} = \alpha_G \frac{\partial^2 T}{\partial x^2}$$

Solid: $$\frac{\partial T_F}{\partial t} = \alpha_F \frac{\partial^2 T_F}{\partial x^2}$$

Mass Diffusion:

$$\frac{\partial C_{ox}}{\partial t} = D \frac{\partial^2 C_{ox}}{\partial x^2}$$

These equations are assumed to have the following constraints:

$t \leq 0$:

$$C_{ox} = C_{ox}^{\infty}$$
$$T_G = T_F = T_o$$

$t > 0$:

$$-D \frac{\partial C_{ox}}{\partial x} = C_{ox}^{n} Z e^{-E/RT}$$
$$T_F = T_G$$
$$-\lambda_G \frac{\partial T_G}{\partial x} = -\frac{\lambda_F \partial T_F}{\partial x} + q C_{ox}^{n} Z e^{-E/RT}$$

} $x = 0$

$$C_{ox} \rightarrow C_{ox}^{\infty}, \quad x \rightarrow +\infty$$
$$T_G \rightarrow T_o, \quad x \rightarrow +\infty$$
$$T_F \rightarrow T_o, \quad x \rightarrow -\infty$$

In writing these equations, the following assumptions are made:

1) Convective mass transport can be neglected
2) Density is independent of temperature
3) Molecular weights and diffusion coefficient of all gases are equal
4) The surface reaction is of order "n" and can be represented by an Arrhenius function
5) The temperature of the system is initially uniform.

Anderson and Brown (20) solved a similar set of equations numerically, and found that the ignition delay was proportional to the oxygen concentration raised to a power approximately twice the order of the surface reaction. This solution was fitted to some of the data reported in reference (12) with the assumption of a first order surface reaction; the fit was offered in support of the validity of the model. A more complete discussion of the properties of the above set of equations is contained in Appendix A—8. The consequences of variation of parameters other than oxygen concentration are included in this discussion. It is very hard, however, to establish the dominance of surface reactions during the ignition event, because oxygen also affects reactions occurring purely in the gas phase. In particular, both the gas phase and surface reaction models show that the apparent effect of oxygen concentration on the ignition delay may be greater than the assumed order of chemical reaction. Therefore, the possibility of experimentally distinguishing between these two processes, each involving an oxidizing gas, is difficult. Such differentiation could be made by the separate variation of surface temperature and gas temperature adjacent to the surface in the same experiment. No such experiment has been performed, however.

C. EXPERIMENTAL STUDIES OF SOLID PROPELLANT IGNITION

1. General Considerations

In this section an attempt is made to sum up some recent experimental studies which are pertinent to the understanding of solid propellant ignition. However, a complete survey of the literature of this field was not attempted. Before discussing the individual experiments, consideration will first be given to what experimental evidence is actually needed in order to distinguish between the different mechanisms outlined in the previous chapter.

Almost all experiments measure a total ignition time as characterized by either pressure or luminosity. If the heating is not immediate (as it is, for example, in some shock tube experiments), there will always be a time span during which all chemical kinetic processes can be neglected. This is true for all the processes mentioned, except ignition due to low temperature hypergolic reactions. The total ignition time can, therefore, be divided into several parts:

$$t_{ignition} = t_1 \text{ (heat-up)} +$$

$$t_2 \text{ (triggering reaction solid, solid-gas or gas phase)} +$$

$$t_3 \text{ (final flame development)}$$

For high activation energy and low heat flux processes, the heat-up time will dominate the observed ignition delay, since in most cases both t_2 and t_3 will be small compared to t_1. Slow ignition experiments provide some valuable information and sometimes allow an estimate of a so-called ignition temperature. Actually this is not a fixed temperature, but the narrow temperature range in which chemical reactions first become rapid enough to contribute to ignition. This could be the temperature at which an exothermic reaction starts in the solid or it could be the temperature at which significant evaporation starts to occur. However, such experiments tend to obscure the most vital piece of information which could give some clue as to the mechanism of ignition, namely, the pressure dependence of the ignition event. Now, conclusive interpretation of this observed pressure dependence is not easy, for in most experiments the applied heat flux as well as the ignition reaction itself is dependent on the pressure. The apparent pressure effect, therefore, has to be corrected by separate estimation of the influence of pressure on heat transfer. The confidence limits of the corrections are often too large to allow any reliable conclusions as to the pressure effect.

Other important evidence in the determination of the ignition mechanism is the influence of oxidizing gases on the ignition. Again, a distinction must be made between slow and fast ignition, with only the latter being of real significance. Finally, an unfortunate limitation of most experiments is that they do not provide means for independently varying over wide limits the solid surface temperature and the nearby gas temperature. The dependence of ignition delay on these two temperatures as independent variables would be an important clue to the process by which ignition occurs.

In all these researches, it must be remembered that the objective is to determine the processes that control ignition in a rocket motor. The conditions should be chosen to bring out the effects of the pertinent processes. In order for an ignition experiment to simulate conditions in a rocket motor as closely as possible, the following requirements should be met:

a) the total ignition time should be very small (several milliseconds and less)
b) the heat flux should be high
c) the gas temperature should be very high (otherwise a gas phase delay might be introduced which does not necessarily exist in practical situations)
d) pressure should be varied over a wide range, including near atmospheric pressures.

It is very hard to design such an experiment. In experiments which do not fulfill the above conditions, it must always be remembered that in complicated reactions the controlling mechanism often changes with conditions. However, by summing up all the experimental evidence available, some significant insight as to the nature of the ignition process in solid propellants is possible.

2. Hot Wire Ignition of Composite Solid Propellants

Altman and Grant (5) reported a study of the ignition of composite ammonium perchlorate propellants by heat transfer from a straight, electrically heated wire embedded in the propellant. The temperature of the propellant adjacent to the wire at ignition was computed from the measured ignition delay. They attempted to show that ignition was governed by a specific ignition temperature regardless of the magnitude of the heat flux.

In the experiments, the ignition delay was the interval between the onset of heating and the burn-out of a fuse wire. The operation of this system was checked, in early experiments, by high speed photographs.

Data obtained from this experiment are presented in a graph of power input versus ignition delay, see Figure 1, abstracted from reference (5). This curve is the authors' correlation of their results, using a one-dimensional heat conduction solution and an ignition temperature of 368° C. The results are in fairly good agreement with their hypothesis.

It should be pointed out that the results do not prove anything with regard to the propellant ignition mechanism. At these ignition times, longer than one second, almost any process having a high activation energy should be correlated by an ignition temperature, provided the pressure and gas composition are not varied.

In view of the preceding discussion of ignition theories, it must be noted that the experiment was incomplete with respect to possible effects of total pressure and test atmosphere composition. It would be interesting to have results at higher pressures and also at higher heating rates. An incidental observation reported by the authors which could be significant for the interpretation of the ignition process, is that in these slow ignition tests a considerable gas evolution was noticed prior to the appearance of a flame. This could indicate that the decomposition vapors play a role in ignition, in a manner according to one of the models discussed above.

3. Explosion Tube
Propellant Ignition Experiments

Cook and Olson (6) reported a series of experiments in which ignition of propellants was caused by impingement and reflection of a complex explosion or detonation front from a nitrate ester propellant sample mounted in an explosion tube. The tube was filled with various detonable mixtures of hydrogen and oxygen. The experiment was conceived as a test procedure for determination of propellant ignitability, with no consideration given to separation of pressure, temperature, and chemical effects from effects caused by the hydrodynamic situation or model mounting methods. However, the authors were cognizant of the importance of the ignition criterion in ignition studies, and observed that any criterion must be such that full scale burning always develops after its attainment.

The significant experimental results were reported in terms of the minimum hydrogen-oxygen charging pressure necessary to cause ignition of the propellant in the explosion tube, see Figure 2 abstracted from (7).

The most interesting feature of the results given in Figure 2 is the influence of oxygen concentration on the minimum charging pressure necessary for ignition. It is impossible to get any quantitative estimate of this effect as the final temperature, pressure, and wave front speed depend upon oxygen concentration also. The fact that the curves have a minimum at oxygen concentrations much above stoichiometric clearly indicates an influence of oxygen

concentration on propellant ignition. If oxygen concentration were to have no influence, an approximate symmetry would be expected around the stoichiometric region.

4. Ignition of Nitrate Ester Propellants by Forced Convection

Churchill, Kruggel, and Brier (8) reported experiments in which cylinders of nitrate ester propellant were ignited in a crossflow of a heated test gas at atmospheric pressure. The gas composition and temperature were varied to include several oxygen-nitrogen mixtures, carbon dioxide, and pure nitrogen. The experimental ignition criterion used in the ignition delay determinations was the establishment of a luminous flame, close to the propellant surface, which led to combustion of the propellant sample. Their results are reported in Figure 3 in terms of an "ignitability function" versus the percent oxygen in the test gas.

Experimentally, it was observed that the ignition delay depended upon test gas temperature, flow rate, and composition; separate increases in test gas temperature, flow rate, and oxygen mole fraction were all observed to decrease the ignition delay. It was concluded that oxidation reactions were the controlling mechanism in double base propellant ignition under these experimental conditions.

A very interesting observation not stressed in the paper was the fact that consistent ignitions could not be obtained in inert atmospheres under the conditions employed. Also, ignition as defined by the appearance of a luminous flame, was not obtained at high flow rates and low temperatures. In some cases, the grain decomposed completely without the appearance of a luminous flame. This illustrates how strongly the ignition time measured in an experiment can depend upon the ignition criterion and the method used for measurement. The results also show that the time needed to establish a luminous flame is not necessarily negligible, compared to the time needed for the start of solid decomposition.

The influence of such parameters, such as test gas composition and temperature, could be completely different under the high pressure and temperature conditions which prevail in actual rocket motors. Thus, for example, in other experiments, propellants ignite consistently in inert atmospheres at high pressures. It would have been valuable if additional experiments of this type had been performed at higher pressures.

5. Ignition of Nitrate Ester Propellant in a Pressurized Oven

Roth and Wachtell (9) studied the ignition of nitrate ester propellant samples subjected to radiant and convective heat transfer inside an oven in which pressure, temperature, and test gas composition were varied separately. Oven pressure and luminosity were monitored simultaneously to determine the total ignition delay and the delay between the start of fizz decomposition and a luminous flame reaction. Ignition delays between one and thirty seconds were obtained.

Little effect of oxygen concentration on the overall ignition delay was noted in experiments with M2 propellant tested in nitrogen, air, and helium over a 300 psi pressure range. Two stage ignitions, and a marked effect of oxygen concentration on the fizz-to-flame delay period was observed in ignition tests of M9 propellant. This effect was observed in tests of M10 propellant at an initial propellant temperature of $0^{\circ}C$, but the effect disappeared with an increase in the initial temperature to $30^{\circ}C$. The experimental data are shown in Table I and Figure 4 which were abstracted from reference (9).

Because of the good fit which was obtained between the ignition delay and the heat flux, Roth and Wachtell concluded that pressure and oxygen concentration had no detectable effect and, therefore, that the overall ignition reaction was controlled by a solid phase decomposition. However, further examination of the data of reference (9) show that the fizz-to-flame delay could be quite significant, depending upon the test gas composition and pressure. It should be mentioned that the observed fizz-to-flame delay was, in itself, large compared to the total ignition delay in a rocket motor. The dependence of the fizz-to-flame delay on oxygen concentration has been replotted from the reported data in Figure 5. It can be seen that pressure and oxygen concentration have a marked effect on this delay.

The conclusions in reference (9) about the dependence of the fizz reaction delay on pressure and gas composition are at least open to question for, as mentioned previously, it is hard to measure such effects at low heat fluxes. The apparent effect of pressure which can be noted in Table I, was explained in terms of an increased heat transfer rate; however, the confidence limits of the heat transfer calculations are not sufficiently narrow to allow a definite conclusion with respect to a pressure effect.

6. Propellant Ignition by High Convective Heat Fluxes

Ryan, Baer, and Salt (10), (11) have reported studies of propellant ignition. In one series of tests (10),

composite propellant samples mounted in a constant area duct were ignited by a hot gas flow which was generated by the exhaust of shock tube driven gas. This gas was generated by a shock tube operating in a tailored interface mode. Test gas pressure and flow velocity were varied to produce a range of heat flux conditions and the gas composition was either nitrogen, air, or oxygen.

In another series of experiments (11), use was made of a low pressure radiation furnace in which temperature and gas composition were varied. No gas composition effect on ignition delay was observed in the furnace tests. At reportedly equal heat transfer rates, ignition delays were larger, by a factor of two to three, in the furnace than in the shock tube experiments.

Data from both of these experiments, abstracted from references (10) and (11), are shown in Figures 6, 7, and 8. The data treatment reported was suggested by an interpretation and development of Hicks' (18) linear surface temperature criterion in which a solid phase decomposition ignition mechanism was assumed. This method is illustrated by equation [3] above.

Ryan, Baer, and Salt concluded that composite propellant ignition data were explained by Hicks' empirical ignition temperature criterion, and that the overall activation energy was fairly well determined by their tests. They also concluded that the more rapid ignition of propellants exposed to pure oxygen test gas was due to an enhanced heat transfer to the propellant caused by an oxygen-fuel binder reaction.

The total pressure range (250 and 350 psig) in these experiments was much too small to permit any definite conclusion regarding the pressure dependence of the ignition reaction. The fact that the ignition delay in the radiation furnace at atmospheric pressure is three times longer than at elevated pressure in the shock tube is interesting, but not conclusive. The difference only illustrates the danger of using heat flux as the sole variable for comparison of ignition times measured under different experimental conditions. It has been pointed out already that, by itself, the form of the dependence of ignition times on heat flux gives no indication as to the ignition mechanism.

7. The Ignition of Composite Solid Propellants in a Shock Tube

McAlevy, Cowan, and Summerfield (12) investigated the ignition of a composite propellant sample mounted flush with the end wall of a simple shock tube which was operated

such that the pressure after the reflected shock remained constant (tailored interface operation). The action of the shock tube exposed the propellant sample instantaneously to a stagnant, doubly shocked, high temperature, high pressure gas. Ignition was detected by a filter-photocell system sensitive to radiation in the violet region of the spectrum.

The effect of variations in the oxygen content of the test gas on ignition delay was obtained under constant shock tube operating conditions. The results are shown in Figure 9 as abstracted from references (12), and (21). Tests in pure oxygen in which the pressure level behind the reflected shock was varied, gave the results shown in Figure 10. It was observed that no ignition was possible with an oxygen concentration less than 3×10^{-3} gm/cc in the test gas behind reflected shock. This might be explained by the limited test time of only five milliseconds. Samples of the propellant fuel binder tested under similar conditions also ignited, but with slightly longer ignition delays. Parallel experiments, as reported in reference (13), were carried out with nitrate ester propellants under the same test conditions. The data which was obtained are also shown in Figures 9, 10, and 11. The nitrate ester propellants ignited more slowly than the composite propellants. It is interesting to note that some of the results reported in reference (21) seem to indicate that the dependence of ignition delay on oxygen concentration decreases at higher concentrations.

On the basis of these results and a simplified analysis of heterogeneous ignition, it was concluded that the dominant ignition delay for composite propellants was caused by a gas phase reaction between pyrolized fuel binder and the oxygen present in the test gas. The experiments do not allow such a definite conclusion as to the mechanism of the ignition and the nature of the oxygen effect. They do, however, clearly indicate that solid phase reactions do not dominate the composite propellant ignition process.

An important feature of these experiments, compared to all other solid propellant ignition experiments, was the instantaneous establishment of high propellant surface temperatures by the shock reflection process. After the initial temperature jump, the surface temperature remains quite constant in the absence of any chemical reactions. This makes it difficult to compare these results with those of constant heat flux experiments.

8. Ignition of Composite Propellants by a Radiant Energy Flux

The ignition of composite propellants by intense radiant energy in an arc-image furnace has been studied in

considerable detail at the Stanford Research Institute (14), (15). In these experiments the intensity of radiant flux incident on the propellant sample was varied over a wide range, as was the pressure at a single flux level.

Fishman and Beyer (14) measured minimum ignition energy defined as the minimum quantity of radiant energy, applied in a pulse, needed to produce ignition some time after the application of radiant flux was terminated. Specific attention was paid to the important problem of the minimum time for which the radiant flux had to be applied for propellant ignition to occur. In reference (15), ignition delays were measured; the radiant flux was maintained at a constant level until ignition occurred. Ignition was detected photoelectrically in both cases. High speed photographic observations (14) seemed to indicate that at least the final stages of composite propellant ignition occurred in the gas phase. Voluminous evolution of gases was noted considerably before the appearance of a flame. The visible reaction started at a considerable distance from the surface and flashed back to it.

In Figure 11 the minimum exposure time causing ignition is plotted against pressure at a constant flux level. It should be pointed out that the exposure time reported was not an ignition time, as ignition occurred after the radiant flux was removed. The ignition times themselves were not reported. It is evident from this figure that the ignition processes are strongly pressure dependent, especially at low pressures. At high pressures, minimum ignition exposure times are less sensitive to pressure. This can be explained because as previously mentioned, the magnitude of the pressure effect depends on the ratio of flame development time to heat-up time. If this explanation is correct, the pressure dependence could be expected to become steeper at higher flux levels. That this is actually the case is seen in Figure 12 in which minimum ignition exposure time for different pressures are plotted as a function of the flux. In addition, it is apparent from this figure that at high flux levels the minimum ignition exposure time does not continuously decrease, but tends to a constant value. As yet there is no quantitative explanation for the apparent plateau in the dependence of minimum ignition exposure time on flux at low pressures as shown in Figure 12.

Figure 13, obtained from reference (15), shows that even with a constant flux applied up to and including ignition, the ignition delay is pressure sensitive. A comparison of Figures 11 and 13 indicate that in Fishman and Beyer's short ignition time experiments, ignition occurred at the end of the minimum energy exposure interval. Measurements of minimum ignition energy with a constant flux

level at atmospheric pressure in a test gas containing oxygen, show a very pronounced oxygen effect. This is illustrated in Figure 14.

The above results indicate convincingly the importance of gas phase reactions in the ignition of composite propellants. It is interesting to note that a simplified model based on the ignition temperature concept would lead to erroneous conclusions for this case. The assumption of an ignition temperature is justified only if heat-up is the controlling element in the total ignition delay.

Ignition by radiant flux is advantageous because it allows variation of ignition time over a wide range at reproducible and controlled conditions. Its main disadvantage is that it involves the presence of a cold gas near the surface. This introduces an additional gas phase resistance which is not present in rocket motors where the temperature close to the surface is very high. For gas phase ignition processes, there is a basic difference between a case where the dimensionless gas temperature (RT/E) is high (0.1 or larger) at the beginning, and one in which (RT/E) is very small. In the first case, any gases coming off from the surface will tend to react immediately while diffusing into regions of high gas temperature. The heat fed back from the reaction will then increase the temperature at the surface causing a still higher gas evolution. In the second case, there must be a buildup of concentration of reactive gases near the surface, before a runaway reaction may occur.

9. Composite Propellant Ignition in a Small Rocket Motor

Grant and Lancaster (16) and (17) have reported a study of the ignition of ammonium perchlorate composite propellants in a small rocket motor. Hot gaseous products from a gas fed, pyrogen-type igniter were used to apply a convective ignition stimulus to the internal surface of a thin-webbed, cylindrical solid propellant grain. A schematic diagram of the experimental system is shown in Figure 15.

Ignition was detected from pressure records and was identified as the first rise over the dummy chamber pressure established by the igniter. An idealized pressure record is shown in Figure 16. The gas mixtures introduced into the igniter contained various proportions of methane, oxygen, and nitrogen. The mixtures were selected to have the same adiabatic flame temperature, but a wide range of equilibrium oxygen concentration in the burnt gases. The

mass flux through the motor was also held constant in an attempt to maintain a constant heat transfer rate in all experiments.

Ignition delays for a series of experiments conducted with a PBAA-80% ammonium perchlorate composite propellants are shown in Figure 17, plotted as a function of the oxygen weight fraction in the burnt igniter gas. It can be noted that strong pressure and oxygen effects on ignition delay are evident even with an ostensibly constant heat flux. The pressure effect even persists when there is no oxygen in the igniting gases. These factors strongly support the contention that the controlling step in the ignition involves a gas phase process.

It is also evident that the effect of oxygen weight fraction changes with pressure. At a pressure of 35 psig the oxygen effect is hardly significant, whereas at 110 psig there is a strong oxygen effect with the ignition delay decreased almost by a factor of five. At each pressure, a threshold effect was noted such that below a certain value, the effect of oxygen concentration was negligible.

Certain aspects of this experimental technique are open to some criticism. The gas temperatures and oxygen concentrations were calculated from equilibrium thermodynamic data and were not measured. These properties could vary due to changes in flow rates, poor mixing or failure to establish equilibrium. Based upon empirical correlations, the heat flux was kept constant by maintaining constant mass flow. Heat flux and oxygen concentrations in these experiments might have differed from their predicted behavior. There might have been variations in the heat flux in different experiments, and the actual oxygen concentrations might have been larger than were calculated to exist. However, the pressure and oxygen effects are so large that they cannot be explained away by experimental error. In order to explain the difference between maximum and minimum ignition delays, one would have to assure that the actual heat flux in one case was 400 times larger than in the other case.

D. DISCUSSIONS AND CONCLUSIONS

In the preceding sections, an intricate array of facts and speculations have been presented. In addition, the experiments and methods of data acquisition have been quite varied. However, despite the apparent complexity of the experimental problem, several definite trends are clearly evident from the collected results to date.

Several of the experiments show that composite propellant ignition is stimulated by pressure increases, an observation which is important in a practical sense. Other experiments clearly showed that the ignition of composite and nitrate ester propellants is aided by the addition of gaseous oxidizer to the ignition environment. The practical consequences of this aid is less evident than in the case of pressure increases. Finally, the concept of a specific ignition temperature which is independent of heating rate and pressure, is demonstrably invalid. This concept is still valuable if it is regarded as an approximate temperature at which decomposition reaction rates become significant. A careful distinction should be made, however, between the heat-up process and the actual ignition event.

The ignition mechanism of either composite or nitrate ester propellants still cannot be stated with any assurance. However, it is possible to make some observations concerning the ignition mechanism of these propellants.

The assumption that composite propellant ignition is controlled by solid phase reactions appears to be refuted by the mass of experimental evidence cited above. At present, there is insufficient evidence to make a proper evaluation of the role of solid phase reactions in nitrate-ester propellant ignition. No pressure effects were detected in some low heat flux experiments with these propellants, but the pressure was not varied over wide ranges independent of heat flux. Therefore, this data is inconclusive with regard to the ignition mechanism.

In several experiments, an effect of oxygen concentration on ignition delay was noted for both composite and nitrate ester propellants. The composite propellant ignition data clearly indicates that gas phase chemical kinetics dominate the ignition process, even in inert environments. However, the effect was not constant and varied with experimental conditions; therefore, the mechanism by which the ignition delay was affected is not clearly evident. In fact, all the experimental evidence reported above could be explained by either the purely gas phase reaction, or the surface reaction, outlined in sections B-3 and B-4, respectively.

Concerning nitrate ester propellants, several investigators found an oxygen effect on the ignition delay. It was shown that the time necessary to establish a luminous flame after the start of a fizz reaction was sensitive to the oxygen concentration. In fact, this fizz-to-flame delay time is comparable to the ignition delay of many rocket motors.

As an addition to the just reported experiments on solid propellant ignition, the experiments which are described in the following chapter were performed. These experiments were concerned with obtaining additional data on composite propellant ignition, for it was felt that the ignition mechanism for this type of propellant was of greatest interest in a practical sense. As shown to be necessary by the preceding discussion, the experiments were designed to cause fast ignitions in chemically reactive and inert atmospheres at some constant, but variable, pressure level.

CHAPTER II-2

EXRERIMENTS ON THE IGNITION OF COMPOSITE SOLID PROPELLANTS CONVECTIVELY HEATED IN A SHOCK TUNNEL

This investigation was undertaken with the view of conducting ignition experiments with a composite propellant placed in a clearly defined flow field. It was reasonable to assume that such experiments would shed further light on the ignition mechanism of composite propellants. The reasoning was that the convective heat fluxes would be of sufficient magnitude to cause composite propellant ignition in all test gases, ranging in potential chemical reactivity from inert (100% nitrogen) to highly reactive (100% oxygen). Experiments were performed in supersonic and subsonic flow fields using several propellant sample configurations. In addition, the ignition of the polymeric fuel used in the propellant formulation, was studied separately in subsonic flow.

A. EXPERIMENTAL

1. Basic Equipment Selection

A shock tunnel was selected to generate the high temperature, high pressure test gas to flow past a composite propellant model, providing the necessary stimulus for ignition of the propellant. The close control over the temperature, pressure, and composition of the test gas afforded by a shock tunnel/shock tube was the basis for this choice of equipment. Additional benefits were fast propellant heat-up and ignition times; it was shown in the last chapter that these characteristics were necessary for experimental determination of the composite propellant ignition mechanism. Finally, the use of a shock tunnel was a logical continuation of the "end wall," ignition studies carried out by McAlevy (12).

The shock tube which was used in the experiments discussed in the following sections, was 71 feet long, 6 inches in internal diameter, with a 56 foot long driver section and 15 foot long driven section. Conversion to a shock tunnel was accomplished simply by addition of a nozzle, concentric with the tube centerline, at the end of the driven section. The hot gas generated by reflection of the incident shock wave from the end wall of the driven section flowed through this nozzle, passed over the propellant sample in the exhaust process, and provided the desired convective heating.

In terms of operating characteristics, the shock tunnel used in these experiments was basically a "simple shock tube." The general operation of such a simple shock tube, and variations on the simple shock tube have been discussed completely in the vast literature on the subject. A good summary of the properties of a simple shock tube may be found in references (12), (22), (23), (24), and (25); references (26) and (27) contain experimental results obtained from shock tubes. A brief discussion of the simple shock tube is given in Appendix A-1. Shock tube operating characteristics and theoretical results which are pertinent to this experiment will be described as necessary.

2. Shock Tunnel Operating Conditions

The shock tube was operated in a manner which produced the necessary reservoir of test gas having uniform stagnation temperature and pressure, and the greatest possible testing time. (The testing time was that time interval between the reflection of the incident shock wave from the end wall and the arrival of the expansion fan after its reflection from the opposite end of the tube. This expansion fan originated at the burst diaphragm position.) Production of these desired conditions was accomplished by operating the shock tube in the "tailored interface" condition. A more detailed treatment of this condition is given in Appendix A-2. In the tailored interface operating condition of a simple shock tube, the reflected shock wave stagnates the incident interface between the driver and driven gases. The result is the formation of a region of stagnant, high temperature and high pressure gas between the interface and the end wall of the shock tube. A wave diagram--a diagram depicting the positions of the shock wave and expansion fan in the tube produced at diaphragm rupture as a function of time--representing the tailored interface condition in the shock tunnel is shown in Figure 18. It may be noted that with 100% He driving air, and a $M_s = 3.5$, a testing time of 27½ msec was available in theory. In practice, the testing time was found to be 25 msec's.

Test gases used in the experiment were mixtures of oxygen and nitrogen. For practical purposes these mixtures were considered to have the properties of air for the calculation of tailored interface conditions under various modes of operation.

With helium driving air, the tailored interface condition in the shock tunnel was obtained with an incident shock Mach number between 3.5 and 4.0. Figure 19 shows the burst pressure ratios which were necessary. The shock tunnel, with gas flowing through the exhaust nozzle, was found to be slightly more sensitive to the value of the incident shock Mach number than the simple shock tube used by McAlevy (12).

He reported that tailored conditions were achieved with $3.0 \leq M_s \leq 4.2$. When various percentages of nitrogen were mixed with helium and the mixture used as a driver gas, the tailored interface condition was obtained between $2.0 \leq M_s \leq 4.0$. Results of theoretical calculations using constant specific heats are presented in Figures 20 and 21. These figures show the Mach number required for tailored interface operation as a function of the percentage of helium in a helium-nitrogen driver gas mixture. The theoretical burst pressure ratios which are necessary to achieve a desired shock Mach number with a range of helium-nitrogen gas mixtures in the driver section are shown in Figure 22. Details concerning the necessary calculations are given in Appendix A-2.

3. Other Equipment

A special test section, which held the desired supersonic and subsonic nozzles and the necessary propellant models was constructed. Provision was made for photographic viewing of the models during experimental tests. This test section is shown in Figure 23, together with the supersonic nozzle, model holder, and one of the propellant model types used in the supersonic tests.

Both the supersonic and subsonic nozzles were exhausted into a large dump tank, flanged to the test section. The dump tank was evacuated and pressurized with the desired test gas simultaneously with the shock tunnel driven section.

The instrumentation consisted of the shock wave sensors and pressure gauges which were necessary to determine the actual operating characteristics of this particular shock tunnel. A high speed framing camera, focused on the propellant model being tested, was used to obtain the ignition data.

The shock sensors consisted of two simple, Pyrex glass backed, platinum thin film resistance thermometers. Pulse amplifiers amplified the shock sensor signals to provide trigger pulses for the start and stop gates of an electronic time interval meter. The shock transit time was measured directly over a known distance, allowing accurate determination of the actual shock Mach number.

The pressure gauges were of the piezo-electric type (Type 601) manufactured by the Kistler Corporation. These gauges were used to determine the pressure-time history near the end wall, and in the subsonic nozzle. The gauges were calibrated and their signal displayed on an oscilloscope operating in single sweep mode.

Ignition data were recorded by a "Fastax" high speed framing camera focused on the propellant sample being tested. Dupont, Type 93A-A, 16 mm. film was used. The

diaphragm burst and subsequent shock wave formation/reflection was synchronized with the starting of the camera such that the camera was operating at a high framing speed (4000-7000 fps) when the shock wave reflected from the end wall of the shock tunnel. The shock wave reflection triggered a light, internally mounted in the camera, to turn on and expose one margin of the film, thus providing a known "zero" time. An internal camera timing light marked the other film margin at millisecond intervals and provided a known time scale from which ignition delays could be found.

A detailed discussion of the instrumentation problems found during the course of the experiments may be found in Appendix A-3; electrical schematics of the shock sensor amplifiers and a block diagram of the instrumentation system are shown in Figures 24 and 25.

Details of the supersonic and subsonic nozzle designs and associated model holders are presented in Appendix A-4, as are the details of solid propellant model preparation.

4. Experimental Results

a. Supersonic flow tests

A series of tests were made in which propellant samples were exposed to a supersonic flow ($M_s = 2.35$) of either nitrogen, air, or oxygen. The shock tube was operated to produce an incident shock Mach number of 3.65, and therefore a tailored interface condition. The stagnation temperature and pressure after the reflected shock was approximately 2200° K. and 330 psi, respectively. Three differently shaped samples were tested in order to vary the boundary layer thickness over the model, and the velocity field in which chemical combustion reactions could take place. The three shapes were those of a hemisphere-cylinder, a two-dimensional wedge having a semi-vertex angle of 25°, and a two-dimensional wedge having a semi-vertex angle of 45°. A sketch of the wedges is shown below, where α is the semi-vertex angle.

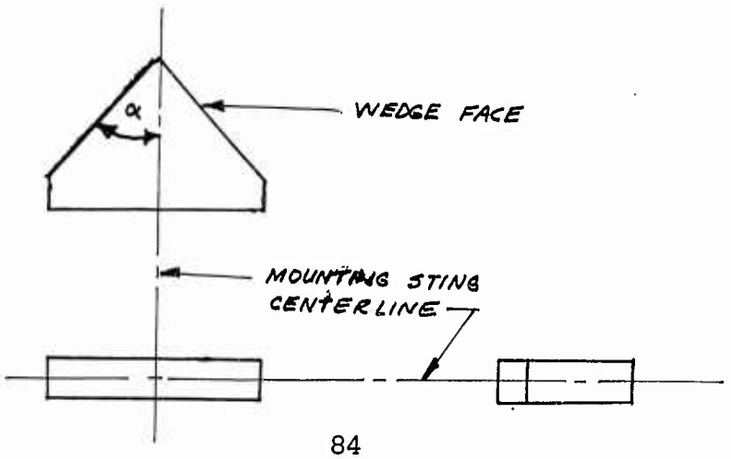

A planar shock was attached to the leading edge of the 25° wedges placed in the flow field of the supersonic nozzle. The gas velocity vector after the shock wave was parallel to the wedge face. Wedge models with the 45° semi-vertex angle forced the formation of a strong shock, detached from the leading edge of the wedge face, when placed in the same supersonic flow. This detached shock, according to reference (28), was stronger than the attached shock and produced greater gas temperature and pressure in the flow region between the shock wave and the propellant sample being tested.

A description of the experimental results and observations obtained during the course of the supersonic tests follows. All data concerning the behavior of the samples during the test period were obtained from the Fastax camera film records.

b. Tests of hemisphere-cylinder propellant models

The chief result obtained from the tests of the hemisphere-cylinder models placed in high temperature supersonic flow, was that ignition could not be obtained. "Ignition" is defined to be the establishment of chemical reaction leading to substantial consumption, or complete burnout, of the propellant model. Film records obtained from tests in pure oxygen and air, showed the presence of discrete points (regions) of luminosity scattered over the hemispherical nose of the samples. These points of luminosity were not continuous in time, but appeared and disappeared in a seemingly irregular fashion. Such points were far more prevalent when pure oxygen was used for the test gas than when air was used. With air as the test gas, the luminous regions were in evidence for about five milliseconds only. Figure 30 depicts the most vigorous and persistent luminous reactions obtained in any of the hemisphere-cylinder propellant sample ignition tests. The test gas was pure oxygen and the light streaks were due to the passage of glowing dirt particles from the shock tunnel. More stringent cleaning of the shock tunnel almost completely eliminated the presence of dirt, but the film records of the tests showed substantially the same behavior.

Tests of the hemisphere-cylinder propellant samples in pure nitrogen did not result in the spotty luminous reactions observed in air and oxygen. In fact, in only one test was the model at all visible in the film record. This one record showed only two frames in which the hemispherical nose of the sample was barely discernible.

Since in no case was ignition obtained in this test series, each sample was examined under a binocular

microscope after being tested. The appearance of the samples was the same, regardless of the test gas used in the ignition test. In each case, the ammonium perchlorate crystals in the immediate region of the stagnation point had disappeared, and the propellant surface was covered by small craters where the perchlorate crystals had been originally. The craters in this region appeared to be larger than the original perchlorate particle size, indicating a loss of fuel from this region. Whether the fuel loss was due to erosion or pyrolysis is not known. In axisymmetric regions surrounding the stagnation region, ammonium perchlorate crystals were observed to be present in the bottom of the craters. The amount of perchlorate decomposition, and degree of cratering, varied with the surface distance from the stagnation point region to the shoulder of the hemisphere-cylinder sample. This decomposition decreased as the shoulder of the sample was approached, and appeared to be axisymmetric. In the regions near the shoulder of the sample, the ammonium perchlorate crystals were only slightly below the mean fuel surface and were milky white and porous in appearance. According to reference (29), such an appearance is associated with ammonium perchlorate decomposition below 503° K. This condition seemed to be established in axisymmetric regions closer to the stagnation region as the amount of oxygen available in the test gas decreased. The amount of the shift was slight, however, between pure oxygen and pure nitrogen test gases. Visual examination of the hemisphere-cylinder samples also revealed an interesting formation of "stringers" which appeared to be the same color and texture as the polymeric (P-13) fuel, at least under 400X magnification. The "stringers" appeared to originate from the fuel, particularly at edges of the craters left by the decomposed perchlorate crystals. The origin and nature of the "stringers" is not known, but may have been due to an "unzipping" of the cured polymer during decomposition/pyrolysis. "Stringers" were formed on a hemisphere-cylinder model of pure fuel tested in nitrogen, and to a much lesser extent were found on some unburned propellant and pure fuel samples tested in the subsonic flow nozzle. No charring of the binder was found in any of the hemisphere-cylinder samples tested.

c. Tests of two-dimensional wedge propellant samples

In this section and hereafter, the term "α°-wedge" should be taken to mean a two-dimensional wedge propellant sample having a semi-vertex angle of α°. One may refer to the sketch drawn in the first part of section 4.

Both types of wedge samples were tested in supersonic flows of oxygen, air, or nitrogen. No luminosity was ever detected in tests of the 25° wedges. In contrast, tests of the 45° wedges showed strong luminous reactions in

oxygen, less strong reactions in air, and barely discernible reactions in nitrogen, see Figures 31, 32, and 33.

The 25° wedges were slightly charred in pure oxygen, only, and the ammonium perchlorate crystals were milky white only at the apex of the wedge angle. No charring was evident on the 45° wedges in any of the test gases. In addition, the perchlorate had been turned milky white over significant portions of the wedge face in each test gas. The extent of this portion depended on the test gas, and was greatest on the samples tested in oxygen.

A quasi-periodic appearance and disappearance of strong luminous reactions on the wedge face was an interesting feature of the 45° wedges test results, see Figures 31 and 32, especially. Close scrutiny of the oxygen test results reveal, see Figure 31, that each appearance of strong luminous reactions was a little further downstream from the leading edge of the model. This progression of reaction centers was not as apparent in the air tests, Figure 32, and was not at all apparent in the nitrogen tests.

5. Conclusions Obtained from Supersonic Flow Ignition Tests

It should be recalled that the definition of "ignition" is very important in discussing the ignition of heterogeneous systems. In the context of the present experiments, ignition is defined as the development of chemical reactions which are sufficiently intense to cause full scale combustion during the available testing time.

It must be concluded, then, that none of the propellant samples were ignited in the supersonic flow tests. However, strongly luminous chemical reactions were observed under certain conditions.

It is significant to note that sufficient surface temperatures were produced in regions of the propellant samples tested, to cause the ammonium perchlorate to decompose at a faster rate than the polymeric (P-13) fuel binder. This fact supports the data presented in Figure 29 of reference (21) which indicated that for sufficiently great surface temperatures, the pyrolysis/decomposition rate of ammonium perchlorate exceeds that of P-13 fuel. The loss of perchlorate definitely was due to decomposition rather than an ejection of perchlorate crystals by the mechanical shock associated with the start of gas flow over the propellant sample. Proof of this assertion was the presence of partially decomposed perchlorate crystals in the bottom of craters near the shoulder of the hemisphere-cylinder samples, and on the 45° wedge propellant samples.

According to references (19) and (21), the existence of rapid perchlorate decomposition, such as just mentioned, requires perchlorate temperatures greater than 500° K. Therefore, it is concluded that the ignition of composite propellants is not governed by a solid phase decomposition and heat generation.

Now, in the 45° wedge sample tests, the luminous reactions decreased in intensity as the oxygen mole fraction decreased, and were very weak in the nitrogen tests. Therefore, it is concluded that a gas phase reaction occurred between the perchlorate decomposition products and the oxygen in the test gas. Such reaction would increase the heat transfer to the sample surface downstream of the leading edge. Therefore, the perchlorate decomposition rate increased and caused the decomposing crystals of oxidizer to disappear fairly rapidly. It is concluded that the quasi-periodic nature of the luminosity observed in these tests was due to a depletion of the rapidly decomposing crystals because of the increased heat transfer from chemical reaction. A delay period then occurred, during which new perchlorate crystals could be heated sufficiently to cause renewed rapid decomposition and subsequent gas phase reaction of the decomposition products and the ambient oxygen.

Further, it is concluded that this gas phase reaction was inhibited by the thin boundary layers associated with high flow velocities over the propellant sample. A boundary layer is thin if its thickness is of the order of a gas phase reaction zone. In such a case, the reactant mixture will be diluted and, consequently, the reaction will be weakened. In addition, even though the gas at the edge of the boundary layer is hot, it is cooler than the flame temperature associated with intense chemical reaction. Therefore, there is a loss of heat to the free stream and a further weakening or dilution of any chemical reaction.

This combination of high flow velocities and reaction dilution makes flame stabilization difficult, and causes the above-mentioned inhibition of gas phase reactions. Consequently, intense, steady state reactions were not observed in the supersonic flow tests.

6. Subsonic Flow Propellant Ignition Tests

Ignition tests of propellant and fuel samples placed in the constant area test section of the subsonic nozzle were conducted. The samples were shaped in the form of a thick flat plate, with a 46° bevel to a sharp leading edge, and were prepared from a cured block of a composite solid propellant or a cured fuel binder. A description of the sample size, shaping technique, and mixing formulations are given in Appendix A-4. The samples were one and one-half inches long, one-half inch wide, and approximately one-quarter inch thick.

A series of tests were conducted using pure helium driver gas and the same shock tunnel operating conditions as in the supersonic flow ignition tests. As before, the incident shock Mach number was 3.65, and oxygen, air, and nitrogen were used as test gases. The velocity of the gas flowing over the propellant sample was controlled by the size of the orifice at the exit of the subsonic nozzle. Using an assumed orifice discharge coefficient of 0.62 and an incident shock Mach number of 3.65, the gas velocity was calculated to be 62 feet/second when exhausted through an 0.25 inch diameter, sharp edged orifice. This value agreed closely with the flow velocity found by observing the residence time of small dust particles through the nozzle. These particles were accelerated by the flow through the nozzle after the incident shock wave. Of course, the flow velocity depended upon the molecular weight of the test gas, but it was estimated that the velocity was constant within $\pm$ 5 percent for test gases ranging from pure nitrogen to pure oxygen. The shock filter described in Appendix A-4 was not used for any of the subsonic flow propellant ignition tests.

7. Results of Subsonic Flow Ignition Tests

a. Propellant ignition tests; helium driver gas

True ignition leading to complete model burnout was obtained in all test gases. Ignition delay times were quite small, and ranged from 0.25 to 0.3 milliseconds in pure oxygen to a maximum of 4.0 milliseconds in pure nitrogen. The development of ignition was almost everywhere simultaneous on samples which were tested in oxygen, while ignition mainly developed just downstream of the leading edge of the models tested in nitrogen. These rapid ignitions occurred, in general, during the two to three millisecond period of unsteady flow and wave interaction in the subsonic nozzle before steady state flow was established.

In all these ignition tests, ignition on any but the top surface of the sample was undesirable. Such undesirable ignition was particularly prevalent in test gases containing large oxygen concentrations. Consequently, an inhibiting method was tried, in which all surfaces but the top surface of the samples were leached in a flow of distilled water. Tests of these samples in pure oxygen showed preferential ignition on the surfaces which had been leached. In addition, the ignition delays in oxygen were reduced to 0.1 to 0.15 milliseconds. Completely leached samples did not ignite when tested in nitrogen. Samples left unleached on the top surface of the flat plate ignited, in nitrogen, in a manner identical with unleached models.

A puzzling phenomenon was observed in the nitrogen tests of the leached propellant samples. This was the appearance of a luminous "cloud" which appeared to originate from the leached surfaces. After approximately one millisecond, the cloud was sufficiently dense to obscure the sample partially; after approximately five milliseconds the cloud was observed to disperse and to be exhausted as steady flow was established in the nozzle. The luminous cloud was much less apparent in the tests of unleached samples in nitrogen test gas.

Because of the rapid ignition, this test series was terminated and a test series, in which tailored operation of the shock tunnel was obtained with lower incident shock Mach numbers was initiated. It was reasoned that a reduction in the heat transfer rate to the propellant sample through reduction of the test gas temperature would increase the ignition delay. With long ignition delays, the two to three millisecond period of unsteady wave motion in the subsonic nozzle before steady flow was established would be a small fraction of the total delay. Therefore, it was expected that any unreproducible events that occurred during this period could be neglected.

b. Propellant ignition tests; mixed driver gas

The method of achievement of tailored interface operation of a shock tube at low values of incident shock Mach numbers is described in Appendix A-2, assuming constant specific heats. Experimentally, it was found that a driver gas mixture of 94% helium - 6% nitrogen produced an excellent tailored condition with a shock tunnel burst pressure ratio, $P_{41} = 39$. The standard, acceptable incident shock Mach number used in these tests was 2.55 $\pm$ 1.5% in oxygen, air, and nitrogen test gases. The calculated temperature after the reflected shock was 1120^{o} K. Standard operation, with a 0.050 inch thick diaphragm which burst at 398 psia, resulted in a pressure of 330 psia after the reflected shock and a pressure of 300 psia in the constant area test section of the subsonic nozzle. An exhaust orifice diameter of 0.294 inches produced a gas flow velocity of approximately 62 feet/second in the nozzle. The available test time was 37 milliseconds. These conditions were the standard shock tunnel operating conditions. The propellant samples were formulated according to the listing given in Figure 34.

The previously mentioned luminous glow was eliminated and a large increase in ignition delay was obtained. Ignition delays of 25 milliseconds were obtained for propellant samples tested in nitrogen, compared to the 4 millisecond delays previously obtained.

The scatter in the data obtained from tests with any one test gas was too great to allow more than the establishment of a definite trend concerning the influence of the mole fraction of oxygen on the propellant ignition delay. This trend is shown graphically in Figure 36 where the circled points refer to the propellant tests. Many more tests were conducted than are presented in Figure 36, but some of these test results were discarded for one or more of the reasons which are listed below.

(1) The shock Mach number differed from 2.55 by more than 1.5%.

(2) Dirt was observed to be present in the shock tube. This was easily determined from the film records.

(3) The sample was mounted insecurely and was observed to bounce or wobble during the start of the test period and the flow of the test gas.

(4) The sample broke, or the tip bent during the test. This occurred, if at all, during the start of the test period.

Ignition and consumption of the propellant samples was observed in all tests. The ignition point was always within a region 1/2 millimeter downstream of the sample leading edge. Close examination of the film records showed that this ignition always occurred on the top flat plate surface of the samples. A flow velocity increase by a factor of four showed no downstream shift of the ignition point in a manner analogous to the flame of a premixed gas held on a heated flat plate, see reference (34), nor was any change in the ignition delay observed. Possibly this was because the data scatter was too great to indicate even a trend. Figure (35) shows a section of the high speed film record of a typical propellant ignition test in subsonic flow.

8. Discussion of Results of Supersonic and Subsonic Propellant Ignition Tests

It may be recalled that the propellant samples tested in supersonic flow could not be ignited in either pure oxygen or pure nitrogen. True, some luminous regions which appeared to be centered around ammonium perchlorate crystals were observed, but no steady deflagration was obtained. Though the intensity of the luminosity was greatest in pure oxygen and least in a pure nitrogen test gas, there was no apparent difference between the appearance of the propellant surfaces after testing in either gas. In both cases, the ammonium perchlorate crystals had been completely decomposed

in the region of highest heat transfer to the propellant samples. These results provide several good clues concerning the ignition mechanism of composite propellants.

The combination of nonignition and significant ammonium perchlorate decomposition clearly refutes the notion that only solid phase decomposition reactions control the ignition process of these propellants. On the other hand, the prevention of steady state flame establishment by a supersonic gas flow could be a useful method for solid phase surface decomposition studies of propellants or polymers. This method may well be superior to the hot plate pyrolysis methods presently used.

It has been proposed (20) that a gaseous oxidizer-fuel surface interaction is the controlling ignition mechanism for composite propellants. Such a mechanism supposes a significant decomposition of the fuel, particularly when an oxidizer is present in the external environment, even at low initial surface temperatures around 130° C. Now, rapid perchlorate decomposition was observed, and all indications point to the presence of a mean surface temperature well in excess of 130° C. In addition, the quantity of oxygen in the test gas had no apparent effect on the amount of fuel decomposed during a test of a propellant sample. Therefore, although this evidence is not conclusive, these tests cast very serious doubt upon the concept of an ignition controlling gas-solid interaction in composite propellants, at least when oxygen is the externally supplied oxidizer.

Finally, one must consider the supersonic test results with respect to the concept of an ignition controlled by a pure gas phase reaction. Now, the boundary layer over the propellant samples was thin because of the high flow velocities. As previously discussed in section 5, it is easily conceivable that such a thin boundary layer could cause significant decreases in the chemical reaction rate. Therefore, no strong gas phase reaction could exist, and no weak reaction could be stabilized in the high velocity flow field. Consequently, it appeared that ignition and flame stabilization required thicker boundary layers.

Turning now to the results of the subsonic flow tests, one will recall that ignition was always obtained. The ignition point was consistently near the leading edge of the propellant sample, and the delay depended upon the environmental oxygen concentration. In addition, the tests of partially and completely leached samples indicated that the ignition delay depended upon the area of available fuel surface. No velocity effect on either the ignition point or delay was observed, but all the subsonic tests were plagued by a fairly large data scatter under constant test conditions.

In these tests, the observation that ignition occurred near the leading edge was contrary to expectation. It may be recalled that the supersonic flow tests indicated that a thick boundary layer was required for ignition. Incidentally, this expectation was borne out in the fuel ignition tests described in the next section. Returning to the subsonic flow propellant test results, however, it was concluded that under the test conditions of nearly parallel, subsonic flow, ignition occurred in the wake region formed by the protrusion of oxidizer crystals above the mean surface of the propellant sample. The data scatter was too large, however, to permit anything but a tentative conclusion that the experimental velocity variation had no effect on either the ignition delay or the ignition point. It may be that near the leading edge, the wake region behind a protruding oxidizer crystal was unaffected by the flow velocity variations.

The observed dependence of the ignition delay on both the test gas oxygen concentration and the amount of exposed fuel surface is interesting. In fact, this behavior agrees with either a surface or gas phase reaction mechanism controlling composite propellant ignition. However, the propellant used in these tests was formulated with the same components as the propellant used by McAlevy (12). Therefore, correlation of the present data and that of (12) by the surface reaction theory of Anderson (20), is very difficult.

In view of the observed dependence of the ignition delay on the oxygen concentration in these tests, the concept of a gas phase mechanism controlling the ignition of composite propellants cannot be neglected. Either the surface reaction or gas phase reaction concepts, therefore, could be the controlling composite propellant ignition mechanism according to the subsonic test results. However, the combined results of the supersonic and subsonic flow ignition tests do indicate that the establishment of a pure gas phase flame is essential for practical ignition of composite propellants.

At this point, composite propellant ignition tests were concluded. It was felt that a major effort would be required to obtain very smooth propellant samples and overcome the tip ignition property of the subsonic flow tests. Furthermore, it was thought that the boundary layer thickness effect could be investigated by using smooth samples of the propellant's polymeric fuel binder. In addition, concentration on the ignition characteristics of these fuel samples could provide additional information concerning the respective validity of the surface reaction, and pure gas phase reaction, ignition concepts.

The next section contains a description of the pure fuel ignition tests and the results obtained.

9. Pure Fuel Ignition Tests, Technique and Results

In view of the preceding discussion, a series of tests were conducted in which samples formulated from pure polymeric (P-13) fuel binder were placed in the subsonic nozzle. These samples were identical in shape and dimensions to the solid propellant samples, and were mounted in the subsonic nozzle in the same way. Shock tunnel operation and sample test conditions were very similar to those given in the section describing the propellant tests using mixed driver gases. The only deviation from the experimental methods used in the subsonic propellant ignition tests was the addition of the shock filter described in Appendix A-4. All pure fuel ignition tests were conducted with this shock filter installed in the entrance of the subsonic nozzle. As mentioned in Appendix A-3, the shock filter was installed in order to make the nozzle filling process free of strong shocks. Pressure traces taken from inside the subsonic nozzle showed that no strong shocks were present when the filter was used. The nozzle filled in one millisecond.

A series of tests was conducted in which no inhibitor was used on the fuel models. Ignition, and significant amounts of fuel decomposition, were obtained in test gases ranging in composition from pure oxygen to a 50% oxygen-50% nitrogen mixture. Ignition delays ranged from 2 milliseconds in 80% oxygen-20% nitrogen to 4.5 milliseconds in the 50% oxygen-50% nitrogen mixture. No reproducible ignition of the fuel samples was obtained with less than fifty percent oxygen present in the test gas; however, ignition was observed to occur, sometimes, in the wake region of the model, see sketch in Appendix A-6. The wake region was formed by the cessation of the machined model surface and the step down to the metal mounting sting to which the model was bonded. Sporadic ignition in the wake region made it difficult to determine whether ignition actually occurred on the flat plate surface of the model or in the wake region. However, this ambiguity occurred only if the test gas oxygen percentage was slightly less than or equal to fifty percent.

An inhibiting technique was developed in which the desired portions of the fuel models were covered with a coating of aluminum approximately one micron thick. The aluminum coating was done by a vacuum evaporation technique, and is described in Appendix A-6.

With models which had been aluminum coated in the wake region only, it was observed that ignition definitely

could not be obtained in test gases which contained less than fifty percent oxygen. An interesting aspect of these tests was the observation that after ignition in the fifty-two percent oxygen test gas, the flame gradually crept upstream along the model to a point about one inch downstream of the leading edge. In test gases containing sixty percent oxygen, the flame would develop until the entire model was flame covered.

Uninhibited and samples inhibited in the wake region only were often observed to ignite on portions of the specimen other than the top flat plate surface when tested in test gases which contained eighty to one hundred percent oxygen. These tests were discarded.

Quite reproducible ignition was obtained by aluminum coating all the fuel sample surfaces with the exception of a one square centimeter area on the top of the flat plate surface. The uninhibted area was placed two and one half centimeters downstream of the leading edge of the sample. It was found that the aluminum coating failed in the pure oxygen tests; the coating was observed to be shed from the leading edge portion of the sample and swept downstream by the flowing test gas. The film records indicated that the aluminum was burning as it was swept downstream, and was ignited at the point from which it was shed. No inhibitor failure was observed with eighty percent, or less, oxygen present in the test gas; however, no ignition was obtained with less than sixty-two percent oxygen in tests of samples which had only one square centimeter of uninhibited area. Several tests were conducted with samples in which uninhibited area was extended downstream of the normal limit until only the wake region and the first two and one half centimeters were inhibited. Again, no ignition was obtained in test gases which contained less than sixty-two percent oxygen. Several tests were conducted in pure nitrogen to determine the extent of fuel decomposition by pyrolysis alone. No difference in the amount of decomposition was detected between tests in pure nitrogen and gases containing less than 50% oxygen. These tests were conducted with fuel samples inhibited in the wake region only; maximum decomposition occurred near the leading edge.

Measurement was made of the temperature of the top flat plate surface of an instrumented model identical in shape to the fuel samples. This model was subjected to the standard test conditions which were used in the subsonic flow ignition tests of fuel and propellant. Thin film resistance thermometers were mounted on a Pyrex glass plate, and the voltage-time traces recorded. Details of the construction of this gauge are given in Appendix A-4. Platinum resistance films were placed one millimeter and

two centimeters downstream of the leading edge of the gauge; the surface temperature of the Pyrex at these respective positions were 108° C. and 66° C. It was observed that practically steady surface temperatures were obtained after approximately one millisecond, see Figure 41. Based upon average values of the quantity β ,

$$\beta = \frac{(\lambda \rho c_p)^{1/2}_{Pyrex}}{(\lambda \rho c_p)^{1/2}_{P-13}}$$

for the test gas and P-13 fuel binder, these steady state temperatures were converted to the approximate values of temperature which was expected on the fuel samples, by the relationship

$$T_{P-13} = \beta \cdot T_{Pyrex}$$

Thus, the calculated fuel surface temperatures at the one millimeter and two centimeter positions downstream of the leading edge were 261° C. and 159° C., respectively.

An analytical prediction of the temperatures at the one millimeter and two centimeter positions was made which substantially agreed with the calculated values just given. The details of this analytical treatment are given in Appendix A-5.

10. Summary of the Pure Fuel Ignition Test Results

Several significant results were obtained from the experiments on the ignition of pure fuel samples in subsonic flow. The most informative of these results are, however, not quantitative in nature, but obtainable only from examination of the film records obtained from the tests. Consequently, one must be satisfied with verbal descriptions rather than concise, numerical compilations of cause and effect.

It was observed that the ignition delay depended quite strongly upon the oxygen mole fraction of the test gas. This data is shown quantitatively by the data points enclosed by a box in Figure 36. No ignition was observed at the leading edge of the fuel sample. The point of ignition on the top plate portion of the sample shifted downstream as the oxygen

content of the test gas was decreased; however, it could not be ascertained whether or not this shift was linear with respect to the oxygen content. Eighty percent oxygen caused ignition at the front of the sample but downstream of the leading edge, whereas ignition occurred at the downstream end of the sample in fifty percent oxygen. It should be mentioned that in pure oxygen, the ignition point was definitely downstream of the leading edge of the sample. The ignition delay, however, could not be accurately determined because ignition was very fast. Therefore, the tests in pure oxygen were not included in the fuel ignition data shown in Figure 36.

A sharp ignition cutoff was detected, and was observed to depend on the area of fuel exposed to the test gas, as well as the oxygen mole fraction present in the test gas. Uninhibited samples could not be ignited in less than 50% oxygen, while ignition of inhibited samples required greater than 60% oxygen in the test gas.

With regard to the dependence of fuel sample ignition on the amount of exposed fuel surface, two additional characteristics were observed. First, uninhibited fuel samples ignited in 62% oxygen at a point corresponding to the beginning of the exposed fuel surface of the inhibited samples. On the other hand, inhibited samples ignited at the most downstream portion of the exposed fuel surface under identical test conditions. Secondly, the uninhibited samples became completely enveloped in flame when tested in 62% oxygen; while the inhibited samples burned only on the far downstream portion of the exposed fuel surface.

Another significant result was obtained from examination of uninhibited samples tested in gas flows of pure nitrogen and oxygen-nitrogen mixtures containing less than 50% oxygen. No difference in the amount of fuel decomposition could be detected between samples tested in nitrogen and samples tested in the oxygen containing test gas mixtures. The test conditions, insofar as pressure, temperature, and flow velocity of the test gas are concerned, were the same as when ignition was obtained; only the oxygen content of the gas flow was changed.

Finally, the maximum surface temperature of a fuel sample in an inert gas flow was estimated to be 260° C. under the standard test conditions. The minimum temperature, at the end of the sample, can be estimated to be approximately 120° C. These estimates are based on the measurements obtained from Pyrex model, instrumented with thin film resistance thermometers.

11. Discussion of the Pure Fuel Ignition Test Results

As was expected from the results of the propellant ignition tests in supersonic flow, the fuel ignition tests indicated that a minimum boundary layer thickness was necessary for ignition. It may be noted that the shift in the ignition point is in qualitative agreement with a gas phase reaction. Intuitively, one would suspect that with a constant surface area of fuel supplying fuel vapors to the boundary layer, a decrease in oxygen concentration would decrease the diffusion of oxygen into the boundary layer. Therefore, a greater boundary thickness would be required in order to allow a stablized, reacting mixture to exist in the boundary layer. In addition, the fact that such a shift was observed indicates the dependence of ignition upon fuel supplied by convection from an upstream portion of the boundary layer, as well as the local supply directly from the fuel surface. Thus, the ignition point shift is quite easily explained on the basis of variations in concentration of reactants in the gas phase.

The existence of a sharp cutoff of ignition and its observed dependence on both oxygen mole fraction and the amount of exposed fuel surface, is most interesting. It may be recalled that the pure gas phase ignition model discussed in Part I, predicted the existence of such an ignition cutoff. This model showed that the cutoff would be observed if: (1) insufficient fuel was supplied to the hot gas environment, or (2) the consumption of gaseous oxidizer was very high, causing the temperature rise to be limited by oxidizer diffusion. In each case then, the maximum attainable temperature in the system was limited by the supply or consumption of one of the reactants. Furthermore, the intuitive argument of the preceding paragraph leads to the conclusion that limited oxygen diffusion could inhibit ignition.

On the other hand, the explanation of the results of the fuel ignition tests on the basis of an ignition controlling surface reaction is difficult. In the first place, no ignition cutoff is predicted by a surface reaction ignition mechanism, at least in the formulation given by Anderson and Brown (20). It's possible that a new formulation might predict such a result.

Disregarding the problem of the ignition cutoff, however, the dependence of the ignition point on the amount of exposed fuel surface with otherwise identical test conditions, might be attributed to differences in boundary layer cooling. It could be argued that a decrease in boundary layer cooling would be caused by heat generation at the surface on the upstream portions of the sample. Consequently, there would be decrease in the heat transfer to that portion of the sample,

causing a higher temperature boundary layer flow over the downstream portion of the sample and subsequently cause ignition there. Inhibition of the upstream portion of the sample would prevent such a heat generation, and cause a downstream movement of the ignition point. This argument could be applied to explain the differences which were observed in the extent of flame development between uninhibited and inhibited fuel samples tested in a sixty-two percent oxygen test gas. However, even though the argument just presented could be valid, the final result of the fuel ignition tests further tends to discredit the possibility of an energetic surface reaction existing, and controlling the ignition of the fuel samples. That is, one must consider the implications of the sample surface temperature estimates.

Now, the surface temperatures which were estimated to exist along the surface of these fuel models were entirely sufficient to initiate energetic surface reaction of the type used in (20) to correlate the data of McAlevy (12). It may be recalled that the fuel binder used in (12) and in the present tests was the same. In fact, according to (20), relatively rapid ignition of the order of five milliseconds should occur in forty percent oxygen, even at surface temperatures around 120° C. Therefore, one might expect significant differences in the amount of fuel decomposed in tests of uninhibited fuel samples exposed to a flow of pure nitrogen or a test gas containing forty percent oxygen. One may recall that this behavior was not observed, even within the relatively long testing time of thirty-five milliseconds which was available. Consequently, it is unlikely that such reactions were present to any great extent in the fuel ignition tests having higher percentages of oxygen in the test gas.

At this point, the results of some experiments in which polymeric fuels were exposed to a steady flow of oxygen and nitrogen at 300° C. for two hours should be mentioned. No significant differences in the amount of fuel decomposition were found between tests in the two gases. These experiments were independently carried out in this laboratory by Mr. Allen Giese.

Combination of the results of the fuel ignition tests and the tests performed by Giese, indicate that a surface reaction does not control the ignition of composite propellants insofar as exposure to oxygen is concerned. For more reactive oxidizers, the mechanism could well be correct.

12. Necessary Considerations in the Planning of Future Composite Solid Propellant Ignition Experiments

In conceiving future experiments on composite propellant ignition, it is necessary to keep several considerations clearly in mind. The usefulness of any new experimental data and the validity of its interpretation should be determined on the basis of the considerations discussed below.

By this time, the many studies of composite propellant ignition have substantiated the fact that increases in both pressure and quantity of externally supplied gas phase oxidizer, decrease the ignition delay. The former factor is important in a practical sense, but the practical consequences of the ignition delay's sensitivity to external gaseous oxidizer concentration less easy to see.

Now, it is most likely that any experiment conducted for the purpose of determining the ignition mechanism will include the above environmental changes and their apparent effect on the ignition delay. Accurate, unambiguous separation of pressure and heat transfer effects must be possible, however, if the experiment is to provide interpretable information about the ignition mechanism of the propellant.

The presently available mass of experimental data clearly demonstrates that gas phase chemical kinetic processes dominate the composite propellant ignition event, and not solid phase decomposition processes. In fact, there is good evidence that the establishment of a gas phase flame is necessary, if a practical ignition is to be achieved. In experiments in which the propellant heat-up times are long, these gas phase processes are obscured. Therefore, this type of experiment is unsuited for investigations of the composite propellant ignition mechanism.

One may recall that there remain two other concepts which have been proposed as the controlling mechanism of composite propellant ignition. These are an exothermic gas-solid reaction, and a purely gas phase reaction. It is clearly evident that none of the experiments to date allow positive proof of either mechanism. However, the experiments which have just been described strongly indicate that pure gas phase reactions control the practical ignition of composite propellant ignition. An obvious conclusion, therefore, is that any further experiments which only measure the ignition delay's dependence on gross environmental changes, are limited in value. The reason is that such experiments lack the resolution necessary for ignition mechanism determination. Consequently, experiments which measure or detect events during

the ignition process itself, are needed if the ignition mechanism question is to be resolved. Alternatively, subtle, comparative experiments are required, providing the results can be positively interpreted.

An example of the former type of experiment is simultaneous monitoring in time of the light emission and surface temperature of a propellant sample exposed to a hot, reactive environment. A knowledge of the relative times at which sharp changes occur in these quantities would give valuable insight into the nature of the ignition process of the propellant. If light emission is detected before, or at the start of, a rapid climb in the propellant surface temperature, it must be concluded that it is the start and development of a gas phase ignition which controls the propellant ignition. On the other hand, if the surface temperature exhibits a sharp runaway before any light emission is detected in the gas phase, then it must be concluded that a heterogeneous, exothermic reaction at the propellant surface is important in the ignition event. Such evidence would strongly indicate the dominance of surface reactions in the ignition of solid propellants exposed to highly oxidative gases.

Another attack on the problem of the composite propellant ignition mechanism requires a theoretical description of both gas phase and surface reactions occurring in the presence of a gas flow over a propellant sample. The results of these theories could be compared to the experimental results described earlier.

Finally, a theoretical description of gas phase ignition of vapors issuing from a propellant sample heated in an arc-image furnace would be valuable. This theory would indicate the conditions under which a propellant sample heated in this manner could ignite well away from the surface. Agreement of this theory, with further arc-image furnace propellant ignition studies in which the sample is irradiated up through the ignition delay, would provide significant discrimination between the gas phase or surface reaction ignition mechanisms.

REFERENCES FOR PART I

I.1 Van't Hoff, Etudes de Dynamique Chimique, 161, Amsterdam, 1844

I.2 Quoted after Jouget, Mechaniqu des Explosifs, 141, Paris, 1937. See also: TAFFANEL, Comptes Rendes, 156, 1544 (1913); 157, 469, 595, 714 (1913).

I.3 N. N. Semenov, Z. physik. Chem., 48, 571 (1928)

I.4 P. H. Thomas; Proc. Roy. Soc., A262, 192 (1961)

I.5 P. W. M. Jacobs and A. R. Tariq Kureisky, Ninth Symposium (International) on Combustion, Academic Press, New York, 366 (1963)

I.6 D. A. Frank-Kamenetskii, Diffusion and Heat Exchange in Chemical Kinetics, Princeton University Press, (1955)

I.7 Todes, Zhur. Fiz. Khim.; 4, 71 (1933); 13, 868 (1939); 13, 1594 (1939); 14, 1026 (1940); 14, 1447 (1940); 14, 1447 (1940); Acta Physicochimica, 5, 785 (1936)

I.8 Rice, J. Amer. Chem. Sec. 57, 310, 1044, 2212 (1935); J. Chem. Phys., 7, 701 (1939)

I.9 L. N. Khitrin and S. A. Goldnburg, 6th Symposium (International) on Combustion, Rheinhold, New York, 545 (1957)

I.10 L. N. Khitrin, 7th Symposium (International) on Combustion, Butterworths, London, 470 (1959)

I.11 Tau-Yi Toong, 6th Symposium (International) on Combustion, Rheinhold, New York, 532 (1957)

I.12 F. E. Marble and T. C. Adamson, Jr.; Selected Combustion Problems, Butterworths (London), 111 (1954)

I.13 D. A. Dooley; Combustion in Laminar Mixing Regions and Boundary Layers; Calif. Inst. of Technology, JPL Memorandum 20-151, June 1, 1956

I.14 W. Jost; Zeit. Phys. Chem., 4, 196 (1950)

I.15 G. von Elbe, 4th Symposium (International) on Combustion, Williams and Wilkins, Baltimore, Md., 13 (1953)

I.16 B. P. Mullins, Spontaneous Ignition of Liquid Fuels, AGARDograph No. 4, Butterworths, London, (1955)

REFERENCES FOR PART I-contd.

I.17 R. S. Brokaw, Selected Combustion Problems, II; AGARD Publication, Butterworths, London, 115 (1956)

I.18 C. C. Swett, Jr., 3rd Symposium (International) on Combustion, Williams and Wilkins Co., Baltimore, Md., 353 (1949)

I.19 M. V. Blanc, P. G. Guest, G. von Elbe, and B. Lewis, 3rd Symposium (International) on Combustion, Williams and Wilkins Co., Baltimore, Md., 363 (1949)

I.20 C. C. Swett, Jr., 6th Symposium (International) on Combustion, Rheinhold, New York, 523 (1957)

I.21 J. W. Mullen, II, J. B. Fenn, and M. R. Irby, 3rd Symposium (International) on Combustion, Williams and Wilkins Co., Baltimore, Md., 317 (1949)

I.22 H. P. Stout and E. Jones, 3rd Symposium (International) on Combustion, Williams and Wilkins Co., Baltimore, Md., 329 (1949)

I.23 S. Kumagai and I. Kimura, 6th Symposium (International) on Combustion, Rheinhold, New York, 554 (1957)

I.24 M. Steinberg and W. E. Kaskan, 5th Symposium (International) on Combustion, Rheinhold, New York, 664 (1955)

I.25 W. C. F. Sheperd, 3rd Symposium (International) on Combustion, Williams and Wilkins Co., Baltimore, Md., 301 (1949)

I.26 T. V. Bozhenova and R. J. Soloukhin, 7th Symposium (International) on Combustion, Butterworths, London, 866 (1959)

I.27 T. Asaba, K. Yoneda, N. Kekihara, and T. Hikita; 9th Symposium (International) on Combustion, Academic Press, New York, 193 (1963)

I.28 N. S. Enikolopyan, 7th Symposium (International) on Combustion, Butterworths, London, 157 (1959)

I.29 R. S. Brokaw and J. L. Jackson, 5th Symposium (International) on Combustion, Rheinhold, New York, 563 (1955); NACA RME54B19

I.30 R. E. Miller, 7th Symposium (International) on Combustion, Butterworths, London, 417 (1959)

REFERENCES FOR PART I-contd.

I.31 C. J. Chang, A. L. Thompson, and R. D. Windship, 7th Symposium (International) on Combustion, 431 (1959)

I.32 H. F. Coward, J. Chem. Soc., 1382 (1934), (Work of H. B. Dixon)

I.33 B. P. Mullins, Fuel, London, 32, 343 (1953), N.G.T.E. Report R96, (1951)

I.34 N. Nishiwaki, 5th Symposium (International) on Combustion, Rheinhold, New York, 148 (1955)

I.35 W. J. Levedahl, 5th Symposium (International) on Combustion, Rheinhold, New York, 372 (1955)

I.36 B. P. Mullins, Fuel, 28, 205 (1949)

I.37 E. Lonn, Luftfarht-forschung, 19, 344 (1943)

I.38 Y. Laure, C. R. Congr. Chim. Ind. 18th Cong., 412, Noncy, Sept.-Oct. (1938); Publ. Sci. Aviat., 162 (1943); Publ. Sci. Minist. Air, 91, 67 (1950)

I.39 H. H. Wolfer, Torschungsh. Forsch. Geb. Ing., 392, 15 (1938)

I.40 J. O. Hirschfelder, 9th Symposium (International) on Combustion, Academic Press, New York, 553 (1963)

I.41 R. Anderson and R. Brown; oral presentation, AFOSR Contractors Meeting, Applied Physics Laboratory of Johns Hopkins, March, 1963

I.42 R. F. McAlevy, III, P. L. Cowan, and M. Summerfield, Solid Propellant Rocket Research, Vol. 1 of ARS series on Progress in Astronautics and Rocketry, Academic Press, 623 (1960). See also: R. F. McAlevy, III, The Ignition Mechanism of Composite Solid Propellants, Ph.D. Thesis, Princeton University, Aeronautical Engineering Laboratory Report No. 557, June, 1961

I.43 Robert D. Richtmeyer, Difference Methods for Initial Value Problems, Interscience Publishers, Inc., New York, (1957)

I.44 Fritz John, On the Integration of Parabolic Equations by Difference Methods, Communications on Pure and Applied Mathematics, 5, 155 (1952)

REFERENCES FOR PART I-contd.

I.45 G. E. Forsythe and W. R. Wasow, Finite-Difference Methods for Partial Differential Equations, John Wiley and Sons, New York (1960)

I.46 B. L. Hicks, J. Chem. Phys., 22, 414 (1954)

I.47 J. B. Zeldovich, J. Exp. Tech. Phys. (URSS), 9, 1530 (1939)

I.48 E. S. C. Meyerink and S. K. Friedlander, Diffusion Controlled Reactions in Fully Developed Turbulent Pipe Flow, Johns Hopkins University, Dept. of Chem. Eng'g., May, (1960)

I.49 D. E. Rosner, A.I.Ch.E. Jour., 9, 3, 321 (1963)

I.50 R. B. Biad, W. E. Stewart, and E. N. Lightfoot, Transport Phenomena, 1st Ed., John Wiley & Sons, New York, (1960)

REFERENCES FOR PART II

1. D. A. Frank-Kamenetskii; Acta Physiochim, URSS, 10, 365 (1939)

2. E. K. Rideal and A. J. B. Robertson; Proc. Roy. Soc. A, 195, 135 (1948)

3. G. B. Cook, Proc. Roy. Soc. A, 246, 154 (1958)

4. J. Zinn and C. L. Mader; J. Applied Phys., 31, 323 (1960)

5. D. Altman and A. F. Grant, Thermal Theory of Solid Propellant Ignition by Hot Wires - Fourth Symposium on Combustion, Williams and Wilkins Co., Baltimore, Md., 158, (1950)

6. M. A. Cook and F. A. Olson, A.I.Ch.E. Jour., 1, 391 (1955)

7. M. A. Cook; The Science of High Explosives, ACS Monograph No. 139, Rheinhold Co., (1958)

8. S. W. Churchill, R. W. Kruggel, and J. C. Brier, A.I.Ch.E. Jour., 2, 4, 568 (1956)

9. J. F. Roth and G. P. Wachtell, I&EC Fundamentals, 1, 1, 62 (1962)

10. N. W. Ryan, A. D. Baer, and D. L. Salt, Solid Propellant Rocket Research, Vol. 1 of ARS series on Progress in Astronautics and Rocketry, Academic Press, 623 (1960)

11. A. D. Baer, Ignition of Composite Rocket Propellants, Ph.D. Thesis, University of Utah, June, 1959

12. R. F. McAlevy, III, P. L. Cowan, and M. Summerfield, Solid Propellant Rocket Research, Vol. 1 of ARS series on Progress in Astronautics and Rocketry, Academic Press, 623 (1960)

13. R. F. McAlevy, III, and M. Summerfield; ARS Jour., 32, 2, 270 (1962)

14. N. Fishman and R. B. Beyer; Solid Propellant Rocket Research, Vol. 1 of ARS series on Progress in Astronautics and Rocketry, Academic Press, 673 (1960)

15. H. Wise and M. Evans; private communication, March, 1963

16. E. H. Grant, Jr., Lt. USN, A Study of the Ignition Process of Composite Solid Propellants in a Small Rocket Motor, Master's Thesis, Princeton University, October, 1963

17. R. W. Lancaster, Lt. USN, Experimental Investigation of the Ignition Process of Solid Propellants in a Practical Rocket Motor Configuration, Master's Thesis, Princeton University, 1961

18. B. L. Hicks; J. Chem. Phys., 22, 414 (1954)

19. T. L. Bircumshaw and B. H. Newman, Proc. Roy. Soc. A, 227, 228 (1954-1955)

20. R. Anderson and R. Brown; oral presentation, AFOSR Contractors Meeting, Applied Physics Laboratory of Johns Hopkins, March, 1963

21. R. F. McAlevy, III, The Ignition Mechanism of Composite Solid Propellants, Ph.D. Thesis, Princeton University, Aeronautical Engineering Laboratory Report No. 557, June, 1961

22. I. I. Glass, W. Martin, and G. N. Patterson, A Theoretical and Experimental Study of the Shock Tube, Institute of Aerophysics, University of Toronto, UTIA Report No. 2, November, 1953

23. Bureau of Ordnance Publication, Handbook of Supersonic Aerodynamics, NAVORD Report No. 1488, Vol. 5 (1953)

24. C. E. Wittliff, M. R. Wilson, and A. Hertzberg, The Tailored Interface Hypersonic Shock Tunnel, paper presented at the ASME-ARS Aviation Conference, Dallas, Texas, March 16-20, 1958. Also, see Journal of the Aero/Space Sciences, Vol. 26, No. 4, April, 1959

25. R. J. Vidal and J. H. Hilton, The Construction and Application of a Rapid Response Resistance Thermometer Probe, C.A.L. Report No. 1M-1062-A-1, April, 1956

26. J. N. Bradley, Shock Waves in Chemistry and Physics, Wiley Press, (1962)

27. A. Ferri, Fundamental Data Obtained from Shock Tube Experiments, Pergamon Press, (1961)

28. W. B. Brower, An Investigation of the Flow Due to Shock Impingement on a Constriction, RPI TRAE6107, August (1961)

29. Sibulkin, JAS, 19, 8, 570 (1952)

REFERENCES FOR PART II-contd.

30. M. F. Romig, ARS Jour. (JP), 26, 12, 1098 (1956)

31. R. Mark, Compressible Laminar Heat Transfer Near the Stagnation Point of Blunt Bodies of Revolution, CONVAIR, Report ZA-7016, 11 April, 1955

32. H. S. Carslaw and J. C. Jaeger, Conduction of Heat in Solids, 2nd Ed., Oxford Press, London, (1959)

33. L. Holland, Vacuum Deposition of Thin Films, Wiley, (1958)

34. S. H. Goldenburg, ARS Jour., 31, 5, Russian supplement, 691, (1961)

35. C. A. Ford, I. I. Glass, An Experimental Study of Shock Wave Refraction, University of Toronto, Institute of Aerophysics, UTIA Report No. 29

APPENDICES

A-1. THE BASIC SHOCK TUBE

An exceedingly brief description of a shock tube follows, for the benefit of those unfamiliar with this prevalent basic research tool. For scientific purposes, the shock tube is a valuable tool for controlled creation of very high temperatures and pressures for times of a few milliseconds duration. In essence, the simple shock tube is a closed tube divided into two sections separated by a frangible diaphragm. One section, termed the "driver" section, is pressurized to some desired level and the diaphragm burst at that point, either by ordinary pressure stress or some mechanical means. At diaphragm burst, the high pressure gas contained in the driver section is released into the other section of the shock tube, which is termed the "driven" section. Because of the disparity of pressures in the driver and driven sections, a shock wave is formed and propagates down the driven section and is maintained by the expansion of the high pressure driver gas into the driven section. An expansion wave, or fan, is generated, ideally at the instant of diaphragm burst and the shock wave formation. This expansion fan is necessary to decrease the driver gas pressure remaining in the driver section to the pressure behind the shock wave propagating into the driven section. Consequently, the expansion propagates into the driver section, opposite to the direction of the shock wave propagation. Both waves reflect from their respective ends of the shock tube and interact a number of times and become steadily weaker until a quiescent state is obtained in the shock tube as a whole.

For shock Mach numbers ≤ 2, the gases in the shock tube may be considered to have constant specific heats, and it is possible to determine an algebraic relationship between the pressure ratio across the diaphragm, at burst, (P_{41}) and the pressure ratio across the shock wave, (P_{21}). The relationship, from reference 23, is

$$P_{41} = P_{21}\left[1-(P_{21}-1)\sqrt{\frac{\left(\frac{\gamma_4-1}{2\gamma_4}\right)\frac{1}{e_{41}}}{\left(\frac{\gamma_1+1}{\gamma_1-1}\right)P_{21}+1}}\right]^{\frac{2\gamma_4}{\gamma_4-1}}$$

where P_{41} is the internal energy ratio across the diaphragm. For $M_s > 2$, variable specific heats and iterative numerical calculations must be used to compute the desired parameters. Fortunately, constant specific heat calculations

are reasonably correct up to $M_s = 4$, and were used for the necessary calculations pertinent to this experimental program. In passing it may be noted, from the above equation, that an increase in $(\mathcal{C}_{41})$ decreases the value of P_{41} required for any specific shock strength P_{21}. It is desirable, therefore, to use a gas having a higher specific heat as the driver gas, driving a gas having a low specific heat. For ease of operation and safety, helium with a Cv = 0.746 cal/gm° K., was the standard driver gas used in these experiments. The specific heat of the driven gas, a mixture of nitrogen and oxygen, was approximately 0.17 cal/gm° C.

In general use of shock tubes for research purposes, the useful experimental conditions are immediately after the shock wave and after the reflected shock wave. Both regions are limited to short experimental test times; however, extended test times after the reflected shock wave may be obtained by operation of the shock tube in the "tailored interface" condition.

A-2. THE TAILORED INTERFACE CONDITION

The tailored interface condition is defined as that condition where the reflected shock wave stagnates the incident interface between driver and driven gases which follows the shock wave, passing smoothly through the interface and leaving a volume of stagnant, doubly shocked gas at the highest temperature in the system near the end wall. Thus, it is necessary that both the driver and driven gases be brought to equal pressure and velocity by the passage of the reflected shock wave. Ideally the stagnant gas volume is at uniform temperature and pressure and practically these quantities are quite uniform. The tailored interface is destroyed by the arrival of the expansion fan which was reflected from the head end of the driver section; therefore, the testing time is the time interval between shock reflection and the arrival of the expansion fan.

Theoretically, it is possible to determine the initial driver gas temperature and pressure to have the reflection of any incident shock "tailor" the interface, see references (22), (23), and (24). However, in practical shock tube operation, the driver and driven gases are at the same temperature and there is a unique M_s which will produce the tailored condition, depending upon the driver and driven gas compositions. For helium driving air assuming constant specific heats, this M_s was calculated to be 3.4, which agrees with the experimental results of reference (35). In reference (24), experimental results showed that effective tailored interface conditions were obtained for $3.4 \leq M_s \leq 4.2$ for

helium driving air. Reference (21) showed tailoring could be accomplished down to $M_s = 3.0$.

Establishment of the tailored interface condition was slightly more critical in the shock tunnel used by the author. Tailoring was accomplished over the range $3.5 \leq M_s \leq 3.9$ for helium driving air. The probable explanation is that the presence of the nozzle and the consequent exhaust gas flow to the dump tank made the tailored interface condition more difficult to achieve. Since the author's investigation was not concerned primarily with shock tunnel operation, this criticality of the condition was accepted and no theoretical explanation was searched for.

It was desirable, in the course of these experiments, to attain a tailored condition at lower incident shock Mach numbers. Now, the condition for tailored interface operation may be stated in two equivalent ways. The first way is to state that the velocities and pressures on either side of the interface must be equal after the passage of the reflected shock. The second way is a requirement on the specific energy ratio across the interface. For computational purposes, the second statement allows straightforward calculations.

$$\left(\frac{C_{v_3}}{C_{v_2}}\right)\left(\frac{\bar{M}_2}{\bar{M}_3}\right)\left(\frac{T_3}{T_2}\right) = e_{32} = \frac{\frac{\gamma_3+1}{\gamma_3-1} + P_{25}}{\frac{\gamma_2+1}{\gamma_2-1} + P_{25}}$$

Assuming constant specific heats, the above equation may be written as

$$\left(\frac{C_{v_4}\,\bar{M}_1}{C_{v_1}\,\bar{M}_4}\right) T_{34} \cdot T_{12} = \frac{\frac{\gamma_4+1}{\gamma_4-1} + P_{25}}{\frac{\gamma_1+1}{\gamma_1-1} + P_{25}} = e_{41}$$

It is evident that with an increase in molecular weight and a decrease in the specific heat of the driver gas, the specific energy ratio, e_{41}, is decreased and the tailored interface net at reduced values of the incident shock Mach number.

The necessary reduction of ϵ_{41} was obtained by using a mixed helium-nitrogen driver gas; results of calculations to determine the shock Mach number for tailoring with varying percentages of nitrogen driver gas diluent are shown in Figures 20 and 21. The theoretical pressure ratio across the diaphragm, P_{41}, necessary to attain a given shock Mach number, when various percentages of nitrogen are present in the helium driver gas, is shown in Figure 22 for the range of nitrogen percentages of interest in the experiment. Figure 23 shows the temperature and pressure ratios after tailored interface shock reflection as a function of helium mole fraction in the driver gas. The helium mole fraction in the driver gas was checked with a thermal conductivity cell manufactured by the Gow-Mac Instrument Company, model number 210-L. Sampling was done from high pressure tanks used for mixing and storage of the driver gas.

A-3. INSTRUMENTATION

1. Shock Sensors

The shock sensors were used to obtain shock velocity measurements and the necessary trigger signals for other instrumentation, and consisted of thin-film, platinum resistance thermometers mounted in the wall of the shock tube near the end wall.

Their construction was as follows:

a. Pyrex glass sheets, 2 mm. thick, were uniformly painted with Hanovia-05X Bright printed circuit paint, thinned with Trichlorethylene to about 1/2 the "out of the bottle" consistency. The glass plates were wiped clean with acetone prior to painting.

b. Painted plates were oven dried at 52° C. for about 5-8 hours or until the characteristic odor of the paint had disappeared. The oven was ventilated to remove the paint vapors.

c. Dried plates were then baked in a high temperature oven at 250° C. until the brown paint residue had disappeared, approximately 2 hours. The oven door was slightly ajar to allow paint vapors to escape. Once the residue had disappeared, the oven temperature was raised to 700° - 750° C. until the glass had slightly softened, causing a good bond between the glass and platinum film. The glass was removed, then allowed to cool, and cut to the desired size for mounting.

To obtain a useful signal for triggering purposes, the mounted gauges complete an electrical circuit

as sketched below.

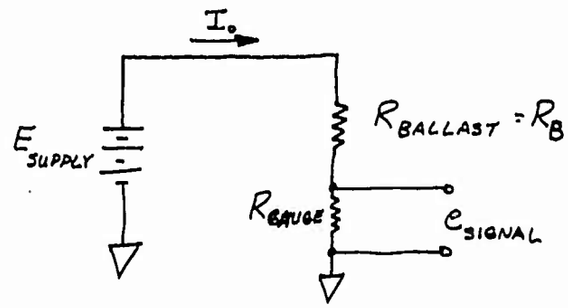

The gauge resistance changes with temperature. This resistance change, for small temperature changes, is given by $R_G = R_o (1 + \alpha \cdot \Delta T)$ where R_o is the ambient temperature resistance, (α) is the temperature coefficient of resistance in ^oK and ΔT is the temperature change. The magnitude of the signal is given by

$$e_s = E_s R_o \left(\frac{1+\alpha \Delta T}{R_B + R_o(1+\alpha \Delta T)} - \frac{1}{R_B + R_o} \right) \simeq \frac{I_o R_B \Delta R}{R_o + R_B}$$

where I_o = current through the undisturbed circuit. The maximum signal, e_s, is obtained when

$$R_B = R_o (1 + \alpha \Delta T)$$

A current of I_o = 12 ma was used for all thin film gauges.

These thin-film gauges had an $\alpha = 0.00224/^o$ C., which is in close agreement to the value found in reference (25). Reference (25) contains an expanded account of resistance thermometer development and use in shock tube research. Thin-film gauges have a response time of about one microsecond when the film thickness of platinum is one micron or less.

2. Amplifiers

The signal obtained from the shock sensors were amplified by three-stage, solid state amplifiers developed for this purpose. Solid state amplifiers were chosen because of their insensitivity to the intense vibration caused by the

diaphragm rupture. The microphonics of tube amplifiers were far too great for this application causing undesired and premature triggering of electronic recording equipment.

The amplifiers, as finally developed, had a working gain of 8000, providing an 8 volt trigger voltage of 5 usec duration for a one millivolt signal from the shock sensors. These amplified shock sensor pulses triggered the time interval meter used for shock speed determination and the oscilloscope used to obtain a display of the pressure gauge signals.

The presence of high intensity electric noise also caused random, premature signals to be impressed on the shock sensor signal wires. After amplification, these signals were sufficient to trigger the electronic apparatus needed in the experiment. Noise reduction to acceptable levels was accomplished in the following manner. A common ground, the shock tunnel, was made for the entire electrical system, and the shock tunnel itself well grounded at one point only. Secondly, the signal wires from the shock sensors were well shielded with Metex RF screening and two stages of amplification were mounted as close as possible to the shock sensors on vibration absorbing mounts. The power supplies for individual shock sensors were contained in the close mounted two-stage amplifier associated with each sensor. These precautions were necessary because of the large quantities of electrical noise generated by the starting up of the Fastax camera which of necessity was in close proximity to the sensors. Before these measures were taken, the start up of the Fastax camera shortly prior to the diaphragm burst, triggered the electronic apparatus needed for recording the shock tunnel operation during each test run.

A schematic of the amplifiers, as finally developed, is shown in Figure (24).

A-4. OTHER EQUIPMENT

1. Supersonic Nozzle Design

A conical, converging-diverging supersonic nozzle was designed on the basis of tailored interface shock tunnel operating conditions. These conditions, for pure helium driving air are typically--using ambient conditions of 300° K. and one standard atmosphere--2200° K. and 330 psia. The experimental observations of Ryan (10) indicated that approximately 70% of the available test gas was cooled by interface mixing under tailored interface operating conditions. Therefore, the supersonic nozzle was designed to exhaust 25% of the test gas during the available testing time of about

24 msec., resulting in a steady state mass flow rate of 0.687 pounds/second. Calculation showed a throat diameter of 0.624 inches was necessary to achieve this mass flow for the minimum projected test gas pressure of 200 psia. The final nozzle design had the following dimensions and characteristics:

Throat Diameter = 0.624"
Exit Diameter = 1.00"
Area Ratio = 0.435
Exit Mach Number = 2.35

The calculated starting time for this nozzle under average conditions was approximately 50 microseconds.

The nozzle exhausted into a dump tank of sufficient volume to maintain a subatmospheric pressure during the testing time. Therefore, the nozzle was operating in a normally underexpanded condition, resulting in a region of expansion which started at the periphery of the nozzle exit and extended downstream. A two-dimensional analysis of such underexpanded operation indicated that the head of the expansion fan reached the nozzle center line three inches downstream of the nozzle exit plane.

The nozzle projected through the end wall of the shock tube, with the entrance plane flush with the wall, and was retained by a flush mounted retainer ring.

A "spider" assembly, affixed to the rear portion of the nozzle, allowed installation of aerodynamically shaped propellant models on the nozzle center line and in the region of constant pressure, undisturbed nozzle flow after the exit plane.

Figures 26 and 27 show the supersonic nozzle configuration, including the retainer ring, spider assembly, and mounted hemisphere cylinder propellant sample. Figure 28 shows nozzle and model mounted in the test section, as seen through one of the viewing ports of the test section, and Figure 29 shows an overall view of the test section, dump tank, and camera mounting.

For average shock tunnel operating conditions, the exhaust gas static and stagnation temperatures were 940° K. and 2200° K. respectively, at the exit plane. For models in a M = 2.35 flow, the ideal stagnation pressure ratio across the bow shock is 0.708. Therefore, the stagnation pressure at the model's stagnation point was 230 psia, typically.

2. Subsonic Nozzle

A two-dimensional nozzle was designed to test composite propellant ignition in a low speed, high temperature,

high pressure gas flow. Provision for viewing the model under test was accomplished by gluing "selected commercial" quality quartz windows to inset regions on the sides of the nozzle with Eastman Kodak-910 cement, a pressure setting epoxy cement. This method was very satisfactory and was used for sealing all inspection ports in the shock tunnel. A scale drawing of the subsonic nozzle, showing the mounting technique of the propellant samples is given in Figure 37.

For ease of construction, the nozzle was made axisymmetric, with steel inserts which faired smoothly with the inset inspection windows. The internal bore of the nozzle was, therefore, almost two-dimensional, having a 30^{o} converging entrance section, with a three-inch long, constant area, test section followed by a further 30^{o} converging section to the throat diameter. All metal parts were constructed of carbon steel, nickel coated to prevent rust formation and corrosion caused by the deposit of propellant sample combustion products.

Standard shock tunnel operation during subsonic ignition tests utilized mixed 94% helium-6% nitrogen driver gases to obtain a tailored interface condition at $M_s = 2.55$. Test gas temperatures after shock reflection were calculated to be 1120^{o} K. With this gas temperature and a 0.294 inch diameter orifice, the test gas flow velocity was approximately 60 feet per second. In theory, for constant incident shock Mach number and constant area ratios between the nozzle test section and exit orifice, the gas velocity is independent of pressure level. Experimentally, this was shown to be true by determining the transit time of small glowing particles, recorded by high speed photography, introduced into the shock tunnel for this purpose.

Reference (28) showed that a shock wave, incident upon a constriction, is partially transmitted and partially reflected, the transmitted shock being slightly stronger than the incident shock. A shock diffuser consisting of a steel plate having a 40% open area, was installed in the nozzle entrance to prevent passage of a strong transmitted shock through the nozzle. Calculations predicted a temperature drop of approximately 50^{o} K. would occur in the test gas flowing through the shock diffuser. Such a temperature drop was negligible in terms of the experiment and was reproducible, for constant shock tunnel operating conditions. Experiments showed that the nozzle fill time was one millisecond--a small time compared to observed ignition times--and free from strong shocks.

The exhaust gas flow from the subsonic nozzle was absorbed by the dump tank, and the exit orifice remained choked during the test time. Pressure measurements in the

nozzle test section showed constant pressure throughout the test time, after the one millisecond nozzle fill time.

Propellant samples, machined in the shape of a thick flat plate with a sharp leading edge, were mounted in the constant area section of the nozzle. The mounting post, inserted through the wall of the nozzle and held in place by a screwed-on cap, was pressure sealed by an O-ring around the periphery of its base.

The propellant samples were cast on a metal sting and secured to the mounting post by means of a bolt passed through the mounting post, as shown in Figures 37 and 39.

3. Ignition Model Preparation

1. Formulation

Solid propellant samples used in these experiments were of the composite type, formulated from Rohm and Haas polyester styrene resin Type P-13 fuel binder and ammonium perchlorate oxidizer. Two basic compositions were used during the course of the experiment. Supersonic flow ignition tests were made with a propellant formulation 80%, by weight, of ammonium perchlorate having a bimodal distribution and 20%, by weight, of fuel binder. Figure 34 gives a detailed formulation list. In the subsonic flow tests, a 78% oxidizer and 22% fuel propellant formulation was used; because of model shaping requirements the oxidizer was unimodal, with a mean particle diameter of fifty microns. The complete formulation is given in Figure 34. Ignition experiments were performed in subsonic flow with models constructed from the same fuel binder as used in the propellant formulations. The detailed formulation of this fuel is also given in Figure 34.

2. Casting and Shaping of Models

Hemisphere-cylinder propellant models for supersonic ignition tests were cast in the form of strands and shaped to the desired hemisphere-cylinder configuration with a special model shaper. This shaper was mounted on a small bench-top lathe and the propellant strand chucked into the lathe; high turning speeds and small cuts resulted in acceptably smooth and regular finishes on the models.

The two-dimensional wedge models were formed by cutting the desired shape and size propellant sample from 6" x 1" x 1/4" cast strips of propellant. New, degreased razor blades were used for the cutting of the propellant; the cuts were guided by a homemade jig to obtain reproducible models.

Both the propellant and pure fuel mixes for the subsonic flow ignition tests were cast into Teflon molds capable of holding the necessary sample stings. Figure 38 shows a typical mold; one side is left off in order to show the stings to which the mix adhered. After curing the mix, the mold was disassembled and cut into blocks. Each block contained a mounting sting. The stings were mounted in a milling attachment placed on a large lathe and shaped to the desired form--a thick flat plate with a sharp leading edge--with an end mill. Figure 39 shows a completed subsonic test sample mounted on the sample mounting post used to hold the sample in the subsonic nozzle. The best wedge angle was found to be 46°, see sketch.

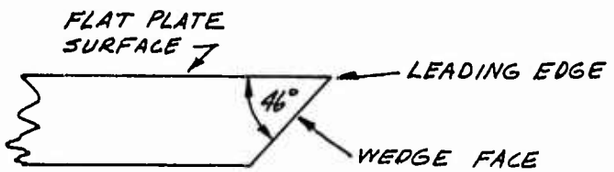

A-5. SAMPLE SURFACE CONDITIONS

1. Supersonic Flow: Stagnation Point Heat Transfer, Surface Temperature

The region of highest heat transfer to a hemisphere-cylinder exposed to hypersonic or supersonic flow, is in the neighborhood of the stagnation point. Heat transfer calculations for this region have been prevalent in recent literature because of the interest in missle nose cone re-entry and high speed flight, see references (29) and (30). A simple estimation of the heat transfer to the hemisphere cylinders of propellant used in the supersonic flow ignition experiments was made. The method of estimation was based on Romig's (30) treatment of stagnation point heat transfer for nonablating surfaces. The steady state heat flux was estimated to be 740 BTU/ft^2 sec., approximately; the enthalphy of the test gas at the surface of the model was neglected compared to the test gas stagnation enthalpy.

It was assumed that the estimated heat flux was constant during the time period between nozzle flow start and any chemical reaction. Mass transfer cooling effects were neglected also. Using the estimated heat flux of 740 BTU/ft^2 sec., a transient solution, reference (32), of a semi-infinite body subjected to this constant heat flux was obtained and used to estimate the temperature-time history at the stagnation point of the model. Results of this calculation are given in

the following table for a solid like the polymeric P-13 fuel and solid ammonium perchlorate. Approximate material property values were used.

Time, msec.	$(T_{surface}-T_{ambient})^{\circ}K.$	
	Fuel (P-13)	NH_4ClO_4
0	0	0
0.1	167	91
1.0	576	314
2.0	745	406

The temperature-time history of the propellant model's stagnation point probably was a step jump in temperature followed by a slow rise and the calculated history is undoubtedly only a rough estimate. However, the estimate does indicate that model surface temperatures of sufficient magnitude to cause ammonium perchlorate and P-13 pyrolysis rates competitive should have been attained, see reference (21), Figure 29.

2. Subsonic Flow Model Surface Temperature

a. Measurement

An instrumented, thick flat-plate model was constructed, with thin film platinum resistance thermometers located 1 mm. and 2 cm. back from the leading edge of the model. The flat plate surface and leading edge was constructed of Pyrex glass and was fastened to the Kel-F main body of the model with Eastman Kodak 910 glue. The necessary instrumentation leads were passed through a special mounting post, also constructed of Kel-F, and brought outside the shock tunnel. Figure 40 shows the completed gauge for surface temperature measurement at the 2 cm. position.

A voltage trace obtained from the leading thin-film gauge (1 mm. from leading edge) is shown in Figure 41. The temperature corresponding to the voltage measured was obtained from the relation

$$\Delta T = \frac{\Delta E \left(R_B + R_{GAUGE}\right)}{I_o \left(R_B \cdot R_{GAUGE}\right) \cdot \alpha}$$

The shape of the voltage/temperature signal in Figure 41 is interesting because of the relative constancy of signal level after the fast initial rise. A simple, transient,

heat conduction model was formulated to check the temperature history indicated by the thin-film gauge trace. Results of this calculation, given in the next section, indicate that the behavior shown in Figure 41 is to be expected.

b. Heat conduction model for a model placed in a subsonic flow

Consider a slab, $0 \leq x \leq a$, suddenly in perfect contact with a semi-infinite solid, $x > a$, at a time greater than zero. It is assumed that the slab is composed of a constant density gas at a high uniform temperature Tg, with the X = 0 boundary maintained at Tg for all time, and the solid is initially at a temperature To. We desire to determine the temperature-time history of the boundary, X = a.

Mathematically, the problem is the solution of the following partial differential equations with the given initial and boundary conditions. A sketch is given for reference.

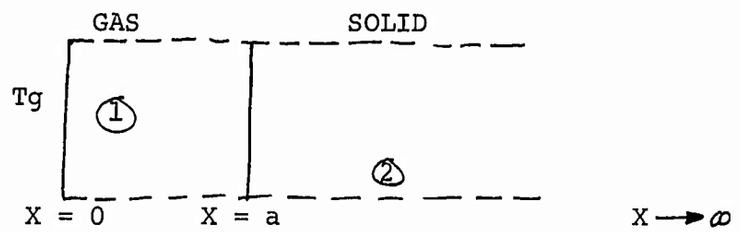

Region $0 \leq x \leq a$ $\quad \frac{\partial \theta_1}{\partial t} = \alpha_1 \frac{\partial^2 \theta_1}{\partial x^2}$

Region $x > a$ $\quad \frac{\partial \theta_2}{\partial t} = \alpha_2 \frac{\partial^2 \theta_2}{\partial x^2}$

$t \leq 0$: $\theta_1 = \theta_0 \quad 0 \leq x \leq a$

$\theta_2 = 0 \quad x > a$

$t > 0$: $\theta_1 = \theta_0 \quad x = 0$

$\theta_1 = \theta_2 \quad x = a$

$-k_1 \frac{\partial \theta_1}{\partial x} = -k_2 \frac{\partial \theta_2}{\partial x} \quad x = a$

$\theta_2 \to 0 \; ; \; x \to \infty$

WHERE $\theta = T - T_0$, $\theta_0 = T_g - T_0$

Taking the Laplace transform of equations and constraints, we obtain

$$\frac{d^2\bar{\theta}_1}{dx^2} - q_1^2\bar{\theta}_1 = -\frac{\theta_0}{p}$$

$$\frac{d^2\bar{\theta}_2}{dx^2} - q_2^2\bar{\theta}_2 = 0$$

$$\bar{\theta}_1 = \frac{\theta_0}{p}, \quad x=0$$

$$\bar{\theta}_2 = \bar{\theta}_1, \quad x=a$$

$$-k_1\frac{d\bar{\theta}_1}{dx} = -k_2\frac{d\bar{\theta}_2}{dx} \quad x=a$$

$$\bar{\theta}_2 \to 0, \quad x \to \infty$$

WHERE $q_i^2 = \frac{p}{\alpha_i}$ AND $\bar{\theta}_i = \mathcal{L}\{\theta_i\} = \int_0^\infty e^{-pt}\theta_i(t,x)\,dt$.

The general solution of the equations are

$$\bar{\theta}_1 = Ae^{q_1 x} + Be^{-q_1 x} + \theta_0/p$$

$$\bar{\theta}_2 = Ce^{-q_2 x}$$

The boundary conditions are used to evaluate the constants A, B, and C, and the solutions for $\bar{\theta}_1$ and $\bar{\theta}_2$ are

$$\bar{\theta}_1(x,p) = \frac{\theta_0}{p}\left[\frac{1}{\beta\tanh q_1 a + 1} - \frac{1}{2\sinh q_1 a}\right](e^{q_1 x} - e^{-q_1 x}) + \frac{\theta_0}{p}$$

$$\bar{\theta}_2(x,p) = \frac{\theta_0 e^{-q_2(x-a)}}{p[\beta\tanh q_1 a + 1]}$$

WHERE $\beta = \sqrt{k_2\rho_2 c_2}\Big/\sqrt{k_1\rho_1 c_1}$

The interface temperature, at X = a, may be found from the inverse Laplace transform of the equation evaluated at X = a. We write

$$\bar{\theta}_2(a,p) = \frac{\theta_0}{p[\beta \tanh q_1 a + 1]}$$

which after some algebraic manipulation, may be written as

$$\bar{\theta}_2(a,p) = \frac{\theta_0}{1+\beta}\left\{\sum_{n=0}^{\infty}(-1)^n \tau^n \frac{e^{-2nq_1 a}}{p} + \sum_{n=0}^{\infty}(-1)^n \tau^n \frac{e^{-(2n+2)q_1 a}}{p}\right\}$$

WHERE $\tau = \frac{1-\beta}{1+\beta}$

The inverse Laplace transform of $\bar{\theta}_2(a,p)$, $\theta_2(a,t)$ gives the interface temperature directly, as follows, as

$$T_2(a,t) - T_0 = \frac{\theta_0}{1+\beta}\left\{\sum_{n=0}^{\infty}(-1)^n |\tau|^n \left[\operatorname{erfc}\frac{na}{\sqrt{\alpha_1 t}} + \operatorname{erfc}\frac{(n+1)a}{\sqrt{\alpha_1 t}}\right]\right\}$$

or, with $\varphi = a/\sqrt{\alpha_1 t}$ the general interface solution is

$$\theta_2(\varphi) = T_2(\varphi) - T_0 = \frac{\theta_0}{1+\beta}\left\{\sum_{n=0}^{\infty}|\tau|^n \left[\operatorname{erfc} n\varphi + \operatorname{erfc}(n+1)\varphi\right]\right\}$$

Observe that as $\varphi \to 0$, $T_2(\varphi) \to T_g$. As $\varphi \to \infty$, $T_2(\varphi) \to T_0 + \frac{\theta_0}{1+\beta}$, or the solution approaches that of the problem of two semi-infinite bodies at different, uniform temperatures brought into sudden contact. These observations may be easily checked by the reader.

For the sake of completeness, the solution for $\theta_2(x,t)$ is

$$\theta_2(x,t) = \frac{\theta_0}{1+\beta} \sum_{n=0}^{\infty} |\sigma|^n \left[\operatorname{erfc}\left(\frac{x-a}{\sqrt{4\alpha_2 t}} - \frac{na}{\sqrt{\alpha_1 t}} \right) + \operatorname{erfc}\left(\frac{x-a}{\sqrt{4\alpha_2 t}} - \frac{(n+1)a}{\sqrt{\alpha_1 t}} \right) \right]$$

A graphical plot of the general solution of $\theta_2(a,t)/\theta_0$ versus $\phi = a/\sqrt{\alpha_1 t}$ is given in Figure 42, and a plot of $(\theta_2(a,t)/\theta_0)$ versus (t) is given in Figure 43. In both of these plots, a value of $\beta = (k_2\rho_2 c_2/k_1\rho_1 c_1)^{1/2} = 24.4$ was assumed, based upon average property values of the gas (air) and the solid (cured P-13). It must be pointed out that the ratio (θ_2/θ_0) depends upon the ratio $\sigma = \left(\frac{1-\beta}{1+\beta}\right)$ used in the evaluation; consequently, the curves shown in these figures will be shifted up or down, depending upon the physical properties assumed for the gas and solid. However, the shape of the curve in Figure 43 is substantially that observed in the experimental curve shown in Figure 41. Physically, the shape of the curves are explained as follows. At zero time, the body experiences a temperature jump and remains at a constant temperature until the cooling wave which propagates into the gas is reversed by the presence of a fixed high temperature at X = 0, the edge of the suddenly applied boundary layer. The presence of the fixed high temperature at X = 0 then causes heat to flow into the solid, raising the solid's surface temperature above the initial jump value.

A-6. ALUMINUM EVAPORATION TECHNIQUE FOR FUEL MODEL INHIBITION

Fuel models that were to be inhibited with a coating of aluminum were machined in the manner described in a previous Appendix (A-4). The wake regions, see sketch below, were then carefully trimmed and cleaned of all loose pieces of polymer formed by the shaping process by a careful brushing with Trichlorethylene and scraping with a sharp razor blade.

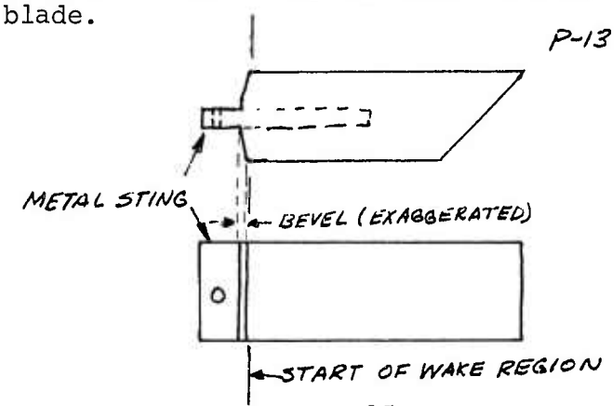

The models so prepared were mounted in holders which are shown in Figure 44. These holders allowed rotation of the models such that each model surface could be exposed to the evaporating aluminum. The holders were mounted on a stand which was internal to the bell jar when the bell jar was in its operating position. Figure 44 shows finished models as they were mounted on this stand. The bell jar is just visible in its withdrawn position. An excellent general reference describing the production and plating of thin metal films is a book by Holland, reference (33).

The aluminum to be evaporated was in the form of three-quarter inch lengths of one-eighth inch diameter wire, and was made to sit upon the heater elements situated in the base of the bell jar stand. The heater elements were three pieces of tungsten rod, one millimeter in diameter and about four centimeters long. They were mounted between heavy copper electrodes connected to the low tension power supply. The power supply was rated at 200 volt-amperes, with an output voltage of six volts.

The method model coating was as follows. The bell jar was placed over the stand which held the model holders and mounted models, and bell jar volume evacuated to a pressure of 3.5×10^{-6} mm. Hg. This was the minimum allowable vacuum for the production of acceptable aluminum films on the fuel models. It was important that the bell jar be left open to the high vacuum pumping system during the actual evaporation of the films. If this was not done, the pressure increased inside the bell jar to such a value that no evaporation was possible. During the evacuation, the models were bombarded by a gas discharge inside the bell jar to cause a further cleaning of the models and removal of any dust particles still present on them. (The gas discharge was not absolutely necessary, but its use appeared to aid the formation of acceptable coverings of aluminum on a greater percentage of the models.) After a pressure of 3.5×10^{-6} mm. Hg. was reached, current was passed through the heater elements until the aluminum was just melted and flowed over the heater elements; at this point, the current was removed and the aluminum allowed to cool slightly. A movable glass shield was kept over the heater elements during the initial melting of the aluminum in order to keep aluminum impurities from being evaporated on to the model surfaces. Current was then reapplied to the heater elements and the aluminum brought to a boil; boiling was observable, visually, by a flowing movement of the aluminum on the heater elements. The glass shield was then rotated away from the heater elements and the aluminum allowed to evaporate into the bell jar and cover the exposed model surfaces. In general, two evaporations were necessary to obtain a coating of aluminum about one micron thick.

A-7. SIMILARITY ANALYSIS OF THE GAS PHASE IGNITION MECHANISM FORMULATED BY McALEVY (12)

Consider McAlevy's (12) experiment, where a shock wave was reflected from a plane wall containing an ignitable substance. The proposed mathematical analogue for predicting the ignition time of the substance was as follows. It is assumed that upon shock reflection, the substance starts vaporizing at a constant rate and that temperature variation and chemical reaction in the gas field do not affect the concentration of vaporized specie up to the instant of ignition. The interface temperature between the gas and the solid is assumed to be constant. It is given by the transient solution of the interface temperature of two semi-infinite bodies--initially at two different, uniform temperatures--coming into contact at zero time. Compressibility effects in the gas are ignored - i.e. - the gas is assumed to have constant density. The shocked gas contains a fixed concentration of oxidizer which is unaffected by diffusion of the igniting vapor. Heat is liberated in the gas phase by a global, second order reaction between the vaporizing substances' vapors and the gaseous oxidizer.

The system of equations used by McAlevy were thus the following:

Mass Diffusion:

$$C_F = 2\dot{m}_F^{\circ}\sqrt{\frac{t}{D}}\ \text{ierfc}\ \frac{x}{\sqrt{4Dt}} \qquad [7\text{-}1]$$

Energy:

$$\frac{\partial T}{\partial t} = \alpha\frac{\partial^2 T}{\partial x^2} + \frac{9\,C_F C_{ox} Z\, e^{-E/RT}}{\rho c_p} \qquad [7\text{-}2]$$

$$t \le 0: \quad T = T_o \quad \text{ALL } x$$

$$t > 0: \quad T = T_s \quad x = 0 \qquad [7\text{-}3]$$

$$T \to T_o \quad x \to \infty$$

Substituting the equation defining C_F as a function of (X) and (t) into the energy equation results in a single equation which was taken as defining the behavior of the system. This equation is

$$\frac{\partial T}{\partial t} = \alpha \frac{\partial^2 T}{\partial x^2} + \frac{9 C_{ox} Z}{\rho c_p} \left(2 \dot{m}_F^{\circ} \sqrt{\frac{t}{D}} \, \text{ierfc} \frac{x}{\sqrt{4Dt}} \right) e^{-E/RT} \qquad [7\text{-}4]$$

where the boundary and initial conditions given in [7-3] still apply.

The ignition criterion used by McAlevy (12) was that ignition occurred when the right hand term of equation [7-4]--the time derivative of the temperature caused by chemical reaction--equalled the time derivative of the temperature caused by cooling, somewhere in the system. The latter temperature derivative was found by the solution of equation [7-4] without the chemical heat generation term, and was termed

$$\left(\frac{\partial T}{\partial t} \right)_{linear}$$

as in Hicks' development of the solid phase, thermal ignition theory for composite propellants. The former temperature derivative, caused by chemical reaction can be termed

$$\left(\frac{\partial T}{\partial t} \right)_{chemical}$$

Thus, the ignition criterion used in (12) was the equality of the above derivatives or

$$\left(\frac{\partial T}{\partial t} \right)_{linear} = \left(\frac{\partial T}{\partial t} \right)_{chemical} \qquad [7\text{-}5]$$

at ignition, somewhere in time and space. The result of this ignition criterion was found to be that

$$t_{IGN} \sim \left(C_{ox}^{\infty} \right)^{-2/3} \qquad [7\text{-}6]$$

Now, it is quite easy to show that the above relationship between ignition delay and oxygen concentration is completely inherent in the assumptions made in the above theoretical development. To show this, define

$$t = \frac{\tau}{\alpha}\left(\frac{c_p E \alpha^2 Le}{2\rho Z R \dot{m}_F^{\circ} C_{ox}^{\infty}}\right)^{2/3} \qquad [7\text{-}7]$$

$$x = \xi \left(\frac{c_p E \alpha^2 Le}{2\rho Z R \dot{m}_F^{\circ} C_{ox}^{\infty}}\right)^{1/3} \qquad [7\text{-}8]$$

$$\theta = \frac{RT}{E} \qquad [7\text{-}9]$$

Substituting these definitions into equation [7-4] and its constraints given by [7-3] results in the following dimensionless differential equation and constraints:

$$\frac{\partial\theta}{\partial\tau} = \frac{\partial^2\theta}{\partial\xi^2} + \sqrt{\tau}\, ierfc\left(\frac{\xi}{\sqrt{4Le\tau}}\right) e^{-1/\theta} \qquad [7\text{-}10]$$

$$\tau \le 0: \quad \theta = \theta_0, \text{ ALL } \xi$$

$$\tau > 0: \quad \theta = \theta_s, \ \xi = 0 \qquad [7\text{-}11]$$

$$\theta \to \theta_0, \ \xi \to \infty$$

Because the above equation and its boundary conditions are completely independent of any factor containing either (Y_{ox}^{∞})

or $(\dot{m}_F^o)$, one concludes that the assumption of any dimensionless ignition criterion will give the results below.

$$t_{IGN.} \sim (C_{ox}^{\infty})^{-2/3} \qquad [7\text{-}12]$$

$$t_{IGN.} \sim (\dot{m}_F^o)^{-2/3} \qquad [7\text{-}13]$$

One may observe that the inherent predictions of this theory concerning the dependence of the ignition delay upon oxidizer concentration do not agree with experiments on solid propellant ignition. In particular, it has been found that the slope of the experimental curves of the logarithm of the real ignition delay versus the logarithm of the oxygen concentration in the environment external to the propellant, often is much greater than unity. Such slopes are clearly inexplicable under McAlevy's development of a gas phase ignition theory. On the other hand, such slopes can be indicative of gas phase ignition in a heterogeneous system, as has been shown in Part I of the present work.

A further interesting conclusion regarding the theoretical development of (12) can be drawn. Consider the necessary condition that at achievement of the criterion $(\partial T/\partial t)_{linear} \equiv (\partial T/\partial t)_{chem}$. That is, the rate at which the fuel is supplied must at least be equal to the rate of its consumption by chemical reaction. If the previous condition of a simultaneous equality of linear and chemical time derivatives of temperature is required in addition, the two conditions are clearly equivalent to the one criterion written below, that:

$$\frac{q}{\rho c_p}\left(\frac{\partial C_F}{\partial t}\right)_{CHEMICAL} \equiv \left(\frac{\partial T}{\partial t}\right)_{LINEAR} \qquad [7\text{-}14]$$

Upon calculating under what mass flux was required for meeting the above condition, certain facts became evident. All of these and the following calculations were for the standard test conditions used in reference (12). First, the

condition was far from satisfied by the fuel mass flux of 1.86×10^{-6} gm/cm^2 sec. used in the calculations in (12), and based upon some steady state, P-13 polyester pyrolysis data, see reference (12). In fact, using the same values for the various physical quantities as were used in (12), a mass flux of 9.2×10^{-1} gm/cm^2 sec. was necessary to satisfy equation [7-14]. In addition, it was found that with this large mass flux, equation [7-14] was satisfied at a time of 1.9×10^{-6} sec.; this was very much shorter than any experimentally observed ignition times for composite propellant.

Now, by assuming a value of 10^{13} instead of 10^{15} for the pre-exponential factor, Z, of the chemical reaction, further calculation showed that [7-14] was satisfied at a time of 0.6×10^{-3} sec. to 0.1×10^{-3} sec. and a mass flux of 2.3×10^{-1} gm/cm^2 sec., over the range of oxygen mole fraction $0.1 \leq (C_{ox}^{\infty}/\rho) \leq 1.0$.

The above very short times, even at the lower and larger mass flux values, strongly indicated that the theoretical development of (12) was incomplete and the simultaneous processes of fuel and oxidizer diffusion and consumption were important in the development of ignition of a diffusion flame.

A-8. SIMILARITY ANALYSIS OF A MODEL FOR HETEROGENEOUS IGNITION BY HYPERGOLIC SURFACE REACTION

Consider the case of a heterogeneous surface reaction between an oxidizer externally supplied and the binder of a solid propellant. A numerical solution of a case similar to that discussed below was done by Anderson and Brown (20).

The mathematical analogue of this ignition model is assumed to be given by the following set of equations for the assumed gaseous hypergolic oxidant and the solid propellant binder.

$$\frac{\partial T_s}{\partial t} = \alpha_s \frac{\partial^2 T_s}{\partial X^2} \qquad X<0 \qquad [8\text{-}1]$$

$$\frac{\partial T}{\partial t} = \alpha_g \frac{\partial^2 T}{\partial X^2} \qquad X>0 \qquad [8\text{-}2]$$

$$\frac{\partial C_{ox}}{\partial t} = D \frac{\partial^2 C_{ox}}{\partial X^2} \qquad X>0 \qquad [8\text{-}3]$$

These equations have the following constraints:

$$
\begin{aligned}
t \le 0: \quad & C_{ox} = C_{ox}^{\infty} && x > 0 \\
& T = T_0 && x > 0 \\
& T_s = T_0 && x < 0 \\
t > 0: \quad & T = T_s^{\circ} && x = 0 \\
& T \to T_0 && x \to +\infty \\
& T_s \to T_0 && x \to -\infty
\end{aligned}
\qquad [8\text{-}4]
$$

$$-D\frac{\partial C_{ox}}{\partial x} = C_{ox}^{n} Z e^{-E/RT}$$

$$-\lambda_g \frac{\partial T}{\partial x} = -\lambda_s \frac{\partial T_s}{\partial x} + q C_{ox}^{n} Z e^{-E/RT}$$

The following simplifying assumptions are implied in the writing of the previous equations:

1. All gas phase properties are constant and independent of the local temperature (though the properties may be averaged).

2. The net mass flow of products from the surface may be neglected.

3. The reaction at the surface is of n^{th} order and its temperature dependence can be represented by an Arrhenius function.

4. Lewis number = $D/\alpha = 1$, for the gas.

The above equations may be nondimensionalized by the following definitions

$$
\begin{aligned}
t &= \frac{\tau}{\alpha_s}\left(\frac{\lambda_s E}{q (C_{ox}^{\infty})^n Z R}\right)^2 \qquad \eta_{ox} = \frac{C_{ox}}{C_{ox}^{\infty}} \\
x &= \xi\left(\frac{\lambda_s E}{q (C_{ox}^{\infty})^n Z R}\right) \qquad \theta = \frac{RT}{E}
\end{aligned}
\qquad [8\text{-}5]
$$

The governing equations can now be written as

$$\frac{\partial \theta_s}{\partial \tau} = \frac{\partial^2 \theta_s}{\partial \xi^2} \quad , \xi < 0 \qquad [8\text{-}6]$$

$$\frac{\partial \theta}{\partial \tau} = \frac{\alpha_g \partial^2 \theta}{\alpha_s \partial \xi^2} \quad , \xi > 0 \qquad [8\text{-}7]$$

$$\frac{\partial \eta_{ox}}{\partial \tau} = \frac{D \partial^2 \eta_{ox}}{\alpha_s \partial \xi^2} \quad , \xi > 0 \qquad [8\text{-}8]$$

with their constraints given by

$$\begin{aligned} \tau \leq 0: \quad & \theta_s = \theta = \theta_0 && \xi \leq 0 \\ & \eta_{ox} = 1 && \xi > 0 \\ & \eta_{ox} = 0 && \xi < 0 \\ \tau > 0: \quad & \theta \to \theta_0 && \xi \to +\infty \\ & \theta \to \theta_0 && \xi \to -\infty \end{aligned} \qquad [8\text{-}9]$$

$$-\frac{\partial \eta_{ox}}{\partial \xi} = \left(\frac{9 (C_{ox}^{\infty})^n RD}{\lambda_s E} \right) \eta_{ox} e^{-1/\theta} \quad ; \xi = 0$$

$$-\frac{\lambda_g}{\lambda_s} \frac{\partial \theta}{\partial \xi} = -\frac{\partial \theta_s}{\partial \xi} + \left(\frac{9 (C_{ox}^{\infty})^n RD}{\lambda_s E} \right) \eta_{ox} e^{-1/\theta}$$

In this complete case we see that τ is a function of a number of dimensionless groups, as well as the definition of ignition. Functionally we may write

$$\tau = f \left(\frac{9 (C_{ox}^{\infty})^n RD}{\lambda_s E} , \frac{\alpha_g}{\alpha_s} , \frac{\lambda_g}{\lambda_s} , \theta_0 \right) \qquad [8\text{-}10]$$

From this functional representation for τ we see that neglect of the gas phase results in a simple functional

relation for τ which may be written

$$\tau = f(\theta_0)$$

[8-11]

$$\text{WHERE} \qquad \tau = \alpha_s \left(\frac{q (C_{ox}^{\infty})^n Z R}{\lambda_s E} \right)^2 t$$

Anderson and Brown (20) reported that neglect of the gas phase did not appreciably alter the results of their numerical solution. Making this assumption, the equations are reduced to the single energy diffusion equation in the solid.

$$\frac{\partial \theta_s}{\partial \tau} = \frac{\partial^2 \theta_s}{\partial \xi^2} \qquad [8\text{-}12]$$

$$\tau \le 0: \quad \theta_0 = \theta_s, \text{ ALL } \xi$$

$$\tau > 0: \quad -\frac{\partial \theta_s}{\partial \xi} = e^{-1/\theta} \qquad \xi = 0$$

$$\theta_s \to \theta_0, \quad \xi \to -\infty \qquad [8\text{-}13]$$

where $\tau = \alpha_s \left(\frac{q (C_{ox}^{\infty})^n Z R}{\lambda_s E} \right)^2 t$, $\xi = \left(\frac{q (C_{ox}^{\infty})^n Z R}{\lambda_s E} \right) x$ and $\theta = \frac{RT}{E}$.

Observe that the oxidizer concentration, C_{ox}^{∞}, appears in the expression for τ only. Pressure, however, appears in two ways. Since $C_{ox}^{\infty} = \rho Y_{ox}^{\infty}$ contains a pressure term, and the expression for the equivalent isothermal temperature--also depends upon pressure, the pressure effect on τ is obscure in this formulation. In other words, with τ functionally related to T_0 or θ_0 as written above, there is no explicit way of determining the effect of pressure on t_{ign}.

However, if it is assumed that $\theta/\theta_0 \big|_{\tau=0}$ AT ignition is small, we can make the Semenov approximation to the

exponential. That is, defining $\theta = \frac{E}{RT_o^2}(T - T_o)$ the exponential can be written in the following manner.

$$e^{-E/RT} \cong e^{-\frac{E}{RT_o}} \cdot e^{\theta}$$

With this assumption, the equations--neglecting the effect of transport processes in the gas phase--become

$$\frac{\partial \theta_s}{\partial \tau} = \frac{\partial^2 \theta_s}{\partial \xi^2} \qquad [8\text{-}14]$$

$$\tau \leq 0: \quad \theta_s = 0 \ , \ \text{ALL } \xi$$

$$\tau > 0: \quad -\frac{\partial \theta_s}{\partial \xi} = e^{\theta_s} \quad \xi = 0 \qquad [8\text{-}15]$$

$$\theta_s \to 0 \ , \ \xi \to -\infty$$

where

$$\tau = \alpha_s \left(\frac{9 (C_{ox}^{\infty})^n Z E e^{-E/RT_o}}{\lambda_s R T_o^2} \right)^2 \cdot t$$

$$\xi = \left(\frac{9 (C_{ox}^{\infty})^n Z E e^{-E/RT_o}}{\lambda_s R T_o^2} \right) \cdot X$$

Now, τ_{ign} is only dependent upon the designated criterion for ignition. For any dimensionless criterion that does not violate the original assumption that (T_s/T_o) is small at ignition, it is apparent that

$$t_{IGN} \sim (Y_{ox}^{\infty})^{-2n} \qquad [8\text{-}16]$$

Again the effect of pressure is not explicit, but one may write

$$t_{IGN} \sim (Y_{ox}^{\infty})^{-2n} \cdot \bar{P}^{-2n} \cdot f(P) \qquad [8\text{-}17]$$

with $$f(P) = \frac{T_o + a\sqrt{P}/(b + a\sqrt{P})}{\exp\left(-E/R\left(T_o + a\sqrt{P}/(b+a\sqrt{P})\right)\right)}$$

The function $f(P)$ appears because the initial surface temperature jump of the fuel surface is dependent upon the pressure level of the gas phase. The function $f(P)$ can be approximated by $(A P^{-m})$, where the value of (m) depends strongly upon the activation energy of the surface reaction. For any range of pressures and initial temperatures, one can find an approximate value of (m) such that

$$t_{IGN} \sim (Y_{ox}^{\infty})^{-2n} \cdot \bar{P}^{-(2n+m)} \qquad [8\text{-}18]$$

Now, for any reasonable values of activation energies (m) is not negligible as compared to $(2n)$. If one, for example, wants to consider McAlevy's case than in the range of pressures investigated by McAlevy, (m) is approximately 1.5 for an activation energy of 15,000 and approximately 5 for an activation energy of 30,000. Anderson and Brown (20) discussed the application of this model to McAlevy's results, and mentioned that they obtained correct slopes of log t_{ign} versus (Y_{ox}^{∞}) for the behavior of the P-13 propellants for both pressure and oxygen effects. They also noted that the slope for $t = t(Y_{ox}^{\infty}, P)$ calculated from this model was virtually independent of the activation energy assumed. These results can actually be obtained by the dimensionless analysis given above. However, the conclusion that t_{ign} is proportional to P^{-2n} is a result of Anderson's assumption that T_o is constant and independent of P. Though there are no data, it is quite difficult to assume that the end wall temperature in the shock tube is independent of pressure. This could be quite easily checked experimentally.

One can now compare the properties of the model described above with the results obtained by McAlevy.

1. The model explains the high sensitivity of ignition time to oxygen concentration.

2. It predicts, however, that unless the activation energy is very low, the influence of pressure on t_{ign} should be much more pronounced then that of oxygen concentration; this has not been found experimentally. Now it is quite reasonable to assume a low activation energy for hypergolic ignition, but not for an oxidation. Otherwise, the reaction would occur at room temperature. To be exact, the above reasoning applies only to the simplified case where heat transfer to the gas phase can be neglected. However, Anderson's results on the computer indicate that the complete solution differs only slightly from the simplified analytical solution. In addition, the dependence of t_{ign} on (y_{ox}^{∞}) remains true for the case where heat and mass transfer in the gas phase can no longer be neglected.

3. Steady state reaction rates between polymer and oxygen are much lower than those required by the model, even for temperatures much higher than those assumed by McAlevy to occur in the experiments. Now, even for the case of an unsteady state surface attack where only the available surface is oxidized, one has to assume very high activation energies. Otherwise, the reaction would occur at room temperature in air. Therefore, the pressure dependence predicted by a surface ignition theory of the Anderson type is much larger than has so far been experimentally observed.

A-9. PROGRAMMING METHODS FOR THE NUMERICAL INTEGRATION OF THE EQUATIONS FOR THERMAL IGNITION OF A DIFFUSION FLAME

It was shown in the preceding chapter, that the differential equations formulated for this problem, could be nondimensionalized in a convenient manner. The properties of the model then could be discussed--before the actual numerical solution--in terms of this set of nondimensional differential equations, boundary conditions, and initial conditions. For convenience, these dimensionless equations and their initial and boundary conditions are repeated.

$$\frac{\partial \eta_F}{\partial \tau} = \frac{\partial^2 \eta_F}{\partial \xi^2} - \eta_F \eta_{ox} e^{-1/\theta} \qquad \text{"Fuel" Diffusion} \qquad [9\text{-}1]$$

$$\frac{\partial \eta_{ox}}{\partial \tau} = \frac{\partial^2 \eta_{ox}}{\partial \xi^2} - A \eta_F \eta_{ox} e^{-1/\theta} \qquad \text{"Oxidizer" Diffusion} \qquad [9\text{-}2]$$

$$\frac{\partial \theta}{\partial \tau} = \frac{\partial^2 \theta}{\partial \xi^2} + B \eta_F \eta_{ox} e^{-1/\theta} \qquad \text{"Energy" Diffusion} \qquad [9\text{-}3]$$

$\tau \leq 0$:

$$\left.\begin{aligned} \eta_F &= 0 \\ \eta_{ox} &= 1 \\ \theta &= \theta_0 \end{aligned}\right\} \text{ all } \xi$$

$\tau > 0$:

$$\left.\begin{aligned} &\text{CASE I}: \quad \eta_F = 1 \\ &\text{CASE II}: \quad -\frac{\partial \eta_F}{\partial \xi} = 1 \\ &\qquad -\frac{\partial \eta_{ox}}{\partial \xi} = 0 \\ &\qquad \theta = \theta_s \end{aligned}\right\} \xi = 0 \qquad \left.\begin{aligned} \eta_F &\to 0 \\ \eta_{ox} &\to 1 \\ \theta &\to \theta_0 \end{aligned}\right\} \xi \to \infty$$

The preceding chapter primarily was concerned with a discussion of the properties of this set of equations; specifically, the variation of the ignition delay with the variation of the physico-chemical parameters absorbed in the

"A" and "B" parameters was discussed in a qualitative manner. In practical terms, then, numerical solution of the above set of equations is necessary for quantitative determination of the functional relationship between the systems ignition delay and

1. ignition criterion
2. variations in A and/or B
3. variations in θ_0
4. variations in activation energy

Mathematically, then, we wish to consider the numerical integration of three, coupled, partial differential equations of the general parabolic form

$$\frac{\partial \beta}{\partial \tau} = \frac{\partial^2 \beta}{\partial \xi^2} + \mu(\xi, \tau, \beta) \qquad [9\text{-}4]$$

Digital techniques to perform the integration of this set of equations.

A. SELECTION AND DISCUSSION OF FINITE-DIFFERENCE TECHNIQUE

Numerical integration of a partial differential equation [9-1], [9-2], and [9-3] requires representation of derivatives in the form of discrete, or finite differences. Many different finite difference methods exist; a good summary of these networks is given in a book by Richtmeyer (I.43) on numerical analysis. The simplest of these finite-difference schemes is the "forward difference" scheme. In this scheme, the independent variable space is divided into a grid of discrete points; in the present problem, the (τ, ξ) space was divided up into a number of pairs of points, (τ_i, ξ_i). The function to be integrated was evaluated at the time (τ_i) over all points (ξ_i), from the values of the function at points ξ_i at time (τ_{i-1}). To be precise, the value of the spacial derivatives function at the point (τ_i, ξ_i) was calculated from the values of the function at the three points (τ_{i-1}, ξ_{i-1}), (τ_{i-1}, ξ_i), and (τ_{i-1}, ξ_{i+1}). From the pictorial representation sketched below, it is easy to see how the designation

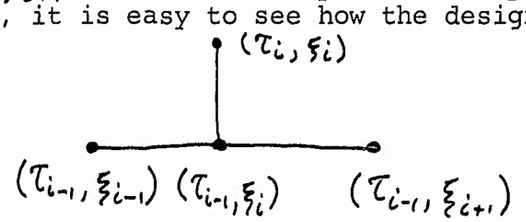

"forward difference scheme" was given to this method.

In the actual use of any finite difference representation of a differential equation, two characteristic problems arise. The first of these is whether the differencing method is "stable" during the entire process of integration. In this case, stability refers to the problem of whether a small error or perturbation process of numerical calculation will propagate and increase during continued calculation, or whether the error will decay and die out. The second problem which is encountered is whether the calculated solution, even if the solution is stable, will converge to the correct solution (in simple cases, the correct solution is the analytical solution) or some other solution--i.e.--the problem of convergence of the numerical solution.

In the case of an ordinary transient diffusion equation of the form

$$\beta_\tau = \beta_{\xi\xi} \qquad [9\text{-}5]$$

the stability of the solution is insured if the grid sizes in the (τ, ξ) plane are made such that the ratio

$$\frac{\Delta\tau}{(\Delta\xi)^2} < \frac{1}{2} \qquad [9\text{-}6]$$

It has been stated, see references (I.43) and (I.45), that the forward difference method of solution of this equation will converge if $[\Delta\tau/(\Delta\xi)^2] \to 0$ as both ($\Delta\tau$) and ($\Delta\xi$) approach zero. In other words, $\beta(\tau_i, \xi_i) \to \beta(\tau, \xi)$ if the above two conditions are fulfilled.

Unfortunately, though convergence of a forward difference scheme is insured if the latter of the last two conditions is met, the practical result of small grid sizes is long computation times. In practice then, the grid size is made only small enough to obtain numerical results which agree with the analytical solution to the desired accuracy. When the analytical solution is not available for comparison--as is the case in the work presented here--convergence usually is assumed to exist when the calculated results for two different grid sizes agree to some arbitrarily chosen number of decimal places. It must be pointed out that this does not mean that the numerical calculations did indeed converge to the correct solution unless there is some analytical evidence to support such a contention. Proof of the convergence and stability

of numerical integration of differential equations is currently an interesting and difficult portion of modern applied mathematics. Indeed, for many mathematical representations of different systems requiring numerical solutions, there is an unfortunate lack of knowledge concerning the conditions necessary for convergence and stability of solution using any particular difference method. Therefore, an empirical approach to these questions often is the only alternative.

Fortunately, Fritz John (I.44) has discussed the numerical integration of the quasi-linear parabolic equation of the form

$$\frac{\partial \beta}{\partial t} = a_0(x,t)\frac{\partial^2 \beta}{\partial x^2} + a_1(x,t)\frac{\partial u}{\partial x} + a_2(x,t)\,u(x,t) + d(u;x,t) \qquad [9\text{-}7]$$

where $d(u;x,t)$ is a general, unrestricted function, by the forward difference scheme previously mentioned. The designation "quasi-linear" refers to the fact that only the nonhomogeneous term(s) are nonlinear. John showed that providing the conditions

$$\Delta t \cdot d(u;x,t) < 1 \qquad [9\text{-}8]$$

and

$$\frac{\Delta t}{(\Delta x)^2} < \frac{1}{2} \qquad [9\text{-}9]$$

were maintained, then the difference solution, $u(k,j)$ was stable and approached the solution $u(x,t)$ as both Δt and Δx approached zero. A short discussion of Fritz John's analysis is given by Richtmeyer (I.43).

The above equation is a general form of any one of the set of equations which were written to describe the thermal ignition of a diffusion flame, see equations [9-1], [9-2], and [9-3]. On the basis of the analysis by Fritz John, it was concluded that the simultaneous integration of this set of equations using standard, simple forward difference scheme previously described would be convergent and stable providing

the following two conditions were maintained:

$$(1) \qquad \Delta\tau \cdot K e^{-1/\theta} \ll 1 \qquad [9\text{-}10]$$

and

$$(2) \qquad \left[\Delta\tau/(\Delta\xi)^2\right] < 1/2 \qquad [9\text{-}11]$$

In condition (1) above, (K) is the greatest of the constant factors "1.0," "A", or "B" which multiply the chemical reaction terms in the set of equations [9-1], [9-2], and [9-3].

The present set of differential equations were rewritten in difference form. For simplicity, the points τ_i and ξ_i are replaced by J and K, respectively, and the ratio $(\Delta\tau/(\Delta\xi)^2)$ was replaced by λ. In writing the difference equations for solution of this problem, the following additional definitions were used:

$$(1) \qquad U(1, J, k) = \eta_F \qquad [9\text{-}12]$$

$$(2) \qquad U(2, J, K) = \eta_{ox} \qquad [9\text{-}13]$$

$$(3) \qquad U(3, J, K) = \theta \qquad [9\text{-}14]$$

where $J = 1, 2$ AND $K = 1, 2, \cdots, K^*, \ldots$

$$(4) \qquad C(1) = +1.0$$

$$(5) \qquad C(2) = +A \qquad [9\text{-}15]$$

$$(6) \qquad C(3) = -B$$

Use of the above definitions make it possible to represent the set of three differential equations by one general difference equation involving $U(I, J, K)$; a particular value of index I refers to one of the three differential equations as defined in definitions [9-12], [9-13], and [9-14] above. The time variable, J, only needs to vary between (1) and (2) since each new series of calculations is based solely upon the immediately preceding calculations. Thus, the set of three differential equations may be written in forward difference form as shown below.

$$\frac{U(I,2,K) - U(I,1,K)}{\Delta\tau} = \frac{U(I,1,K+1) - 2U(I,1,K) + U(I,1,K-1)}{(\Delta\xi)^2} +$$

[9-16]

$$+ U(1,1,K) \cdot U(2,1,K) \cdot C(I) \exp\left(\frac{-1.0}{U(3,1,K)}\right)$$

Since part of the chemical reaction term is identical in all three equations, the quantity $F(K)$ was defined as

$$F(K) = U(1,1,K) \cdot U(2,1,K) \exp\left(\frac{-1.0}{U(3,1,K)}\right) \qquad [9\text{-}17]$$

Equation [9-16] may be solved for the desired quantity, namely, $U(I,2,K)$ as shown below

$$U(I,2,K) = \lambda\left[U(I,1,K+1) + U(I,1,K-1) + \left(\frac{1-2\lambda}{\lambda}\right) U(I,1,K)\right] + \lambda \cdot C(I) \cdot F(K) \qquad [9\text{-}18]$$

In difference form, the initial and boundary conditions for case I - constant fuel concentration at the wall, and case II - constant fuel mass flux from the wall, become:

Initial Conditions:

Cases I and II

$$U(1,0,K) = 0.0$$
$$U(2,0,K) = 1.0$$
$$U(3,0,K) = \theta_0$$

Boundary Conditions:

Case I

$$U(1,2,1) = 1.0$$
$$U(2,2,1) = U(2,2,2)$$
$$U(3,2,1) = \theta_s$$

Case II

$$U(1,2,1) = U(1,2,2) + \sqrt{\Delta\tau/\lambda}$$
$$U(2,2,1) = U(2,2,2)$$
$$U(3,2,1) = \theta_s$$

$$U(1,2,K^*) = 0.0$$
$$U(2,2,K^*) = 1.0$$
$$U(3,2,K^*) = \theta_0$$

Essentially the same difference equations, with the initial and boundary conditions written as above, may be used for the zero activation energy case. Two modifications of the computational technique are necessary, however. The first of these is the redefinition of $F(K)$ as

$$F(K) = U(1,1,K) \cdot U(2,1,K) \qquad [9\text{-}19]$$

The second modification is a large reduction in the size of the time step, $\Delta\tau$. This is necessary in order to maintain the convergence condition of $(\Delta\tau \cdot K \cdot \eta_F \eta_{ox}) \cong 10^{-4}$. Therefore, the numerical solution of the zero activation energy cases required longer computational times than the comparable finite activation energy cases. The nondimensional value of the ignition delay for the former cases may, however, be shorter than the nondimensional value of the ignition delay in the latter cases which have a finite activation energy chemical reaction.

B. COMPUTATIONAL DIFFICULTIES, PROCEDURES, AND OBSERVATIONS

The computer programs for the solution of equation [9-18] were written in the IBM formula translation language Fortran II. Use of this language removed the necessity of programming the necessary instructions in machine language for the IBM 7090 computer which was used for the numerical computation. Though the Fortran II source program was not basically unusual in nature, several features of the programs are worthy of separate mention. These features will be mentioned as the discussion of the program requires.

A simplified and abbreviated flow diagram of the computer program, and a general program is given at the end of this Appendix. The description of the program operation that follows, is easily traced on the flow diagram.

In operation, the values of the function $U(I,2,K)$ were calculated at each space point K ; the limiting value of K was increased, as necessary, such that the "$\xi \to \infty$" conditions were reached during the calculations at each time step. At predetermined numbers of steps $\Delta\tau$, the results of these calculations were recorded on magnetic tape. A plotting routine was incorporated in the program which caused the results $U(3,2,K)$ versus K calculation to be stored in such a manner that a graph could be printed on the high speed printer, along with the numerical values of $U(I,2,K)$ at each K value. This plot of $U(3,2,K)$, the dimensionless temperature, was recorded less often than the numerical results, and was a valuable feature for quickly scanning the results of the calculations.

After calculation of the values of $U(I,2,K)$ and the possible recording of the results, the following options were programmed:

(1) Display a graph of the $U(3,2,K)$ values versus K on the cathode ray tube, then update

(2) Update the calculations

(3) Read in new initial data and start calculation of a new data case.

"Updating" consisted of advancing the base line in (τ, ξ) space from which the next calculations were to be based. Thus, $U(I,1,K)$ values were replaced by the $U(I,2,K)$ values just calculated, and new values of $U(I,2,K)$ were calculated. Updating was the option normally taken. Option (1), above, was a useful feature of the program in that the course of the solution could be checked during operation of the computer; options (2) and (3) could be selected as desired after viewing the course of the solution.

It was found that the conditions for convergence and stability were quite severe for the simultaneous integration of the three equations represented by equation [9-18]. The fact that (λ) was less than unity was insufficient for stable solutions because of the influence of the quasi-linear chemical reaction terms. Unstable solutions resulted in negative values for at least one of the solutions $U(I,2,K)$. In such a case, the computer was programmed to cease computation, record the occurrence of negative values in any $U(I,2,K)$, and start computation of a new data case.

Extensive computation showed that stable and convergent solutions for all cases could be obtained, in general, only if the previously mentioned stability and convergence conditions were of the form

$$\Delta\tau\,(K e^{-1/\theta}) \leq 10^{-3}$$

and

$$\lambda \equiv \frac{\Delta\tau}{(\Delta\xi)^2} < \frac{1}{2}$$

and remained so throughout the calculation. Fortunately, a decrease in ($\Delta\tau$) was a sufficient correction; however, increased computational time was the penalty paid for this reduction of $\Delta\tau$.

In the present calculations, convergence was taken to be agreement in the calculated values for η_F , η_{ox} , and θ

(or $U_I(I,2,K)$, $I=1,3$) to four decimal places between the results for a certain ($\Delta\tau$) value and a ($\Delta\tau$) value four times smaller. It should be emphasized that it was not completely certain, a priori, that the simultaneous integration of the three partial differential equations would be stable, even if each one were stable under the conditions given in [9-10] and [9-11]. The fact that extensive computational effort showed these conditions to be sufficient for convergence and stability, makes it entirely likely that a large class of similar problems, often encountered in chemical engineering, can be treated successfully in a like manner.

Because of long computation times, a most valuable feature of the program was the inclusion of the manually called subroutine "RSOS". This subroutine dumped the current contents of the computer memory and control registers onto magnetic tape in a form which allowed the computer to be reloaded, and restarted from this tape. During the memory and register dumping process, the contents of the tape was checked by the computer to insure an accurate transfer. Therefore, the computation of a particular data case could be interrupted at any point, and later restarted from the same point. This feature allowed continued computation of a data case which required long computation times for completion.

A-10. THE NEGLECT OF CONVECTIVE TRANSPORT OF MASS AND ENERGY

The assumption of equal moles of reactants and products of the chemical reaction means that no volume change, or convective transport, is engendered by the chemical reaction itself. Therefore, only the relative magnitudes of the diffusion process, and the convective process caused by the presence of a surface impermeable to all but fuel molecules, must be considered.

Consider a semi-infinite, one-dimensional, variable density field in which an unsteady diffusion, and chemical reaction, is taking place. The differential equation governing the behavior of a diffusing quantity, (Φ_i), may be written as

$$\frac{\partial \Phi_i}{\partial t} + v_0 \frac{\partial \Phi_i}{\partial y_0} = \frac{1}{\rho} \frac{\partial}{\partial y_0}\left\{\left(\frac{\mu}{N_i}\right)\frac{\partial \Phi_i}{\partial y_0}\right\} - A_i e^{-E/RT} \qquad [10\text{-}1]$$

The correspondence between Φ_i , N_i , and A_i is given in the table below:

Φ_i	N_i	A_i
Y_F	S_c	$C_F C_{ox} Z/\rho$
Y_{ox}	S_c	$n C_F C_{ox} Z/\rho$
T	P_r	$-q C_F C_{ox} Z/\rho C_p$

Now, it can be shown that equation [10-1] may be converted from one-dimensional, unsteady, variable density form to a two-dimensional, steady, variable density form. Application of the Howarth transformation of the (X_o, Y_o) space to an (x, y) space results in an equation for a two-dimensional, steady, constant density space. The result, for the diffusion of fuel through the two-dimensional field, may be written in the following dimensional form:

$$U_o \frac{\partial Y_F}{\partial X} + v \frac{\partial Y_F}{\partial y} = D \frac{\partial^2 Y_F}{\partial y^2} - Y_F C_{ox} Z e^{-E/RT} \qquad [10\text{-}2]$$

In this equation, U_o is some velocity used to scale the real time such that $t = (X_o/U_o)$, U_o = constant. If the following definitions are used, equation [10-2] may be transformed to one describing the unsteady diffusion of fuel vapors into a one-dimensional, constant density field.

Let

$$\tau = (Z C_{ox}^{\infty}) \frac{X}{U_o} \qquad \eta_{ox} = C_{ox}/C_{ox}^{\infty} \qquad [10\text{-}3]$$

$$\xi = y \sqrt{\frac{Z C_{ox}^{\infty}}{D}} \qquad \theta = RT/E$$

then

$$\frac{\partial Y_F}{\partial \tau} + \frac{v}{\sqrt{Z C_{ox}^{\infty} D}} \frac{\partial Y_F}{\partial \xi} = \frac{\partial^2 Y_F}{\partial \xi^2} - Y_F \eta_{ox} e^{-1/\theta} \qquad [10\text{-}4]$$

Equation [10-4] allows determination of the ratio, R, of the convective transport to the diffusion transport which is defined below.

$$R \equiv \frac{v \dfrac{\partial Y_F}{\partial \xi}}{\sqrt{\varepsilon C_{O_2}^{\infty} D}\, \dfrac{\partial^2 Y_F}{\partial \xi^2}} \qquad [10\text{-}5]$$

The convective transport velocity, v , in the (τ , ξ) space is constant because the density is constant in this space.

In case I, where the fuel is assumed to establish a constant mass fraction Y_F^o at the boundary $y = 0$, the velocity v must be identified as

$$v = v_F = \frac{D}{1 - Y_F^o} \left.\frac{\partial Y_F}{\partial y}\right|_{y=0} = \frac{\sqrt{\varepsilon C_{O_2}^{\infty} D}}{1 - Y_F^o} \left.\frac{\partial Y_F}{\partial \xi}\right|_{\xi=0} \qquad [10\text{-}6]$$

Using the definition $\eta_F \equiv Y_F / Y_F^o$, the ratio R in this case is

$$R = \left(\frac{Y_F^o}{1 - Y_F^o} \left.\frac{\partial \eta_F}{\partial \xi}\right|_{\xi=0} \right) \frac{\dfrac{\partial \eta_F}{\partial \xi}}{\dfrac{\partial^2 \eta_F}{\partial \xi^2}} \qquad [10\text{-}7]$$

Now $\eta_F = O(1)$ near the wall, while further away from the wall it must decrease; therefore, R is greatest near the wall and is of order [$Y_F^o/(1-Y_F^o)$]. Clearly, if R is small enough, say ϵ , the effect of convection may be neglected with respect to the effect of diffusion.

In case II, where the mass flux of fuel from the wall was assumed constant, obtaining a value for v is somewhat more laborious. The definition of v is

$$v = \frac{\rho}{\rho_o} v_o + u_o \int_0^{Y_o} \frac{\partial}{\partial x_o} \left(\frac{\rho}{\rho_o} \right) dy_o \qquad [10\text{-}8]$$

where the subscript "o" refers to the real variables in the steady, two-dimensional space. The application of the

continuity equation in the steady, variable density form to the above equation results in

$$v = \frac{\rho}{\rho_0} v_0 - \int_0^{y_0} \frac{\partial}{\partial y_0}\left(\frac{\rho v_0}{\rho_0}\right) dy_0 \qquad [10\text{-}9]$$

Identifying $v_0^{max} = \dot{m}_F^{\circ}/\rho_{min} = \dot{m}_F^{\circ}/\rho^*$ where ρ^* is the density of the gas phase at some temperature $T^* > T_0$, and (ρ/ρ^*) as (T^*/T) results in

$$v \leq \frac{\dot{m}_F^{\circ}}{\rho_0}\left(\rho/\rho^*\right)_{max} - \frac{\dot{m}_0}{\rho_0}\int_0^{y_0} \frac{\partial}{\partial y_0}\left(T^*/T\right) dy_0$$

or

$$v \leq u_0\left(\frac{T^*}{T_s}\right) - u_0 \int_0^{y_0} d\left(\frac{T^*}{T}\right) \qquad [10\text{-}10]$$

The max value of v will occur for the minimum value of the integral in the above equation.

Now, there are two basic types of temperature profiles during the ignition process, sketched below.

(a) Before Ignition

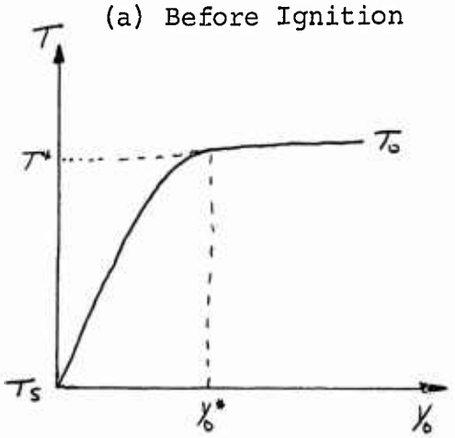

(b) After Ignition

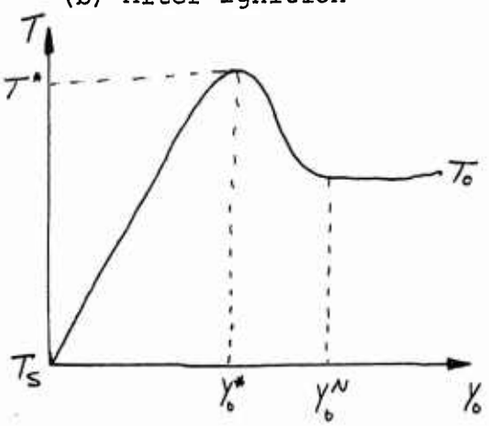

Upon substitution of linear temperature gradients in the above sketches, the integral equation [10-10] can be evaluated.

This shows that case (a), before ignition, results in the most negative value for the integral; consequently

$$|v_{max}| \leq \dot{m}_F^\circ/\rho_\circ \qquad [10\text{-}11]$$

and

$$\frac{v}{\sqrt{2C_{ox}^\infty D}} \leq \frac{\dot{m}_F^\circ}{\sqrt{\rho_\circ^3 Y_{ox}^\infty 2D}} = \left(\frac{c_p E}{qR} B\right) \qquad [10\text{-}12]$$

Therefore, the ratio of convective transport to diffusive transport is

$$R \leq \frac{\left(\frac{c_p E}{qR} B\right)\frac{\partial \eta_F}{\partial \xi}}{\frac{\partial^2 \eta_F}{\partial \xi^2}} = O\left(\Delta\xi \frac{c_p E}{qR} B\right) \qquad [10\text{-}13]$$

As for case I, it appears that if $R \leq \epsilon < 1$ before ignition, then it is possible to neglect convective transport and have the pure diffusion solution of the set of equations similar to [10-4] correct to order ϵ .

Now equations [10-7] and [10-13] predict the error involved in the neglect of convective transport is order (ϵ), where ϵ is determined primarily by (Y_F°) in case I and $(c_p E B/qR)$ in case II. For example, in case I with reference to Figure I-5, B = 0.25, 1/A = 0.2 results in $Y_F^\circ = 3/16$; if q = 4800 cal/gm, C_p = 0.3 cal/gm $^\circ$K, and E/R = 4000° K, the table below shows R at various ξ values:

τ	ξ	R	Comment
6.5×10^4	6	0.19	Near wall, start of ignition
	31	0.01	Middle of temperature bulge
8.75×10^4	6	0.15	Near wall, start of ignition
	41	0.06	Middle of flame

In case II, using Figure I-9, and C_p = 0.3 cal/gm °K, E/R = 4000° K, and q = 4800 cal/gm to obtain Figure (I-17), the most severe effect of neglecting diffusion is for small values of B/A. The following table was computed for these conditions.

$$B/A = 0.333 \quad , \quad B^3/A = 27 \times 10^{-4}$$

τ	ξ	R	Comment
50	4	0.1	Near wall, start of ignition
	20	0.07	Start of temperature bulge
150	4	0.21	Near wall
	16	0.09	Center of flame
	76	0.04	End of flame

$$B/A = 0.12 \quad , \quad B^3/A = 27 \times 10^{-4}$$

τ	ξ	R	Comment
50	4	0.4	Near wall, ignition start
	15	0.01	Center of flame
	41	0.005	End of flame
800	4	1.0	Near wall
	71	0.4	Center of flame
	171	0.05	End of flame

In the case where R approaches unity at some points of space and time, while over the majority of the space time field $R < \epsilon$, the total effect of these large (ϵ) R values is small. This can be seen from an a posteri check of the numerical solution based on the following integral analysis.

The type of equation solved was

$$\frac{\partial \varphi}{\partial \tau} = \frac{\partial^2 \varphi}{\partial \xi^2} + \psi(\varphi, T) = P(\varphi) \qquad [10\text{-}14]$$

whereas the inclusion of convective transport would necessitate solution of

$$\frac{\partial \varphi}{\partial \tau} = \frac{\partial^2 \varphi}{\partial \xi^2} + \sigma \frac{\partial \varphi}{\partial \xi} + \psi(\varphi, T) = Q(\varphi) \qquad [10\text{-}15]$$

Now we note that evaluation, from the numerical solution of the integrals

$$I_1 = \int_0^{\tau^*} \cdot \int_0^{\infty} \frac{\frac{\partial \varphi}{\partial \tau}}{P(\varphi)} d\xi \cdot d\tau \qquad [10\text{-}16]$$

and

$$I_2 = \int_0^{\tau^*} \cdot \int_0^{\infty} \frac{\frac{\partial \varphi}{\partial \tau}}{Q(\varphi)} d\xi \cdot d\tau \qquad [10\text{-}17]$$

allows another determination of the relative error involved in neglecting convection by comparing I_1 to I_2. Thus, the effect of locally large R values, caused by neglecting convection, is a small part of the total integral.

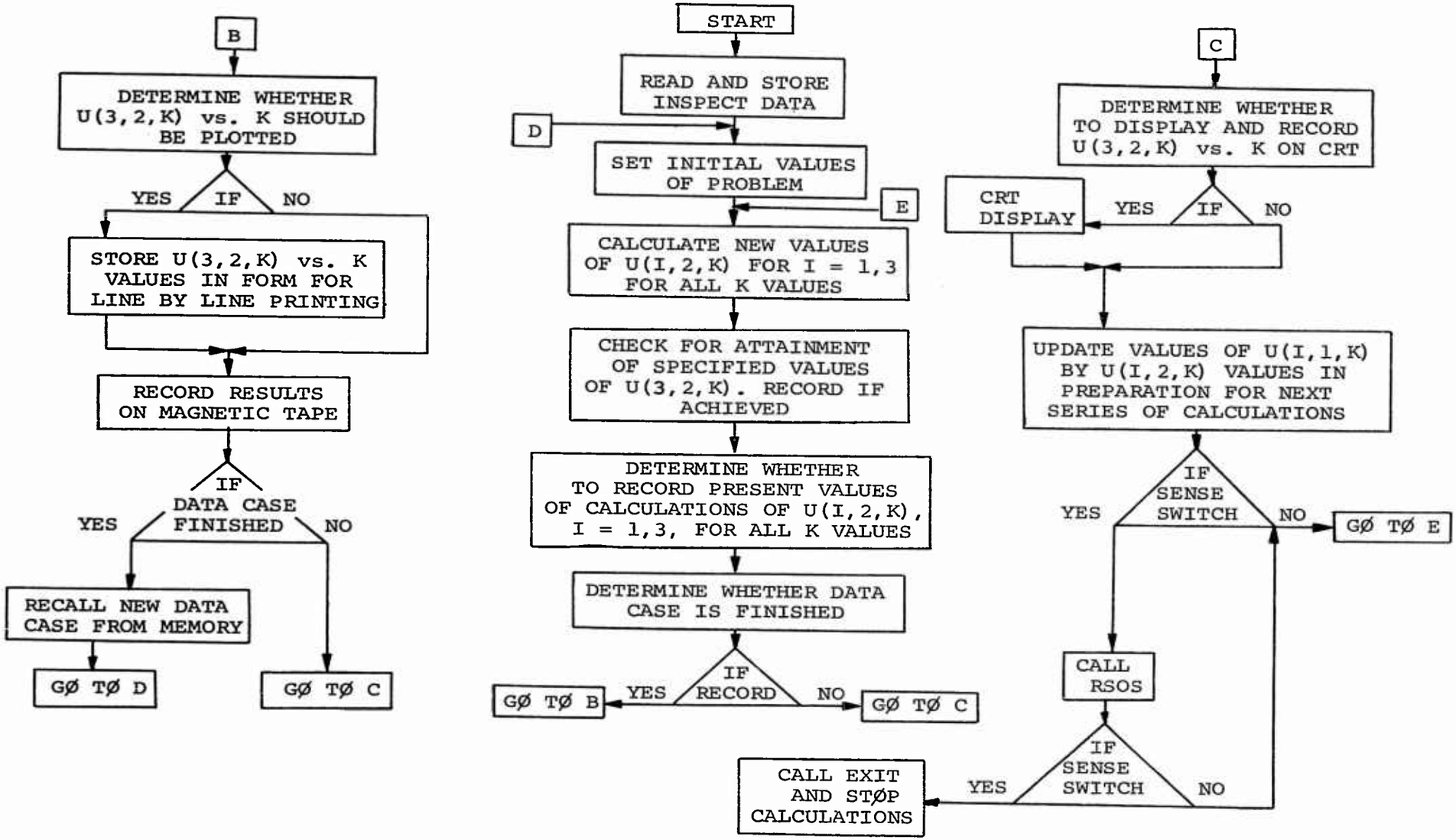

FLOW CHART OF COMPUTER PROGRAM

```
                                        DIFLAME
                                          *
                                          *
A GENERAL PROGRAM FOR THE NUMERICAL INTEGRATION OF THE SET OF
PARTIAL DIFFERENTIAL EQUATIONS DESCRIBING THE THERMAL IGNITION
OF A DIFFUSION FLAME NEAR A COOL WALL, FOR CASES I AND II.
      *
      *
  800 FORMAT (218)
  801 FORMAT (E15.7, E15.7)
  802 FORMAT (4E15.7)
  803 FORMAT (16)
  804 FORMAT (3E16.8,3X,16)
  805 FORMAT (16H TIME STEP NO. =16)
  806 FORMAT (6X,4HFUEL,13X,2HOX,13X,4HTEMP,8X,10HSPACE STEP)
  810 FORMAT (33H THERMAL DIFFUSION FLAME IGNITION)
  811 FORMAT(9H DIFLAME ,11)
  815 FORMAT (3(4H F= ,E10.4,1X,4H K= ,15))
  816 FORMAT(11H U(1,2,K)= ,E12.4,3X,4H K= ,15,3X,9H TO KSTAR)
  820 FORMAT (6H TAU= ,E12.4,3X,5H JJ= ,18)
  821 FORMAT(1H1,6H TAU= ,E12.4,3X,5H JJ= ,18)
  830 FORMAT (3(4H OX= ,E10.4,1X,4H K= ,15))
  831 FORMAT(25H TEMP NEGATIVE, QUIT CASE)
  832 FORMAT (E15.7,18,E15.7)
  850 FORMAT(1H1, 23H DIFLAME, TEMP IN SPACE)
  851 FORMAT (1H )
  855 FORMAT(12H MAXIMUM X= ,E10.4, 31H GRID LINES EVERY 10TH OF MAX X)
  856 FORMAT (48H TEMP HAS EXCEEDED DESIRED MAX, GONE TO NEW DATA)
  857 FORMAT (16,E10.2)
  858 FORMAT (42H  X  COORDINATE IS DISTANCE, LIMIT IS XMAX)
  859 FORMAT (1H1)
  860 FORMAT (35X,17H MONTH/DAY/YEAR= ,12,1H/,12,1H/,2H63)
  861 FORMAT (E15.7,E10.2)
  862 FORMAT(1H1, 30X,41H C.E.HERMANCE, GUGGENHEIM LABS, DIFLAME ,11)
  863 FORMAT(7H  TAU= ,E12.6,3X,7H TEMP= ,E16.8,3X,3H K= ,16)
  864 FORMAT (44H J=1 FOR 1 STEP BACK, J=2 FOR LAST STEP, J= ,12)
  865 FORMAT(60H A U(1,2,K) HAS GONE NEGATIVE, RECORD MADE, GONE TO NEW
     1DATA)
  866 FORMAT(8X,4H ***,11H MAX TEMP= ,E16.8,1X,3H AT,4H K= ,16)
  867 FORMAT(21H CASE ENDED AT  TAU= ,E12.4,9H  AT JJ= ,18,22H  TIME
     8671INTEGRATIONS)
  868 FORMAT(40H THE MAX TEMP ATTAINED AT THIS TAU WAS  ,E16.8,8H  AT K
     1= ,18)
  869 FORMAT(60H A U(1,2,K) WAS NEGATIVE AT THIS POINT, RECOMPUTE THIS
     8691CASE)
  872 FORMAT(34H TEMP EXCEEDED (FAC*W0), WITH FAC= ,E10.2)
  873 FORMAT(39H CASE ENDED BY MANUAL CALL EXIT COMMAND)
  874 FORMAT(39H CASE ENDED BY MANUAL CALL FOR NEW DATA)
  875 FORMAT(43H ALL DATA CASES SUPPLIED HAVE BEEN COMPUTED)
  876 FORMAT(49H SUPPLY INPUT TAPE  A-6  TO THE MACHINA COMPUTANA)
  877 FORMAT( 49H MAKE SURE THAT TAPE  A-6  IS ON 7090 AND REWOUND/
     116H THEN PUSH START////)
  878 FORMAT(30H RSOS TAPE STARTING TO OPERATE)
      DIMENSION C(3),U(3,2,1000), T(15)
      DIMENSION X(1000),Y(1000),KQ(15),R(15),S(15),DUMMY(10)
C     0 IS INDICATOR FOR INITIAL READ IN OF DATA
C     1 IS INDICATOR FOR DATA REMOVAL FROM TABLES STORED IN MACHINE
```

```
      CALL INPUT(Ø,JM,JD,NTP,NSP,A,B,XLAM,DTAU,WØ,W1,RATIO,JJDEL,PCENT,
     1JGRAPH,FAC,ALIMOX,ALIMT,KSTAR)
  1ØØ CALL INPUT(1,JM,JD,NTP,NSP,A,B,XLAM,DTAU,WØ,W1,RATIO,JJDEL,PCENT,
     1JGRAPH,FAC,ALIMOX,ALIMT,KSTAR)
    7 CONTINUE
    8 PRINT 81Ø
      PRINT 811, NFLAME
      PRINT 8Ø1,A,B
      PRINT 8Ø2,XLAM,DTAU,WØ,W1
      PRINT 832, RATIO, JJDEL, PCENT
      PRINT 857, JGRAPH, FAC
      PRINT 861, ALIMOX, ALIMT
      WRITE OUTPUT TAPE 6, 862, NFLAME
      WRITE OUTPUT TAPE 6, 851
      WRITE OUTPUT TAPE 6, 86Ø,JM,JD
      WRITE OUTPUT TAPE 6, 851
    9 WRITE OUTPUT TAPE 6, 81Ø
      WRITE OUTPUT TAPE 6, 851
   1Ø WRITE OUTPUT TAPE 6, 811, NFLAME
      WRITE OUTPUT TAPE 6, 851
   11 WRITE OUTPUT TAPE 6, 8Ø1, A,B
   12 WRITE OUTPUT TAPE 6, 8Ø2, XLAM, DTAU, WØ, W1
      WRITE OUTPUT TAPE 6, 832, RATIO, JJDEL, PCENT
      WRITE OUTPUT TAPE 6, 857, JGRAPH, FAC
      WRITE OUTPUT TAPE 6, 861, ALIMOX, ALIMT
C     INITIALIZE THE PROBLEM
      CHAR=1H*
      XCHAR=1H-
      YCHAR=1H1
      BLANK=2H *
   15 DO 2Ø J=1,2
      DO 2Ø K=1,NSP
      U(1,J,K)=Ø.
      U(2,J,K)=1.
   2Ø U(3,J,K)=WØ
      JJ=1
      MAXU3=1
      ATEMP=Ø.
      MAXK=Ø
      JAP=Ø
      RATIO=RATIO
      KRUEL=Ø
      MYOGL=Ø
      T(1)=1.Ø2*WØ
      T(2)=1.Ø5*WØ
      T(3)=1.1Ø*WØ
      T(4)=1.2Ø*WØ
      T(5)=1.3Ø*WØ
      T(6)=1.4Ø*WØ
      T(7)=1.5Ø*WØ
      T(8)=1.6Ø*WØ
      T(9)=1.7Ø*WØ
      T(1Ø)=1.8Ø*WØ
      T(11)=1.9Ø*WØ

      T(12)=4.Ø*WØ
```

```
      BETA=(1.-2.*XLAM)/XLAM
      DO 24 N=1,15
      KQ(N)=Ø
      R(N)=Ø.
      S(N)=Ø.
   24 CONTINUE
   25 C(1)=1.
      C(2)=A
      C(3)=-B
C     CALCULATE NEW U VALUES FROM OLD,UP TO KSTAR
      M=1
   4Ø KKSTAR=KSTAR-1
      SENSE LIGHT 1
      DO 56 K=2,KKSTAR
      IF(ZIPPER) 3Ø,3Ø,31
   3Ø F1=DTAU*U(1,1,K)*U(2,1,K)
      GO TO 32
   31 F1=DTAU*U(1,1,K)*U(2,1,K)*EXPF(-1./(U(3,1,K)))
   32 DO 56 I=1,3
   41 F=F1*C(I)
      UI2K=XLAM*(U(I,1,K+1)+U(I,1,K-1)+BETA*U(I,1,K))-F
      U(I,2,K)=UI2K
      IF(U(3,2,K)-T(M)) 45,251,251
  251 M=M+1
      XJJ=JJ
      TAU=XJJ*DTAU
      WRITE OUTPUT TAPE 6, 851
      WRITE OUTPUT TAPE 6, 863, TAU, U(3,2,K),K
      WRITE OUTPUT TAPE 6, 851
      N=M-1
      KQ(N)=K
      R(N)=U(3,2,K)
      S(N)=TAU
C     CHECK FOR NEGATIVE VALUES OF U(I,J,K)
   45 IF(U(I,2,K)) 7ØØ,47,47
C     DETERMINATION OF MAX TEMP AT RECORD INTERVAL
   47 IF(I-3) 56,48,48
   48 IF(JJ-KRUEL) 56,5Ø,5Ø
   5Ø IF(M-7) 56,56,51
   51 IF(MAXU3-1) 52,52,56
   52 IF(U(3,2,K)-U(3,2,K-1)) 53,53,56
   53 MAXU3=MAXU3+1
      ATEMP=U(3,2,K-1)
      MAXK=K-1
   56 CONTINUE
      SENSE LIGHT Ø
      GO TO 56Ø
  7ØØ JAP=K
      SENSE LIGHT Ø
      PRINT 865
      WRITE OUTPUT TAPE 6, 865
      WRITE OUTPUT TAPE 6, 851
      XJJ=JJ
```

```
      TAU=XJJ*DTAU
      DO 258 J=1,2
      IF(J-2) 702,701,701
  701 KKSTAR=JAP
  702 WRITE OUTPUT TAPE 6, 864, J
      WRITE OUTPUT TAPE 6, 864,J
      WRITE OUTPUT TAPE 6, 851
      WRITE OUTPUT TAPE 6, 820,TAU,JJ
      WRITE OUTPUT TAPE 6, 851
      WRITE OUTPUT TAPE 6, 806
      DO 255 K=2,KKSTAR
      IF(K-20) 252,252,256
  252 WRITE OUTPUT TAPE 6, 804,(U(I,J,K),I=1,3),K
  255 CONTINUE
  256 DO 258 K=21,KKSTAR,5
      WRITE OUTPUT TAPE 6, 804,(U(I,J,K),I=1,3),K
  258 CONTINUE
  259 WRITE OUTPUT TAPE 6, 862, NFLAME
      WRITE OUTPUT TAPE 6, 851
      WRITE OUTPUT TAPE 6, 860, JM,JD
      WRITE OUTPUT TAPE 6, 851
      WRITE OUTPUT TAPE 6, 801, A, B
      WRITE OUTPUT TAPE 6, 802, XLAM, DTAU,W0,W1
      WRITE OUTPUT TAPE 6, 851
      WRITE OUTPUT TAPE 6, 851
      DO 260 N=1,15
      WRITE OUTPUT TAPE 6, 863,S(N),R(N),KQ(N)
  260 CONTINUE
      WRITE OUTPUT TAPE 6, 851
      DO 261 K=2,KKSTAR
      IF(U(3,2,K)-U(3,2,K-1)) 262,262,261
  261 CONTINUE
  262 ATEMP=U(3,2,K-1)
      MAXK=K-1
      XJJ=JJ
      TAU=XJJ*DTAU
      WRITE OUTPUT TAPE 6, 867, TAU,JJ
      WRITE OUTPUT TAPE 6, 868, ATEMP,MAXK
      WRITE OUTPUT TAPE 6, 851
      IF(JAP) 264,264,263
  263 WRITE OUTPUT TAPE 6, 869
      GO TO 100
  264 IF(SENSE SWITCH 6) 268,265
  265 IF(SENSE SWITCH 5) 266,267
  266 WRITE OUTPUT TAPE 6, 874
      GO TO 100
  267 WRITE OUTPUT TAPE 6, 872, FAC
      GO TO 100
  268 WRITE OUTPUT TAPE 6, 873
      GO TO 913
  560 IF(LAW-1) 565,565,566
  565 U(1,2,1)=1.0
      GO TO 570
```

```
  566 U(1,2,1)=U(1,2,2)+SQRTF(DTAU/XLAM)
  570 U(2,2,1)=U(2,2,2)
      U(3,2,1)=W1
C     CHECK TO SEE IF MORE SPACE POINT ARE NEEDED
      LSTAR=KSTAR-2
      FUEL=U(1,2,LSTAR)
      OX=U(2,2,LSTAR)
      TEMP=U(3,2,LSTAR)
      IF(FUEL-PCENT) 561,562,57
  561 DO 562 K=LSTAR,KSTAR,1
      U(1,2,K)=Ø.
  562 CONTINUE
  563 IF(OX-ALIMOX) 57,564,564
  564 TDIFF=ABSF(TEMP-WØ)
      BARF=9.Ø*ALIMT
      IF(TDIFF-BARF) 58,58,57
   57 KSTAR=KSTAR+1
   58 CONTINUE
      IF(SENSE SWITCH 5) 59,6Ø
   59 PAUSE
      GO TO 259
C     TIME INTTERVAL PRINT DETERMINATION FOLLOWS
   6Ø XJJ=JJ
      TAU=XJJ*DTAU
C     DATA PRINT OUT AT EVERY JJDEL INCREMENTS OF  JJ
      DO 6ØØ4 K=1,KSTAR
      IF(U(3,2,K)-FAC*WØ) 6ØØ4,2ØØ,2ØØ
 6ØØ4 CONTINUE
 6ØØ5 IF(JJ-KRUEL) 6ØØ,61,61
   61 CONTINUE
C     SS3  PRINTS TIME, JJ, AND U(I,2,K), K
      IF(SENSE SWITCH 3) 62,64
   62 PRINT 82Ø, TAU,JJ
   63 PRINT 8Ø6
   64 CONTINUE
   65 WRITE OUTPUT TAPE 6, 851
      WRITE OUTPUT TAPE 6, 851
      WRITE OUTPUT TAPE 6, 82Ø, TAU,JJ
      WRITE OUTPUT TAPE 6, 8Ø6
C     Ø
C     Ø
C     SENSE SWITCH 3  ON  FOR U(I,2,K) PRINT OUT
C     Ø
C     Ø
C     SPACE STEP RECORD DETERMINATION
  411 DO 42Ø K=1,KKSTAR
      IF(K-2Ø) 413,413,65Ø
  413 IF(SENSE SWITCH 3) 414,415
  414 PRINT 8Ø4, (U(I,2,K),I=1,3),K
  415 WRITE OUTPUT TAPE 6, 8Ø4, (U(I,2,K),I=1,3),K
  42Ø CONTINUE
```

```
      WRITE OUTPUT TAPE 6, 851
      IF(SENSE SWITCH 3) 421,422
  421 PRINT 866, ATEMP,MAXK
  422 WRITE OUTPUT TAPE 6, 866, ATEMP,MAXK
      MAXU3=1
      GO TO 500
  200 WRITE OUTPUT TAPE 6, 851
      DO 215 J=1,2
      WRITE OUTPUT TAPE 6, 864, J
      WRITE OUTPUT TAPE 6, 851
      WRITE OUTPUT TAPE 6, 820, TAU,JJ
      WRITE OUTPUT TAPE 6, 851
      WRITE OUTPUT TAPE 6, 806
      DO 205 K=1,KKSTAR
      IF(K-20) 201,201,210
  201 WRITE OUTPUT TAPE 6, 804,(U(I,J,K),I=1,3),K
  205 CONTINUE
      WRITE OUTPUT TAPE 6, 851
      WRITE OUTPUT TAPE 6, 866, ATEMP,MAXK
      WRITE OUTPUT TAPE 6, 851
      PRINT 856
      WRITE OUTPUT TAPE 6, 856
      GO TO 259
  210 DO 215 K=21,KKSTAR,5
      WRITE OUTPUT TAPE 6, 804,(U(I,J,K),I=1,3),K
  215 CONTINUE
      WRITE OUTPUT TAPE 6, 851
      WRITE OUTPUT TAPE 6, 866, ATEMP,MAXK
      WRITE OUTPUT TAPE 6, 851
      PRINT 856
      WRITE OUTPUT TAPE 6, 856
      GO TO 259
C     SPACE STEP JUMP RECORDING DETERMINATION
  650 DO 657 K=21,KKSTAR,5
  654 IF(SENSE SWITCH 3) 655,656
  655 PRINT 804,(U(I,2,K),I=1,3),K
  656 WRITE OUTPUT TAPE 6, 804, (U(I,2,K),I=1,3),K
  657 CONTINUE
      WRITE OUTPUT TAPE 6, 851
C     REPLACE**GO TO 500**WITH--SGRAPH ON SS 4--WHEN AVAILABLE
      IF(SENSE SWITCH 3) 658,659
  658 PRINT 866, ATEMP, MAXK
  659 WRITE OUTPUT TAPE 6, 866, ATEMP, MAXK
      MAXU3=1
      GO TO 500
C     TEMPERATURE PLOT ROUTINE FOLLOWS
  500 IF(JJ-MYOGL) 599,501,501
  501 DO 505 K=1,KSTAR
      X(K)=K
      Y(K)=U(3,2,K)
  505 CONTINUE
      MYOGL=MYOGL+JGRAPH
```

```
      CALL MAXIM(X,XMAX,KSTAR)
      CALL MAXIM(Y,YMAX,KSTAR)
      WRITE OUTPUT TAPE 6, 850
      WRITE OUTPUT TAPE 6, 851
      WRITE OUTPUT TAPE 6, 820, TAU,JJ
      WRITE OUTPUT TAPE 6,851
      WRITE OUTPUT TAPE 6,855, XMAX
      CALL PLOT(X,XMAX, 0.,10, Y, YMAX, 0. , 10 , KSTAR, CHAR, XCHAR,
     1YCHAR, BLANK)
      WRITE OUTPUT TAPE 6, 858
      WRITE OUTPUT TAPE 6, 859
      IF(SENSE SWITCH 4) 510, 597
  510 K0=0
      WRITE OUTPUT TAPE K0, 870, NFLAME,TAU
      READ INPUT TAPE K0,871,DUMMY(9),DUMMY(8),DUMMY(7),DUMMY(6),
     1DUMMY(5),DUMMY(4),DUMMY(3),DUMMY(2)
  870 FORMAT(9H DIFLAME ,I1,24H TEMP IN SPACE AT TAU = ,E12.6,5X)
  871 FORMAT(8A6)
B     DUMMY(1)=-0
      SENSE LIGHT 1
      SENSE LIGHT 2
      SENSE LIGHT 3
      SENSE LIGHT 4
      CALL SGRAPH(X,Y,KKSTAR,0,DUMMY(9),9H DISTANCE,5H RT/E)
      SENSE LIGHT 0
  597 CONTINUE
      IF(SENSE SWITCH 2) 598,599
  598 PAUSE 77777
      CALL RSOS(10)
  599 KRUEL=KRUEL+JJDEL
C     UPDATE PROCEDURE FOLLOWS
  600 DO 605 I=1,3
  601 DO 605 K=1,KSTAR,1
      SENSE LIGHT 3
  605 U(I,1,K)=U(I,2,K)
      IF(SENSE SWITCH 1) 720,750
  720 DO 721 K=1,KKSTAR
      X(K)=K
  721 Y(K)=U(3,1,K)
      K0=0
      WRITE OUTPUT TAPE K0, 870, NFLAME, TAU
      READ INPUT TAPE K0, 871,DUMMY(9),DUMMY(8),DUMMY(7),DUMMY(6),
     1DUMMY(5),DUMMY(4),DUMMY(3),DUMMY(2)
B     DUMMY(1)=-0
      CALL SGRAPH(X,Y,KKSTAR,0,DUMMY(9),9H DISTANCE,5H RT/E)
  750 CONTINUE
      IF(SENSE SWITCH 2) 751,606
  751 PRINT 877
      PAUSE 77777
      CALL RSOS(10)
      PAUSE 11111
      BACKSPACE 6
      PRINT 878
```

```
      WRITE OUTPUT TAPE 6, 862, NFLAME
      WRITE OUTPUT TAPE 6, 851
      WRITE OUTPUT TAPE 6, 800,JM,JD
      WRITE OUTPUT TAPE 6, 851
      WRITE OUTPUT TAPE 6, 801,A,B
      WRITE OUTPUT TAPE 6, 802,XLAM,DTAU,W0,W1
      WRITE OUTPUT TAPE 6, 851
      WRITE OUTPUT TAPE 6, 851
      WRITE OUTPUT TAPE 6, 878
  606 JJ=JJ+1
      SENSE LIGHT 0
C      SS6  STOPS PROGRAM
      IF(SENSE SWITCH 6) 910,607
  607 IF(JJ-NTP) 40,40,259
  910 WRITE OUTPUT TAPE 6, 862, NFLAME
      WRITE OUTPUT TAPE 6, 851
      WRITE OUTPUT TAPE 6, 860, JM,JD
      WRITE OUTPUT TAPE 6, 851
      WRITE OUTPUT TAPE 6, 801, A, B
      WRITE OUTPUT TAPE 6, 802, XLAM, DTAU,W0,W1
      WRITE OUTPUT TAPE 6, 851
      WRITE OUTPUT TAPE 6, 851
      DO 911 N=1,15
      WRITE OUTPUT TAPE 6, 863,S(N),R(N),KQ(N)
  911 CONTINUE
      DO 912 K=1,KKSTAR
  912 U(3,2,K)=U(3,1,K)
      GO TO 260
  913 CALL EXIT
      END
```

.
.
.
.

SUBROUTINE FOR INCLUSION OF ALL DATA CASES IN THE MAIN PROGRAM

```
      *
      *
      SUBROUTINE INPUT(IND,JM,JD,NFLAME,LAW,ZIPPER,KSTOP,FMAX,NTP,NSP,A,
     1B,XLAM,DTAU,W0,W1,RATIO,JJDEL,PCENT,JGRAPH,FAC,ALIMOX,ALIMT,KSTAR)
  800 FORMAT (218)
  801 FORMAT (E15.7, E15.7)
  802 FORMAT (4E15.7)
  803 FORMAT (16)
  832 FORMAT (E15.7,I8,E15.7)
  857 FORMAT (I6,E10.2)
  861 FORMAT (E15.7,E10.2)
  875 FORMAT(43H ALL DATA CASES SUPPLIED HAVE BEEN COMPUTED)
  876 FORMAT(49H SUPPLY INPUT TAPE  A-6  TO THE MACHINA COMPUTANA)
  877 FORMAT(I8,F8.0)
  878 FORMAT(E15.7)
      DIMENSION NTP1(35),NSP1(35),A1(35),B1(35),XLAM1(35), DTAU1(35),
     1W01(35),W11(35),RATIO1(35),JJDEL1(35),PCENT1(35),JGRPH1(35),
     2FAC1(35),OXLIM1(35),ALIMT1(35),KSTAR1(35),FMAX1(35),KSTOP1(35)
      IF(IND) 1,1,2
```

```
    1 READ INPUT TAPE 5, 803, NCASES
      READ INPUT TAPE 5, 800,JM,JD
C     LAW=1 REFERS TO CONSTANT CF CASE
C     LAW=2 REFERS TO CONSTANT MDOT CASE
      READ INPUT TAPE 5, 803, NFLAME
      READ INPUT TAPE 5, 877, LAW,ZIPPER
C     ZIPPER REFERS TO ACTIVATION ENERGY
C     IF ZIPPER IS ZERO, ACTIVATION ENERGY IS ZERO
      DO 3  I=1,NCASES
      READ INPUT TAPE 5, 878, FMAX1(I)
      READ INPUT TAPE 5, 803, KSTOP1(I)
      READ INPUT TAPE 5, 800, NTP1(I),NSP1(I)
      READ INPUT TAPE 5, 801,A1(I),B1(I)
      READ INPUT TAPE 5, 802,XLAM1(I),DTAU1(I),W01(I),W11(I)
      READ INPUT TAPE 5, 832,RATIO1(I),JJDEL1(I),PCENT1(I)
      READ INPUT TAPE 5, 857,JGRPH1(I),FAC1(I)
      READ INPUT TAPE 5, 861,OXLIM1(I),ALIMT1(I)
    3 READ INPUT TAPE 5, 803,KSTAR1(I)
      NCOUNT = 1
      RETURN
    2 IF(NCOUNT-NCASES) 4,4,5
    5 PRINT 875
      PRINT 876
      CALL EXIT
    4 NCOUNT=NCOUNT
      FMAX=FMAX1(NCOUNT)
      KSTOP=KSTOP1(NCOUNT)
      NTP=NTP1(NCOUNT)
      NSP=NSP1(NCOUNT)
      A=A1(NCOUNT)
      B=B1(NCOUNT)
      XLAM=XLAM1(NCOUNT)
      DTAU=DTAU1(NCOUNT)
      W0=W01(NCOUNT)
      W1=W11(NCOUNT)
      RATIO=RATIO1(NCOUNT)
      JJDEL=JJDEL1(NCOUNT)
      PCENT=PCENT1(NCOUNT)
      JGRAPH=JGRPH1(NCOUNT)
      FAC=FAC1(NCOUNT)
      ALIMOX=OXLIM1(NCOUNT)
      ALIMT=ALIMT1(NCOUNT)
      KSTAR=KSTAR1(NCOUNT)
      NCOUNT=NCOUNT+1
      RETURN
      END
```

THE**PLOT**SUBROUTINE IS DUE TO MR.L.L.HOFFMAN, OF GUGGENHEIM LABS, AND WAS WRITTEN COMPLETELY IN FORTRAN II. ALL INQUIRIES ABOUT THIS PROGRAM SHOULD BE ADDRESSED TO MR. HOFFMAN. THE SUBROUTINE **MAXIM** IS A PART OF **PLOT**, AS ARE THE DESIGNATIONS CHAR=1H* , XCHAR=1H- , YCHAR=1H1 , AND BLANK=2H * .

ALL OTHER CALLED SUBROUTINES ARE IN THE LIBRARAY OF THE PRINCETON UNIVERSITY COMPUTING CENTER.

TABLE I

IGNITION OF M2 PROPELLANT

Roth & Wactell, 1962, Ref. (9)

Ignition Time, Seconds

Temp., °K.	Results in Nitrogen				
	0 psig	50 psig	100 psig	200 psig	300 psig
723	30.50	17.50	12.30	8.80	5.40
798	15.40	9.30	6.80	5.00	3.10
873	8.90	5.60	4.10	3.10	2.00
948	5.50	3.70	2.70	2.10	1.35
1023	3.70	2.45	1.85	1.50	1.10
1098	2.60	1.80	1.40	1.10	0.75

	Results in Air			Results in Helium	
	0 psig	100 psig	300 psig	0 psig	50 psig
723	25.80	12.02	4.40	9.12	8.54
798	11.84	5.84	2.94	5.82	4.41
873	7.69	3.62	1.80	3.52	3.22
948	5.22	2.41	1.36	2.41	2.02
1023	3.36	1.57	1.00	1.71	1.28
1098	2.17	1.25	0.74	1.08	0.90

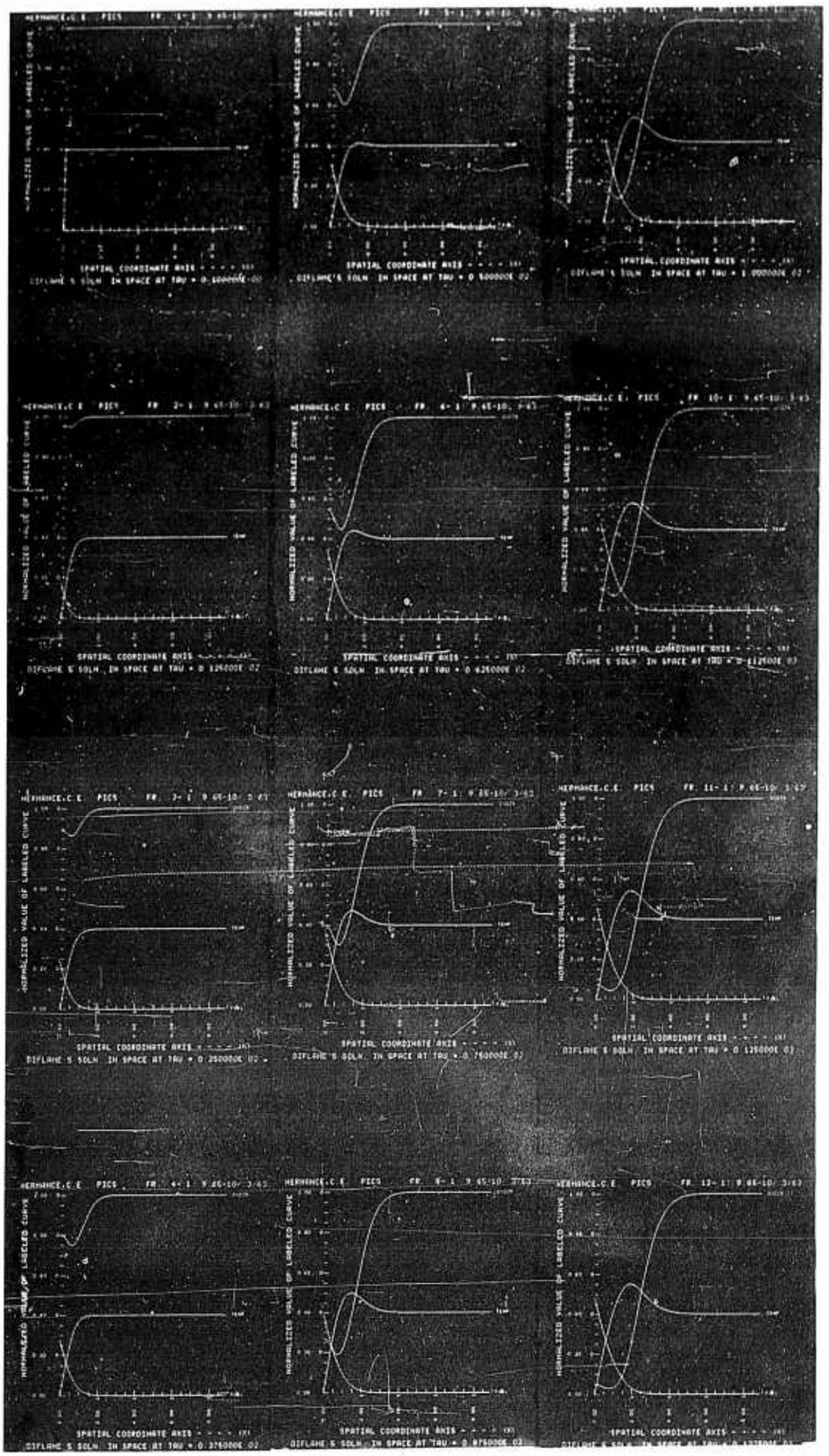

CRT DISPLAY OF NUMERICAL SOLUTION AT SUCCESSIVE TIME INTERVALS TAU

FIGURE I-1

DIMENSIONLESS IGNITION DELAY τ^* VS RECIPROCAL OF A PARAMETER

CASE I: CONSTANT C_F° AT WALL

$(E/R) = 12000°K$ $\quad \theta_0 = 0.10$

$B = 1.0$ $\quad \theta_s = 0.0333$

$L^*(\theta)$: $\theta^* = \alpha\theta_0$

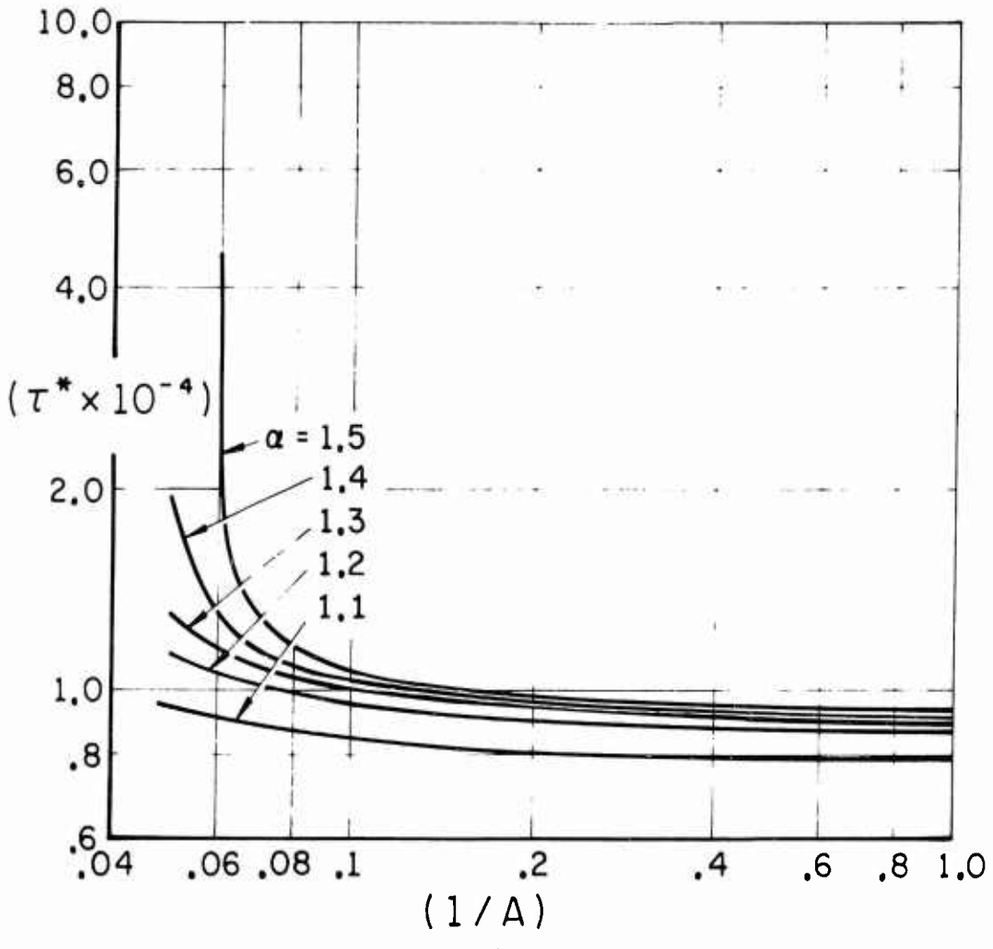

FIGURE I - 2

DIMENSIONLESS IGNITION DELAY τ^* VS RECIPROCAL OF A PARAMETER

CASE I: CONSTANT C_F^o AT WALL

$(E/R) = 4000°\,K$ $\quad \theta_0 = 0.30$

$B = 3.0$ $\quad \theta_s = 0.10$

$L^*(\theta)$: $\theta^* = \alpha\theta_0$

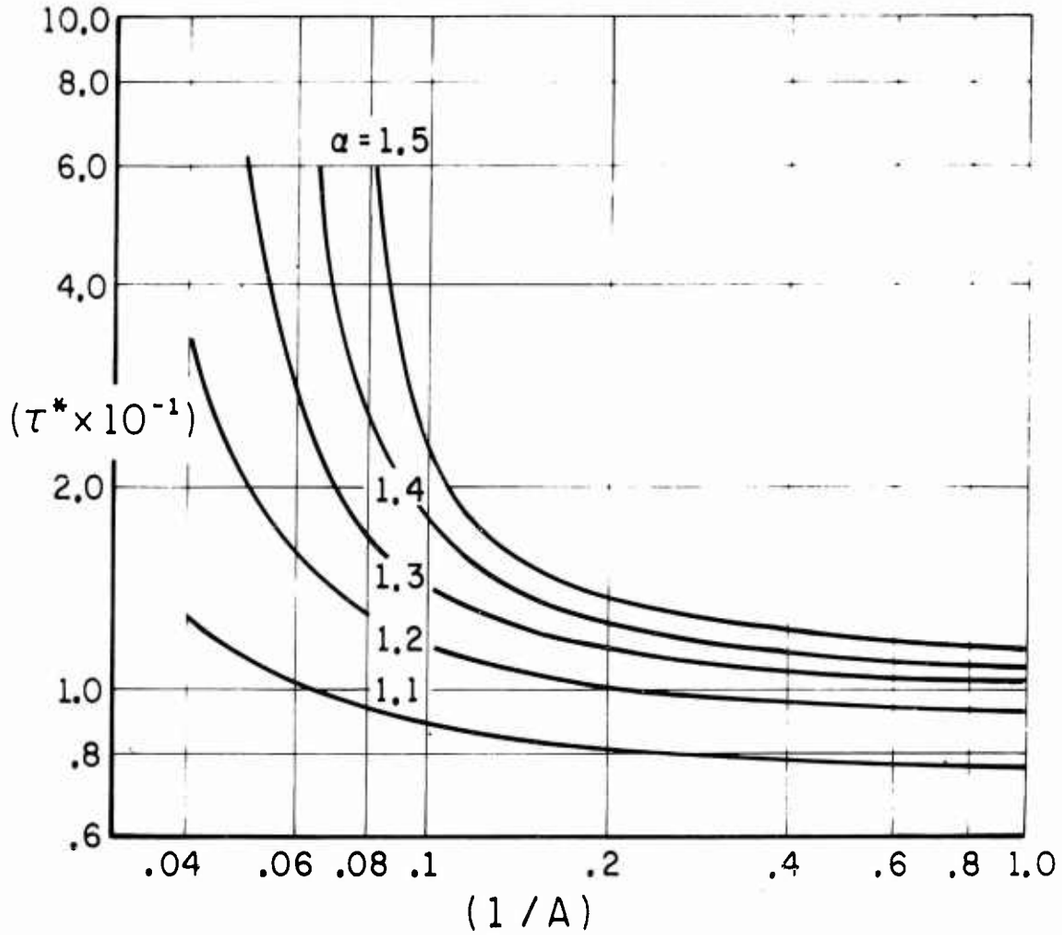

FIGURE I - 3

DIMENSIONLESS IGNITION DELAY τ^* VS RECIPROCAL OF A PARAMETER

CASE I: CONSTANT C_F^o AT WALL

$(E/R) = 0$ $\theta_0 = 0.66667$

$B = 10.0$ $\theta_S = 0.0$

$L^*(\theta)$: $\theta^* = \alpha\,\theta_0$

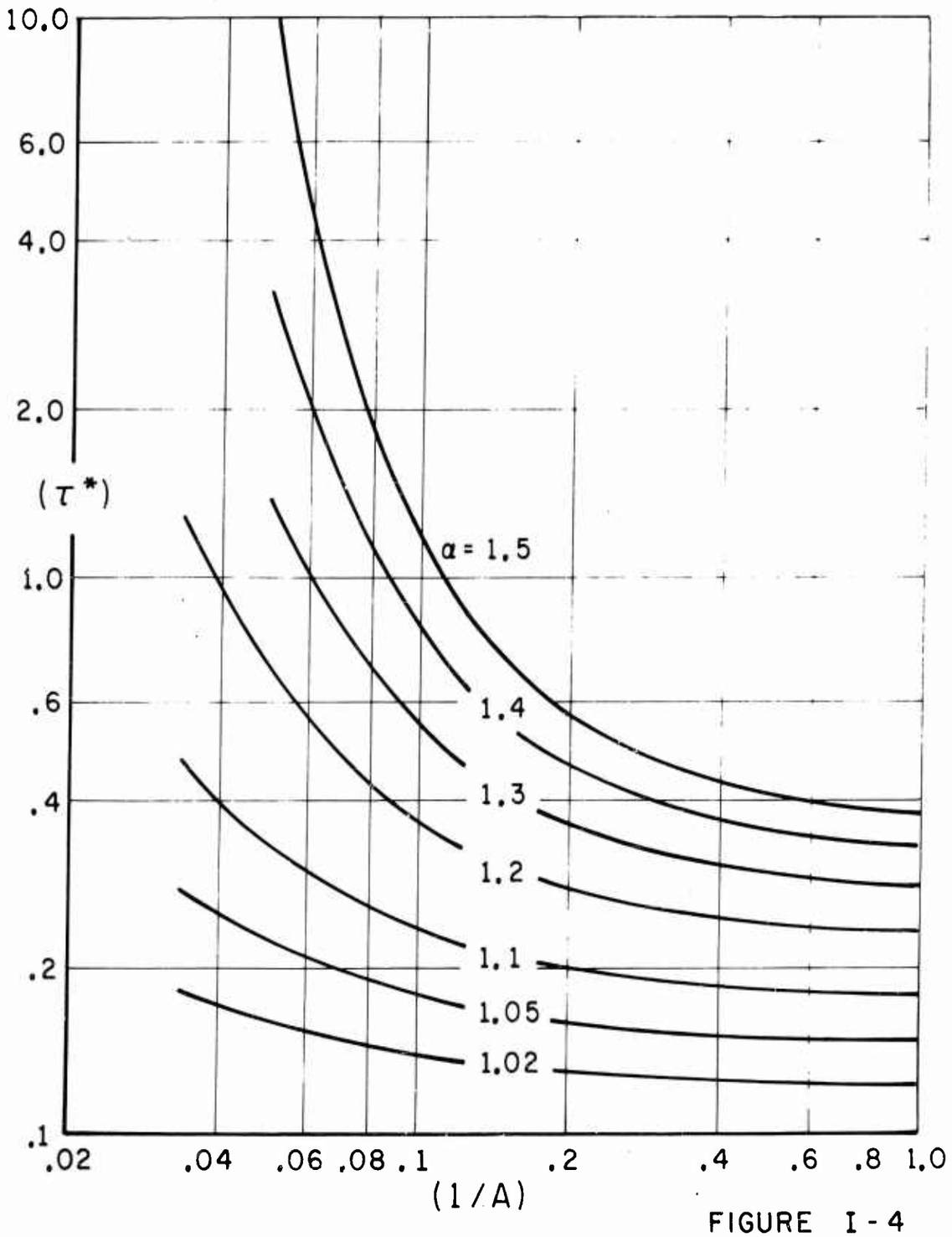

FIGURE I - 4

EFFECT OF B PARAMETER VARIATION ON
DIMENSIONLESS IGNITION DELAY

CASE I: CONSTANT C_F^o AT WALL

$(E/R) = 12000°K$ $\theta_s = 0.0333$

$\theta_0 = 0.10$ $L^*(\theta)$: $\theta^* = \alpha\theta_0$

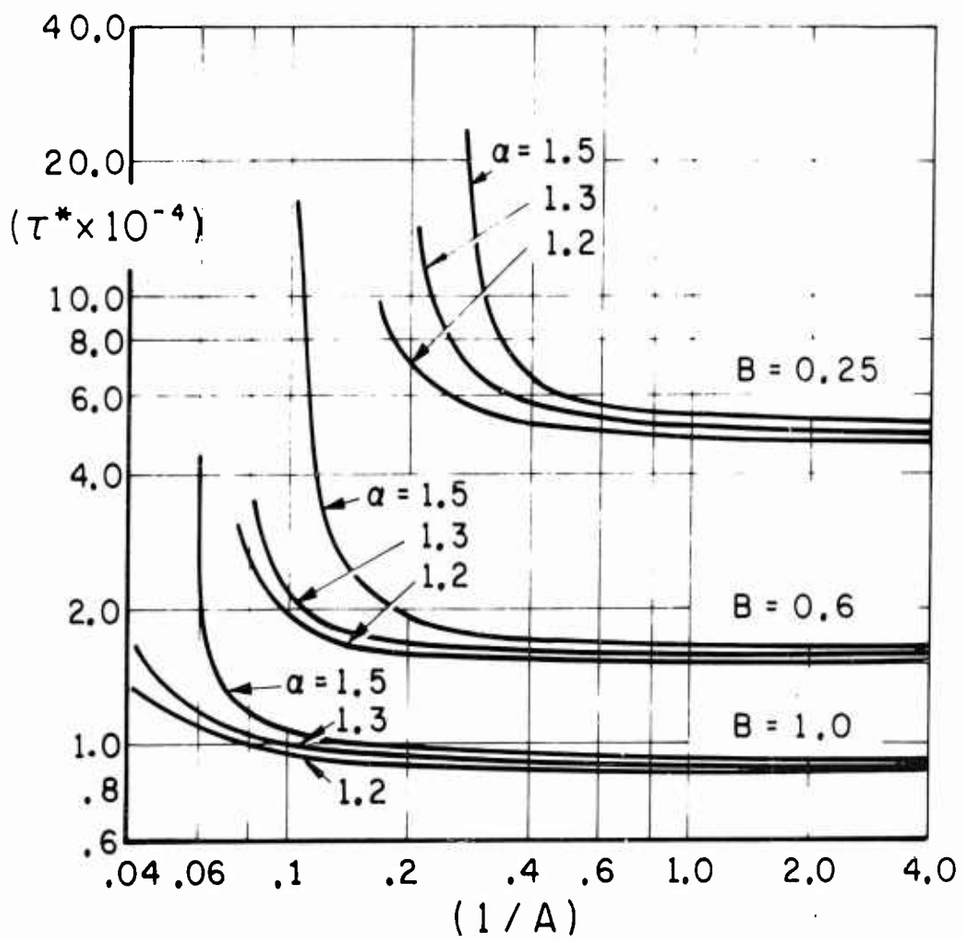

FIGURE I - 5

EFFECT OF B PARAMETER VARIATION ON
DIMENSIONLESS IGNITION DELAY

CASE I: CONSTANT C_F^o AT WALL

$(E/R) = 4000°K$ $\theta_S = 0.10$

$\theta_0 = 0.30$ $L^*(\theta)$: $\theta^* = 0.45$

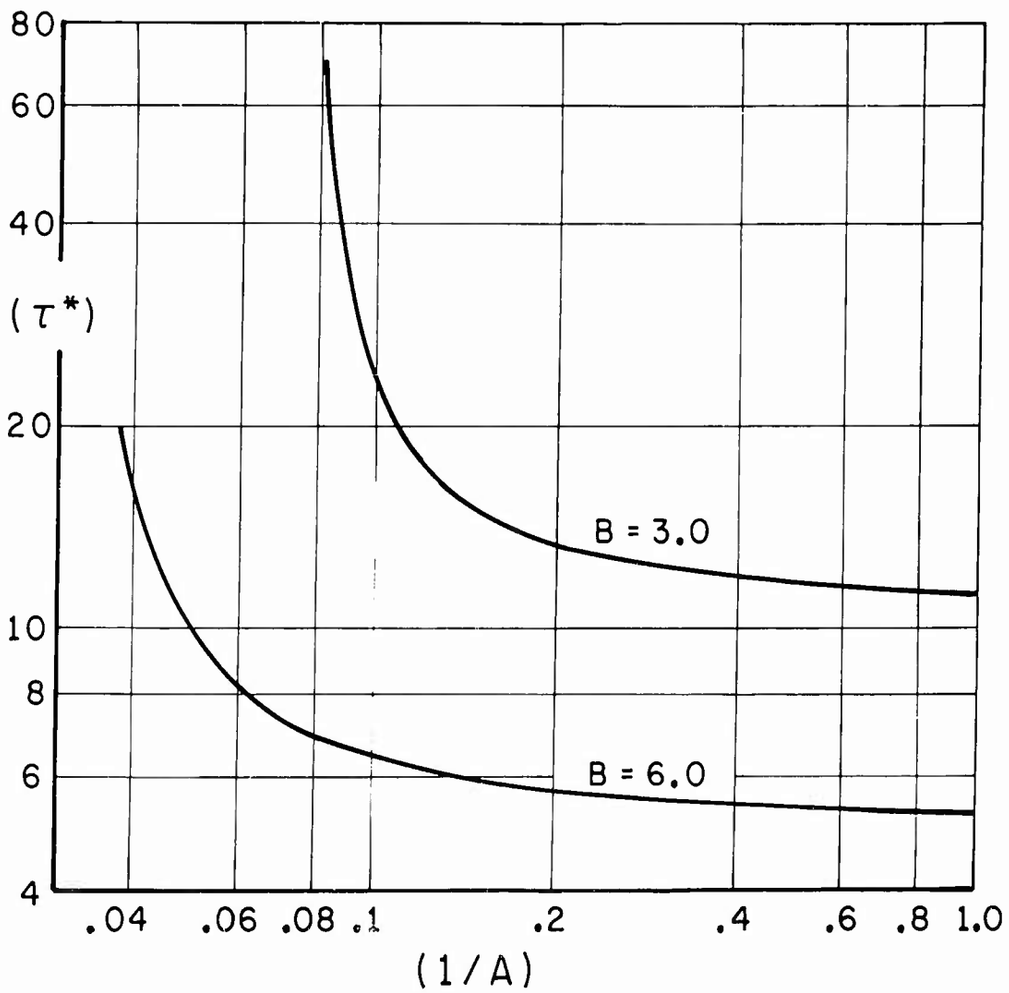

FIGURE I-6

EFFECT OF B PARAMETER VARIATION ON
DIMENSIONLESS IGNITION DELAY

CASE I: CONSTANT C_F^o AT WALL

$(E/R) = 0$ $\theta_S = 0.0$

$\theta_0 = 0.66667$ $L^*(\theta)$: $\theta^* = 1.0$

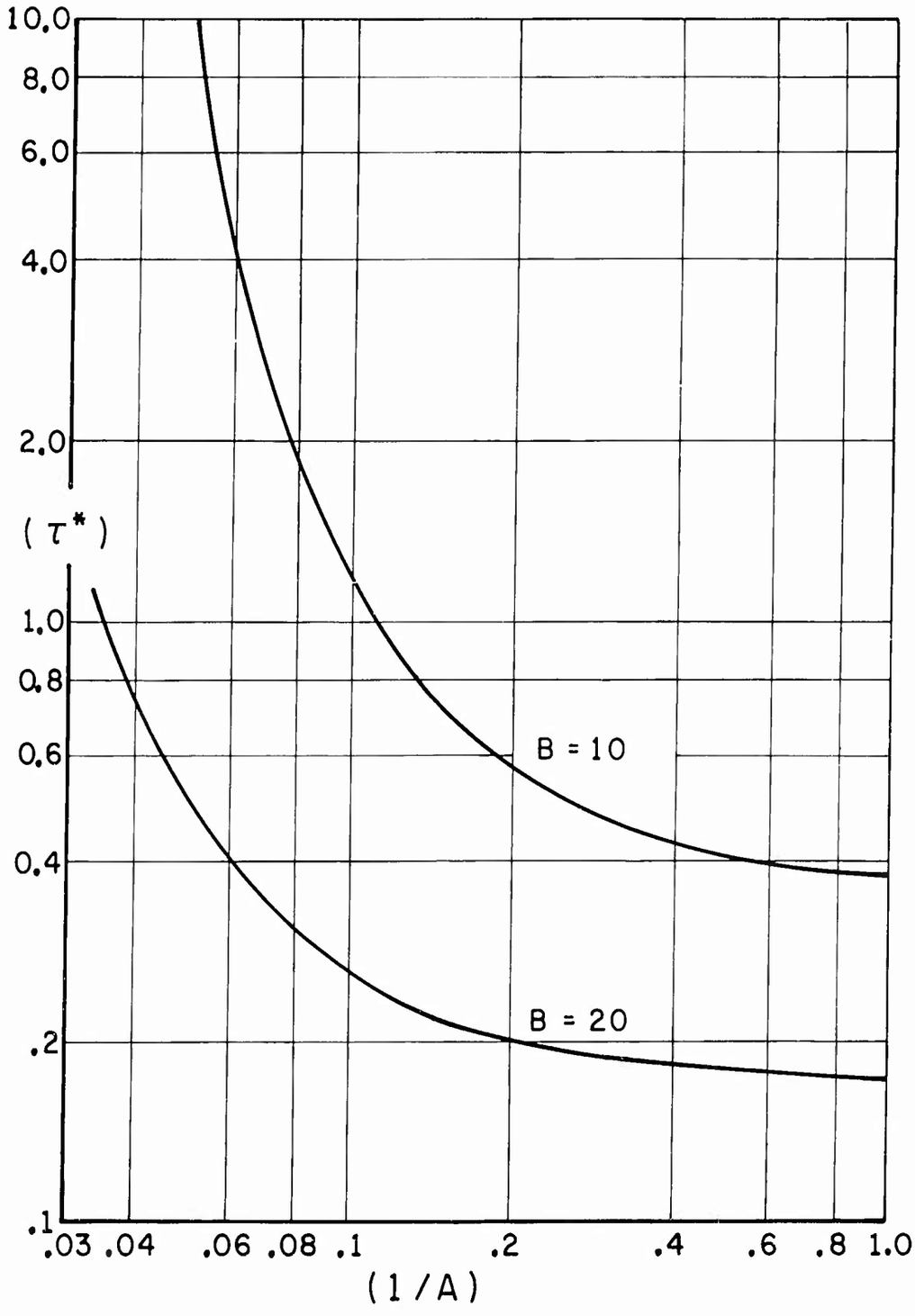

FIGURE I - 7

DIMENSIONLESS IGNITION DELAY τ^* VS RATIO OF A AND B PARAMETERS

CASE II: CONSTANT $\dot{m}_F^o$ AT WALL

$(E/R) = 12000°K$ $\theta_s = 0.0333$

$\theta_0 = 0.10$ $L^*(\theta)$: $\theta^* = \alpha\theta_0$

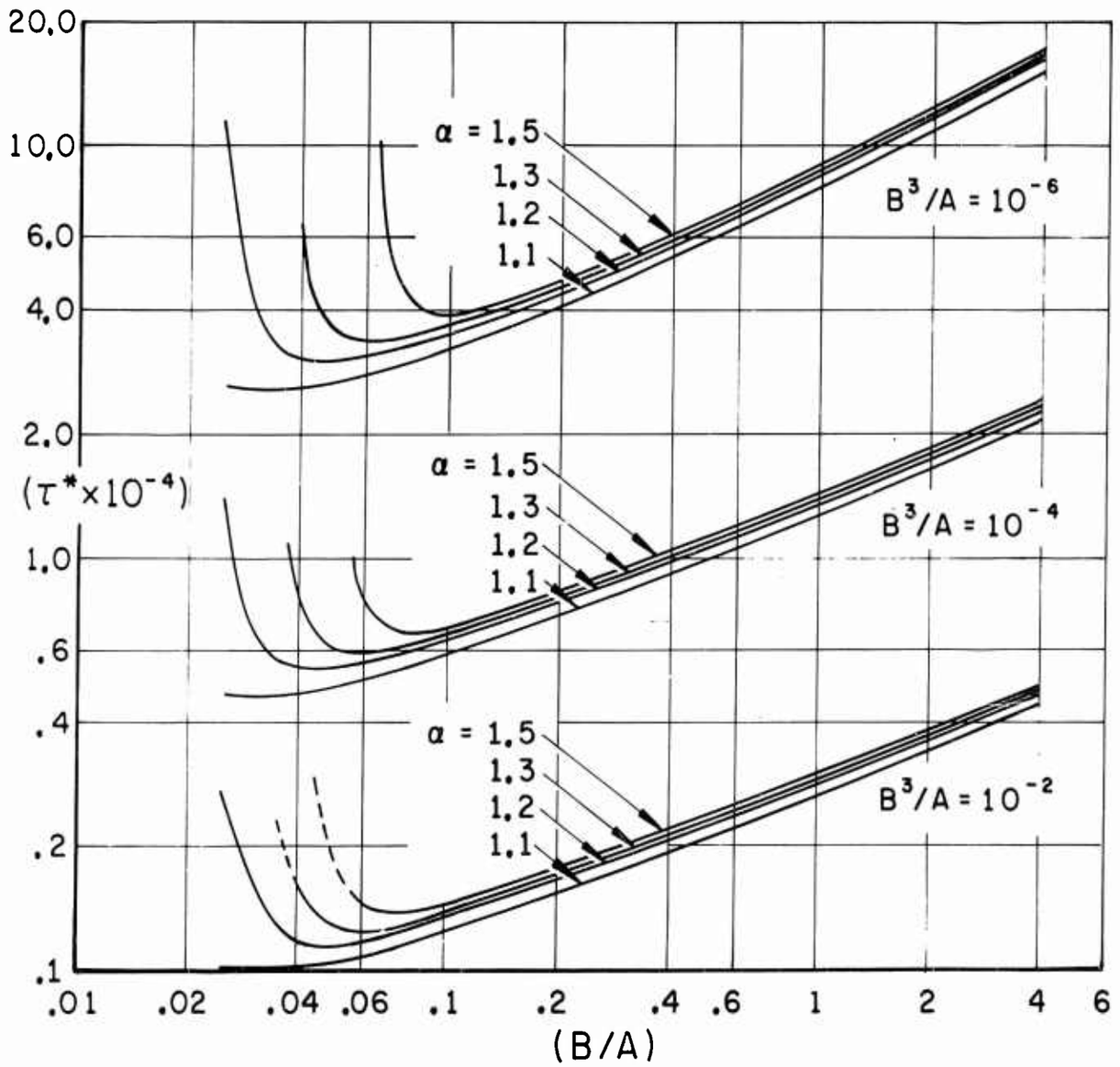

FIGURE I-8

DIMENSIONLESS IGNITION DELAY τ^* VS RATIO OF A AND B PARAMETERS

CASE II : CONSTANT $\dot{m}_F^o$ AT WALL

$(E/R) = 4000°K$ $\theta_0 = 0.30$

$(B^3/A) = 27 \times 10^{-4}$ $\theta_s = 0.10$

$L^*(\theta)$: $\theta^* = \alpha\theta_0$

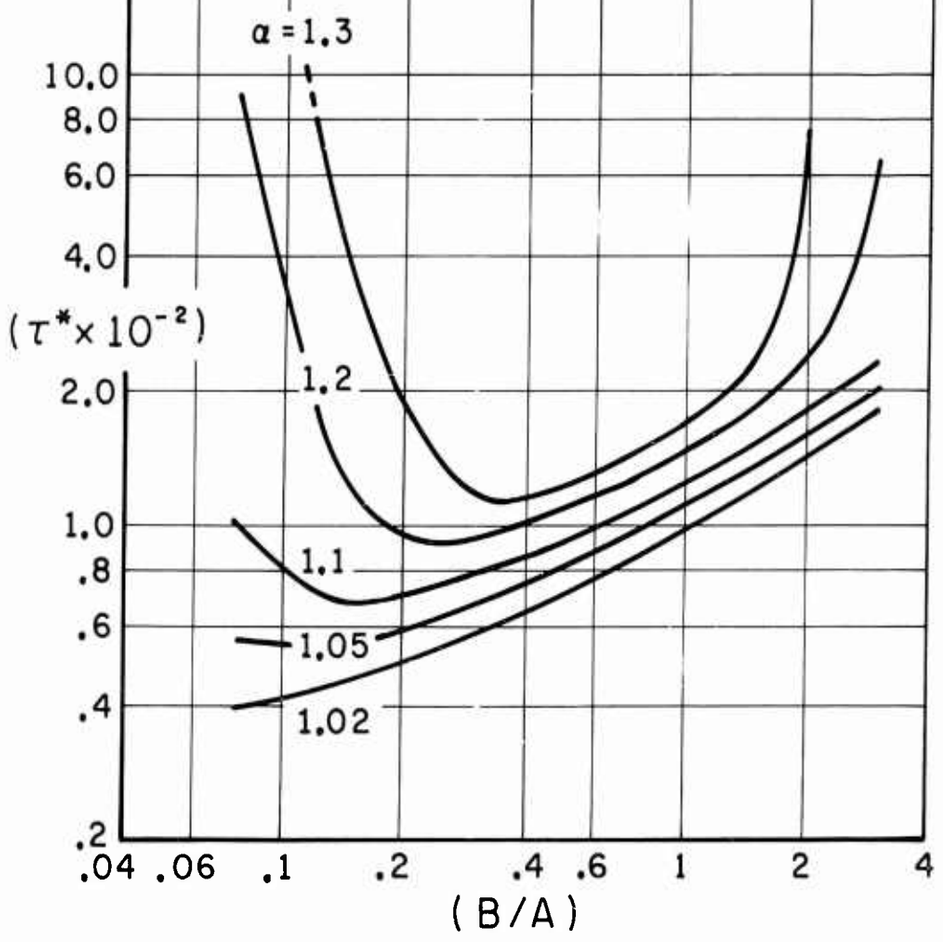

FIGURE I-9

DIMENSIONLESS IGNITION DELAY τ^* VS RATIO OF A AND B PARAMETERS

CASE II : CONSTANT $\dot{m}_F^o$ AT WALL

$(E/R) = 0$ $\theta_0 = 0.66667$

$(B^3/A) = 10$ $\theta_s = 0.0$

$L^*(\theta)$: $\theta^* = \alpha\theta_0$

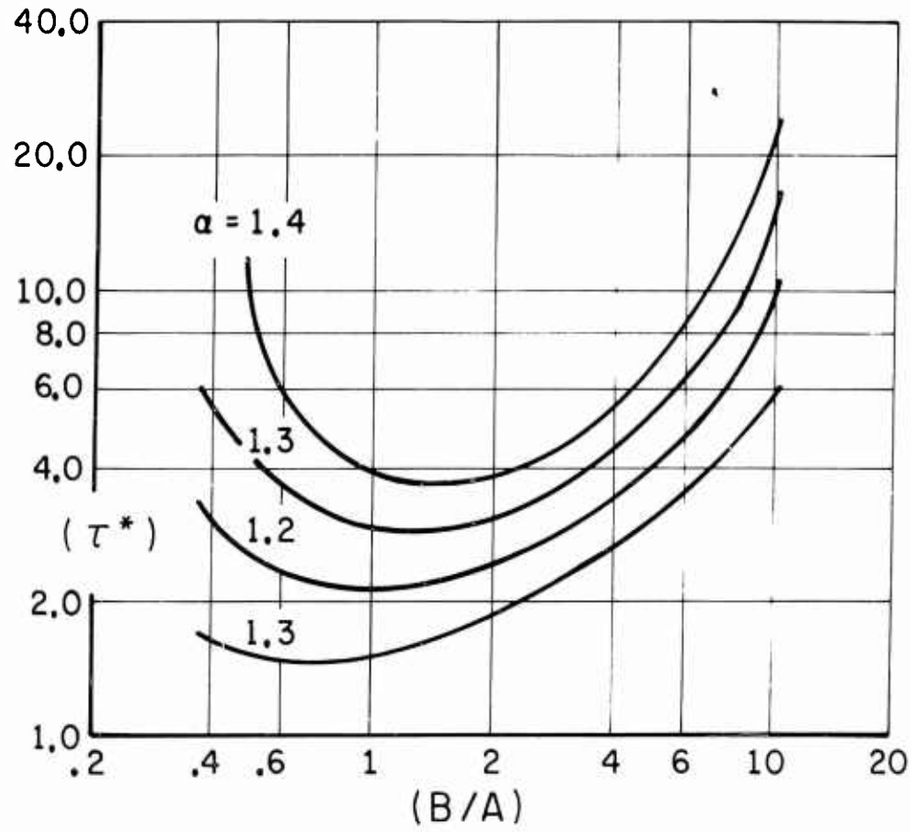

FIGURE I-10

EFFECT OF ACTIVATION ENERGY ON THE DIMENSIONLESS IGNITION DELAY

CASE I: CONSTANT C_F^o AT WALL

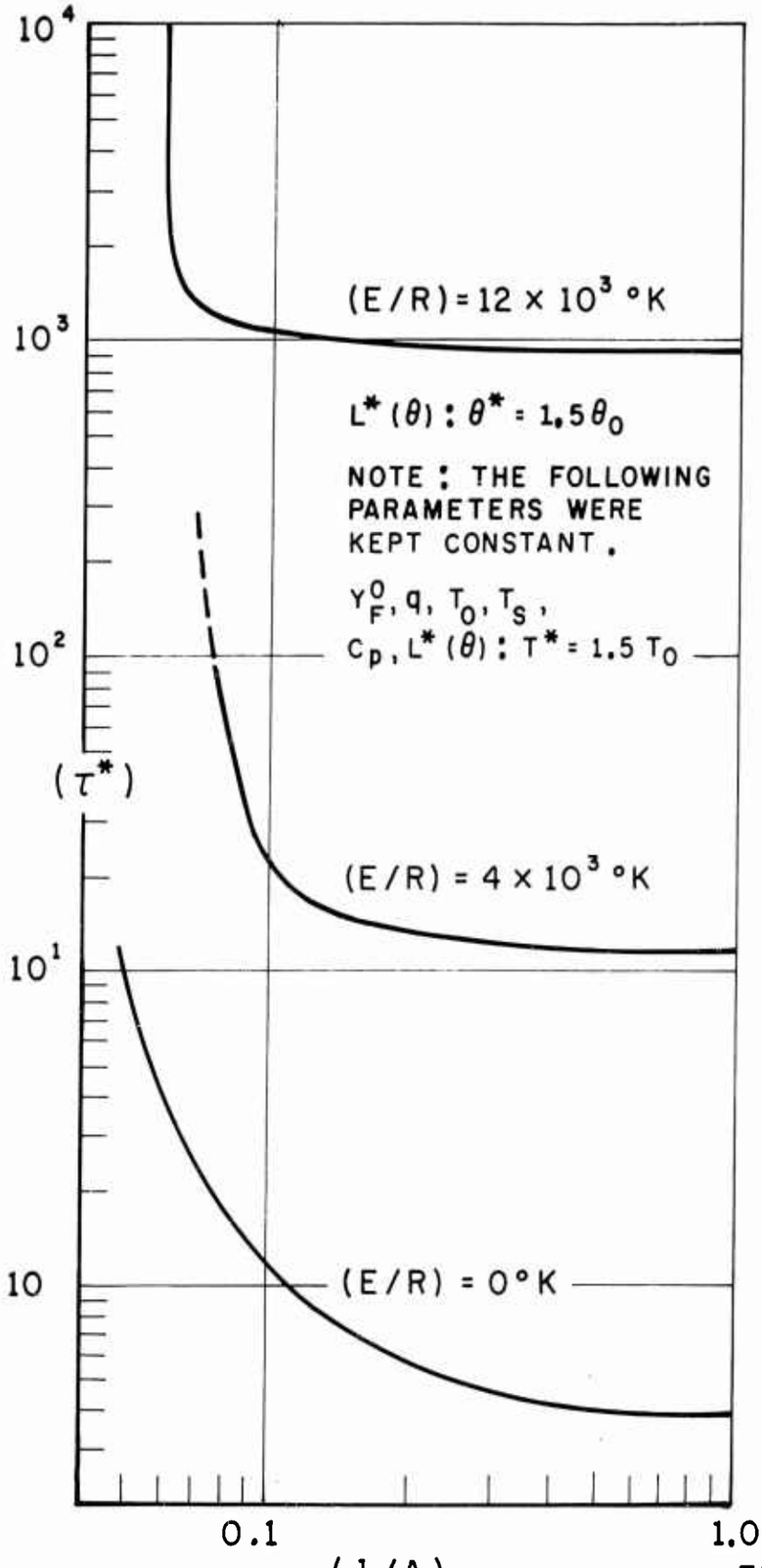

FIGURE I - 11

EFFECT OF ACTIVATION ENERGY ON THE DIMENSIONLESS IGNITION DELAY

CASE II: CONSTANT $\dot{m}_F^o$ AT WALL

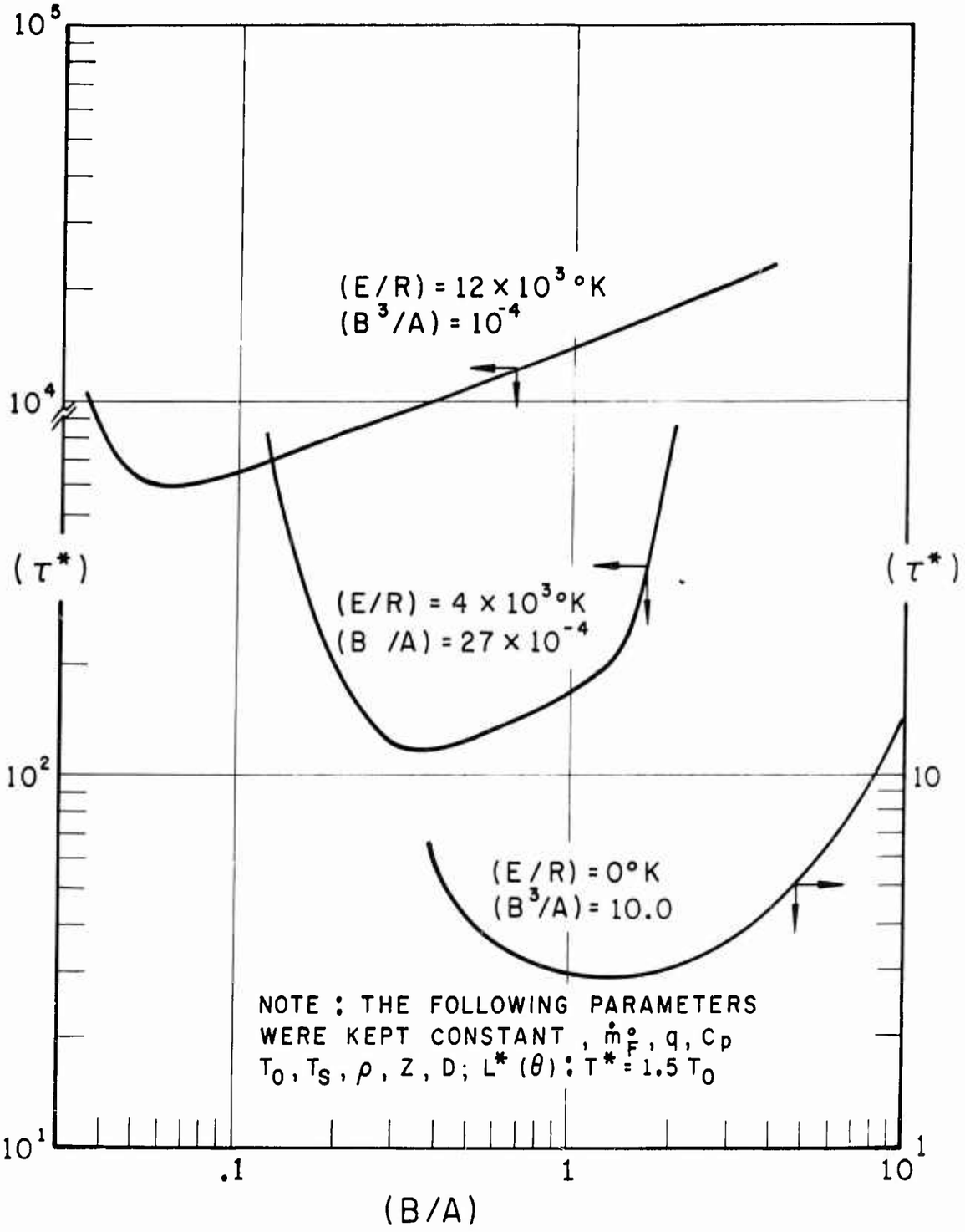

FIGURE I - 12

SENSITIVITY OF IGNITION DELAY TO
INITIAL GAS TEMPERATURE

CASE I: CONSTANT C_F^o AT WALL

(E/R) = 4000°K θ_s = 0.10

B = 3.0 $L^*(\theta)$: θ^* = 0.4

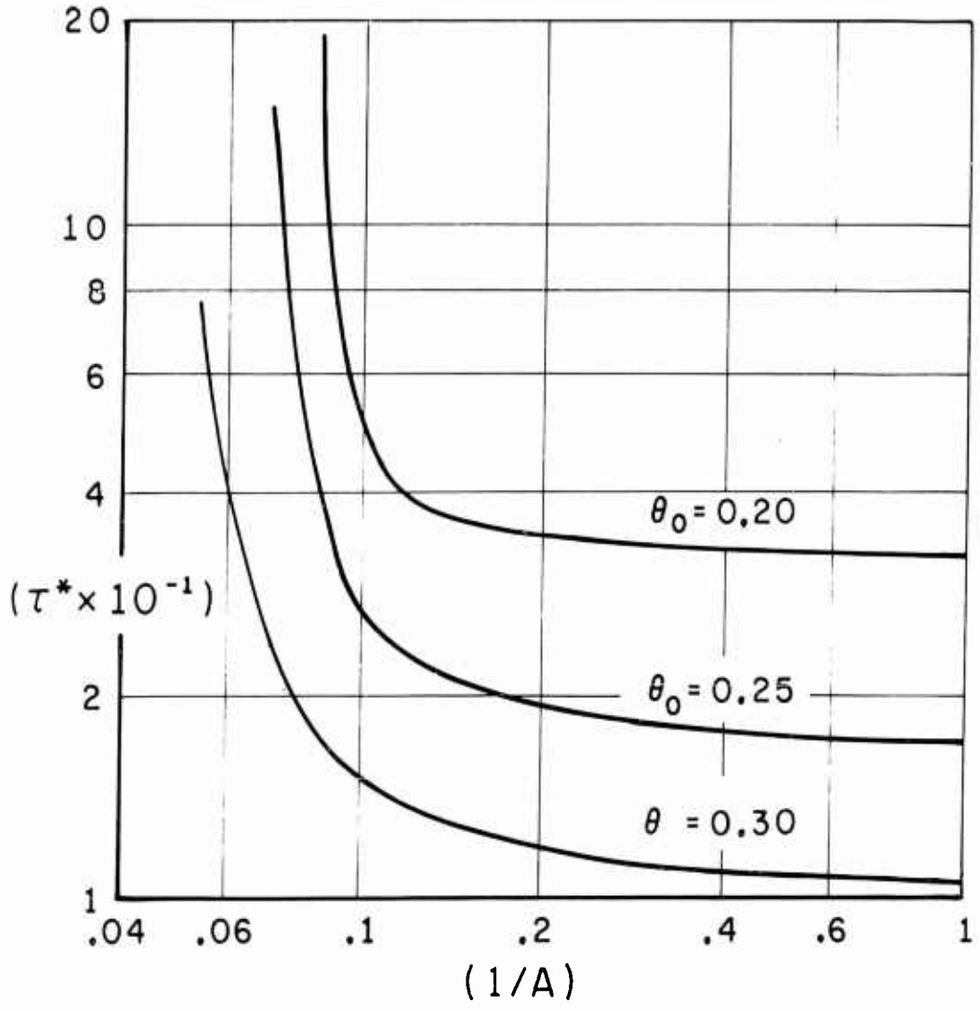

FIGURE I - 13

SENSITIVITY OF REAL IGNITION DELAY TO
INITIAL OXIDIZER MOLE FRACTION
AT CONSTANT PRESSURE
CASE I: CONSTANT C_F^o AT WALL

$B = 3.0$ $q = 12000$ CAL/GM °K
$\theta_0 = 0.3$ $(E/R) = 4000$ °K
$\theta_s = 0.1$ $C_p = 0.25$ CAL/GM °K

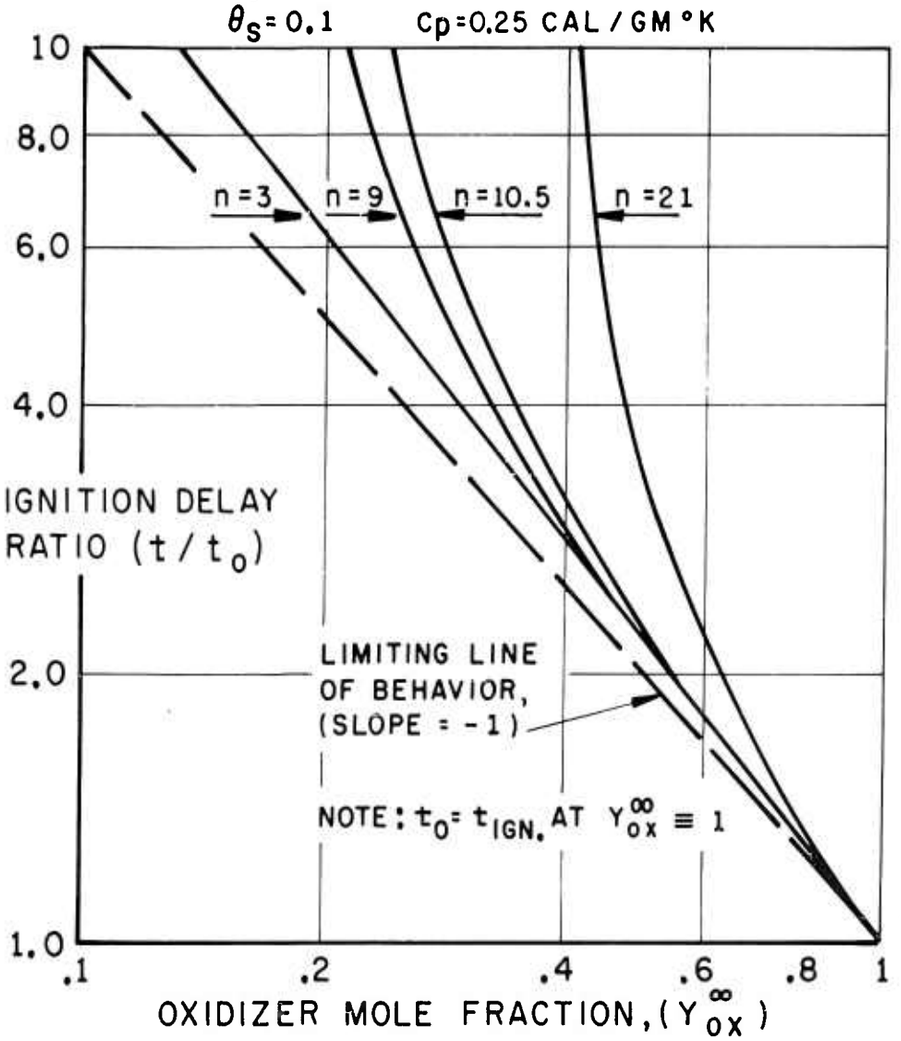

FIGURE I-14

SENSITIVITY OF REAL IGNITION DELAY TO
INITIAL OXIDIZER MOLE FRACTION
AT CONSTANT PRESSURE

CASE II: CONSTANT $\dot{m}_F^o$ AT WALL

$(E/R) = 12000°K$ $\theta_0 = 0.10$

$q = 14{,}400$ CAL/GM $\theta_s = 0.0333$

$C_p = 0.3$ CAL/GM °K $L^*(\theta)$; $\theta^* = 0.15$

$(B^3/A) = 10^{-6}$

$(\dot{m}_F^o / \sqrt{\rho^3 Z D}) = H = \text{CONSTANT}$

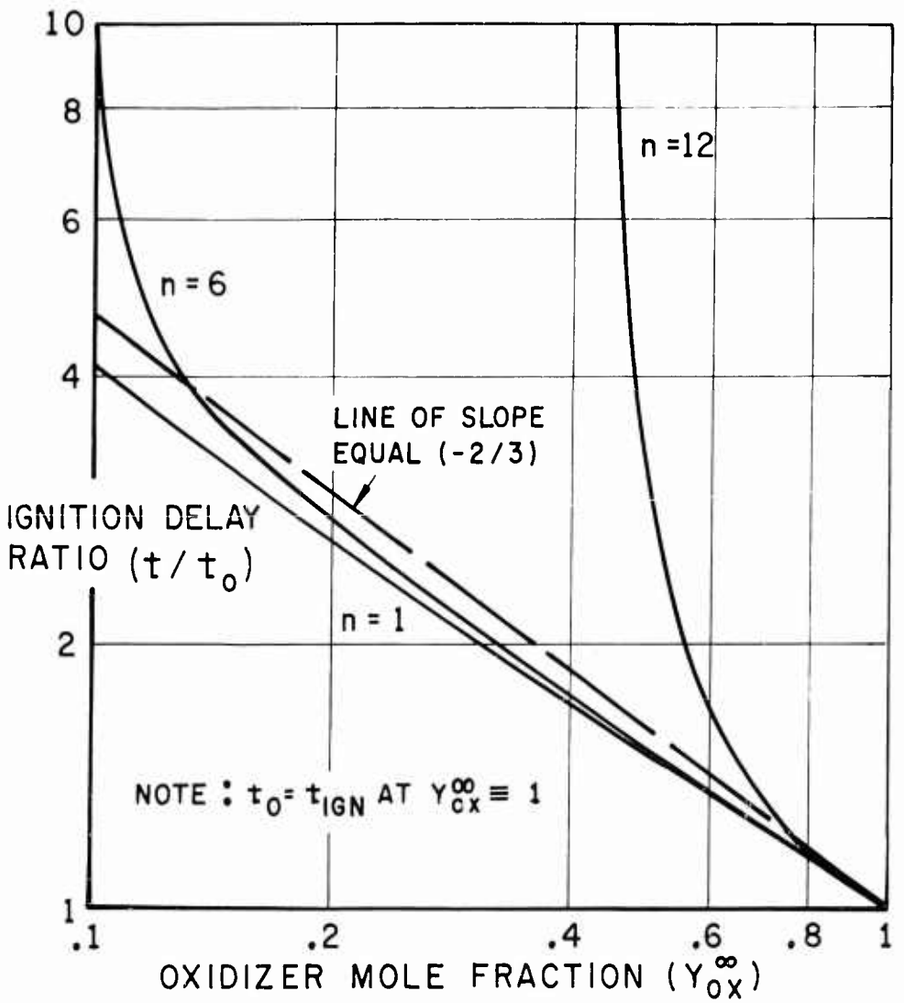

FIGURE I-15

SENSITIVITY OF REAL IGNITION DELAY TO
INITIAL OXIDIZER MOLE FRACTION
AT CONSTANT PRESSURE

CASE II: CONSTANT $\dot{m}_F^o$ AT WALL

$(E/R) = 12000°K$ $\theta_0 = 0.10$

$q = 14{,}400\ CAL/GM$ $\theta_S = 0.0333$

$C_p = 0.3\ CAL/GM\,°K$ $L^*(\theta)$; $\theta^* = 0.15$

$(B^3/A) = 10^{-2}$

$(\dot{m}_F^o/\sqrt{\rho^3 ZD}) = 10^2 H = CONSTANT$

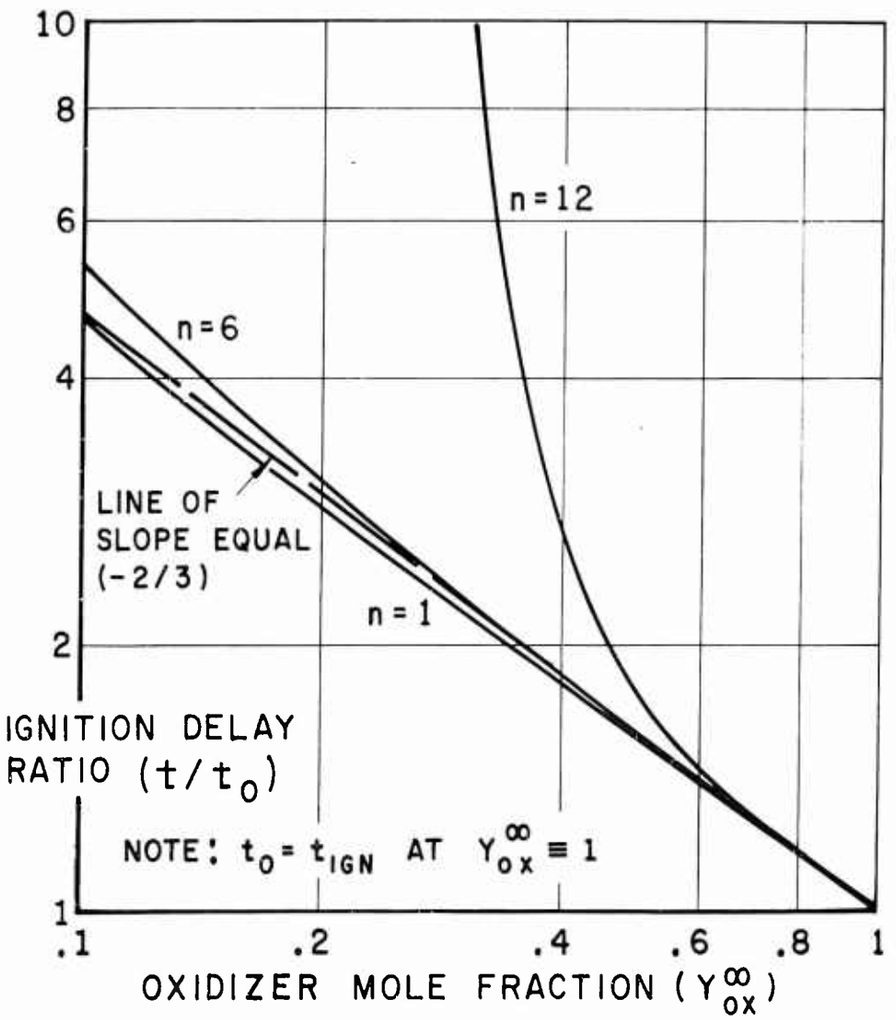

FIGURE I-16

SENSITIVITY OF REAL IGNITION DELAY TO
INITIAL OXIDIZER MOLE FRACTION
AT CONSTANT PRESSURE

CASE II: CONSTANT $\dot{m}_F^o$ AT WALL

$\theta_0 = 0.30$ $\theta_s = 0.10$
$L^*(\theta)$: $\theta^* = 0.45$

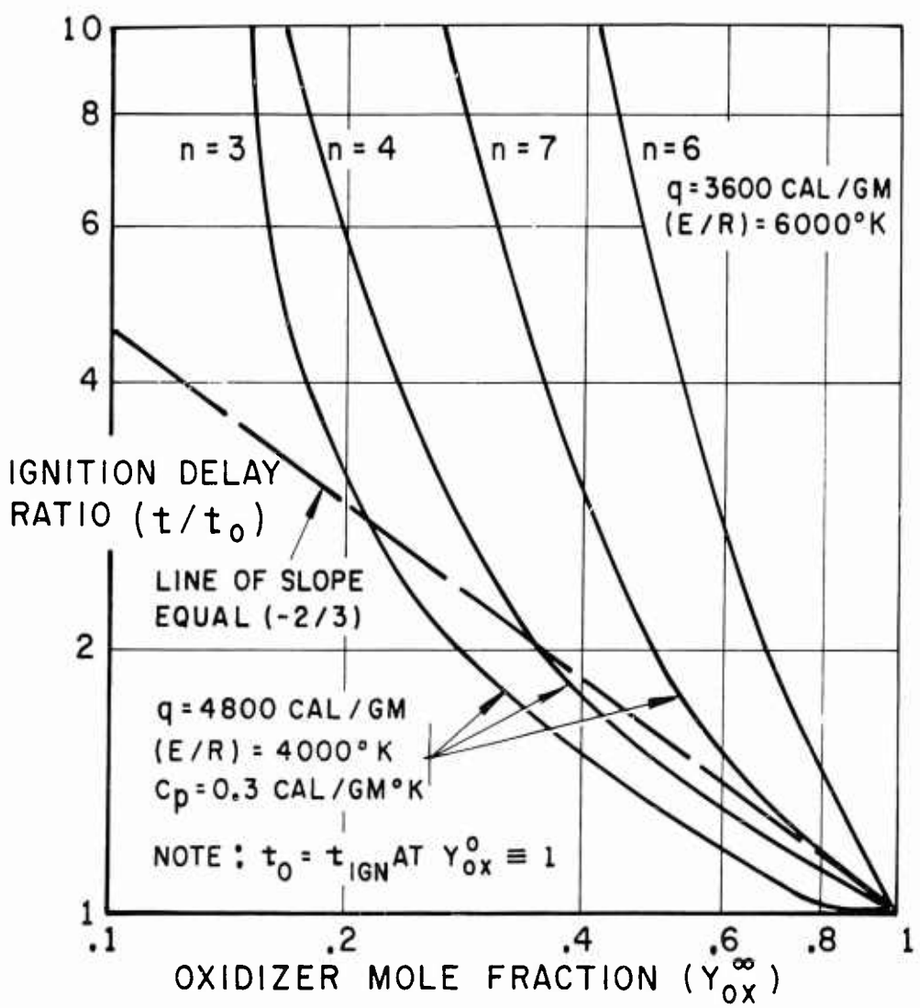

FIGURE I-17

SENSITIVITY OF REAL IGNITION DELAY TO PRESSURE LEVEL, CONSTANT INITIAL OXIDIZER MOLE FRACTION (Y_{ox}^{∞})

CASE I : CONSTANT C_F° AT WALL
$L^*(\theta)$: $\theta = 1.5\theta_0$

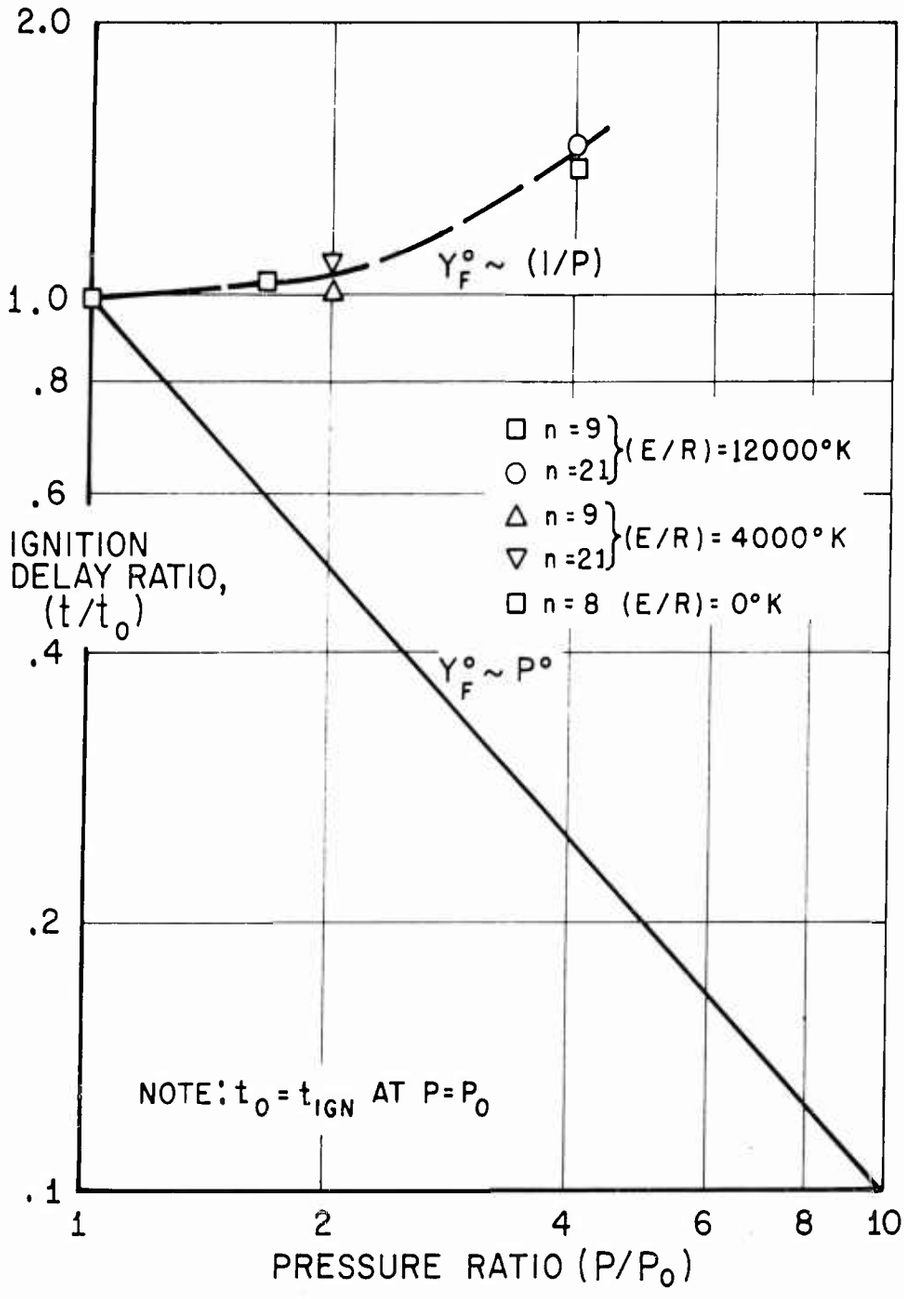

FIGURE I-18

SENSITIVITY OF REAL IGNITION DELAY TO PRESSURE LEVEL, CONSTANT INITIAL OXIDIZER CONCENTRATION

CASE I : CONSTANT C_F^o AT WALL

$L^*(\theta) : \theta^* = 1.5\theta_0$

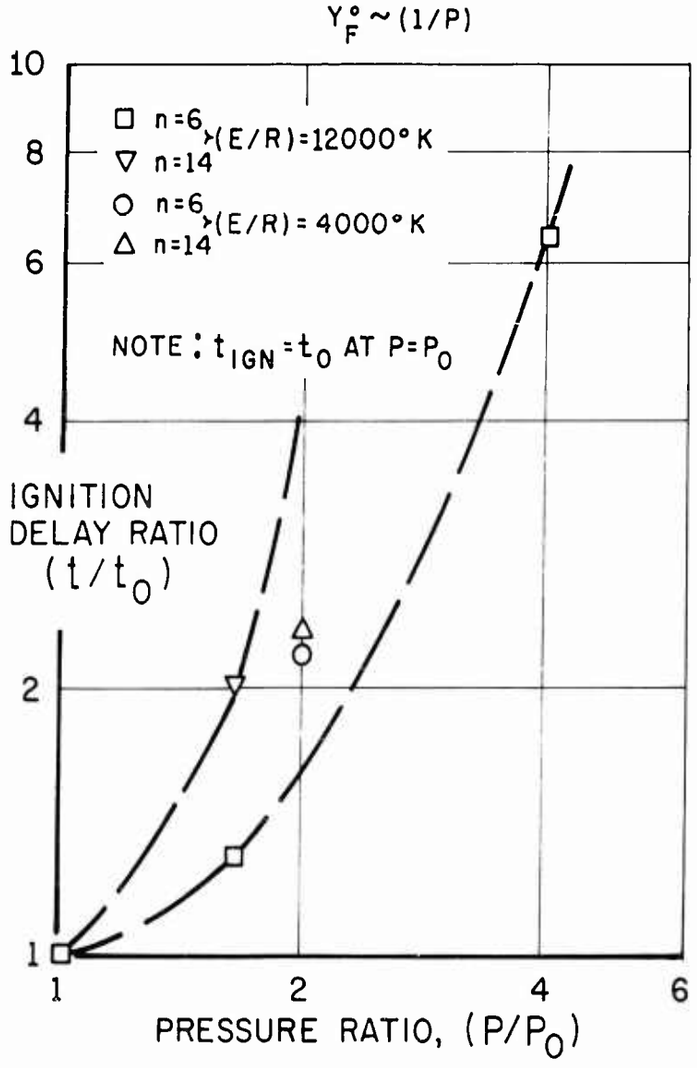

FIGURE I-19

SENSITIVITY OF REAL IGNITION DELAY TO PRESSURE LEVEL, CONSTANT INITIAL OXIDIZER CONCENTRATION

CASE I: CONSTANT C_F° AT WALL

(E/R) = 12000°K $\theta_0 = 0.10$

$L^*(\theta)$: $\theta^* = 0.15$ $\theta_S = 0.0333$

$Y_F^\circ \sim P^\circ$

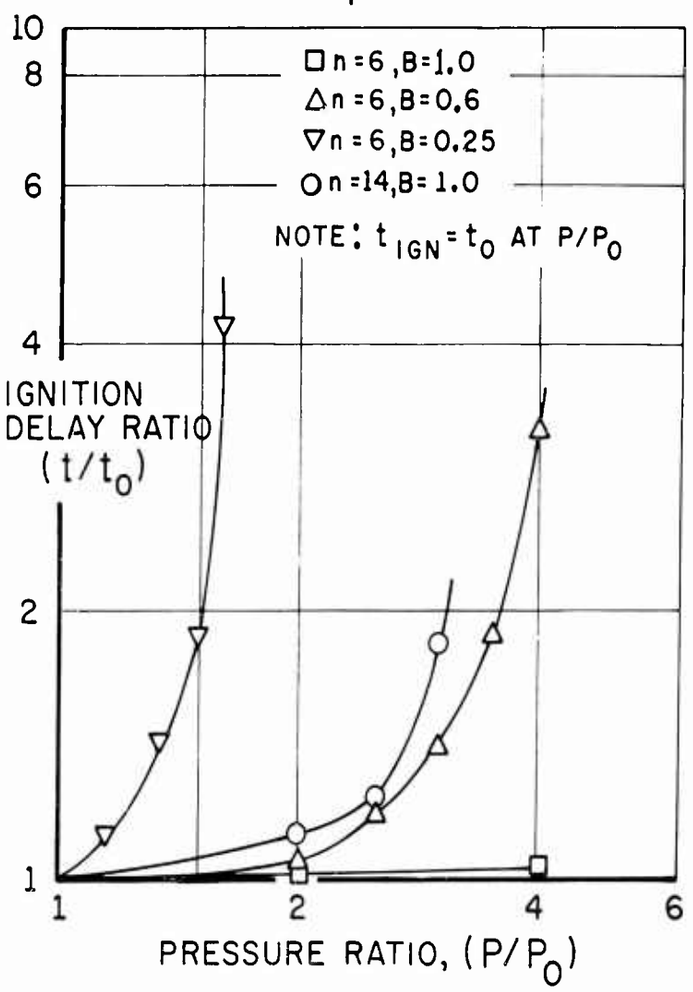

FIGURE I-20

SENSITIVITY OF REAL IGNITION DELAY TO PRESSURE LEVEL, CONSTANT INITIAL OXIDIZER CONCENTRATION

CASE I: CONSTANT C_F^o AT WALL

(E/R) = 4000°K $\theta_0 = 0.30$

$L^*(\theta)$: $\theta^* = 0.45$ $\theta_s = 0.10$

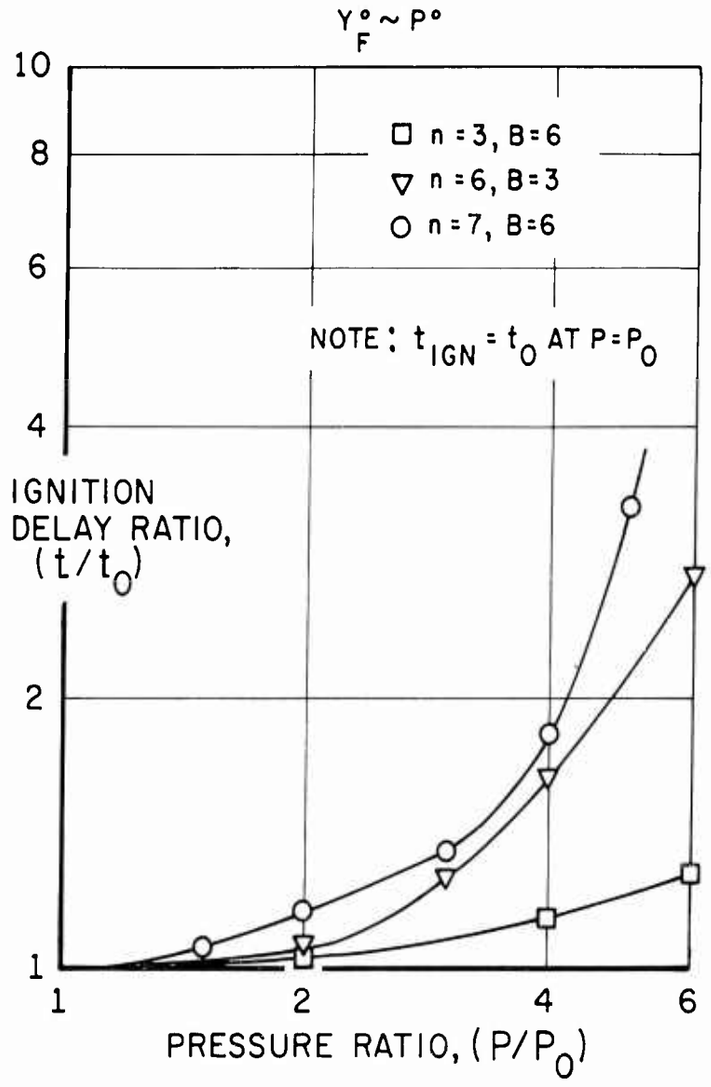

FIGURE I-21

SENSITIVITY OF REAL IGNITION DELAY TO PRESSURE LEVEL, CONSTANT INITIAL OXIDIZER MOLE FRACTION

CASE II: CONSTANT $\dot{m}_F^\circ$ AT WALL

$L^*(\theta)$: θ^*=0.15

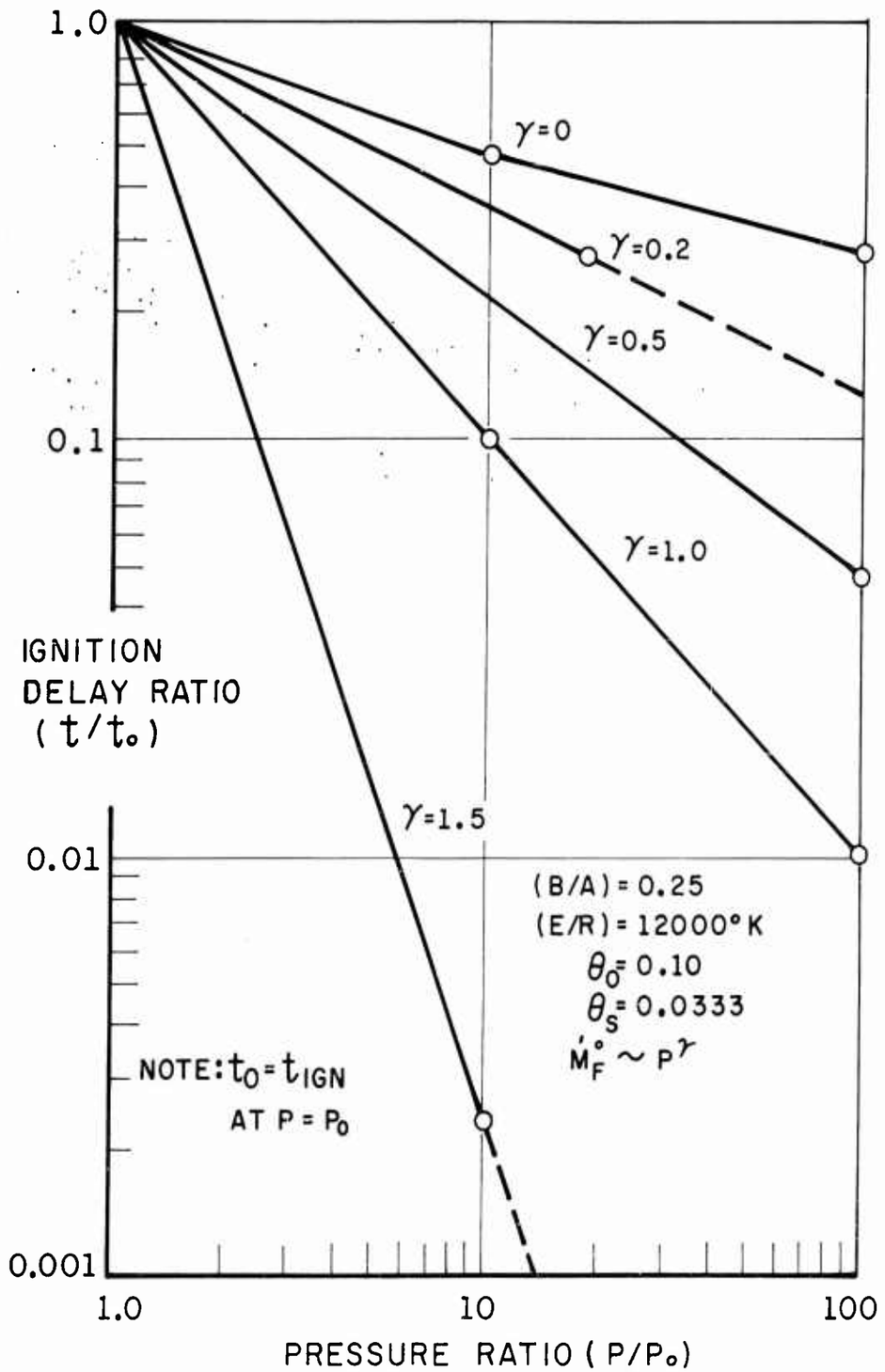

FIGURE I-22

SENSITIVITY OF REAL IGNITION DELAY TO PRESSURE LEVEL, CONSTANT INITIAL OXIDIZER CONCENTRATION

CASE II: CONSTANT $\dot{m}_F^o$ AT WALL

$L^*(\theta)$: θ^*=0.13

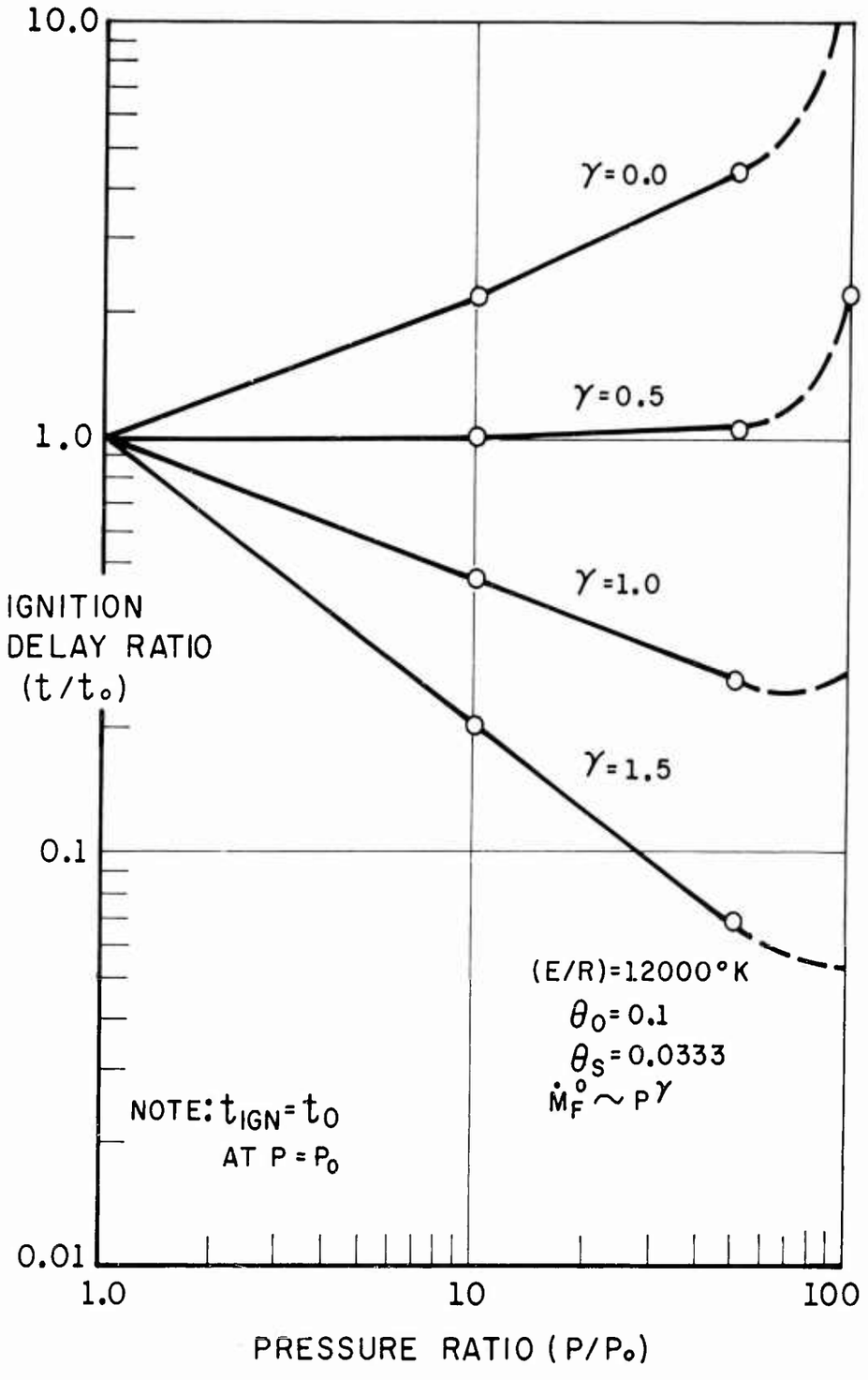

FIGURE I-23

SENSITIVITY OF REAL IGNITION DELAY
TO INITIAL GAS TEMPERATURE LEVEL

CASE I: CONSTANT C_F^o AT WALL

$(E/R) = 12000°K$

$L^*(\theta) : \theta^* = 0.18$

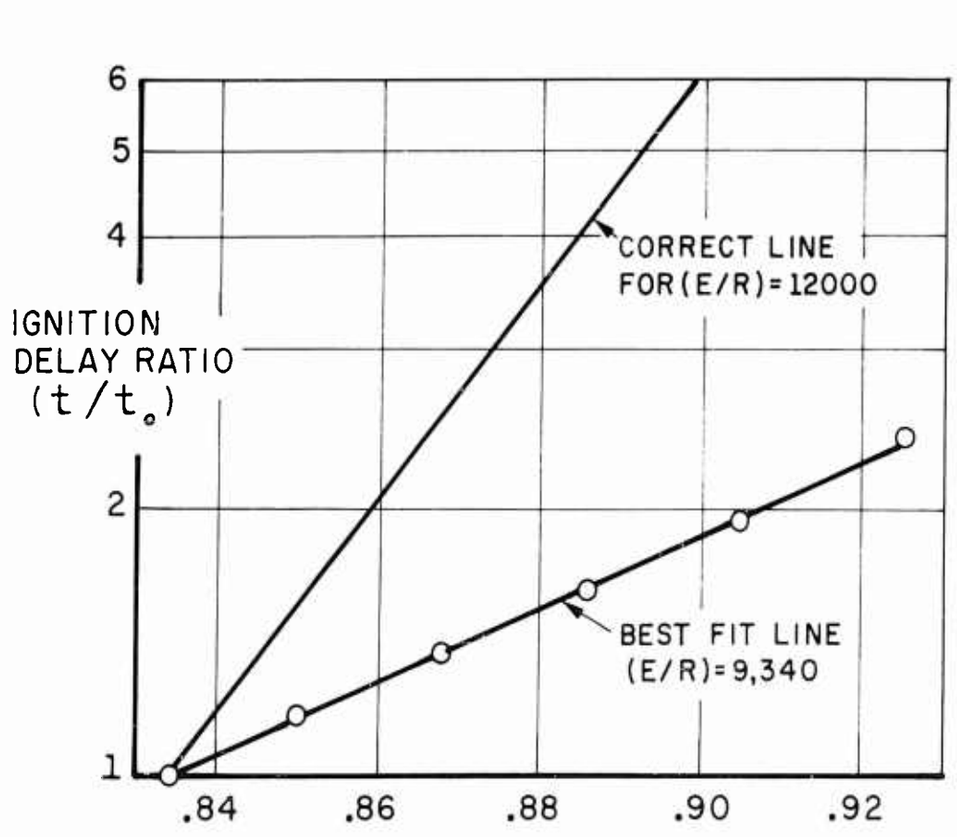

FIGURE I-24

SENSITIVITY OF REAL IGNITION DELAY
TO INITIAL GAS TEMPERATURE LEVEL

CASE I: CONSTANT C_F^o AT WALL

$(E/R) = 4000°K$

$L^*(\theta):\theta^* = 0.4$

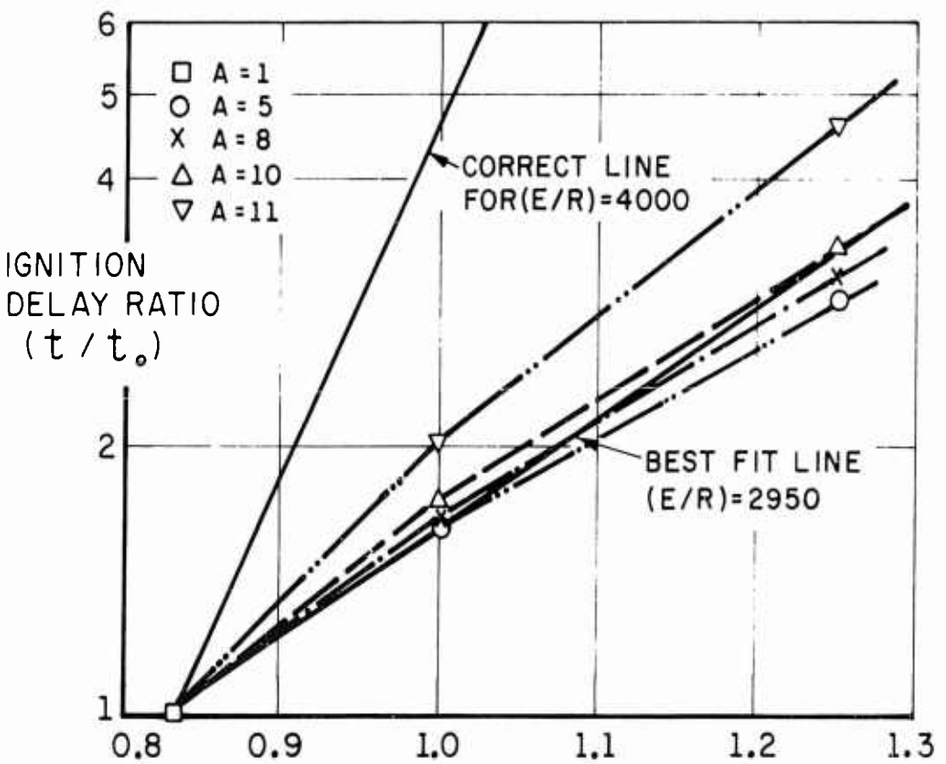

FIGURE I-25

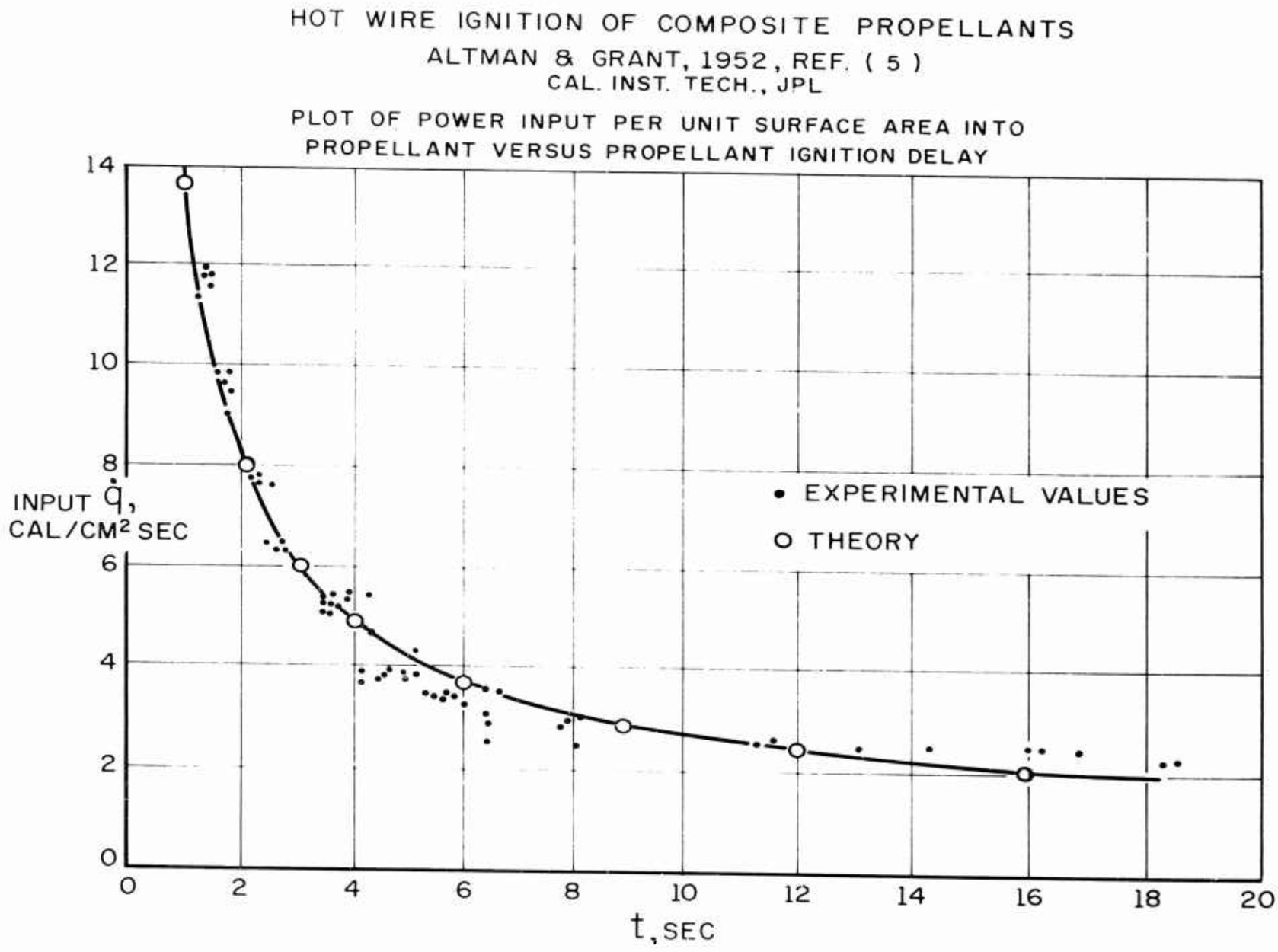
HOT WIRE IGNITION OF COMPOSITE PROPELLANTS
ALTMAN & GRANT, 1952, REF. (5)
CAL. INST. TECH., JPL
PLOT OF POWER INPUT PER UNIT SURFACE AREA INTO
PROPELLANT VERSUS PROPELLANT IGNITION DELAY
INPUT $\dot{q}$,
CAL/CM^2 SEC
0
2
4
6
8
10
12
14
t, SEC
16
18
20
• EXPERIMENTAL VALUES
O THEORY

FIGURE 1

NITRATE ESTER PROPELLANT IGNITION
IN AN EXPLOSION TUBE

COOK AND OLSON, 1955, REF. (6)
UNIVERSITY OF UTAH

PLOT OF MINIMUM CHARGE PRESSURE, P_1°,
REQUIRED FOR IGNITION VERSUS MOLAR H_2/O_2
RATIO OF CHARGING MIXTURE

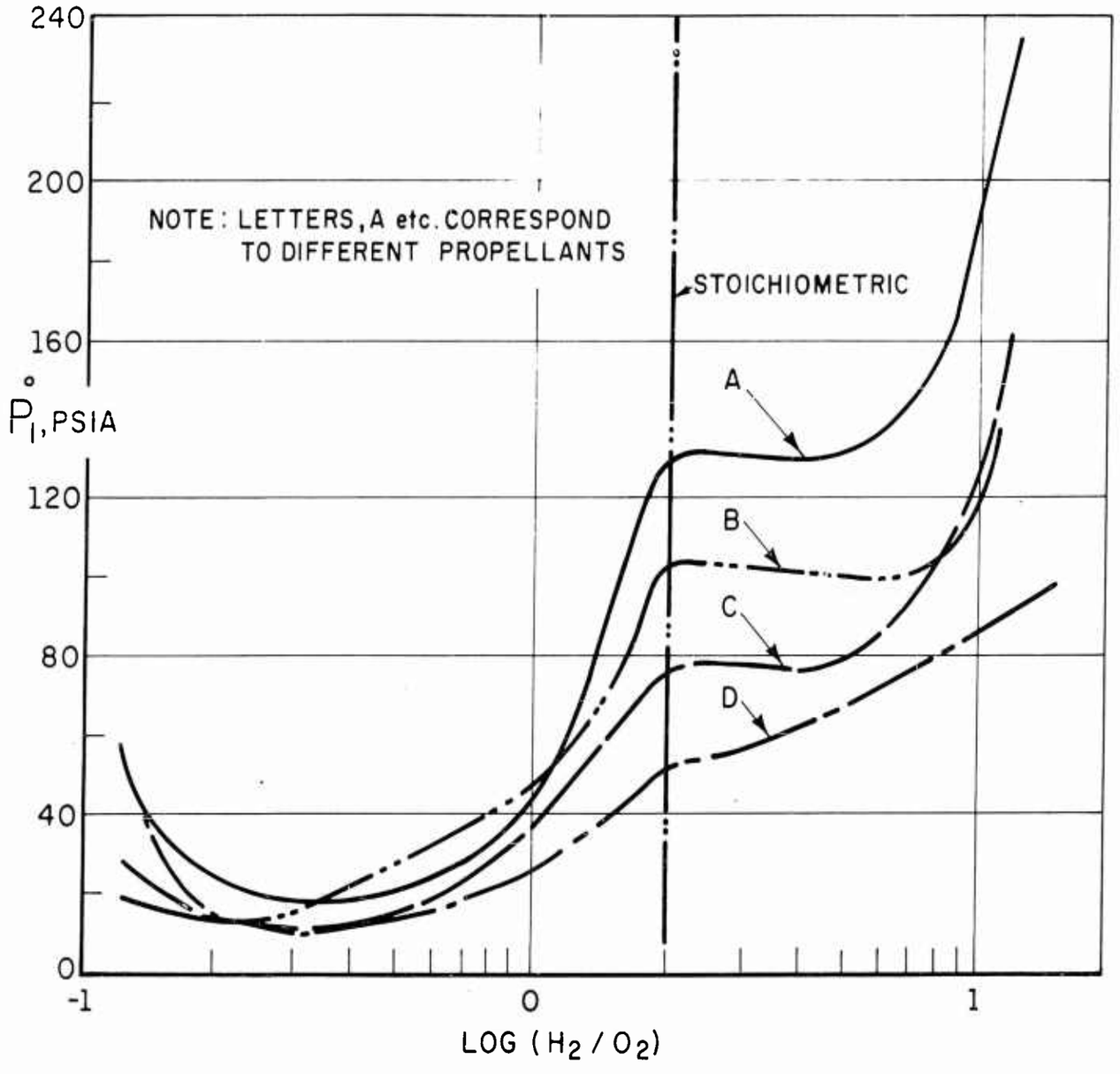

FIGURE 2

CONVECTIVE IGNITION OF NITRATE ESTER PROPELLANTS

CHURCHILL, KRUGGEL, & BRIER, 1956, REF. (8)
UNIVERSITY OF MICHIGAN

PLOT OF AN INVERSE FUNCTION OF IGNITION DELAY VERSUS TEST GAS OXYGEN PERCENTAGE

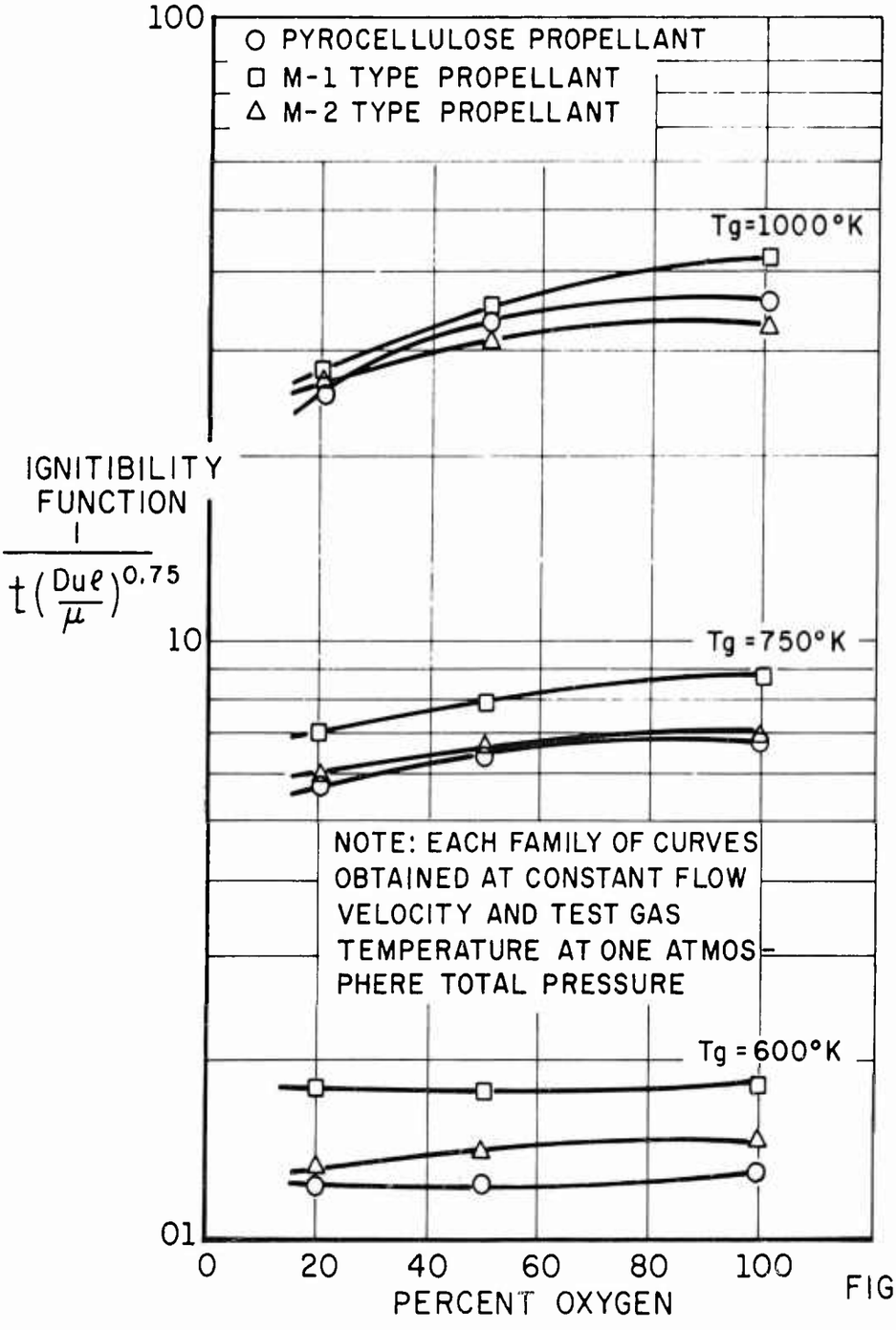

FIGURE 3

M2 NITRATE ESTER PROPELLANT
IGNITION AT ATMOSPHERIC PRESSURE

ROTH & WACHTELL, 1962, (9)
FRANKLIN INSTITUTE

PLOT OF SQUARE ROOT OF IGNITION DELAY
VERSUS CALCULATED HEAT FLUX VALUES

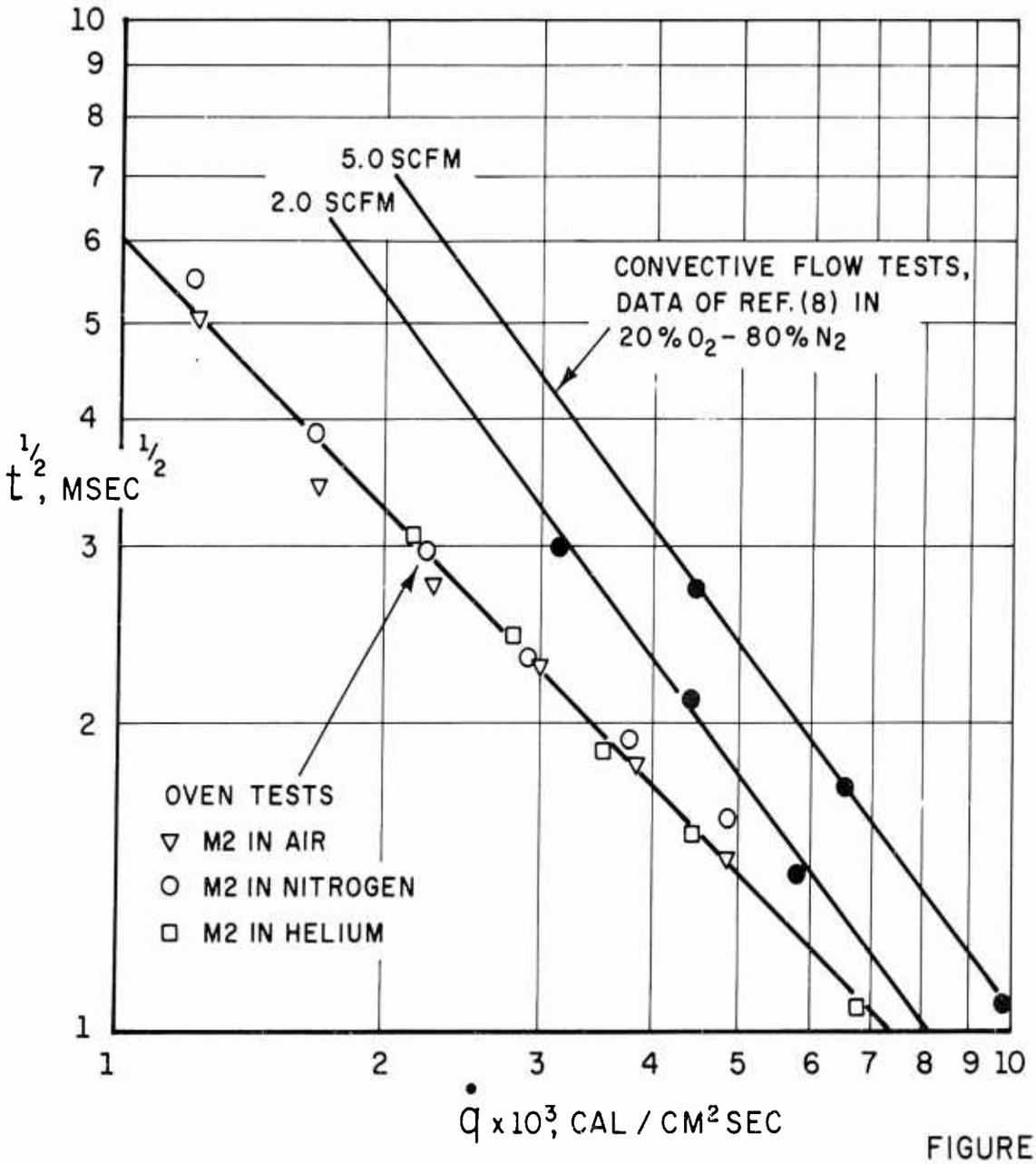

FIGURE 4

M9 NITRATE ESTER PROPELLANT
IGNITION AT ATMOSPHERIC PRESSURE

ROTH & WACHTELL, 1962, (9)
FRANKLIN INSTITUTE

PLOT OF FIZZ-TO-FLAME DELAY VERSUS
OXYGEN PARTIAL PRESSURE IN TEST GAS
(M9 PROPELLANT DISCS)

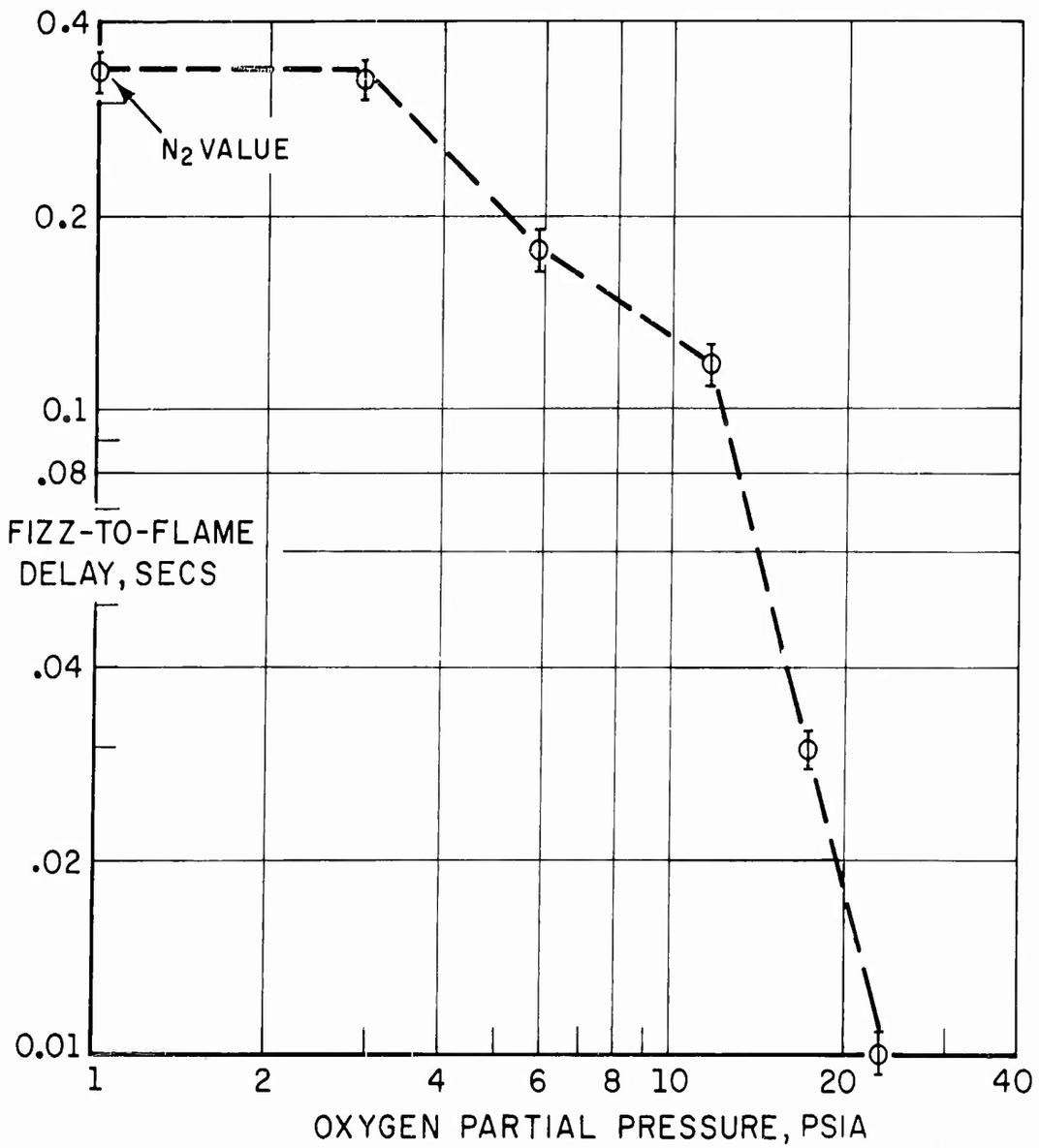

FIGURE 5

COMPOSITE PROPELLANT IGNITION BY CONVECTION
IN A SHOCK TUNNEL

RYAN AND BAER, 1960, REF. (10)
UNIVERSITY OF UTAH

SQUARE ROOT OF IGNITION DELAY
VERSUS MEAN CONVECTIVE HEAT FLUX

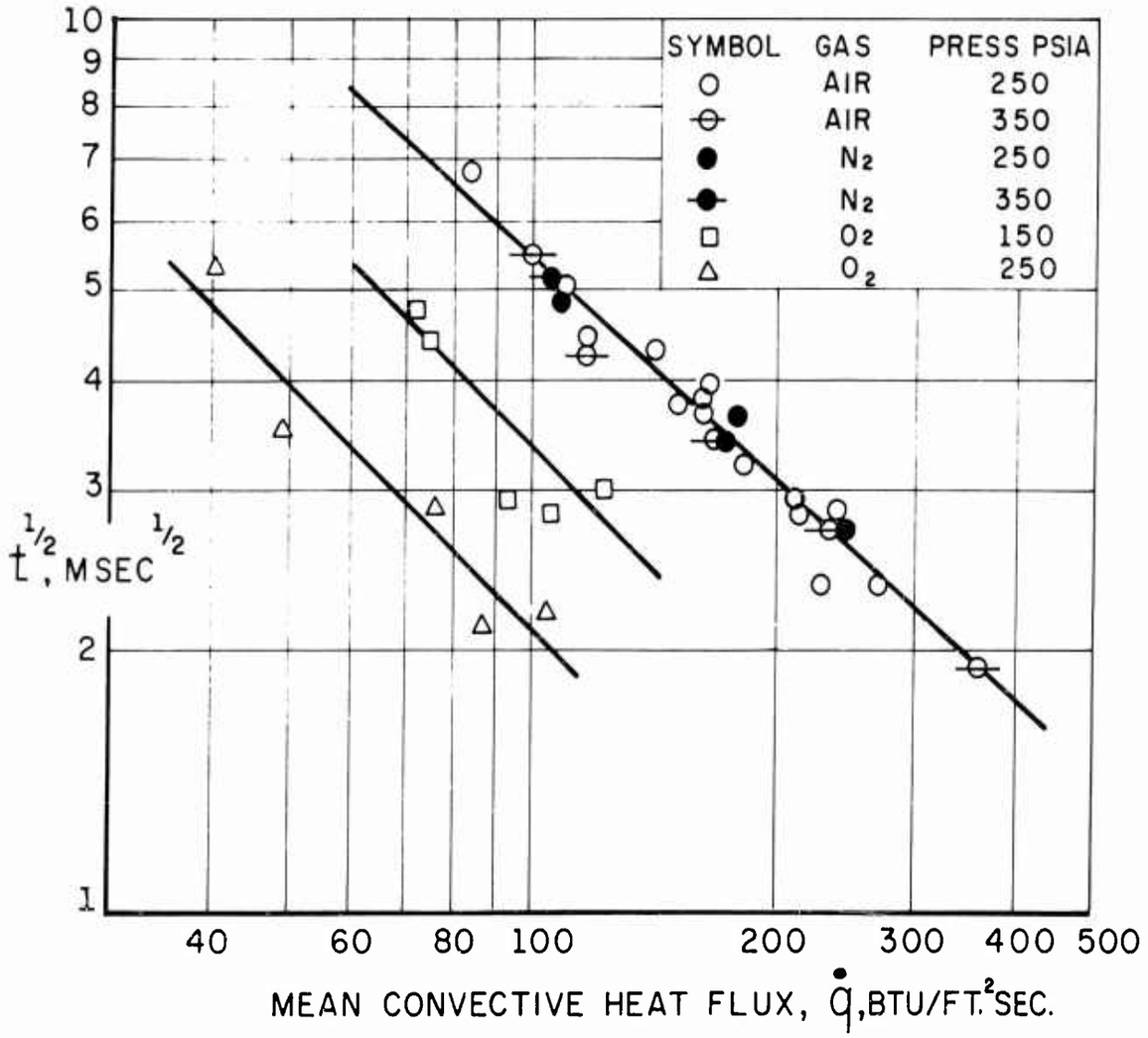

FIGURE 6

COMPOSITE PROPELLANT IGNITION
IN A RADIATION FURNACE

BAER, 1960, REF. (11)
UNIVERSITY OF UTAH

SQUARE ROOT OF IGNITION DELAY
VERSUS APPLIED HEAT FLUX

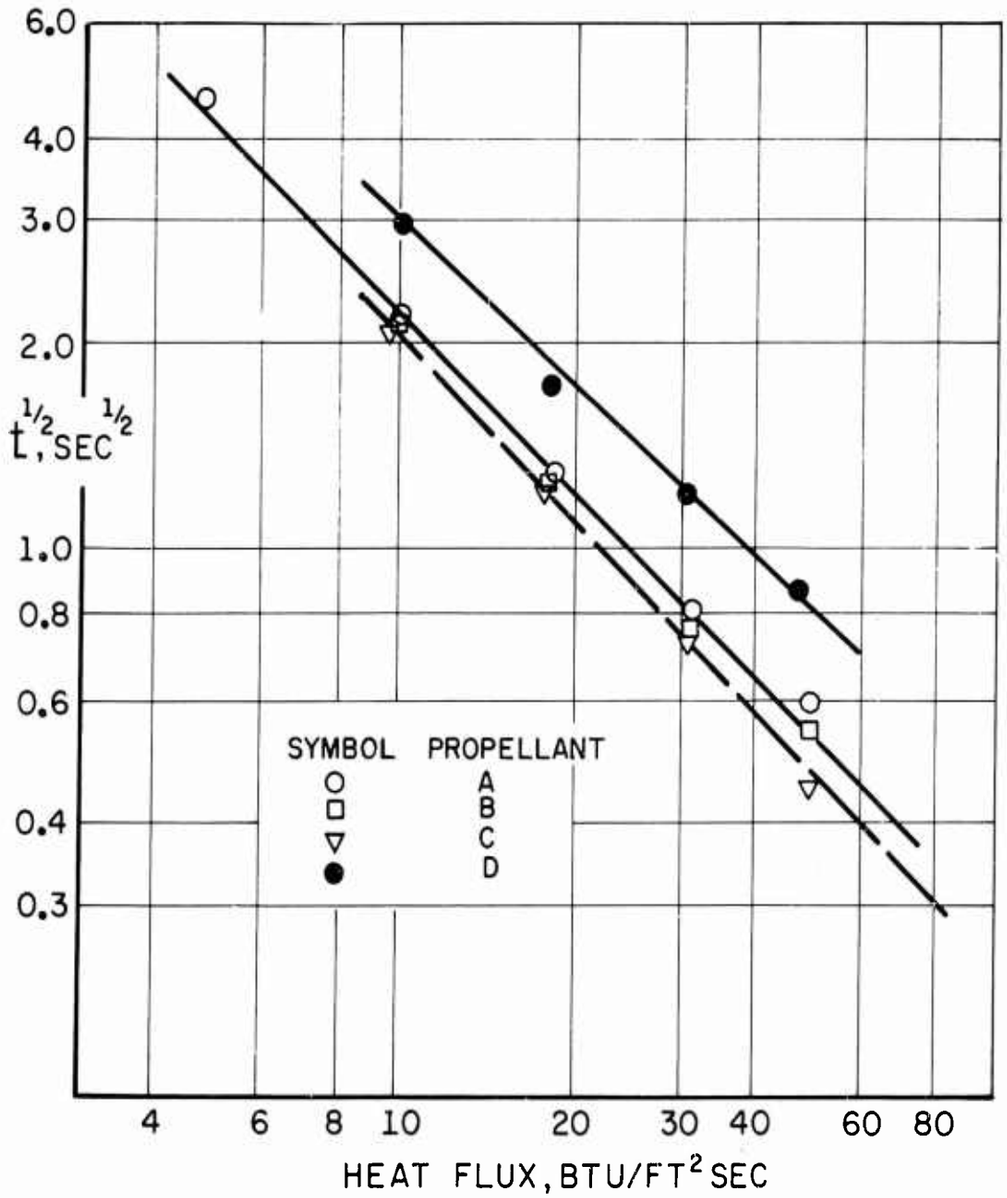

FIGURE 7

COMPOSITE PROPELLANT IGNITION BY CONVECTION
IN A SHOCK TUNNEL

RYAN AND BAER, 1960, REF'S (10) AND (11)
UNIVERSITY OF UTAH

IGNITION DELAY VERSUS OXYGEN
CONCENTRATION IN TEST GAS

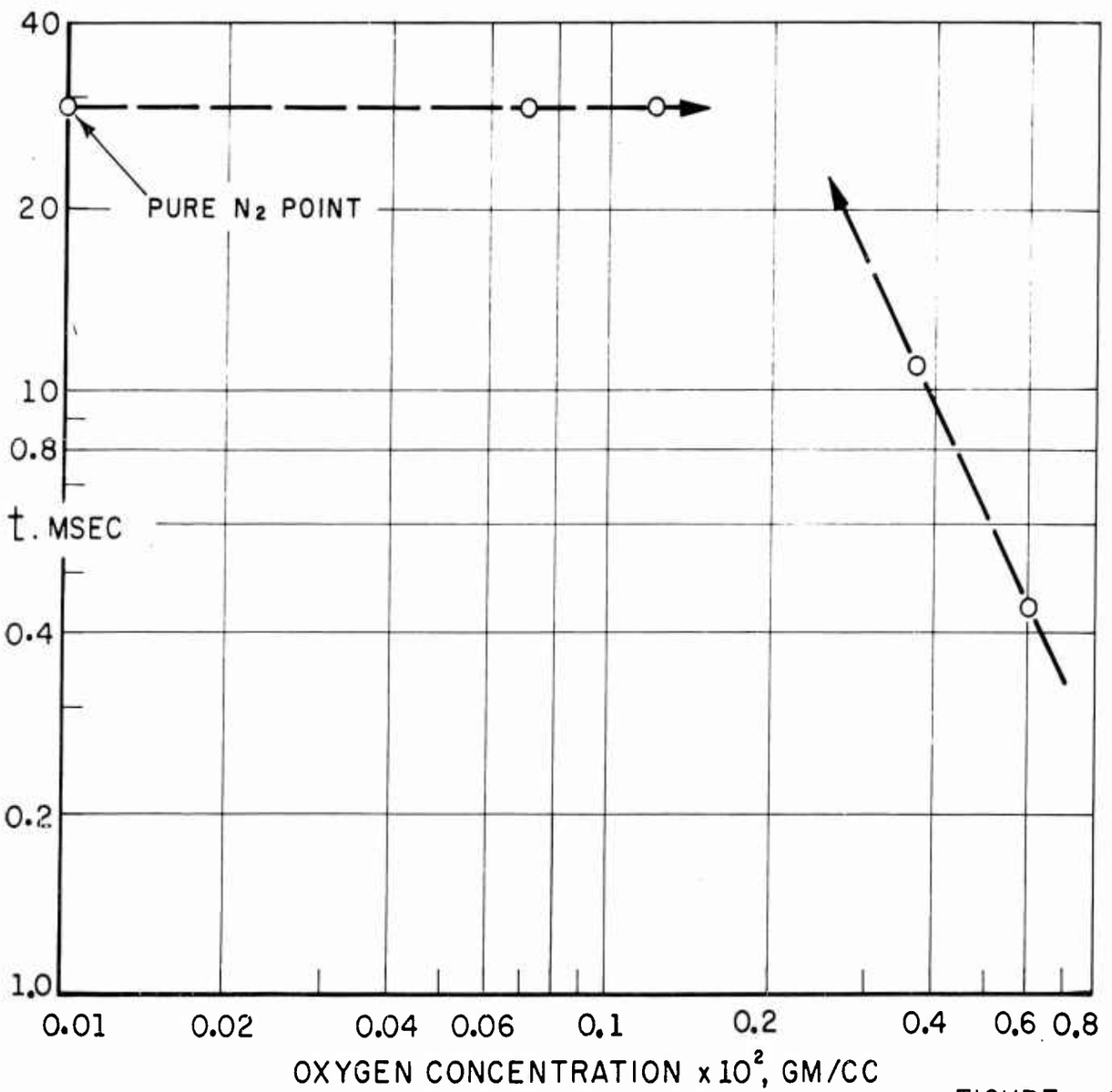

FIGURE 8

COMPOSITE AND NITRATE ESTER PROPELLANT
IGNITION DATA FROM END WALL SHOCK TUBE TESTS

McALEVY, 1960, REF'S (12) AND (13)
PRINCETON UNIVERSITY

IGNITION DELAY VERSUS OXYGEN
MOLE FRACTION IN TEST GAS

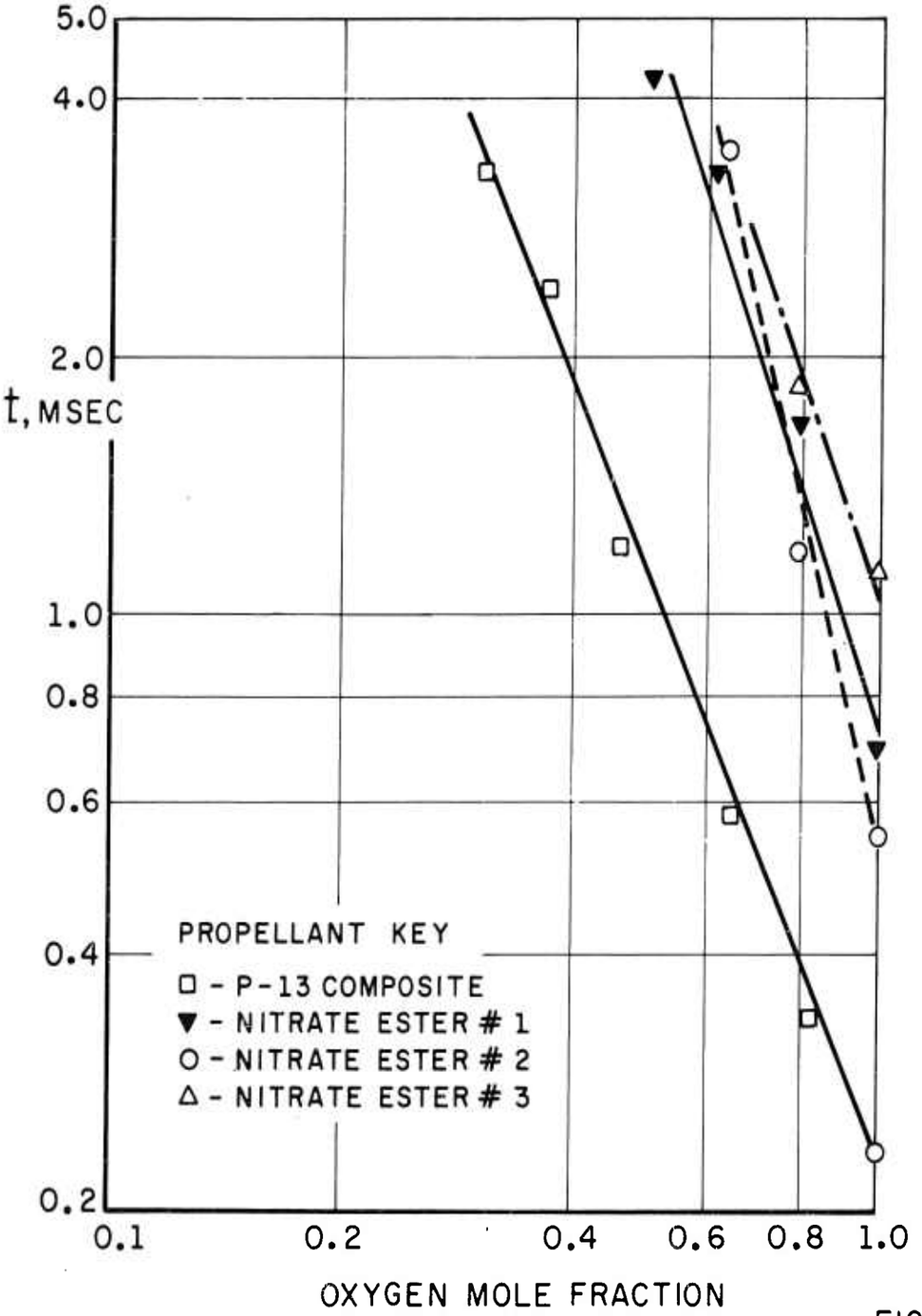

FIGURE 9

COMPOSITE AND NITRATE ESTER PROPELLANT
IGNITION DATA, END WALL SHOCK TUBE TESTS

McALEVY, 1960, REF'S (12) AND (13)
PRINCETON UNIVERSITY

IGNITION DELAY VERSUS OXYGEN
CONCENTRATION IN TEST GAS

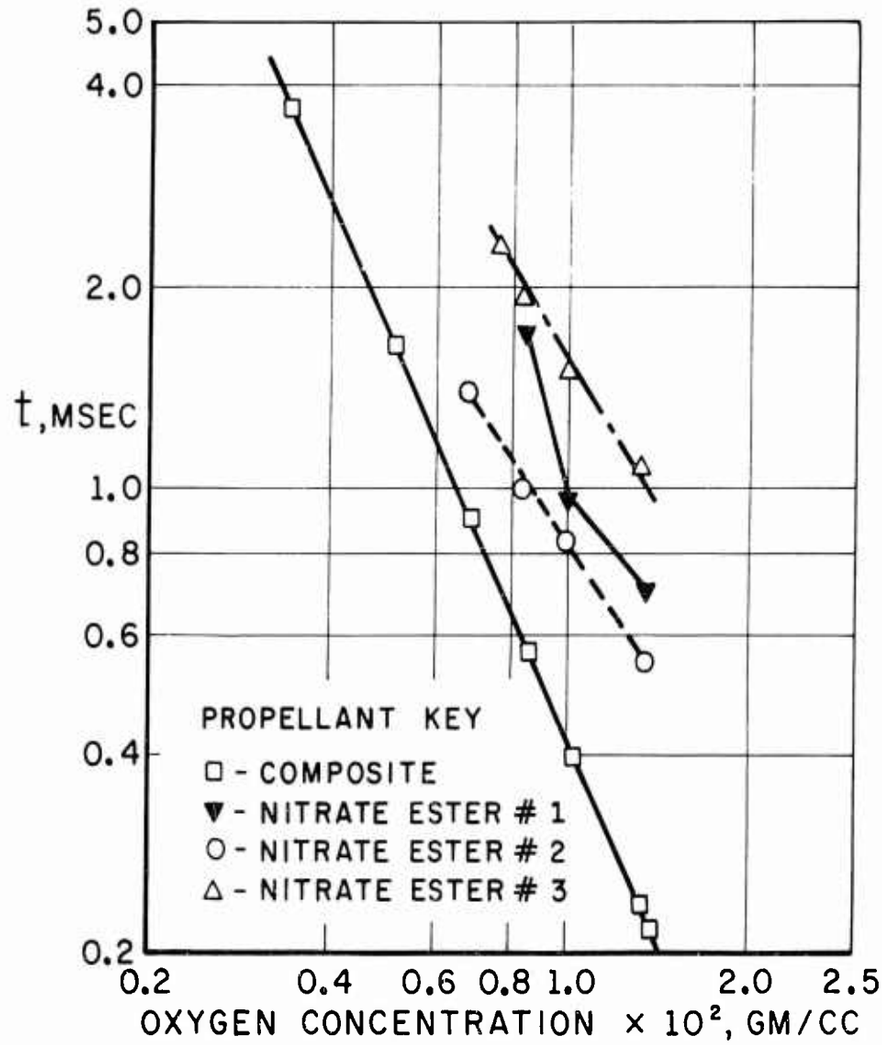

FIGURE 10

IGNITION OF COMPOSITE PROPELLANTS
BY MEANS OF RADIANT HEAT FLUX

FISHMAN AND BEYER, 1960, REF (14)
STANFORD RESEARCH INSTITUTE

PLOT OF MINIMUM EXPOSURE TIME OF PROPELLANT SAMPLES TO A CONSTANT FLUX OF 75 CAL/CM^2 SEC FOR IGNITION AT VARIOUS PRESSURES VS THE PRESSURE LEVEL

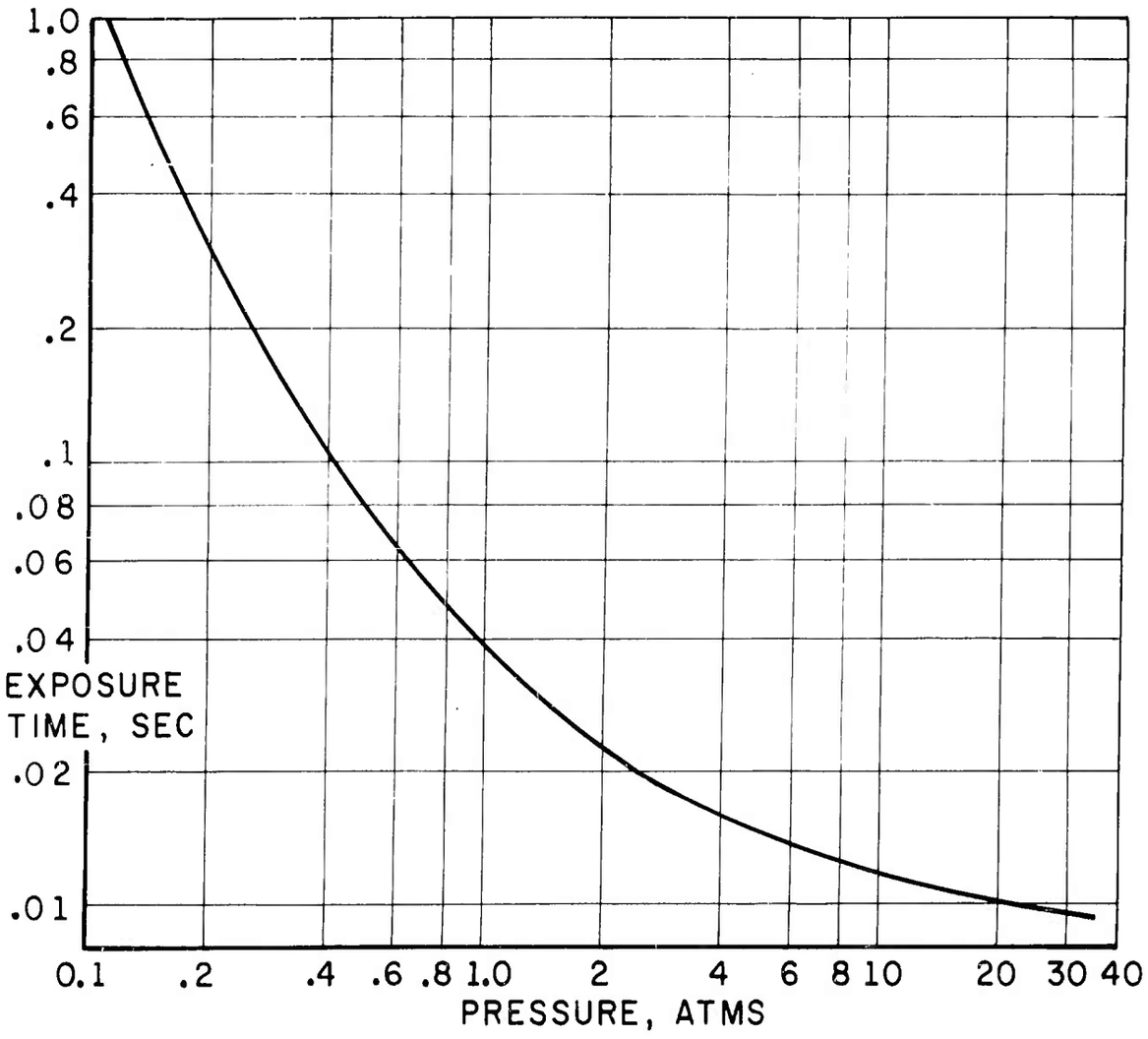

FIGURE 11

IGNITION OF COMPOSITE PROPELLANTS
BY MEANS OF RADIANT HEAT FLUX

FISHMAN AND BEYER, 1960, REF (14)
STANFORD RESEARCH INSTITUTE

PLOT OF MINIMUM TIME OF PROPELLANT EXPOSURE
TO RADIANT FLUX NECESSARY FOR IGNITION
VS. THE RADIANT FLUX LEVEL USED,
PARAMETRIC WITH PRESSURE LEVEL

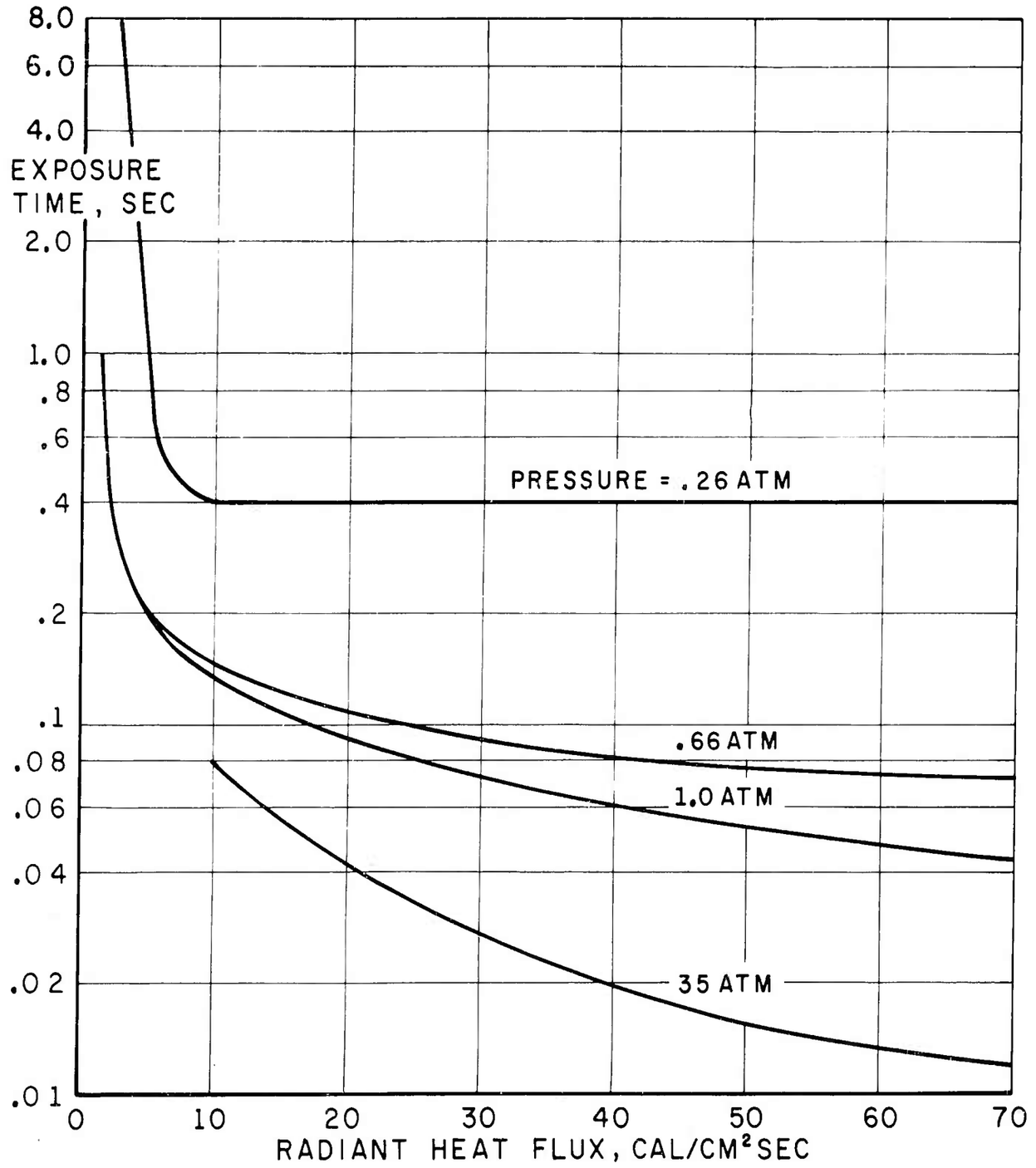

FIGURE 12

IGNITION OF COMPOSITE PROPELLANTS
BY MEANS OF RADIANT ENERGY

WISE AND EVANS, 1963, REF. (15)
STANFORD RESEARCH INSTITUTE

PLOT OF IGNITION DELAY VERSUS ARC-IMAGE FURNACE PRESSURE LEVEL; CONSTANT RADIANT FLUX OF 70 CAL/CM^2 SEC

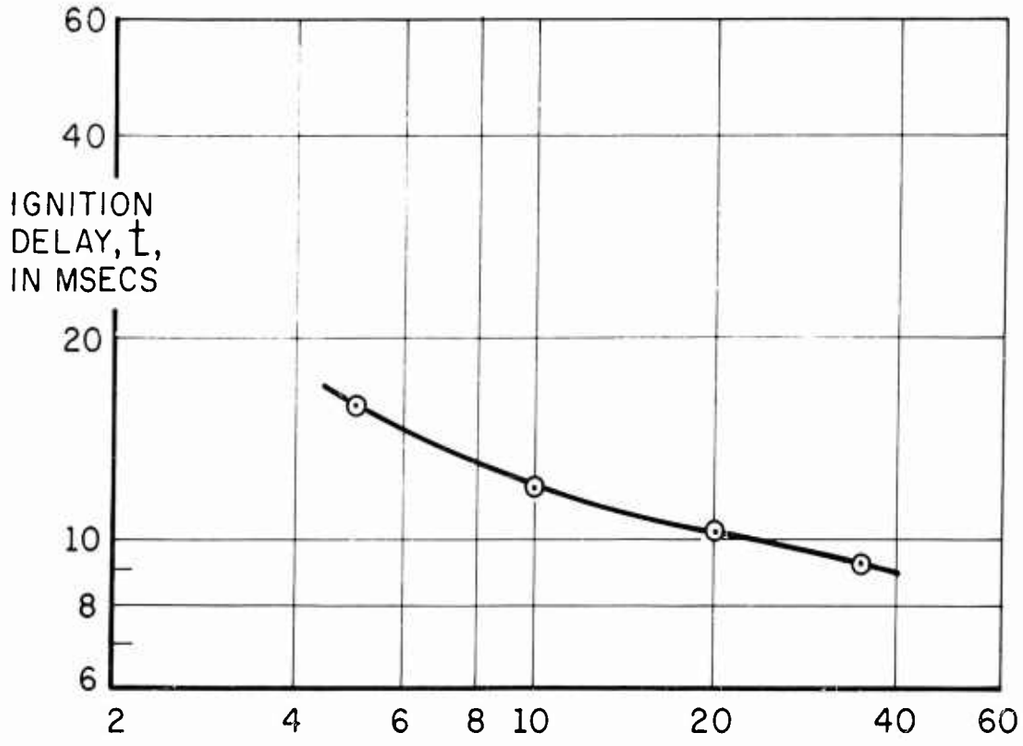

FIGURE 13

IGNITION OF COMPOSITE PROPELLANTS
BY MEANS OF RADIANT HEAT FLUX

FISHMAN AND BEYER, 1960, REF(14)
STANFORD RESEARCH INSTITUTE

PLOT OF MINIMUM EXPOSURE TIME FOR IGNITION OF PROPELLANT SAMPLES EXPOSED TO A CONSTANT FLUX OF 75 CAL/CM^2 SEC VERSUS GAS COMPOSITION AT ATMOSPHERIC PRESSURE

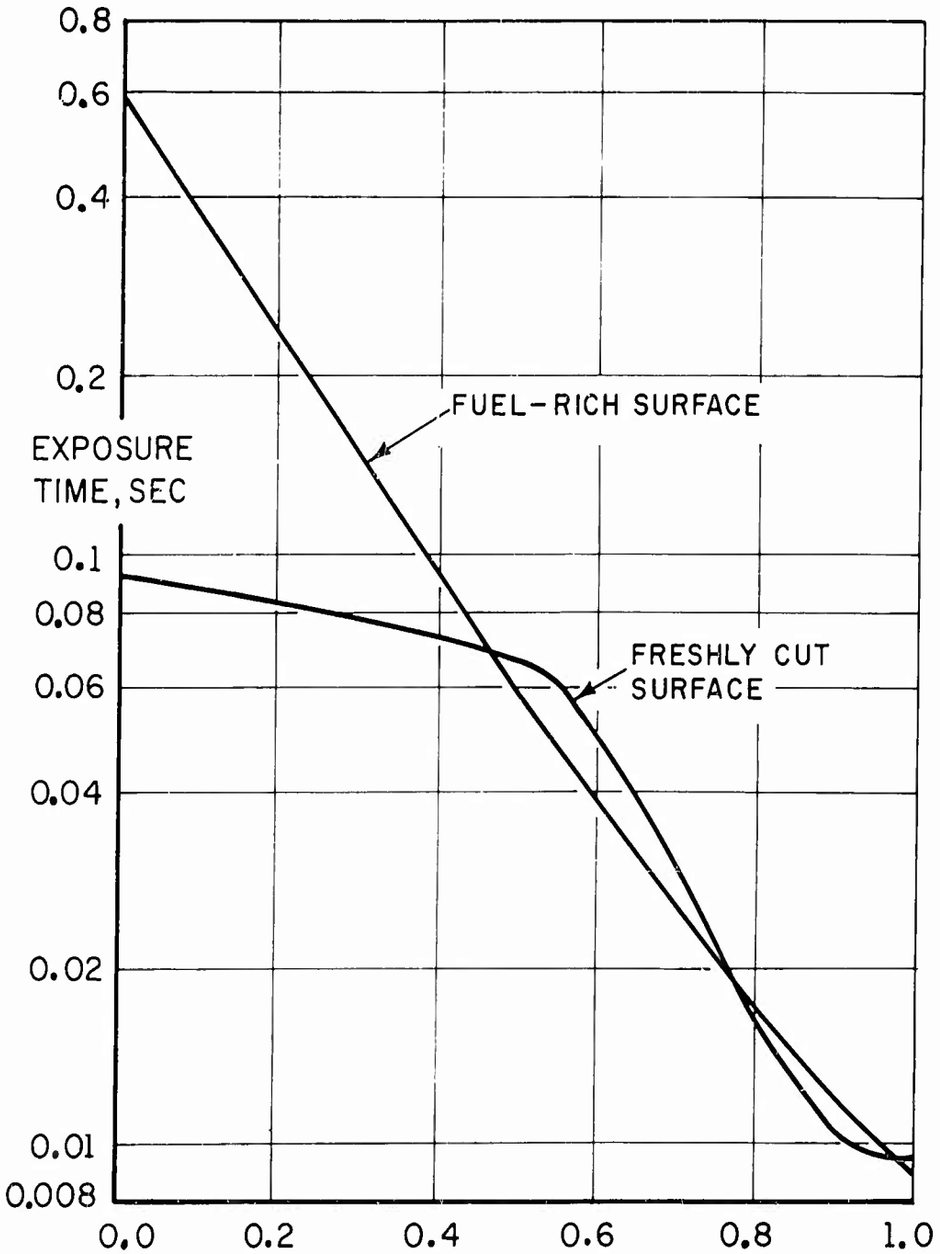

FIGURE 14

IGNITION ROCKET MOTOR EXPERIMENTS
ON COMPOSITE PROPELLANTS

GRANT, 1963, REF. (16) & LANCASTER, 1961, REF. (17)
PRINCETON UNIVERSITY

SCHEMATIC DIAGRAM OF IGNITION ROCKET MOTOR

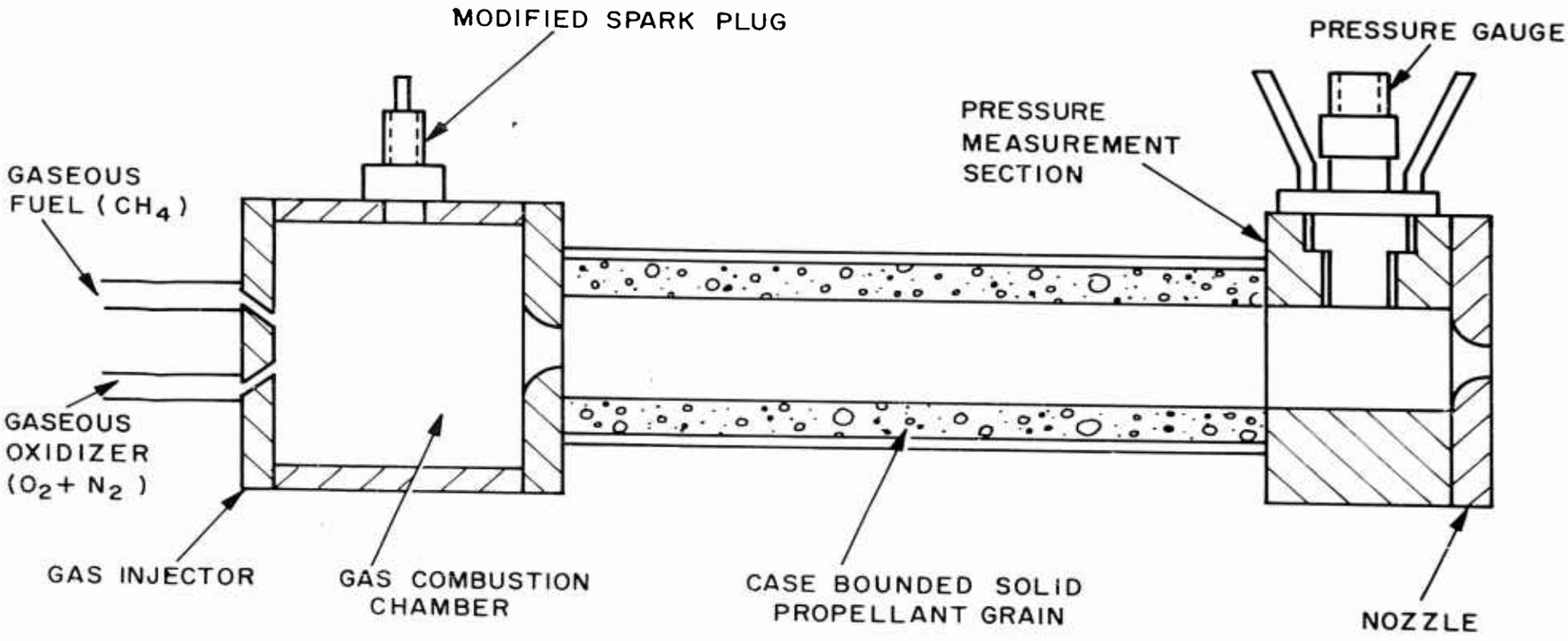

FIGURE 15

IGNITION ROCKET MOTOR EXPERIMENTS
ON COMPOSITE PROPELLANTS

GRANT, 1963, REF. (16) & LANCASTER, 1961, REF, (17)
PRINCETON UNIVERSITY

IDEALIZED AND INTERPRETED IGNITION ROCKET
MOTOR PRESSURE TRACE

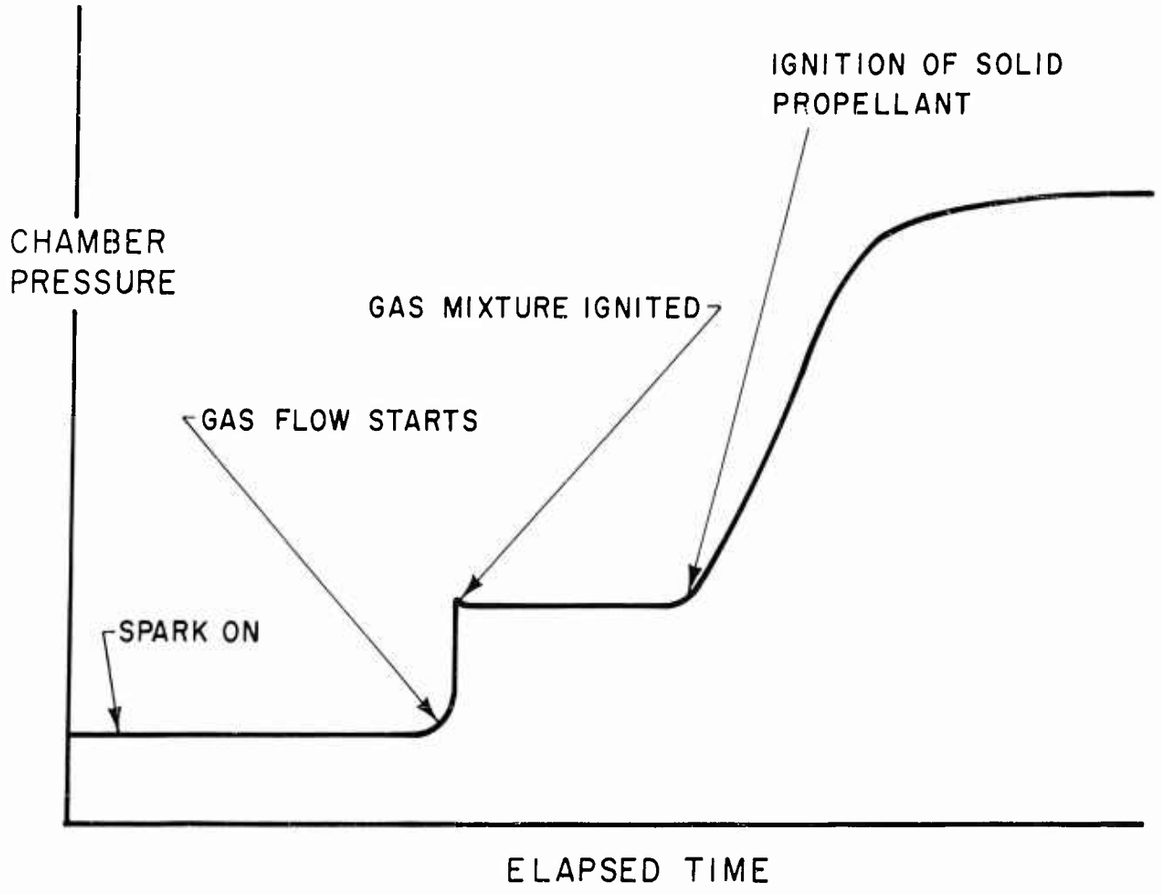

FIGURE 16

IGNITION ROCKET MOTOR EXPERIMENTS
ON COMPOSITE PROPELLANTS

GRANT, 1963, REF. (16) & LANCASTER, 1961, REF. (17)
PRINCETON UNIVERSITY

IGNITION DELAY, t, VERSUS WEIGHT FRACTION OF OXYGEN PRESENT IN COMBUSTION PRODUCTS OBTAINED FROM IGNITER TORCH

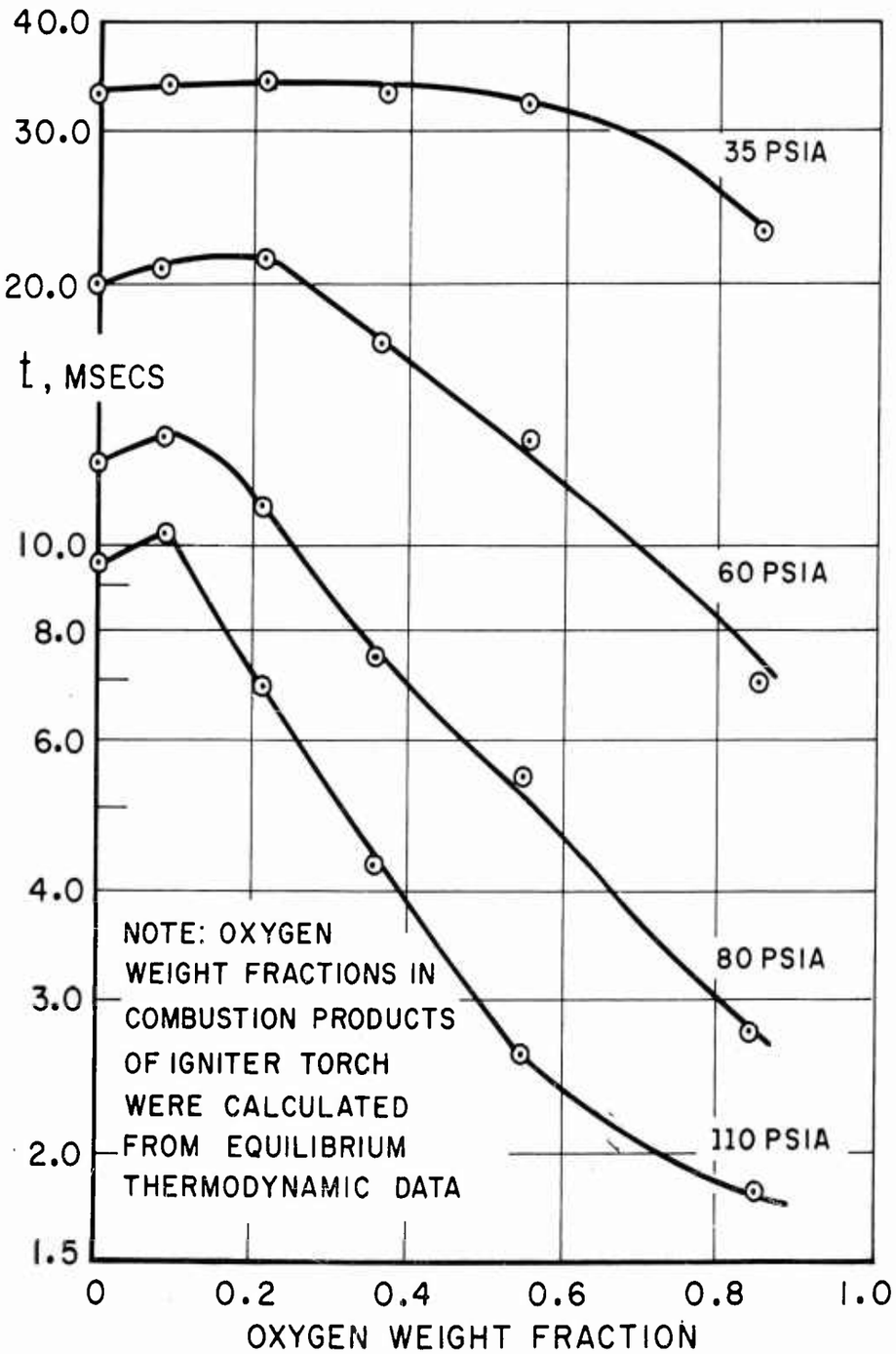

FIGURE 17

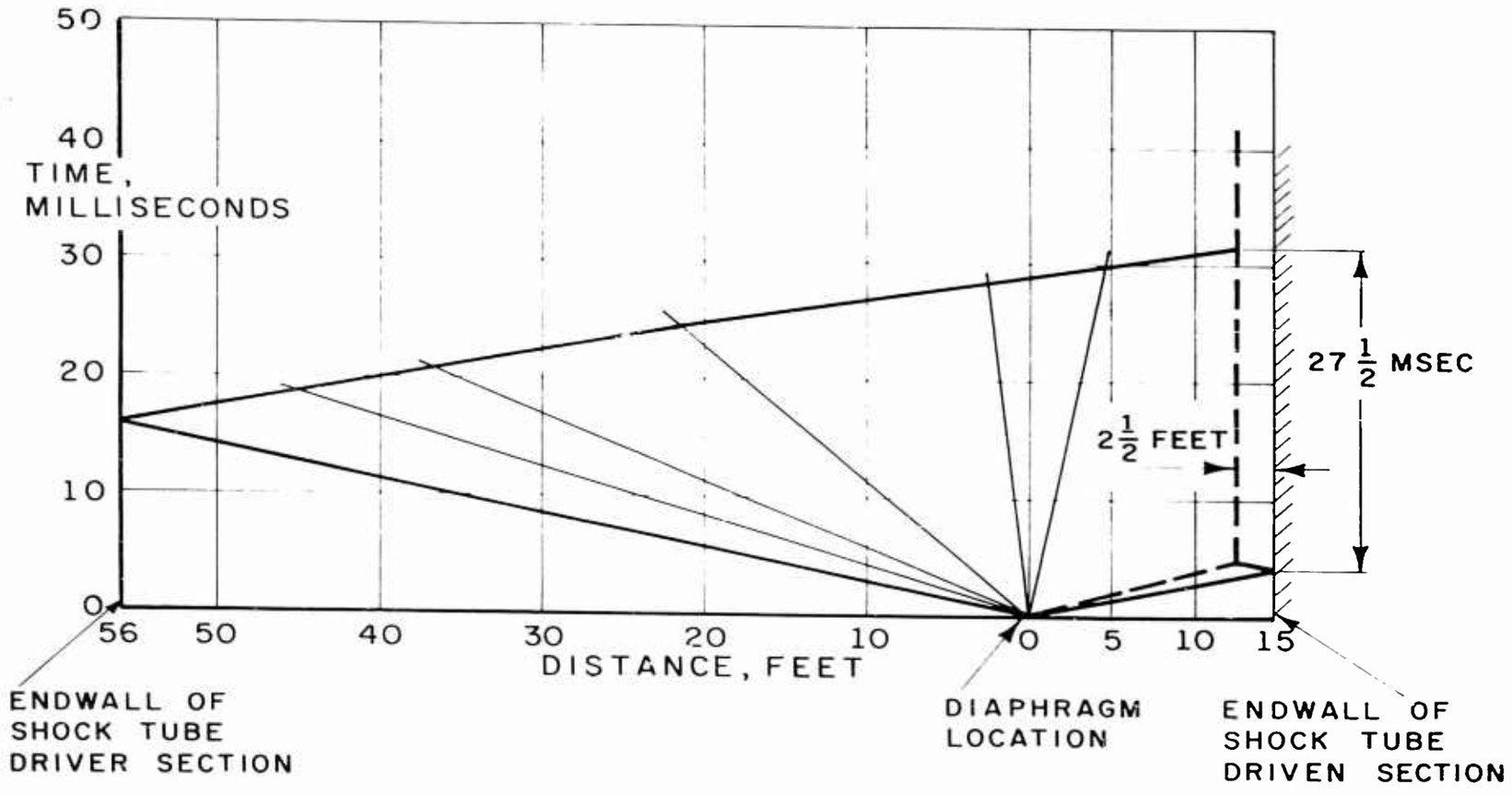

SIMPLIFIED IDEAL WAVE DIAGRAM
SHOCK TUBE DURING TAILORED INTERFACE OPERATION
WITH INCIDENT SHOCK MACH NUMBER OF 3.50
71' LONG 6" DIAMETER SHOCK TUBE

FIGURE 18

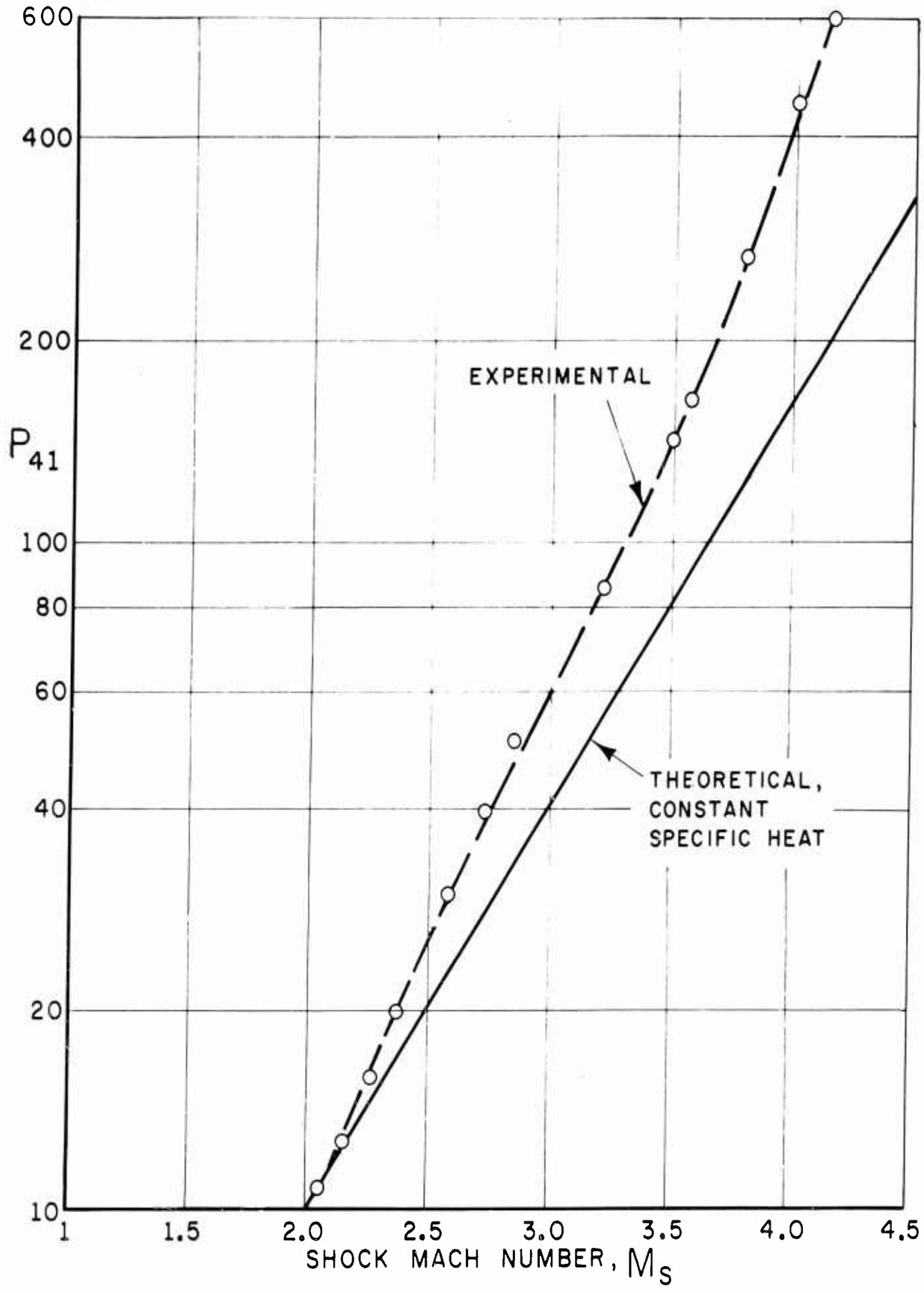

DIAPHRAGM PRESSURE RATIO AT BURST VS MACH NUMBER
SHOCK GENERATED FOR SHOCK TUNNEL WITH
HELIUM DRIVING AIR

FIGURE 19

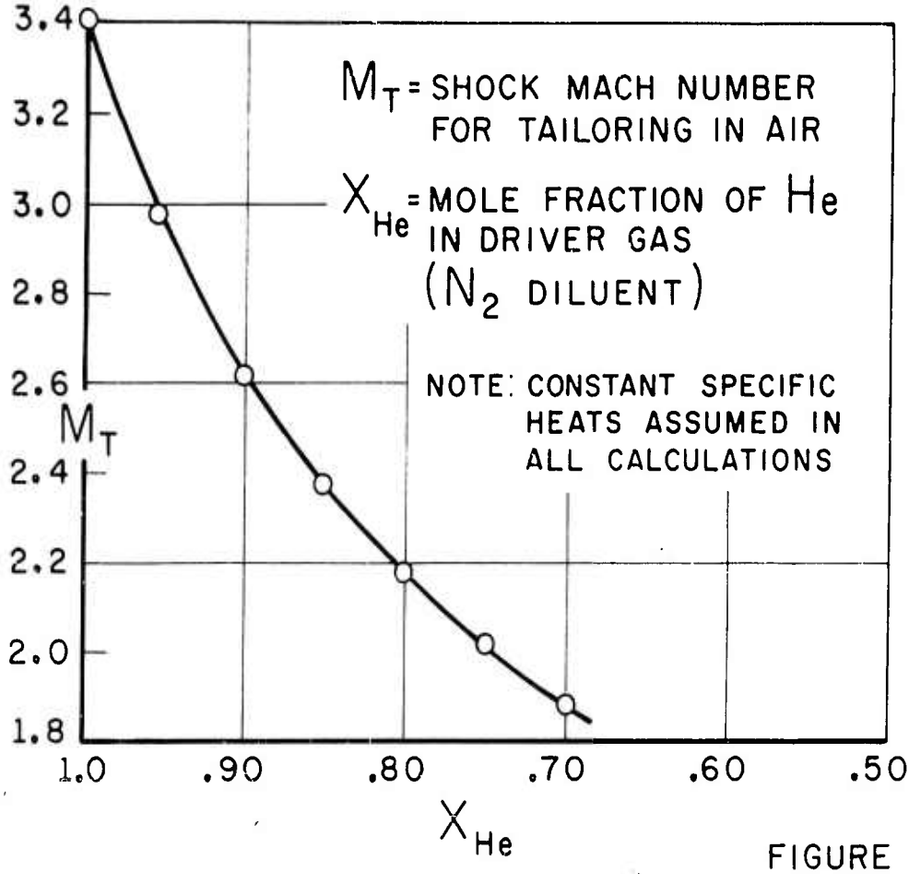

FIGURE 20

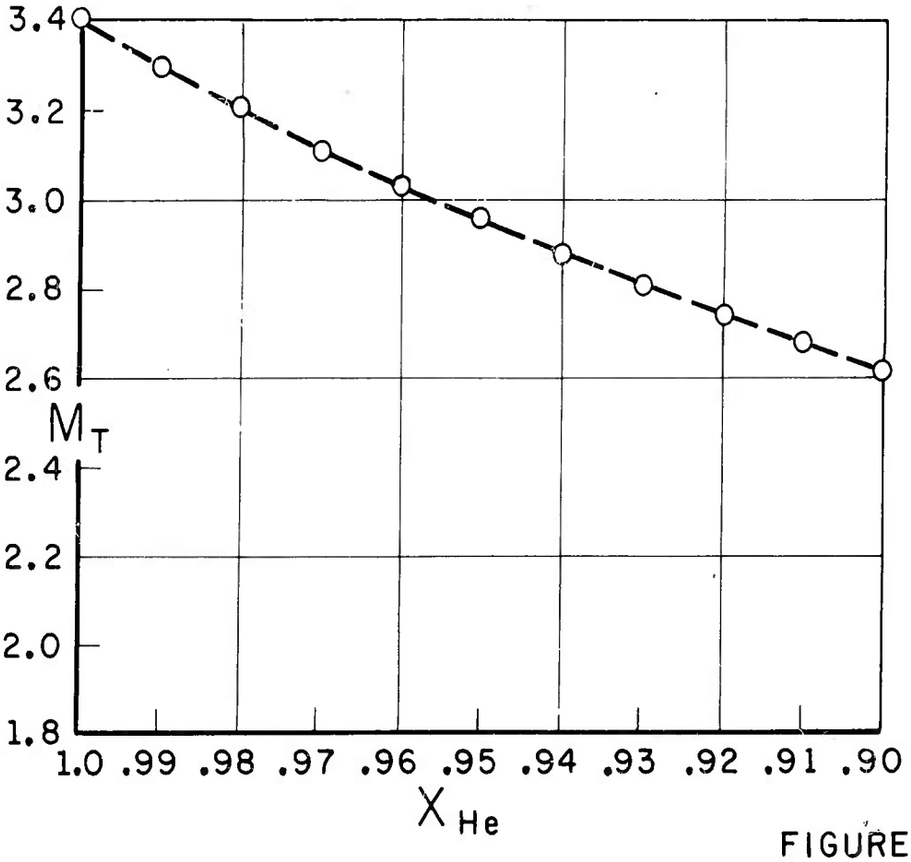

FIGURE 21

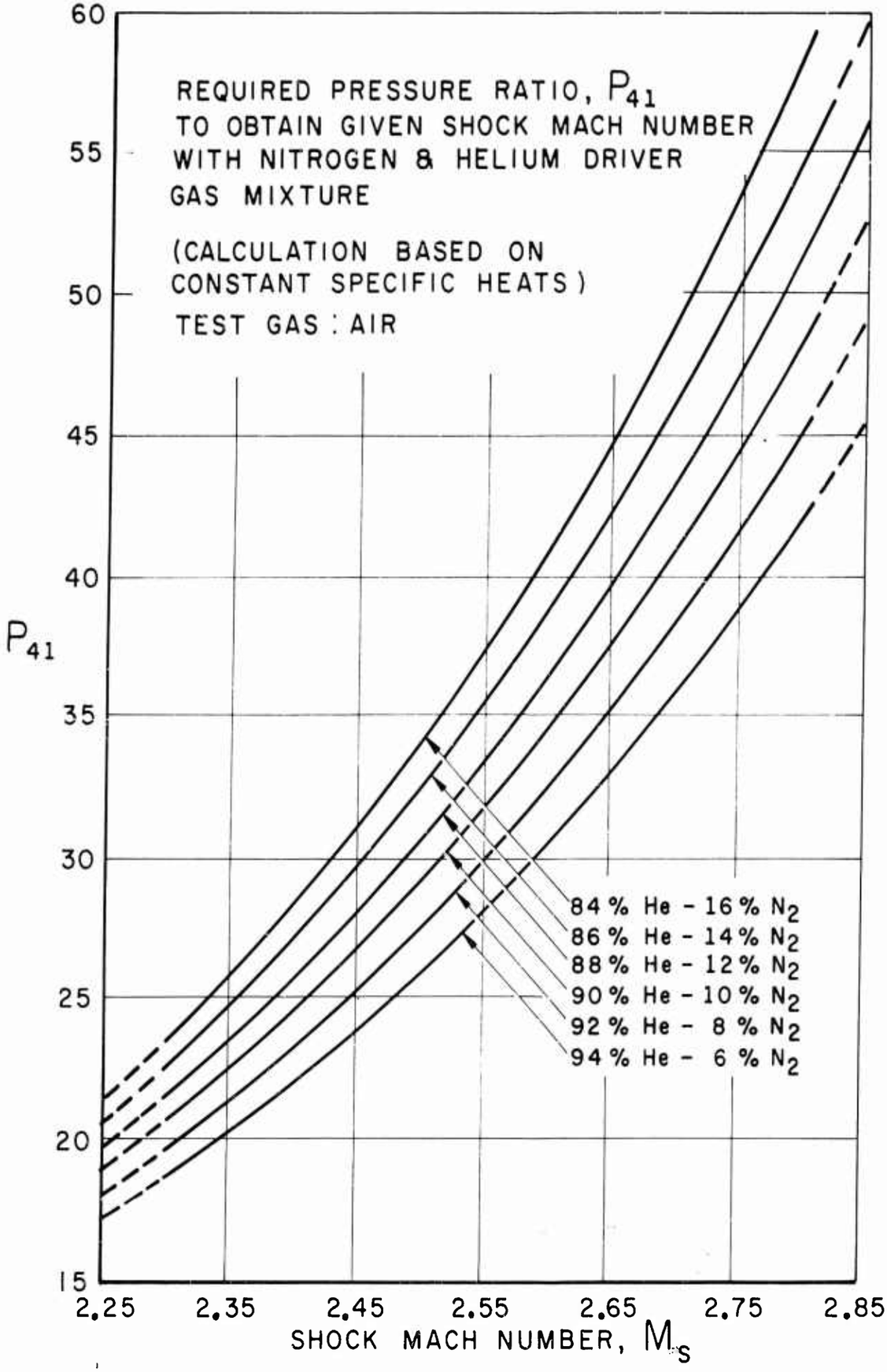
REQUIRED PRESSURE RATIO, P_{41}
TO OBTAIN GIVEN SHOCK MACH NUMBER
WITH NITROGEN & HELIUM DRIVER
GAS MIXTURE
(CALCULATION BASED ON
CONSTANT SPECIFIC HEATS)
TEST GAS : AIR
84 % He - 16 % N_2
86 % He - 14 % N_2
88 % He - 12 % N_2
90 % He - 10 % N_2
92 % He - 8 % N_2
94 % He - 6 % N_2
P_{41}
60
55
50
45
40
35
30
25
20
15
2.25
2.35
2.45
2.55
2.65
2.75
2.85
SHOCK MACH NUMBER, M_s

FIGURE 22

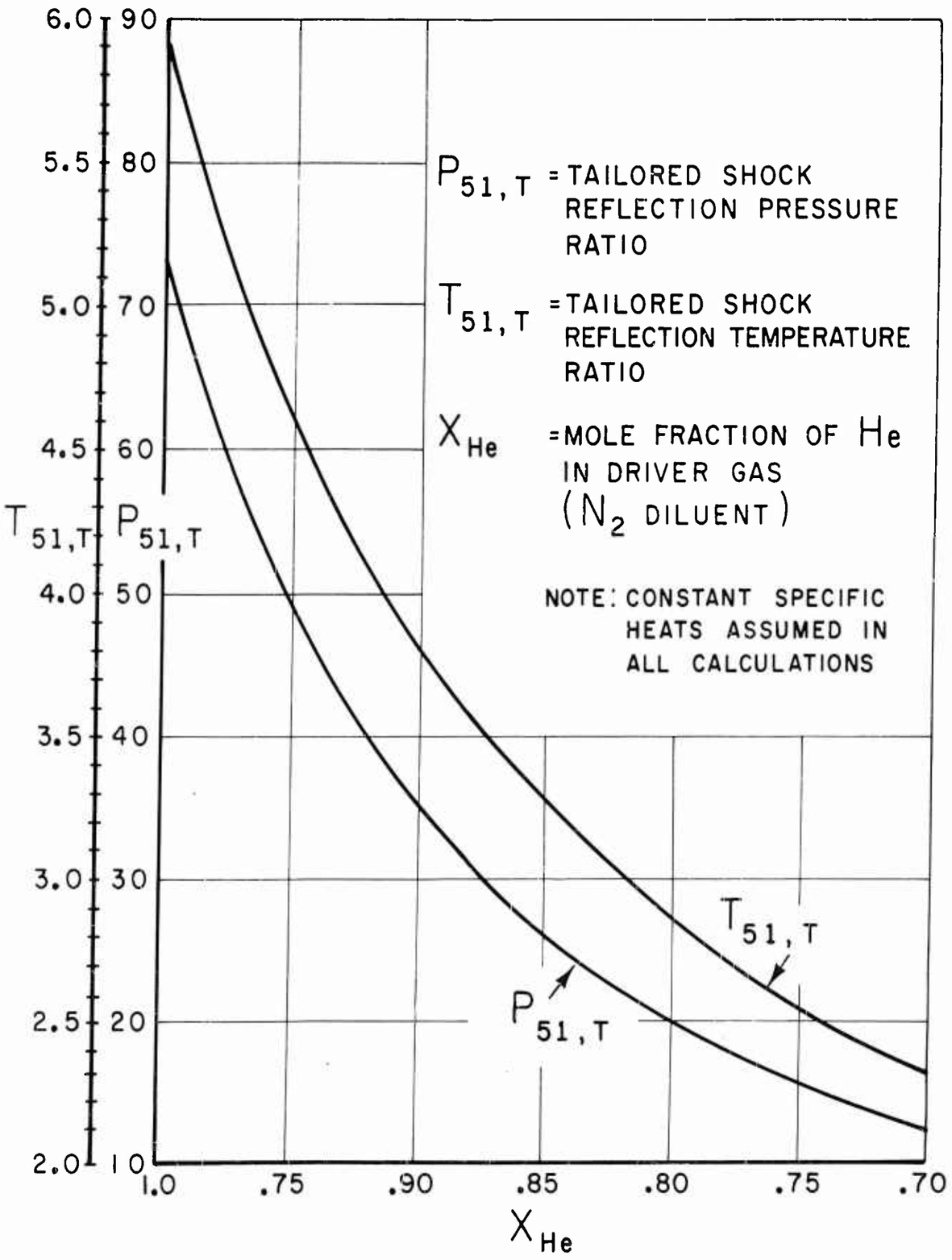
6.0
5.5
5.0
4.5
4.0
3.5
3.0
2.5
2.0
90
80
70
60
50
40
30
20
10
$T_{51,T}$
$P_{51,T}$
$P_{51,T}$ = TAILORED SHOCK REFLECTION PRESSURE RATIO
$T_{51,T}$ = TAILORED SHOCK REFLECTION TEMPERATURE RATIO
X_{He} = MOLE FRACTION OF He IN DRIVER GAS (N_2 DILUENT)
NOTE: CONSTANT SPECIFIC HEATS ASSUMED IN ALL CALCULATIONS
$T_{51,T}$
$P_{51,T}$
1.0
.75
.90
.85
.80
.75
.70
X_{He}

FIGURE 23

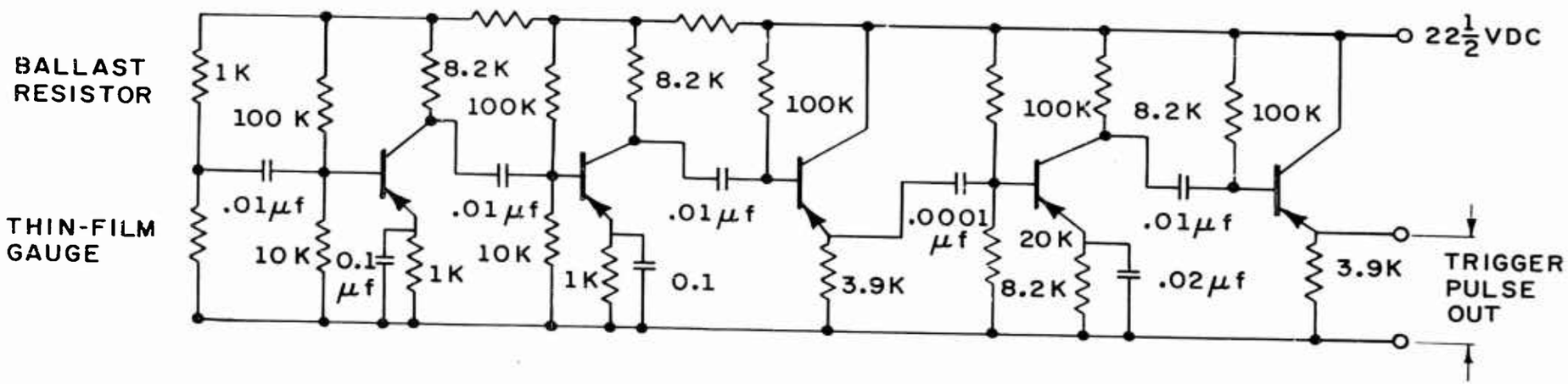

SHOCK SENSOR AMPLIFIER
WITH INTERNAL SENSOR POWER SUPPLY

FIGURE 24

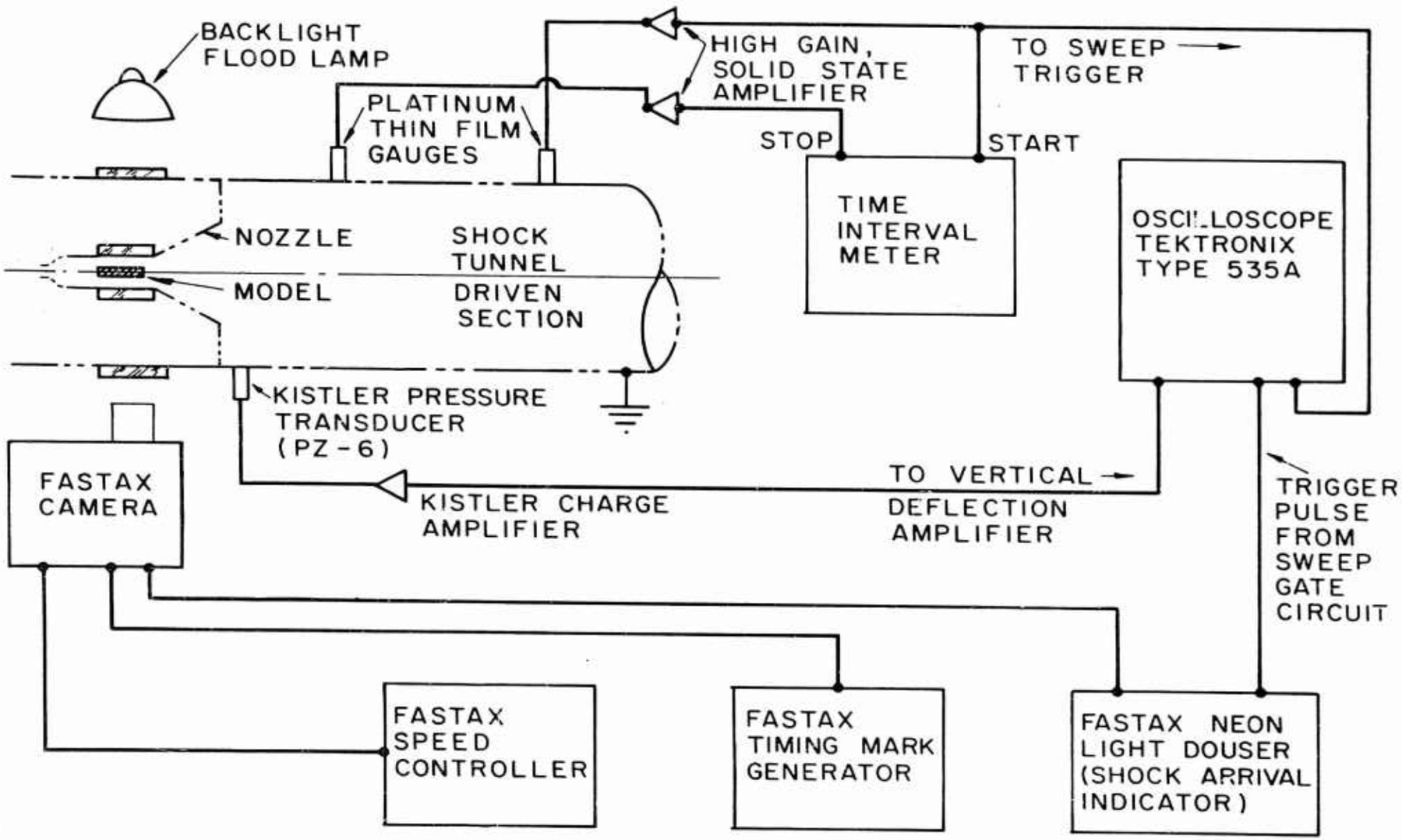

FIGURE 25

SHOCK TUNNEL INSTRUMENTATION

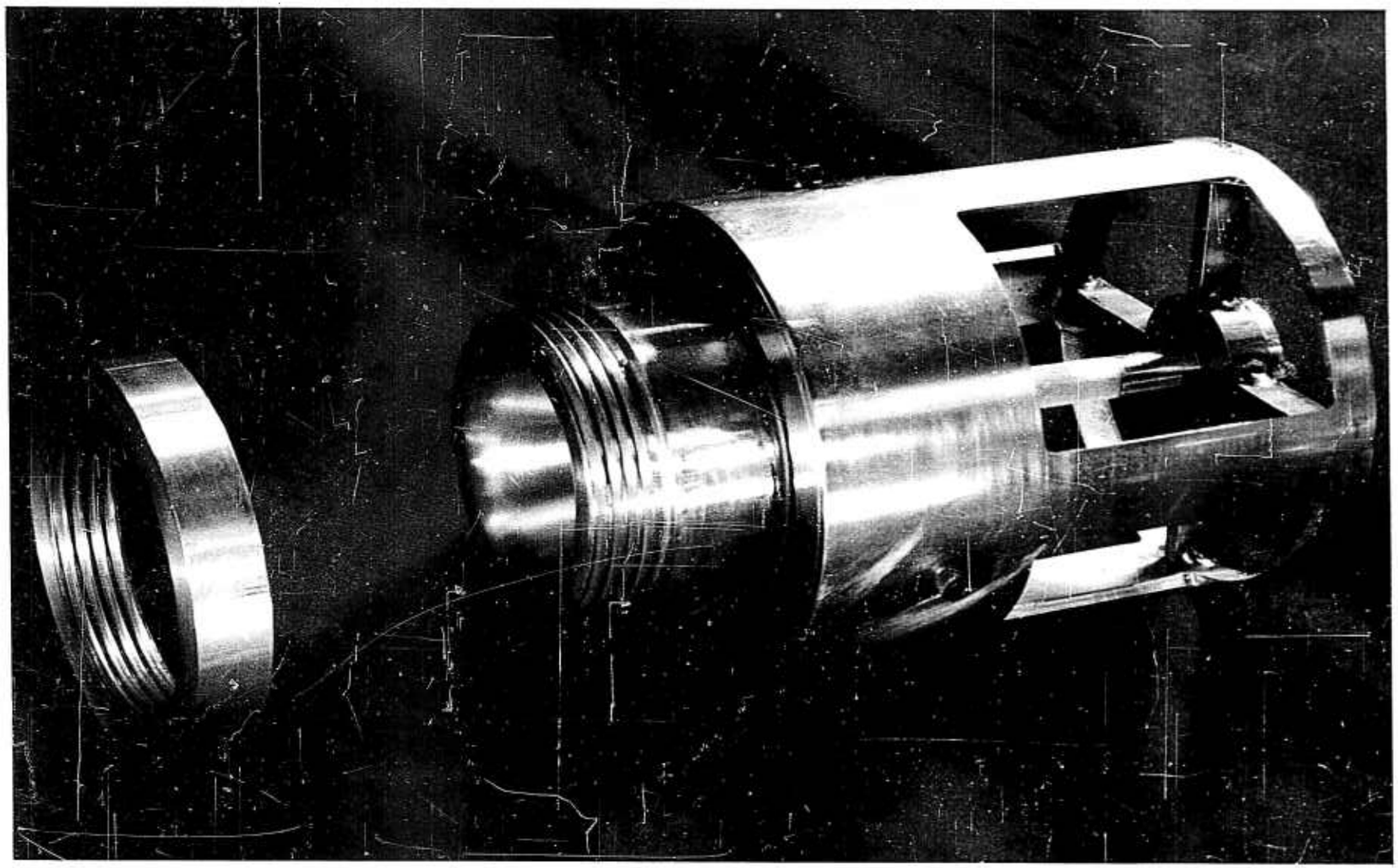

SUPERSONIC NOZZLE WITH PROPELLANT SAMPLE

FIGURE 26

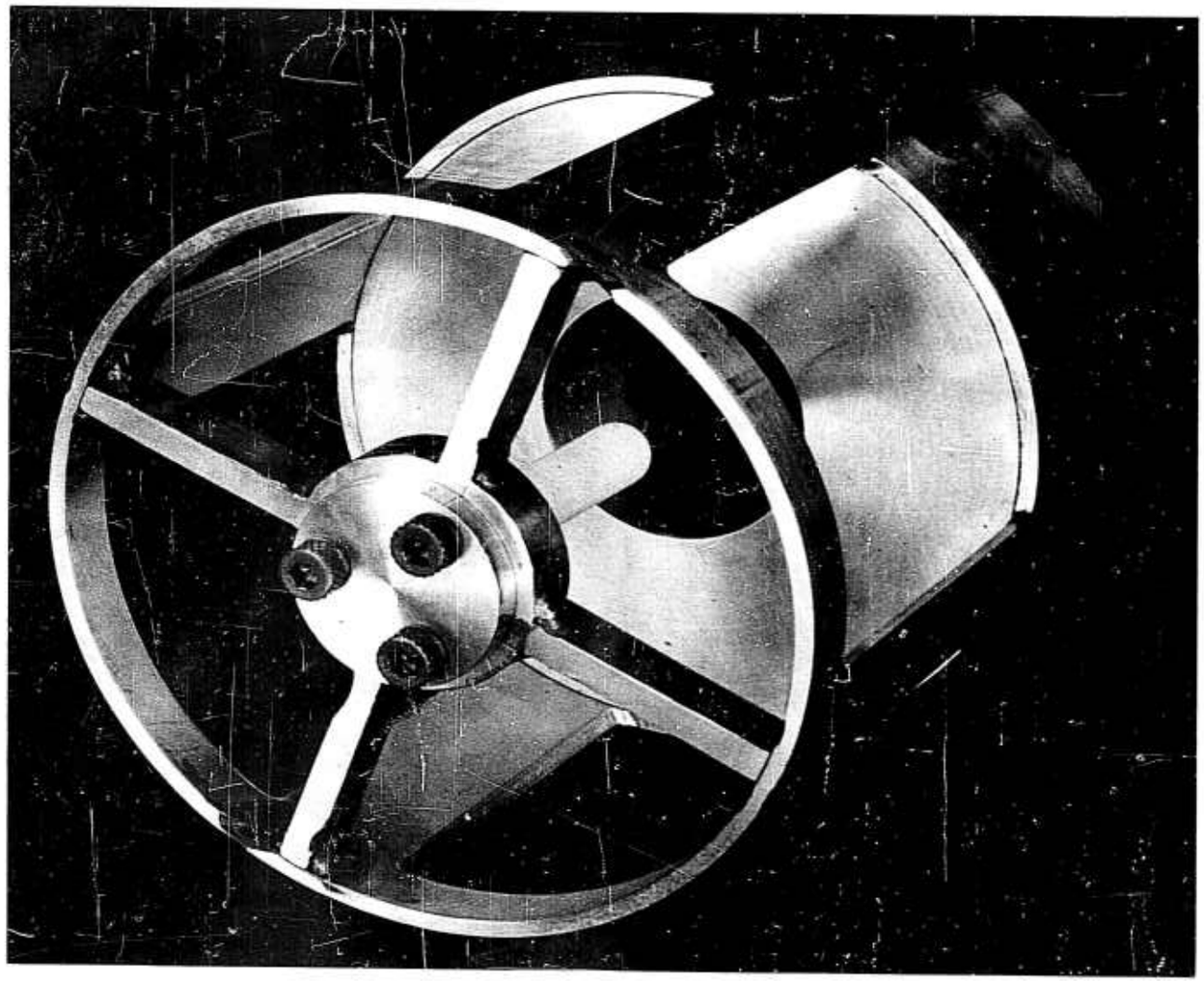

SUPERSONIC NOZZLE WITH PROPELLANT SAMPLE

FIGURE 27

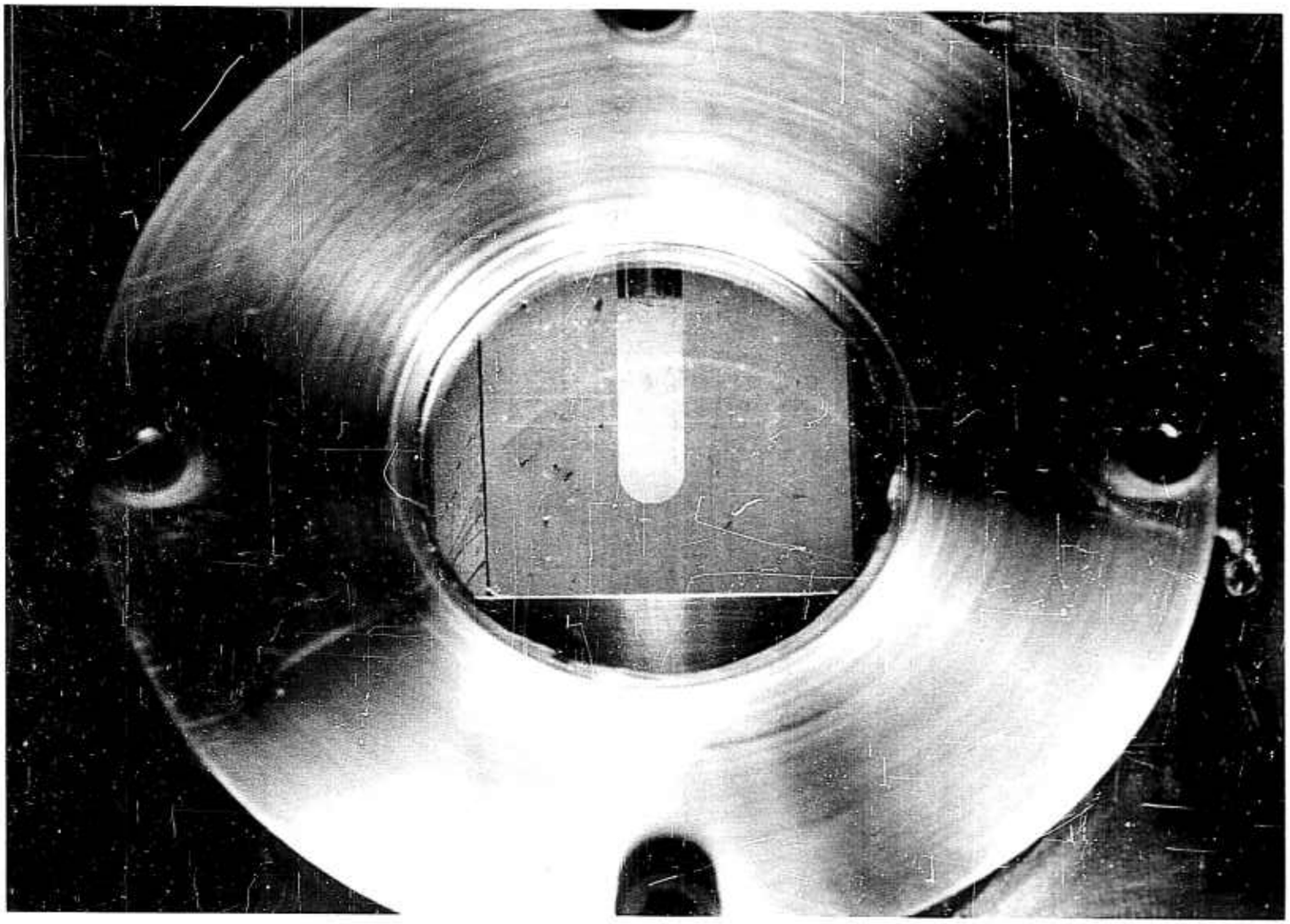

FIGURE 28

HEMISPHERE - CYLINDER SAMPLE VIEWED THROUGH
TEST SECTION WINDOW

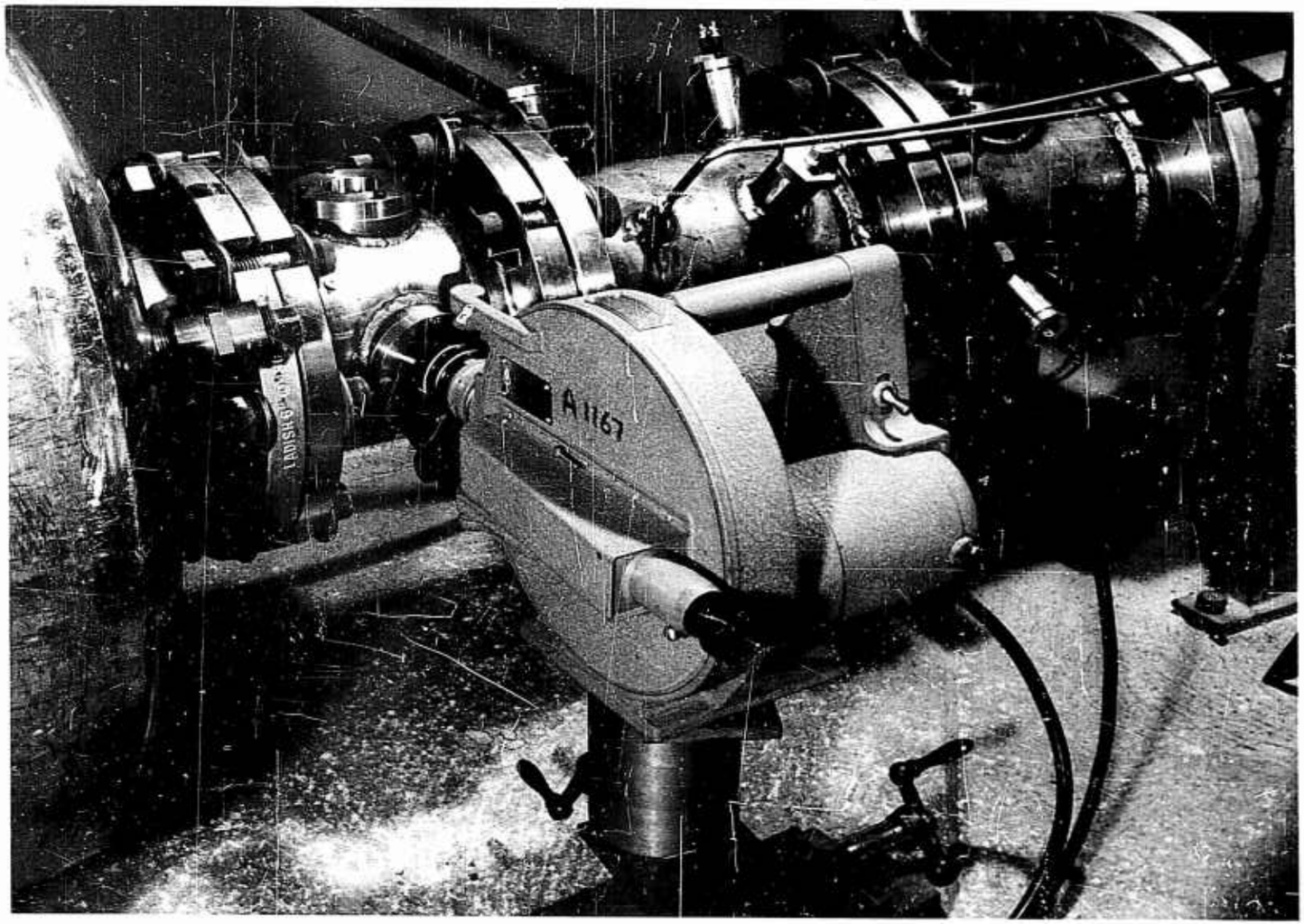

OVERALL VIEW OF TEST SECTION

FIGURE 29

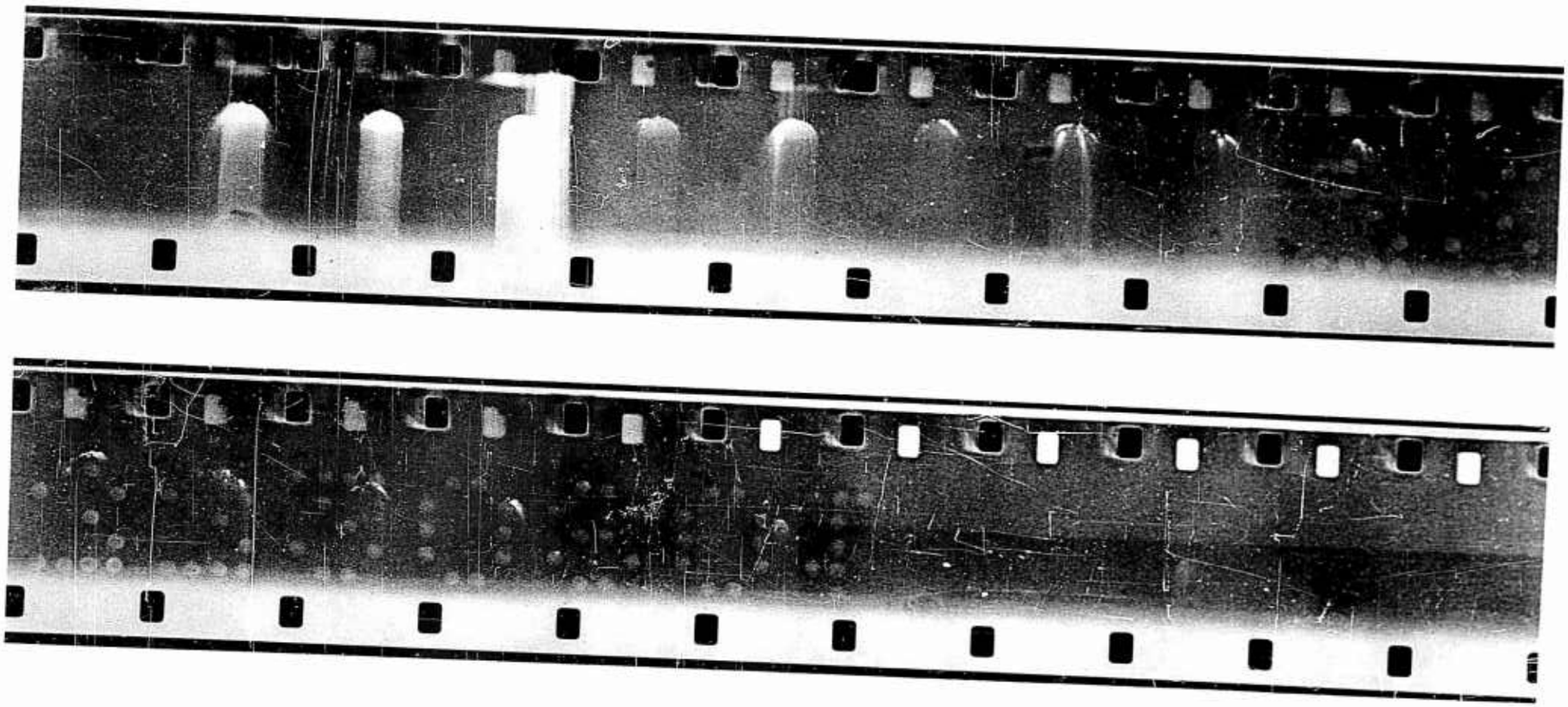

FIGURE 30

HEMISPHERE CYLINDER SAMPLE - IGNITION
IN SUPERSONIC FLOW OF 100 % O_2

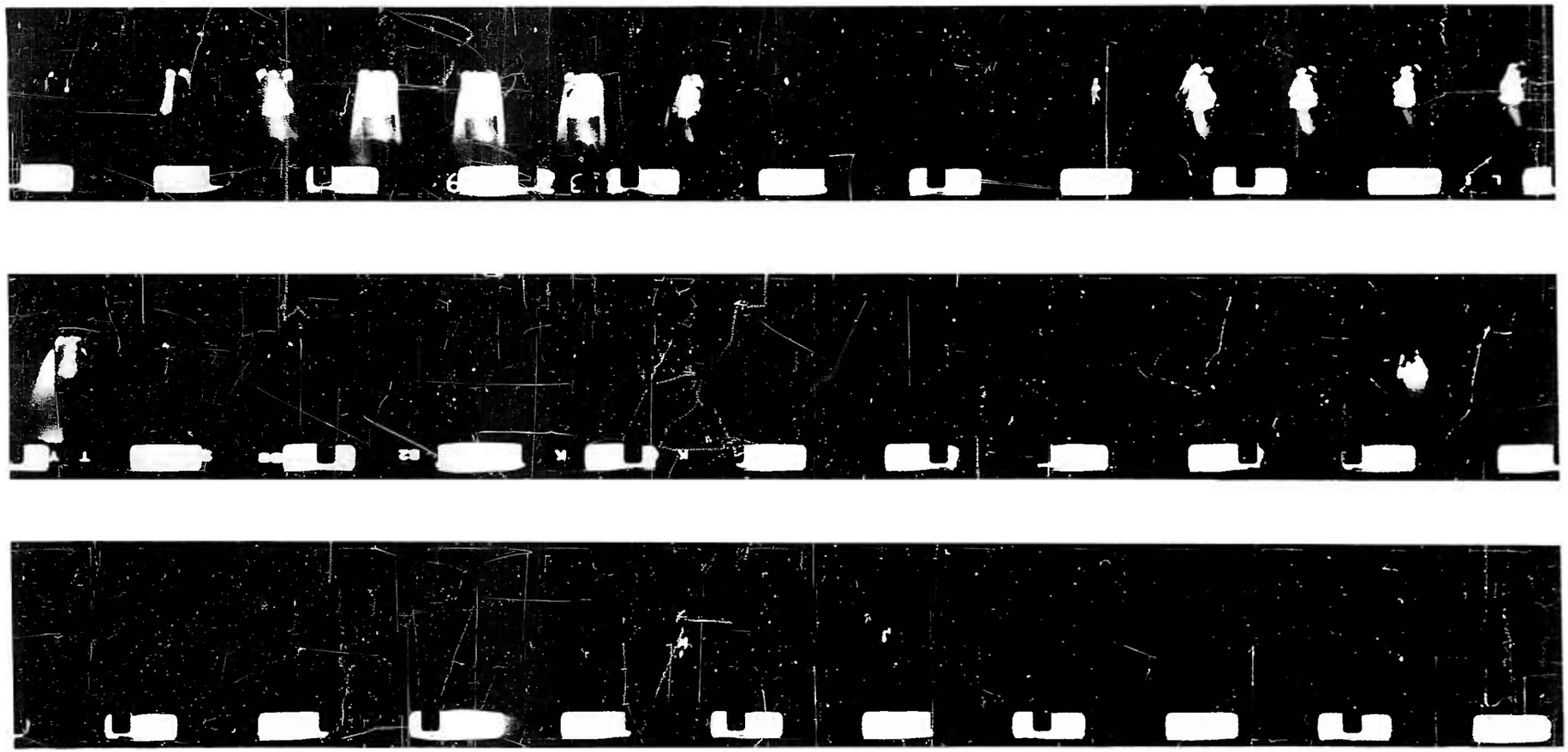

45° WEDGE SAMPLE IN 100% O_2; SUPERSONIC FLOW

FIGURE 31

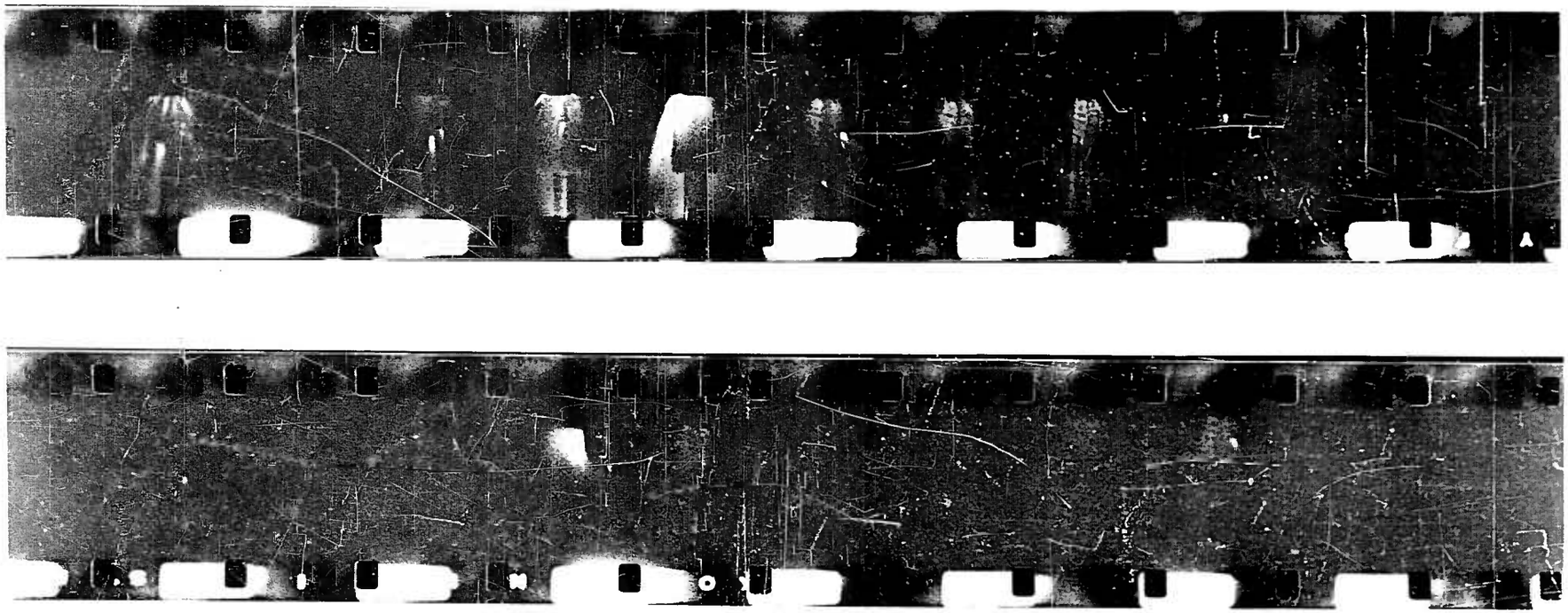

45° WEDGE SAMPLE IN AIR ; SUPERSONIC FLOW

FIGURE 32

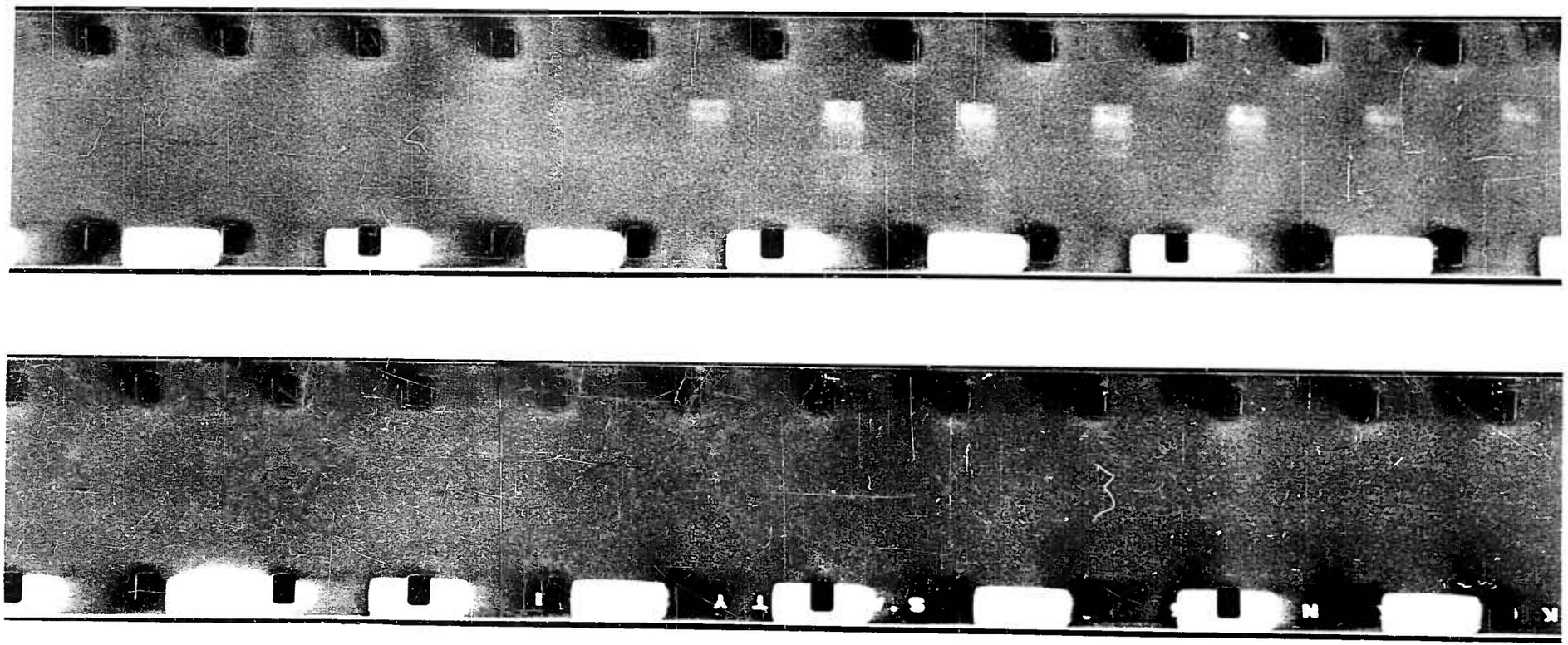

45° WEDGE SAMPLE IN 100 % O_2 ; SUPERSONIC FLOW

FIGURE 33

FORMULATIONS FOR
PROPELLANT AND FUEL SAMPLES

AP/80:20/I: SUPERSONIC FLOW TEST SAMPLES

COMPONENT	PERCENTAGES BY WEIGHT OF TOTAL MIXTURE
Fuel[1]	19.75
Cobalt	0.10
Lecithin	0.10
MEKP[2]	0.05
NH_4ClO_4[3]	80.0
	100.0

AP/78:22/I: SUBSONIC FLOW TEST SAMPLES

Fuel[1]	21.752
Cobalt	0.11
Lecithin	0.11
MEKP[2]	0.028
NH_4ClO_4[3]	78.0
	100.0

PURE FUEL: SUBSONIC FLOW TEST SAMPLES

Fuel[1]	98.7
Cobalt	0.6
Lecithin	0.6
MEKP[2]	0.1
	100.0

[1]Rohm and Haas, P-13 Polyester-Styrene Resin
[2]Methyethyl Ketone Peroxide
[3]Ground, 56 Average Particle Size

FIGURE 34

TYPICAL FILM RECORD OF SUBSONIC FLOW IGNITION TESTS

FIGURE 35

DATA PLOT: SUBSONIC FLOW IGNITION TESTS WITH 94% HELIUM - 6% NITROGEN DRIVER GAS MIXTURE

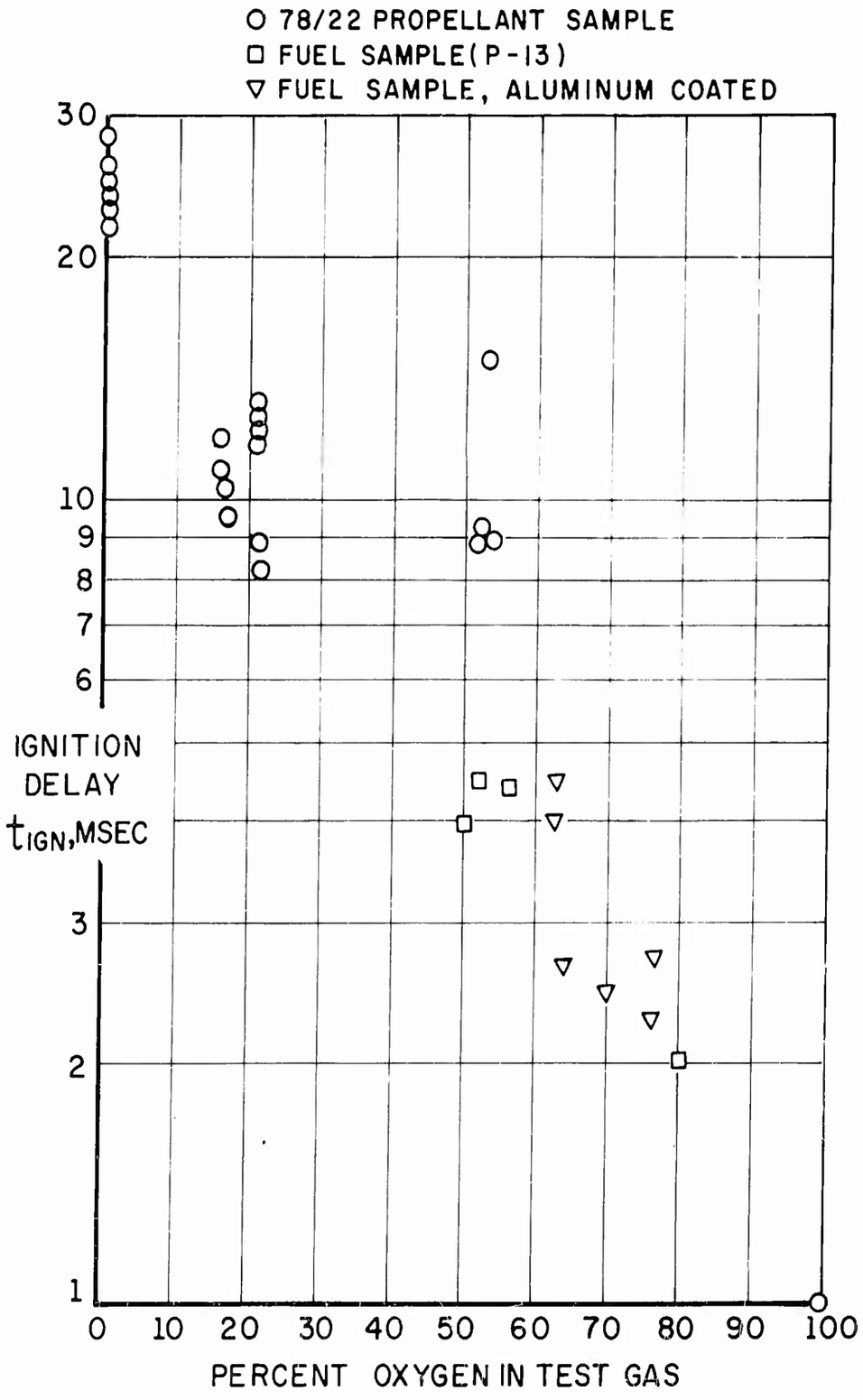

FIGURE 36

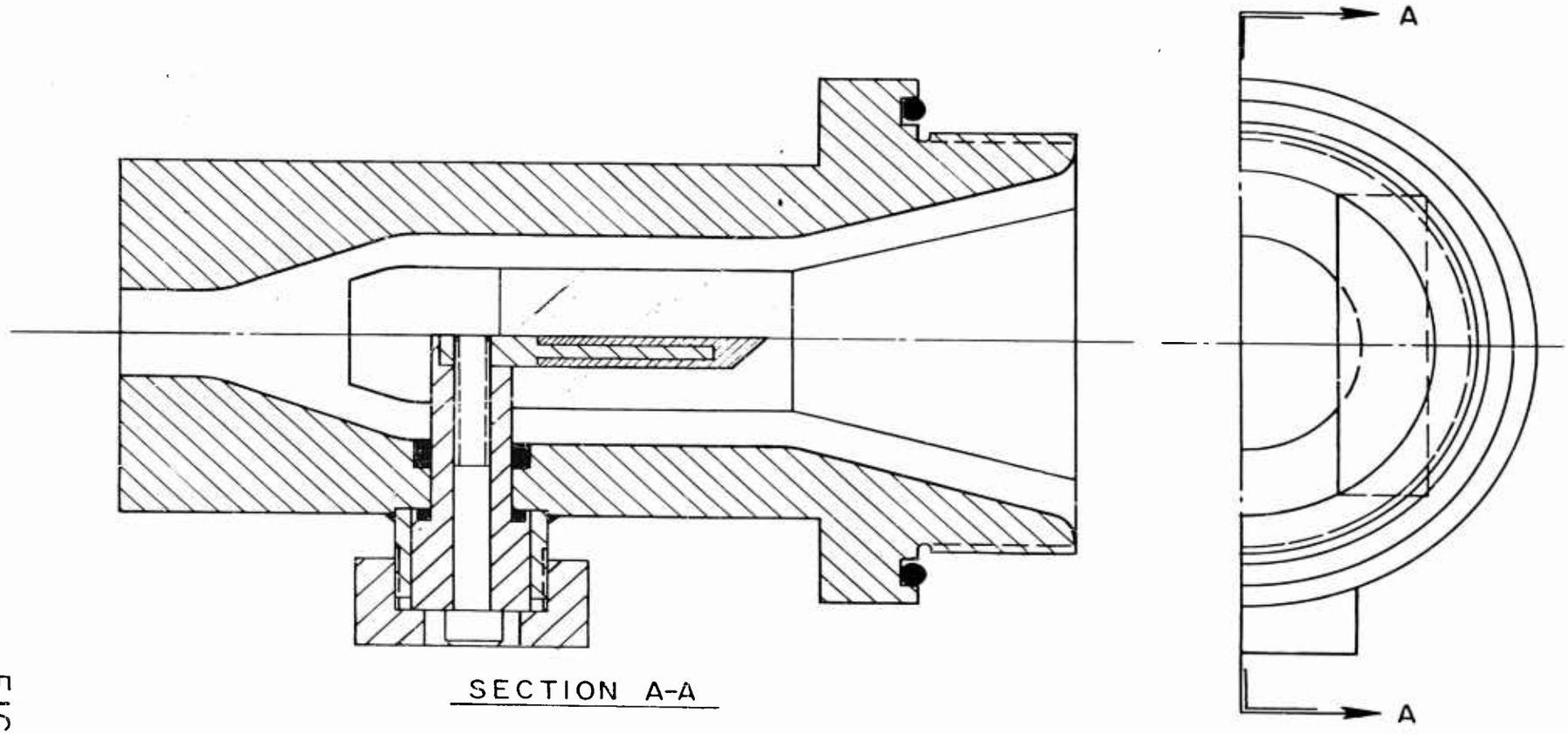

SECTION A-A

FIGURE 37

SHOCK TUNNEL SUBSONIC NOZZLE
SHOWING MOUNTED PROPELLANT MODEL

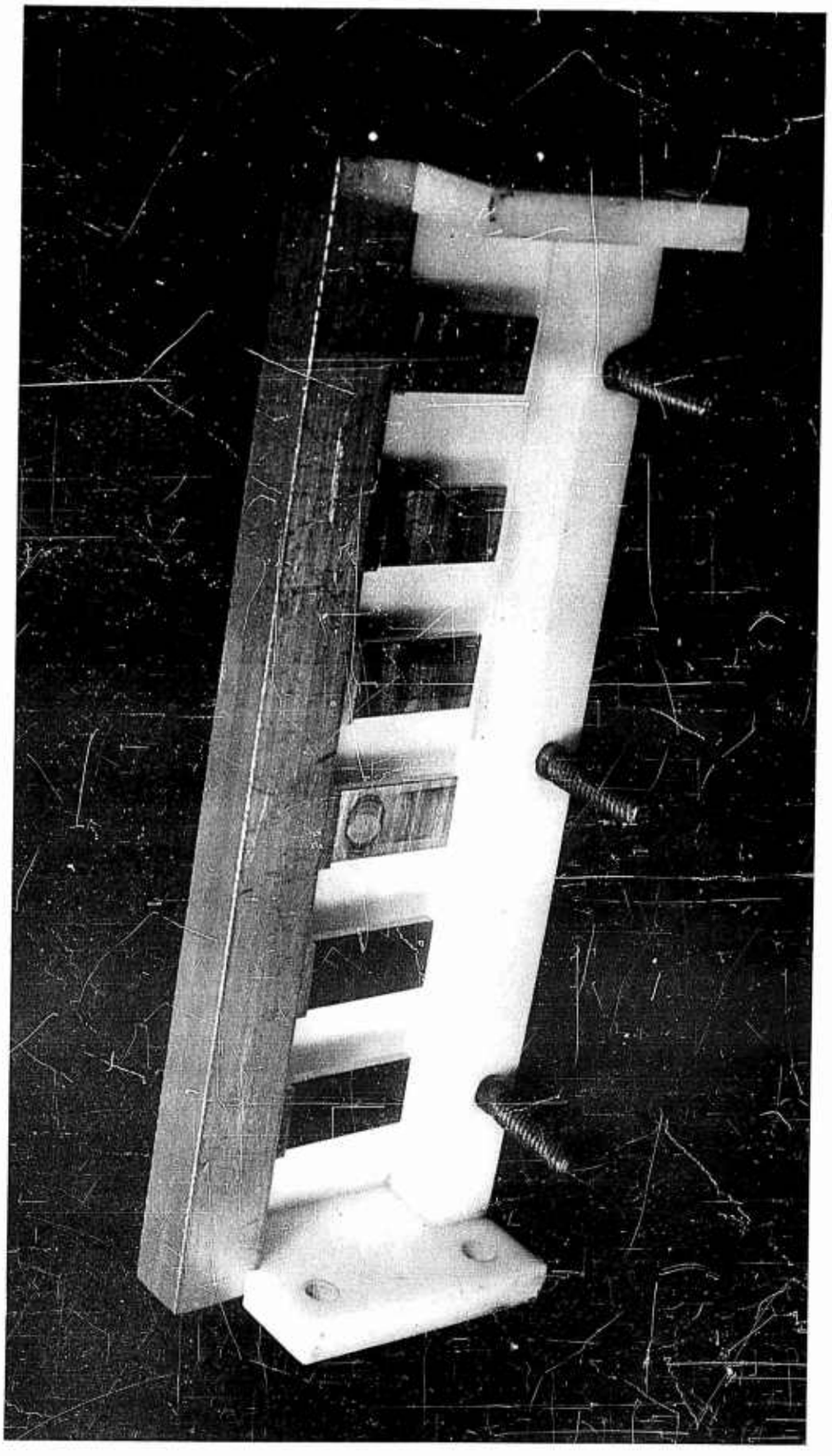

SUBSONIC SAMPLE MOLD

FIGURE 38

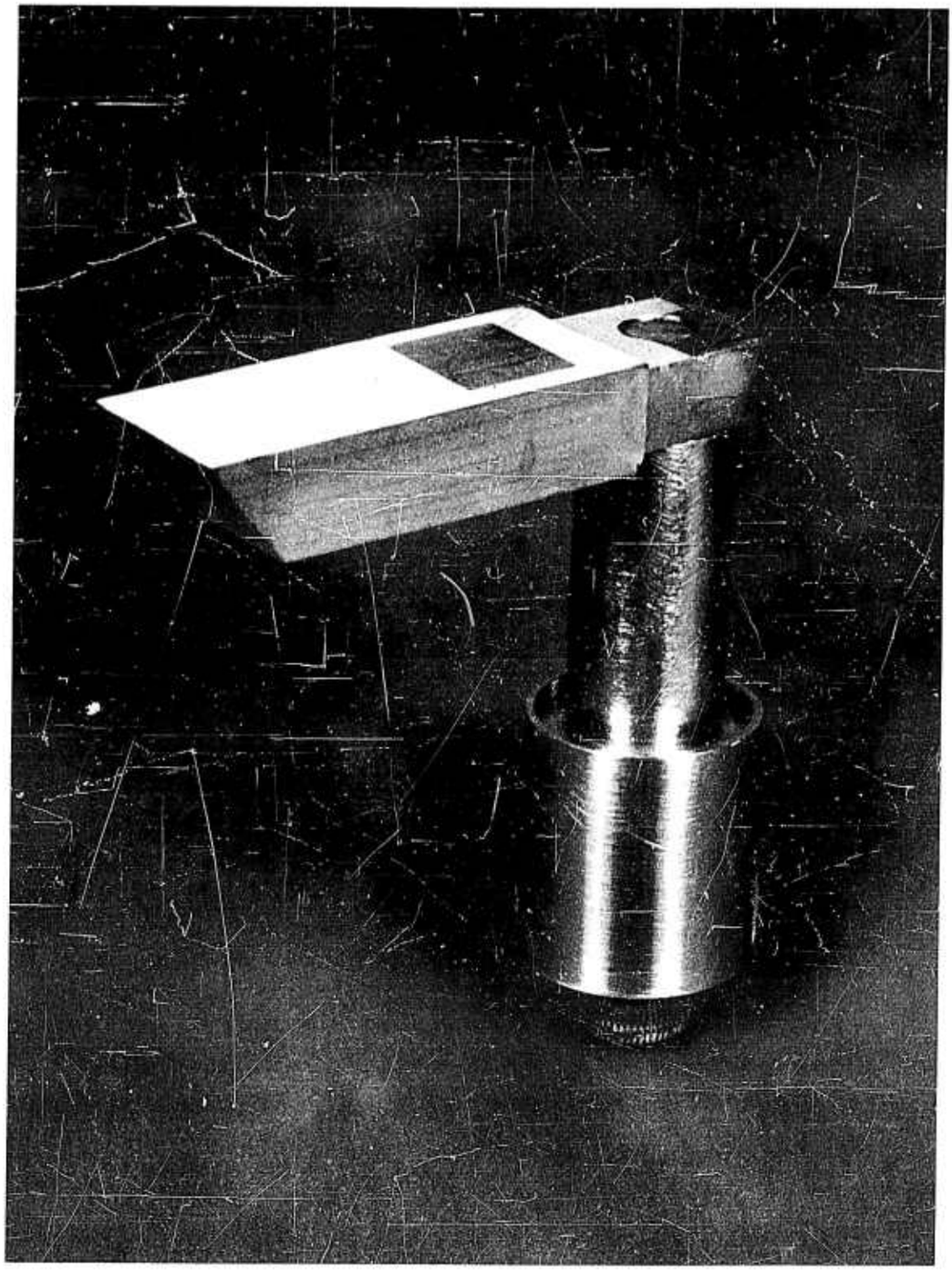

MOUNTED SUBSONIC FLOW SAMPLE

FIGURE 39

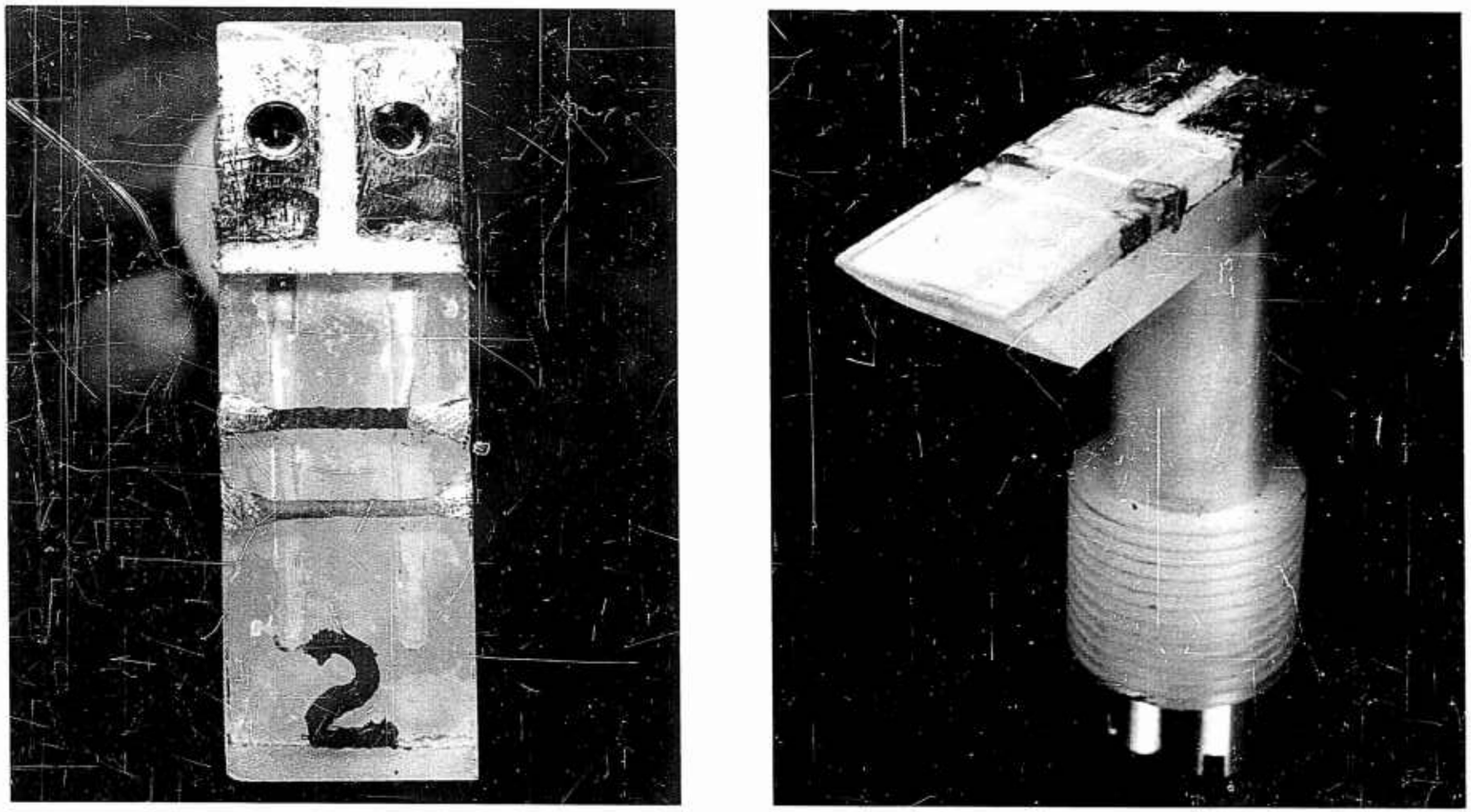

THIN FILM INSTRUMENTED MODEL FOR SURFACE TEMPERATURE MEASUREMENTS

FIGURE 40

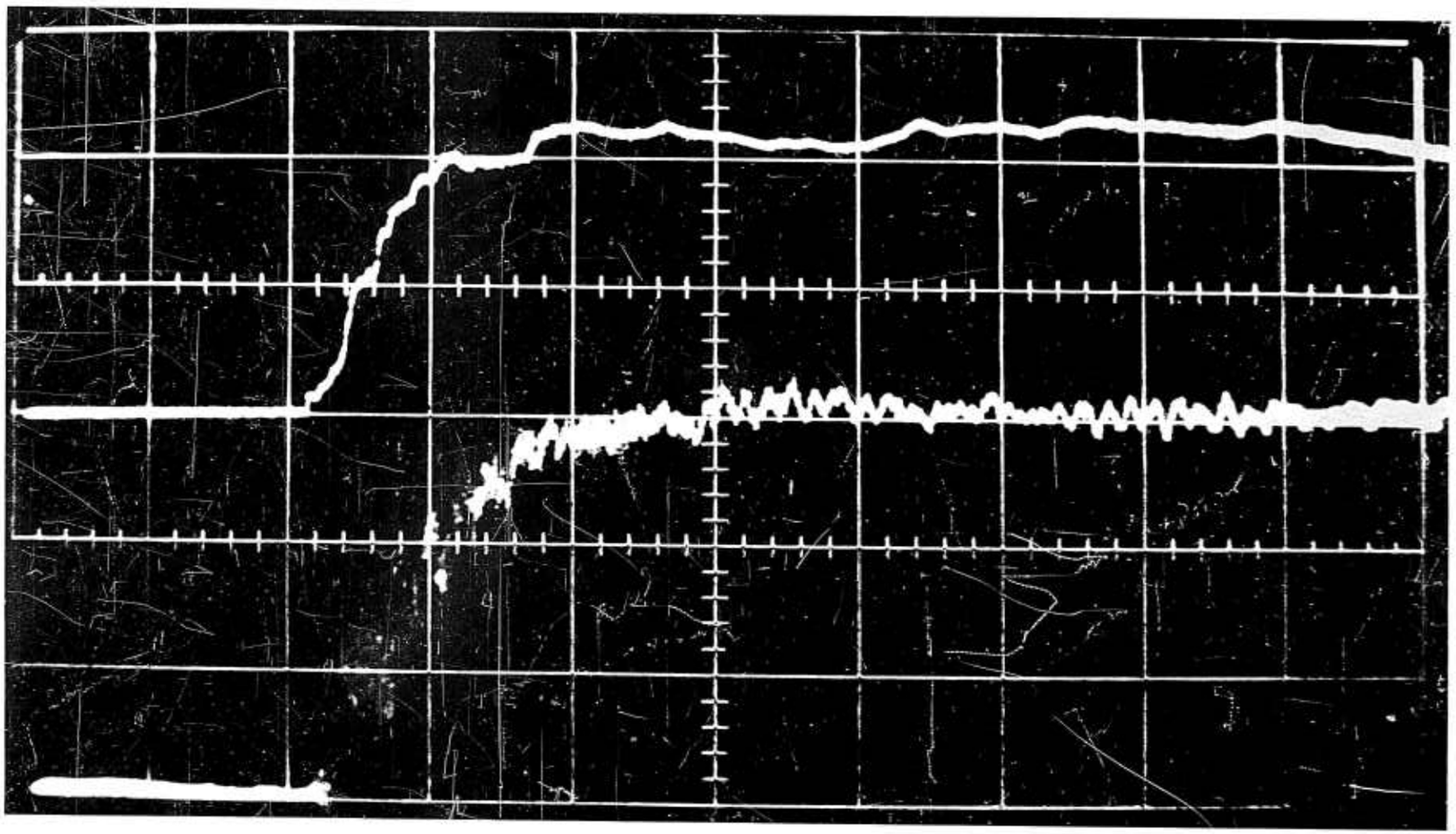

FIGURE 41

TYPICAL VOLTAGE TRACE VS TIME, SURFACE TEMPERATURE MEASUREMENTS

TEMPERATURE DIFFERENCE VERSUS ϕ
AT THE INTERFACE OF GAS SLAB AND SEMI-INFINITE SOLID

$\phi = a/\sqrt{\alpha t}$
a = GAS LAYER THICKNESS

P_{GAS} = 20 ATM
T_{GAS} = 1200 °K
α_{GAS} = 0.103 CM^2/SEC

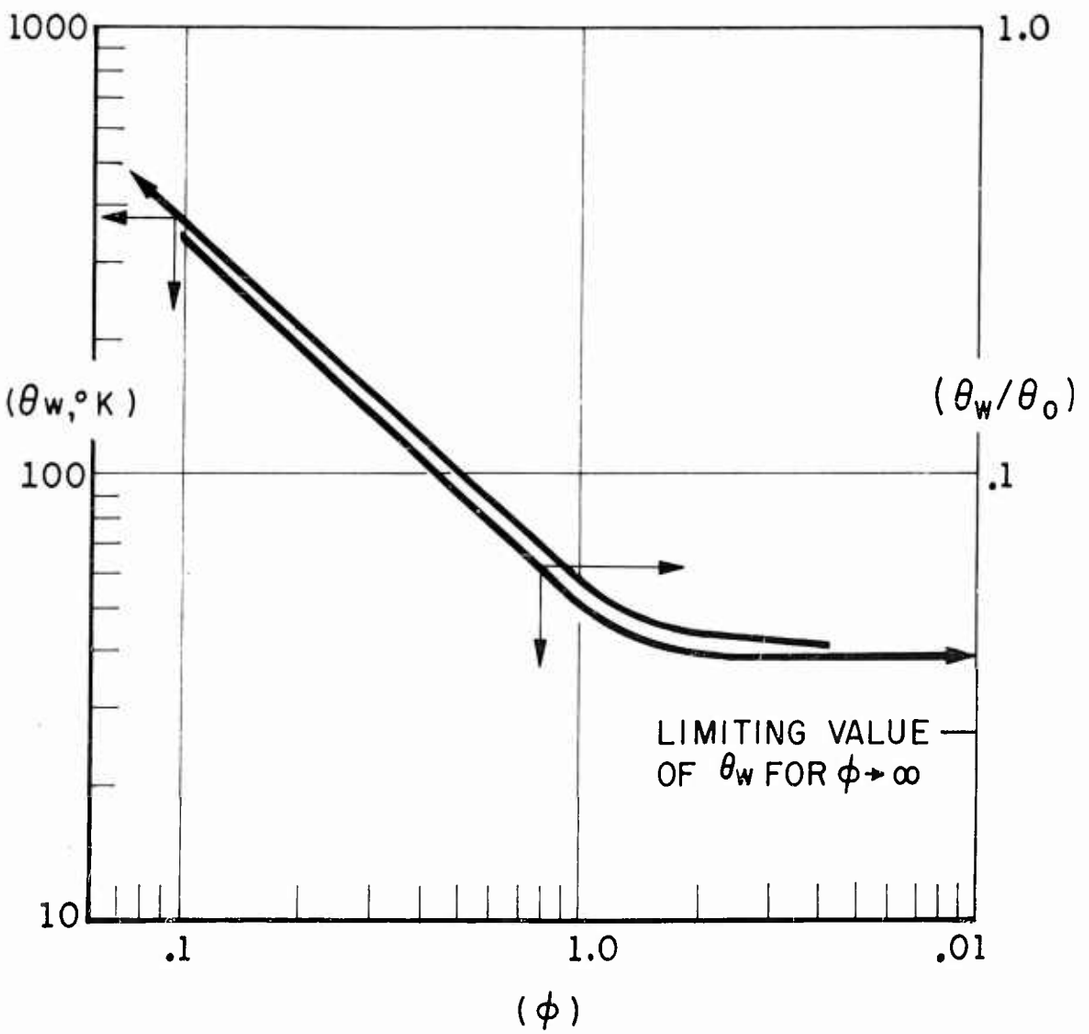

FIGURE 42

TEMPERATURE HISTORY OF GAS-SOLID INTERFACE

NOTE: GAS IS AIR, SOLID IS P-13

θ_w = Twall − To θ_o = Tg − To

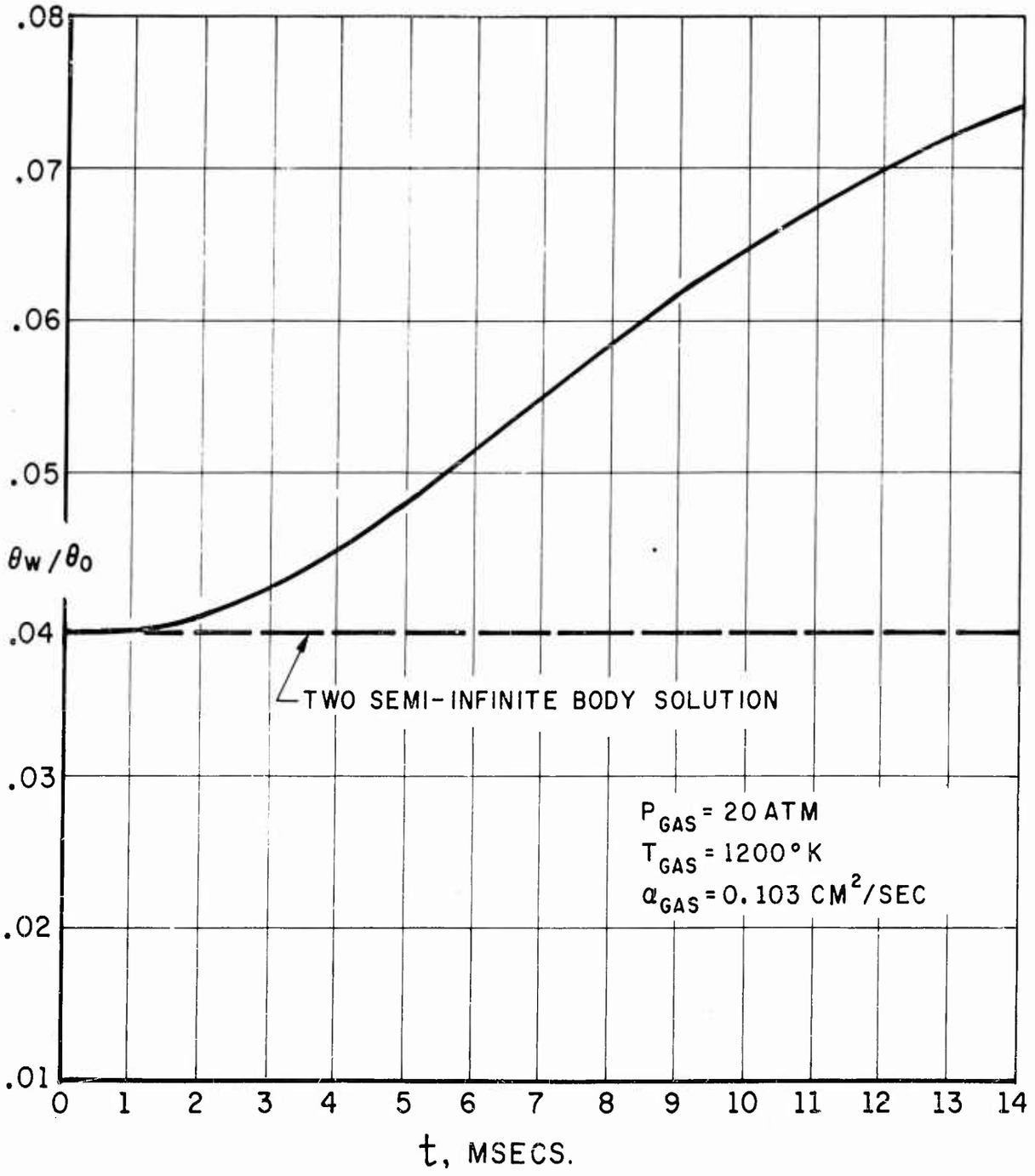

FIGURE 43

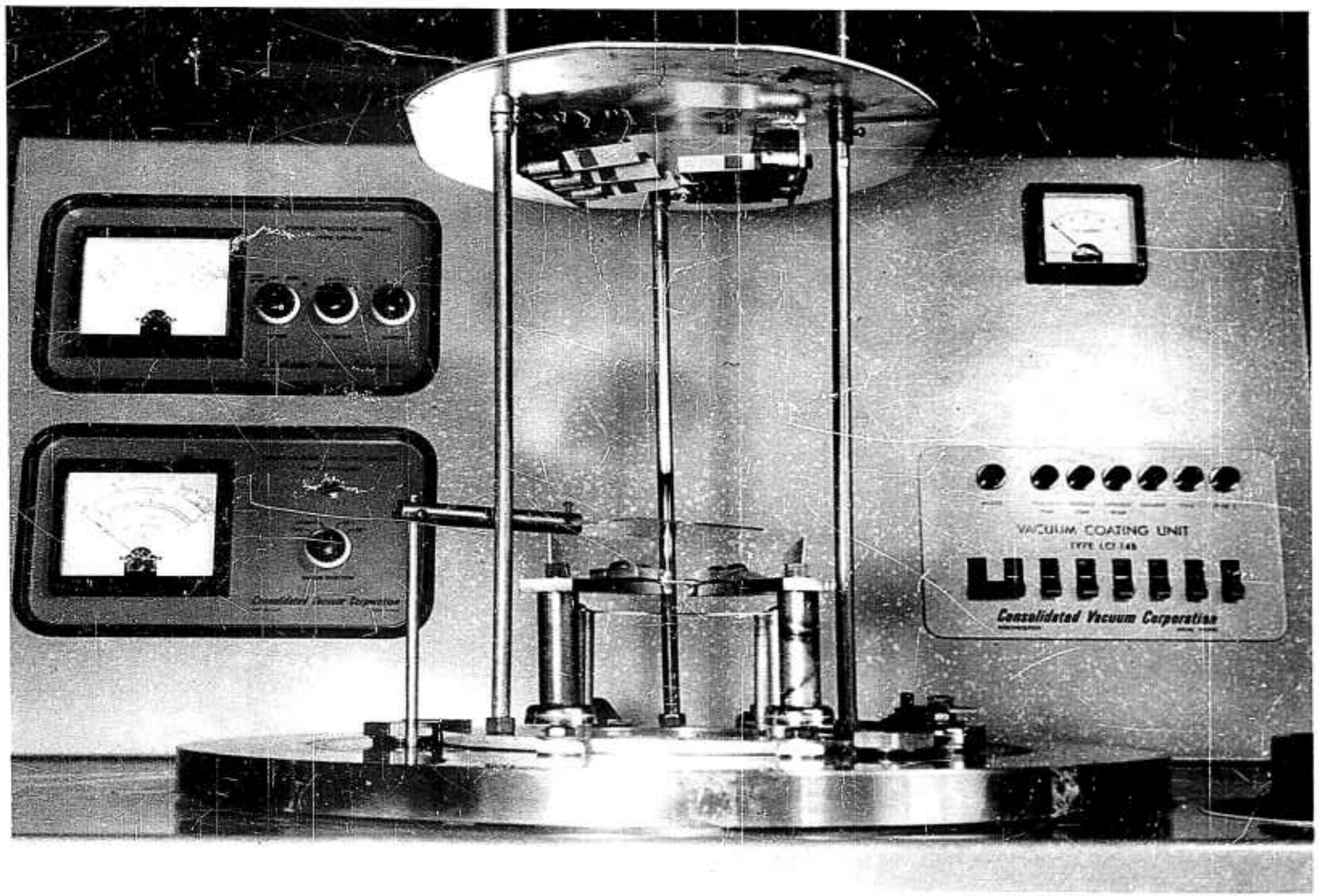

COATED SAMPLES MOUNTED IN VACUUM EVAPORATOR

FIGURE 44